A Molecular, Anatomical and Developmental Account of Copine-6 Protein Expression in the Rodent Brain

Ruth Helen Faram

MRC Anatomical Neuropharmacology
New College

Thesis for the Degree of
Doctor of Philosophy

Medical Sciences Division

University of Oxford

Trinity Term 2013

"Have I gone mad?" asked The Mad Hatter

"I'm afraid so", replied Alice.
"You're entirely bonkers. But I'll tell you a secret. All the best people are".

~Alice in Wonderland

For my parents, Helen and John Faram
And my wonderful sister, Jane.

In loving memory of Laura Howard
1985-2009

♥

Acknowledgments

Firstly, my thanks go to the Medical Research Council; without their generous funding my doctoral training would not have been possible.

I would like to express my greatest appreciation to my supervisor, Dr. Jeff McIlhinney, for his endless support and kindness. Initially as my M.Sc. supervisor, and subsequently as my D.Phil supervisor and mentor, Jeff has played the most important role in my development as a scientist. He has been a source of strength in every possible way, far beyond any reasonable call of duty and I have been privileged to have had such a caring and encouraging supervisor who has inspired me from the beginning. My thanks and gratitude also goes to Dr. Pavel Perestenko, for his help, advice and humour, not to mention his brilliant microscopy skills. I have thoroughly enjoyed working within the McIlhinney lab, which never lacks a healthy dose of wit and comical discussion.

I am sincerely grateful to Dr. Peter Magill for his continuous support and training throughout my D.Phil, and for giving up so much time for fruitful scientific discussion. Without Pete's enthusiasm, wisdom, and expertise, much of this thesis would not have been possible and I would not have had the opportunity to delve deep into the wonderful world of neuroanatomy. I would also like to thank Professor Peter Somogyi, the director of the Unit, who has always given me great advice and focus, particularly with the electron microscopy. His immense knowledge, philosophical insight and eye for detail taught me how to think like an anatomist, which goes far beyond the technical skill. It has been an invaluable and honourable experience to have received training from such highly regarded individuals.

I wish to also pay thanks to Dr. Louise Kay, who made the developmental studies in this thesis possible. The scientific help and assistance resulted in the formation of a friendship, and I am very grateful for your support both in work and when gossiping over a cup of coffee and (bottles) of wine!

I would like to acknowledge Kathryn Newton, Natalia Campo-Urriza, Kristina Detzner, Ben Micklem, Prakash Guna, Kouichi Nakamura, Liz Norman and Robert Stewart for their technical advice and support. You have each played an invaluable part in the production of my thesis and I thank each of you for having so much patience, even when I ask ridiculous questions.

I would like to thank my good friends Jonathan Fitzgibbons and Daniel Walters, who not only shared the unlikely journey to studying at Oxford from the same unlikely secondary school, but provided encouragement, witty conversation and irreverent humour – the perfect combination following an average day working in the lab! On this note, especial thanks also goes to my "chuck" Emma Bolton, a friend worth more than her weight in gold, who has supplied me with support, friendship and laughter, alongside pints of ale and uncountable cups of tea. Since being in Oxford, I have been privileged to meet so many inspiring people; Sarina Agkatsev, Julia Shanks, Simon Hackett and Yvonne Couch, you are wonderful friends and I am lucky to have shared my experiences (including madness) in Oxford with you all.☺ Krysta Melanie "Mole" Munford, thank you for being a fellow neuron and for supporting me throughout our fruitful undergraduate and beyond! And, of course, I would not be the person I am today were it not for my friends from Aston, Sheffield, who I have known for ~15 years. Lauren Ellis, Christopher Stump, Georgie Pope, Kate Earnshaw, and Lucy Simmonite: thank you all for being there for me despite the distance between us. I am proud to have you as my friends and the longevity of our friendship proves how special you all are.

Especial thanks goes to my wonderful partner in crime, Paul Howard, for his love and support over the decade we've spent together. You believed in me more than I believed in myself, and your optimism right at the beginning back at school enabled me to achieve my dream of being a neuroscientist. Who thought it would be at the University of Oxford! Even through the tough times of personal tragedy, you have been my rock, and I simply wouldn't have completed this thesis if it weren't for you.

My ultimate gratitude, however, goes to my parents and my sister, Jane. They have always supported me and have had colossal patience in doing so. Their nurturing created the foundations of a scientist – the bird watching holidays and fishing matches were only the beginning of my curiosity with nature! – but most importantly I would like to thank them for all of their support when I was in hospital and having brain surgery, the *real* reason why I now love neuroscience. My parents have always been selfless and generous in giving Jane and I their love, including during times of personal illnesses and tragedy. It is to them that I dedicate this work, and to the loving memory of Paul's sister Laura, who was one of my best friends, and who shared some of my oldest and most treasured memories throughout my life, from nursery right through to University.

Table of Contents

Chapter 1. Introduction 1

1.1. Cell Signalling 1

1.1.1. Calcium signalling... 3

1.1.2. The Copines are a novel double C2-domain calcium binding protein family ... 13

1.1.3. Structure, sequence homology and function of the Copine family of proteins.. 13

1.1.4. Anatomical distribution of each Copine family member in mammals 23

1.2. Copine-VI (Copine-6).. 24

1.3. Neocortex and the Hippocampus 25

1.4. Olfactory bulb 31

1.4.1. Adult Neurogenesis at the subventricular zone.. 34

1.5. Aims of thesis 38

Chapter 2. Characterising a rabbit polyclonal antibody against Copine-6 40

2.1. Introduction... 40

2.2. Methods 41

2.2.1. Copine-6 protein production and production of the rabbit polyclonal antibody against Copine-6... 41

2.2.2. Indirect Fluorophore- Linked Immunosorbant Assay (FLISA) 43

2.2.3. Production of HEK cells to constitutively express Copines –1, -2, -3, -6, -7 43

2.2.4. Protein immunoblotting of various rat tissues.. 45

2.2.5. Immunohistochemical analysis of tissue using polyclonal antibody against Copine-6 46

2.2.6. Antigen retrieval 48

2.3. Results 49

2.3.1. Indirect FLISA 49

2.3.2. One of the two rabbit polyclonal antibodies specifically targets Copine-6 50

2.3.3. The Copine-6 antibody from rabbit 3 identifies Copine-6 in brain 54

2.3.4. The Copine-6 rabbit polyclonal antibody has an identical neuronal staining pattern as the commercial anti–Copine-6 monoclonal antibodies 56

2.4. Discussion 59

Chapter 3. Immunohistochemical analysis of Copine-6 immuno-positive cells 64

3.1. Introduction 64

3.2. Materials and Methods 65

3.2.1. Dissociated cell culture 65

3.2.2. Section preparation of adult rat brain in the parasagittal plane 68

3.3. Results 72

3.3.1. A general overview of Copine-6 histochemistry 72

3.3.2. Immunohistochemical analysis of cultured dissociated hippocampal neurons.. 74

3.3.3. Immunohistochemical analysis of cultured dissociated olfactory bulb neurons.77

3.3.4. Copine-6 in the adult rat hippocampus 83

3.3.5. Copine-6 in the Olfactory Bulb 88

3.3.6. Copine-6 in the neocortex 99

3.3.7. Copine-6 in layer VI of the neocortex and the corpus callosum 107

3.4. Discussion 120

3.4.1. Copine-6 immunolabelling of some pyramidal cells and granule cells in the rat hippocampus 121

3.4.2. Copine-6 immunolabelling identifies an ‘axonless’ spiny interneuron subpopulation in dissociated olfactory culture, with similarities to olfactory granule and/or periglomerular cells 122

3.4.3. Copine-6 is expressed by certain olfactory granule and periglomerular cell populations in the rat olfactory bulb 123

3.4.4. Copine-6 labels neocortical small pyramidal principal neurons, and a discrete population of calretinin +ve/CCK +ve GABAergic interneuron (the ‘ghost’ cell) ... 126

3.4.5. Copine-6 labels a novel ‘spiny’ interneuron subpopulation in the corpus callosum of the rat with striking similarities to olfactory intrinsic interneurons 128

Chapter 4. Developmental expression of Copine-6 in mouse and rat brain 133

4.1. Introduction 133

4.2. Materials and Methods 137

4.2.1. Protein immunoblotting of developing rat brain from embryo to adult 137

4.2.2. Developmental immunocytochemical analysis of dissociated hippocampal culture 138

4.2.3. Immunohistochemical analysis of Copine-6 in embryonic and postnatal rat brain 139

4.2.4. (BrdU) analysis of Copine-6 cells in the white matter of the adult rat brain ... 139

4.2.5. Embryonic BrdU birthdating analysis of Copine-6 cells in the white matter of mouse brain 140

4.3. Results 141

4.3.1. Copine-6 expression increases during brain development 141

4.3.2. Developmental analysis of Copine-6 expression in dissociated hippocampal culture 142

4.3.3. Copine-6 expression in the embryonic and postnatal rat brain 144

4.3.4. BrdU analysis: Copine-6 spiny interneurons are not born in the adult rat brain 157

4.3.5. BrdU-analysis of embryonic mouse brain: Copine-6 cells are born during embryogenesis 163

4.4. Discussion 169

Chapter 5. Electron Microscopic analysis of Copine-6 immuno-positive neurons........ 174

5.1. Introduction 174

5.1.1. Synaptic neurochemistry and the Copine-6 spiny cells in the corpus callosum 174

5.2. Methods 176

5.2.1. Horseradish Peroxidase (HRP) + 3,3'-Diaminobenzidine (DAB), and Avidin-Biotin Complex (ABC) + 3,3'-Diaminobenzidine (DAB). 177

5.2.2. Silver intensified Gold 178

5.2.3. Controls 178

5.2.4. Postfixation, Uranyl Acetate staining, Dehydration and epoxy resin embedding. 179

5.2.5. Coating of Copper Grids 179

5.2.6. Cutting electron microscopic sections and electron microscopy 180

5.3. Results 181

5.3.1. Fine structure of the Copine-6 spiny interneurons in the corpus callosum 181

5.3.2. Copine-6 spiny interneurons within the corpus callosum receive dendrodendritic synapses 185

5.3.3. Intracellular localisation of Copine-6 protein using silver intensified nanogold particle labelling 192

5.4. Discussion 197

5.4.1. Synaptic relationship of the Copine-6 spiny interneurons in the corpus callosum 197

5.4.2. Intracellular location of Copine-6 in neurons 199

Chapter 6. General Discussion 203

Chapter 7. References 212

TABLE OF FIGURES

Figure 1-1 Schematic representation of rat proteins DOC2b, synaptotagmin 1, and Copine-6. 14

Figure 1-2 A phylogenetic tree of rat Copines -1 to -9. 16

Figure 1-4 Distribution of cortical interneuron markers in adult mouse primary visual cortex (modified from Gonchar *et al*., 2007). 28

Figure 1-5 A sagittal view of the cellular architecture of the hippocampal formation 30

Figure 1-6 A reproduction of an original Cajal drawing from a Golgi stained horizontal section 32

Figure 1-7 A calretinin labelled sagittal section of the main olfactory bulb outlining the different layers. 32

Figure 1-8 A sagittal view of an adult rodent brain, showing the main sites involved in adult neurogenesis. 35

Figure 1-9 A simplified sequence of marker expression during neurogenesis in the adult olfactory bulb. 36

Figure 2-1 Cloning Copine-6. 42

Figure 2-2 FLISA data for Rabbits 3 and 4. 50

Figure 2-3 Protein immunoblotting of HEK cells with constitutive expression of Copines -1, -2, -3, -6 and -7, reacted with the affinity purified antibodies from rabbits 3 and 4. 52

Figure 2-4 Protein Immunoblot analysis of the rabbit polyclonal anti Copine-6 from rabbit 3 compared to two commercially available monoclonal Copine-6 antibodies. 53

Figure 2-5 Rat tissue samples were subjected to protein immunoblotting to investigate the expression of Copine-6 in various tissues. 55

Figure 2-6 Protein immunoblot of adult rat brain pellet and supernatant in the presence and absence of EGTA. 56

Figure 2-7 Immunohistochemical analysis of dissociated hippocampal culture comparing polyclonal rabbit anti- Copine-6 and two commercially available monoclonal anti-Copine-6 57

Figure 2-8 Immunohistochemical analysis of Copine-6 in adult rat brain sections using polyclonal rabbit Copine-6 and commercial monoclonal Copine-6 antibodies. 59

Figure 2-9 An overview of Copine-6 in the adult rat brain 62

Figure 3-1 Mapping the distribution of Copine-6 immunoreactive cells in the rat brain using MBF Stereoinvestigator 73

Figure 3-2 Immunohistochemical analysis of dissociated hippocampal cultures following 21 days *in vitro* show a heterogeneous immunoreactivity for Copine-6. 74

Figure 3-3 Immunohistochemical protein expression analysis of dissociated hippocampal cultures following 21 days *in vitro*. 76

Figure 3-4 A schematic figure of the anatomical areas isolated for the Olfactory bulb (OB) cultures. 78

Figure 3-5 A Copine-6 ‘spiny cell’ in dissociated olfactory bulb cell culture. 79

Figure 3-6 Copine-6 cells in dissociated olfactory bulb culture are not glia. 81

Figure 3-7 Copine-6 immunoreactive ‘spiny’ neurons in olfactory bulb cultures after 21 days *in vitro*. 82

Figure 3-8 Copine-6 mRNA and protein expression in the hippocampus. 84

Figure 3-9 Copine-6 labelling in the hippocampus of the adult rat. 86

Figure 3-10 Copine-6 does not label GAD67/PV/SOM interneurons. 87

Figure 3-11 Co-reactivity of Copine -6 cells in the hippocampus with other cell markers 88

Figure 3-12 Copine-6 labelling in the adult rat main olfactory bulb. 89

Figure 3-13 An example of heterogenic Copine-6 labelling in granule cells of the main olfactory bulb.. 90

Figure 3-14 Copine-6 labelling of Olfactory granule cells.. 91

Figure 3-15 Copine-6 Olfactory granule cells have a heterogenic calretinin expression.... 92

Figure 3-16 Copine-6 granule cells are negative for other olfactory granule cells markers. 93

Figure 3-17 VGAT and gephyrin reactivity in the processes of Copine-6 olfactory granule cells... 94

Figure 3-18 Co-localisation of Copine-6 olfactory granule cells with other olfactory cell markers 95

Figure 3-19 Copine-6 labels cells surrounding the olfactory glomeruli............................. 96

Figure 3-20 Some Copine-6 labelled cells in the olfactory glomerular layer co-express enkephalin and calretinin.. 98

Figure 3-21 Co-localisation of Copine-6 olfactory glomerular cells with other olfactory cell markers 99

Figure 3-22 Copine-6 labelling in the adult rat neocortex. 100

Figure 3-23 Copine-6 labels small pyramidal neurons in layer II/III of the adult rat neocortex. 101

Figure 3-24 Co-localisation of Copine-6 cortical small pyramidal cells with other cell markers 102

Figure 3-25 A typical Copine-6 “ghost cell” in the neocortex of the adult rat brain. 103

Figure 3-26 Copine-6 labelling of ‘ghost cells’ in the neocortex..................................... 104

Figure 3-27 Copine-6 labelling of “ghost cells” in the neocortex (continued). 105

Figure 3-28 Copine-6 “ghost cells” do not express the interneuron markers parvalbumin or somatostatin.. 106

Figure 3-29 Co-localisation of Copine-6 cortical 'ghost' cells with other interneuron cell markers 106

Figure 3-30 Copine-6 spiny cells in the rostral and caudal corpus callosum. 108

Figure 3-31. Typical Copine-6 spiny cells in the corpus callosum of the adult rat brain. 108

Figure 3-32 Copine-6 spiny cells bordering the rostral migratory stream (RMS) and the subventricular zone (SVZ)... 109

Figure 3-33 The Copine-6 spiny cells in the corpus callosum of the adult rat are immunopositive for the neuronal marker NeuN. 110

Figure 3-34 Copine-6 spiny cells are not glia or newborn neuroblasts. 111

Figure 3-35 Copine-6 spiny cells in the corpus callosum are not PSA-NCAM or doublecortin postive. 112

Figure 3-36 Copine-6 spiny cells in the corpus callosum are immunoreactive for GAD67 and lack an Ankyrin –G defined axon. 113

Figure 3-37 Some Copine-6 spiny cells are co-immunoreactive for calretinin................ 114

Figure 3-38 Copine-6 spiny cells are not labelled by other interneuron markers. 115

Figure 3-39 Some Copine-6 spiny cells in the corpus callosum are immunoreactive for enkephalin... 116

Figure 3-40 Co-localisation of Copine-6 'spiny' cells in the corpus callosum with other cell markers representative of cells in the neurogenic location... 117

Figure 3-41 Copine-6 spiny cells are co-immunoreactive with presynaptic VGAT and form appositions with postsynaptic gephyrin.. 119

Figure 3-42 Where the Copine-6 'spiny' and 'ghost' cells fit into the distribution of cortical interneuron markers (image modified from Gonchar *et al*., 2007). 121

Figure 4-1 Schema of a sagittal section through the brain of an embryonic day e12 mouse. 133

Figure 4-2 Protein immunoblot of rat brain at different developmental stages................ 142

Figure 4-3 The developmental expression of Copine-6 in dissociated hippocampal cell cultures at 2, 4, 6, 8, 10, 12, 21 and 28 days *in vitro*. 143

Figure 4-4 A general overview of the developmental expression of Copine-6 and Tuj-1 in dissociated hippocampal tissue cultures. 145

Figure 4-5 Copine-6 in the e12 rodent brain (part 1). 146

Figure 4-6 Copine-6 in the e12 rodent brain (Part 2) 147

Figure 4-7 Copine-6 cells in the marginal zone (MZ) appear to be immunopositive for Tuj-1 and are absent from the ventricular zone (VZ).. 148

Figure 4-8 Copine-6 in the e18 developing neocortex and rostral migratory stream. 149

Figure 4-9 Copine-6 cells in the e18 brain neocortex and neighbouring rostral migratory stream are GABAergic neurons... 150

Figure 4-10 Copine-6 in the e18 developing hippocampus.. 151

Figure 4-11 Copine-6 immunolabelling in the e18 developing olfactory bulb. 152

Figure 4-12 Copine-6 in the post natal day 2 rat brain. 154

Figure 4-13 Copine-6 cells bordering the corpus callosum in the p2 brain. 155

Figure 4-14 Copine-6 expression in the p8 rat brain. 156

Figure 4-15 Copine-6 spiny interneurons in the adult rat brain are not born during adult neurogenesis. 158

Figure 4-16 BrdU labelling in the adult rat hippocampus following x5 days of BrdU dosing and 28 day incubation prior to sectioning. 159

Figure 4-17 Copine-6 spiny interneurons in the subventricular zone (SVZ) and white matter(WM) are not co-labelled by BrdU or Ki67. 160

Figure 4-18 A small number of Copine-6 cells co-label for BrdU in the granule and glomerular cell layers of the olfactory bulbs. 162

Figure 4-19 Some Copine-6 cells are born as early as embryonic day e10.5. 164

Figure 4-20 Copine-6 cells are also born during embryonic day e13.5. 165

Figure 4-21 Copine-6 cells are also born during embryonic day e14.5. 167

Figure 4-22 Copine-6 cells are also born during embryonic day e15.5. 168

Figure 4-23 The majority of Copine-6 spiny interneurons are born during embryonic day e13.5 and e14.5. 169

Figure 5-1 Copine-6 labelled cells in the corpus callosum of the adult rat, immunoperoxidase labelling. 182

Figure 5-2 A x20 light microscope image demonstrating the abundance of Copine-6 spiny processes in the corpus callosum of the adult rat brain. 184

Figure 5-3 Copine-6 spiny interneurons labelled with HRP endproduct. 185

Figure 5-4 Three Copine-6 spiny interneurons in the corpus callosum. 187

Figure 5-5 Ultrastructural analysis of two Copine-6 spiny appendages............................ 188

Figure 5-6 A typical Copine-6 labelled vesicle-filled spine-like appendage. 189

Figure 5-7 Postsynaptic Copine-6 processes. 190

Figure 5-8 An example of putative Copine-6 presynaptic terminals................................ 191

Figure 5-9 Silver intensified gold nanoparticle labelling of Copine-6. 193

Figure 5-10 Copine-6 protein is localised to the inner face of the plasma membrane in neurons. 194

Figure 5-11 Copine-6 protein is localised to the ER and multivesicular bodies in neurons. 195

Figure 5-12 Preliminary evidence for pre- and post- synaptic Copine-6 labelling in CA3 pyramidal neurons in the hippocampus. 196

Chapter 1. **Introduction**

The plasma membrane of all eukaryotic cells consists of a dynamic protein-lipid interface, which acts to separate the intracellular cytoplasmic milieu from the extracellular environment. The plasma membrane is selectively permeable and regulates the transportation of substances both into and out of the cell, in order to maintain cell homeostasis. Multiple cellular mechanisms operate in order to achieve this, including endocytosis for the internalisation of different molecules, exocytosis for their removal, or trans-membrane transportation via selective transport molecules, or ion selective channels, for the active movement of molecules or ions across the plasma membrane. All intracellular components, including minerals and ions, are tightly regulated, therefore cells are required to rapidly detect and respond to changes in intra-, inter- and extracellular environments. Different cells have different requirements, and the homeostatic mechanisms that are essential for maintaining a steady intracellular state reflect this. For example, cells may use, release or be targeted by various different intercellular chemical messengers such as neurotransmitters, growth factors or hormones, which bind to specific receptors expressed on the plasma membrane. Receptor-messenger combinations vary between different cell types, and can therefore produce a variety of intracellular responses. These responses can be subsequently modulated by regulation of receptor number, or by modulation of the signal transduction pathways that are initiated upon receptor binding by the messenger molecule.

1.1. Cell Signalling

The concept of second messengers was first introduced in the 1950s by Sutherland and colleagues and they were envisaged as intracellular signalling factors with the ability able to mediate an intracellular response following extracellular receptor activation, thereby translating an extracellular message into an intracellular code. Cyclic AMP, or in full cyclic adenosine monophosphate (cAMP), was the first compound to be discovered with such signalling properties, since endogenous levels of cAMP were reported to increase intracellularly following the exogenous application of epinephrine (adrenaline) on heart, brain, liver and skeletal muscle (Rall *et al*, 1958). The role, function or origin of this timely increase in intracellular cAMP was not clear at the time of this discovery and publication, however Rodbell and colleagues later confirmed that cAMP concentrations can increase within the cell following extracellular activation of the relevant related receptor, and does so as part of a 'cascade' involving the activation of adenylyl cyclase, an enzyme that catalyses the production of cAMP from ATP (Rodbell, 1980). Since then, the classical idea follows that adenylyl cyclase activity is itself initiated by the binding of a G-protein subunit following receptor activation. This binds to guanine tri phosphate (GTP) in exchange for guanine di phosphate (GDP), undergoes a conformational change in structure, and dissociates from an 'inactive' G-protein complex, to generate separate alpha and beta-gamma subunit complexes each with individual activities and targets (for a review of the advances into various types of G-protein receptors, see (Pierce *et al.*, 2002) Thus following receptor activation and activation of G-proteins, different intracellular signalling pathways are initiated, which results in the timely recruitment of various different intracellular proteins, kinases, enzymes and second messengers. Indeed, G-protein coupled receptors are now recognised as one of the largest gene families, including receptors for a multitude of hormones, neurotransmitters and signalling molecules, and since different G-protein subunits and variations in receptor/G-protein coupling can exist between organisms and different cell types, an enormous diversity in intracellular signalling 'cascades' – involving the specific and controlled activation of different effector molecules within the cell –have been demonstrated. However, it must be noted that G-protein coupled receptors are one of many examples of signal transduction pathways. Various other extracellular or intracellular signalling receptors or molecules may contribute to the physiological state of a cell. Further examples of signalling pathways would include the activation of extracellular ligand-gated ion channels, activation of the integrins, or toll like receptors on the plasma membrane, each with specific conformational changes or binding of particular molecules depending on the cell in question.

Intracellularly, signalling pathways may originate from the activation of intracellular hormone receptors, or perhaps by activation of certain lipophilic second messenger signalling cascades. Furthermore, intracellular ions or free radicals, such as calcium and nitric oxide, respectively, may initiate certain signalling pathways following an increase in intracellular concentrations.

1.1.1. Calcium signalling

Ionised calcium (Ca^{++}) is of particular importance in the majority of intracellular signalling pathways, and was recognised as one of the major intracellular transduction elements in the early 1970s (Rasmussen, 1970). Calcium's pivotal role ranges from vacuole maintenance and cell division in Plantae, to cell contraction in musculature and neurotransmitter release in specialised neurons. Tightly controlled intracellular fluctuations in calcium concentration are responsible for the activation or regulation of various effector moieties, such as kinases and calcium binding proteins, and the specific alterations in calcium concentration may be local or global, varying significantly depending upon the initial trigger. For example, activation of a G-protein coupled receptor on the extracellular plasma membrane may activate a signalling cascade initiating the inositol (1,4,5)-triphosphate (IP3)-mediated pathway; via G-protein activation of phospholipase C which catalyses the breakdown of the substrate phosphatidylinositol (4, 5) bi-phosphate (PiP2) into the active compound IP3. This then binds to IP3 receptors which span the membrane of the endoplasmic reticulum. The activation of these receptors triggers a release of calcium from the intracellular stores, and may cause a global rise of intracellular calcium in the cytosol up to ~1µM. In excitable cells of the cardiac or central nervous system, a variety of signalling cascades such as those mentioned above exist, and these are complemented by the expression of voltage gated calcium channels along the plasma membrane of both the cell and the intracellular components. These voltage gated channels are sensitive to changes in charge across the membrane, and undergo rapid conformational changes following a change in the resting membrane potential. Rapid alterations in the membrane potential of excitable cells, such as in neurons, where cells depolarise from some ~-70mV to ~+40mV during the course of an action potential, will result in a time-limited opening of Ca^{++} selective ion channels owing to unique voltage sensing regions in their channel structure. The calcium signal therefore has the ability to target different signalling effector molecules depending on its size and the cell in question. In the neuron, for example, not only can large increases in calcium concentration occur such as during the initiation and potentiation of the full action potential, but also more localised and independent calcium influxes can occur, in compartments such the dendritic spines. Often these more localised events occur via release of calcium from intracellular stores, and it has been proposed that such events may also occur to shape or modulate larger changes in calcium concentrations (Garaschuk *et al.*, 1997), particularly since the increase in intracellular calcium is the classical trigger for vesicular and neurotransmitter release following action potential and depolarisation of the membrane(for a review see Berridge, 1998)

Since a large number of signalling cascades depend on tightly controlled alterations in calcium concentration, it is no wonder that homeostatic regulations are in place to control calcium concentrations in cells. Persistent elevations or aberrant fluctuations in calcium concentrations are deleterious and cytotoxic, and cause irreversible damage to the cell and its surrounding environment (Jewell *et al.*, 1982; Schanne *et al.*, 2013 For a review, see Harman *et al*, 1995) Normal cytosolic calcium concentration is usually ~100nM, some 20,000-fold lower than the typical 2mM concentration found extracellularly. To reduce intracellular calcium, the endoplasmic reticulum acts as a major sequestering organelle, and active calcium protein pumps present on the plasma membrane of both the cell and on the intracellular stores (endoplasmic reticulum and mitochondria) use ATP to continuously remove calcium from the cytoplasm. The plasma-membrane-Ca^{++}-ATPase (PMCA) extrudes calcium into the extracellular space, and the smooth-endoplasmic-reticulum-Ca^{++}-ATPase (SERCA) sequesters calcium into the ER, therefore ensuring that cytoplasmic calcium concentrations remain at a consistent homeostatic level in the absence of signalling.

In addition to these active pumping mechanisms that maintain homeostatic levels of calcium, a multitude of calcium binding proteins have been recognised to have an important role in both intracellular signalling and calcium homeostasis. In 1976, Kertsinger summarised some 70 proteins that exhibit calcium binding properties; of those, at that time, 2 had been identified in brain: S-100 and Calbindin (of which there were two isoforms, CaBP-I and CaBP-II) (Kretsinger, 1976) Since then, many proteins with calcium binding properties – in particular, the annexin protein family ; 'EF-hand' helix-loop-helix structural domain protein family; and proteins exhibiting the C2 structural domains – have been identified throughout different tissues, including brain. Each of these protein families are categorised structurally, based on the type of helices and the fold of their calcium binding site. Each family consists of several members, the majority of which exhibit sequence homology within highly conserved calcium binding domains, yet have a variety of properties depending on isoform and tissue distribution.

1.1.1.1. **The EF-hand Motif**

The calcium binding protein families exhibiting an 'EF hand' motif have the ability to bind calcium with high affinity, via hydrophobic regions within a C-terminus EF domain. (For a discussion see (Heizmann & Hunziker, 1991). The EF hand motif consists of two alpha helices separated by a calcium binding loop, itself comprising of aspartate and glutamate and glycine residues, the calcium binding is co-ordinated by an oxygen atom which is provided by the carboxyl and hydroxyl side chains and the carbonyl on the peptide back bone (Kretsinger, 1980). Some 200 proteins exhibiting variations of this EF hand motif have since been identified, most of which consist of more than a single EF motif; and the organisation of these domains gives rise to diverse target selectivity and function (Bhattacharya *et al*, 2004). The majority of EF hand proteins have been categorised into either '**effector** proteins' with a function other than the initial calcium binding, or as '**buffer** proteins' with the principle function, to chelate calcium.

<u>EF-hand effector proteins</u>: The classical example of a ubiquitous effector protein with calcium binding properties is Calmodulin (or CaM), which is a relatively small intracellular messenger, which serves as a calcium sensor with multiple downstream functions. It binds calcium at each of its four EF hand motifs, which have high affinity for calcium, the binding of calcium results in a conformational change in protein structure. Hydrophobic residues are exposed, which are then able to bind to the target protein(s), thus promoting various different function(s) depending on the interaction in question. In turn, this facilitates the transduction and amplification of the initial calcium signal, by activation and modification of different downstream interactors. Various effector proteins and enzymes may be targeted by calmodulin, such as CaM kinase-II (CaMKII), which is specifically regulated by the calcium/calmodulin complex. The CaM kinase family themselves are also implicated in many signalling and physiological processes, their main function being to phosphorylate and thus modify a variety of molecules even further downstream in the biochemical cascade. Each of the multiple isoforms of CaMKII consist of an N-terminal catalytic domain, a C-terminal association domain, and a centre auto-regulatory domain, with 80-90% conserved identity across the domains (Tobimatsu *et al*, 1989) . The CaMKII isoforms differ in physiological role and target proteins, depending on tissue expression and the biochemical cascade in which they are associated. For example, in the brain, CaMKII is a very important protein having been implicated in several different intracellular signalling cascades, protein interactions and modifications. These includes roles in presynaptic vesicular docking, where CamKII is reported to phosphorylate the vesicular protein synapsin I thus facilitating vesicle and neurotransmitter release (Greengard *et al.*, 1993), and the kinase has been suggested to have roles in long term potentiation, the strengthening of a synaptic communication, possibly during NMDA receptor mediated induction of LTP (Malinow *et al.*, 1989). Furthermore, in mice mutated in the alpha-isoform of CaMKII, deficiencies in hippocampal long term potentiation (Silva, *et al.*, 1992) and impaired spatial learning (Silva, *et al.*, 1992) are documented, further implicating CaM Kinase in processes underlying synaptic plasticity.

Calcium is a precursor for the downstream activation of CaM Kinase, and the activity dependent changes in intracellular calcium have been found to directly affect the type of potentiation that may occur at any given synapse, whether it be an enhancement or a depression (Lisman, 1989) . The spatial and temporal recruitment of the many different signalling molecules, including calcium, are therefore paramount for specific physiological changes to occur.

EF-hand buffer proteins: These are present intracellularly and have the ability to chelate calcium. Such buffer proteins with the EF-hand motif are abundant in most cells and act primarily to balance leaky calcium currents or to eliminate increased calcium concentrations following signalling. These proteins contribute towards the maintenance of calcium homeostasis, , and cells expressing functional buffer proteins may be particularly well protected against pathological conditions resulting from aberrant calcium signalling (Heizmann, 1993). Buffer proteins do not necessarily have assigned functions other than to control the intracellular concentrations of calcium by chelation (for a review of calcium signalling, see Clapham, 1995), and they are mainly located within the cytoplasm and on the plasma membranes of calcium sequestering organelles such as the endoplasmic reticulum and mitochondria.

In cardiac and skeletal muscle, the major calcium buffer, calsequestrin –which actually lacks any EF-hand motifs, instead binding calcium by exposure of charged residues – is a specific endoplasmic reticulum calcium buffer present in the cisternae of the ER, which reduces cytosolic calcium concentrations by sequestering calcium ions within the organelle (for a more detailed account see (Scott *et al.*, 1988). In the central and peripheral nervous system, however, the majority of calcium buffer proteins exhibit the EF hand motif and therefore chelate calcium with high affinity. A variety of these buffer proteins, for example parvalbumin, calbindin, and calretinin, can be found in different neuronal populations for which they provide useful molecular markers.

Parvalbumin was the first EF hand calcium binding protein to be described following its isolation in skeletal muscle of frog and carp. The ‘EF hand motif’ takes its name following the initial discovery of parvalbumin, owing to the orientation of the helices (with the E and F helices forming a structure similar to a "pointing hand") (Kretsinger *et al*, 1973) . Parvalbumin exhibits 3 of these EF hand motifs, and although it was originally isolated in skeletal muscle, it can also be found in other tissue regions such as smooth muscle, glands, and the peripheral and central nervous system (Heizmann, 1984). The expression of parvalbumin in the brain is restricted to distinct neuronal subpopulations, such as interneurons of the cerebral cortex and periglomerular cells of the olfactory bulb (Celio *et al*, 1981; Heizmann, 1984). It is well documented that parvalbumin is specific to GABAergic neurons in the brain and may therefore have important properties for the specific signalling or active metabolism of these cells (Celio, 1986). Indeed, parvalbumin knockout mice (PV-/-) exhibit a decreased rate of calcium transients decay following stimulus of fast contracting muscle fibres (Schwaller *et al.*, 1999), and paired-pulse modulation is disrupted in cerebellar stellate or basket/Purkinje cell synapses of PV-/- mice (Schwaller *et al.*, 2002).

Calbindin, so named for its calcium binding ability, belongs to the EF hand protein family, having six EF hand motifs. Following its discovery, calbindin was documented to be rich in brain, particularly in the cerebellum (Taylor, 1974). Since then, calbindin expression has been documented in specific subpopulations of the brain including the cortex, hippocampus, and olfactory bulb (Baimbridge *et al*, 1982), and the restricted expression pattern may reflect a unique function in addition to the calcium buffering capabilities, that may shape neuronal excitability in specific cell types (for a review of the functions of calbindin, see Schmidt, 2012) Calbindin shares 58% homology with **Calretinin,** another six EF-hand protein with calcium binding properties initially identified in the chick retina (Rogers, 1987), the expression of which is also restricted to specific neuronal subpopulations of the brain such as some cells of the hippocampus, cerebral cortex, caudate putamen, and olfactory bulb (Jacobowitz & Winsky, 1991). Despite sequence homology between calretinin and calbindin, they are expressed independently in different neuronal subpopulations, which suggests that they may have individual functions or effects perhaps in their buffering capabilities of calcium and how this regulates neuronal excitability (Rogers, 1987; Camp *et al*, 2009).

Owing to the unique distribution and expression patterns of the various different calcium buffer proteins such as those EF hand proteins named above, they are used increasingly as neuroanatomical markers for neuronal subpopulations. There is much heterogeneity in calcium-binding protein expression between different neuronal populations, and it seems likely that the differences in protein expression are implicated in specific roles that are yet to be defined (Baimbridge *et al.*, 1992).

1.1.1.2. **The Annexins**

The annexins consist of a conserved core domain at the C-terminus, and an N-terminus domain that varies in sequence between family members. The core domain of the annexins consists of five alpha helices, four of which form a looped ‘coiled coil’ structure, each loop harbouring the calcium binding site of carbonyl- and carboxyl- oxygen and water molecules. Annexins are identified by the presence of an ‘annexin repeat’ within the core domain. Each family member differs in loop site location, identifiable by the type of coiled coil in each individual isoform (Rosengarth & Luecke, 2004), and variations in both the core domain and the N-terminal sequence have been speculated to give rise to the diverse functions observed between family members (Rosengarth & Luecke, 2004). The annexins chelate calcium with relatively low affinity when compared to other calcium binding proteins, such as those containing the EF hand motif, perhaps owing to the co-binding of water molecules at each of the calcium binding sites (Raynal & Pollard, 1994). In the presence of calcium, annexins bind to negatively charged phospholipids on the inner side of the plasma membrane via the conserved core domain, which takes the shape of a convex disc. Calcium binding co-ordinates this phospholipid and protein interaction. The N-terminus of the annexin structure is unusual, since it is documented not only to bind target ligands, but it has been shown to interact with other calcium binding protein families, particularly those exhibiting the EF hand motif, which also have the ability to bind the plasma membrane such as S100 (Seemann *et al.*, 1996). Indeed, it has been postulated that the binding of other calcium binding proteins such as S100 allow a double membrane binding domain, such that two annexin monomers may be ‘bridged’ by an EF-hand calcium binding protein – the function of this complex is yet to be elucidated, but may facilitate or inhibit either the activity of the proteins within the complex, or the function of other downstream interactions (Gerke *et al.*, 2005). The annexin family consists of various different isoforms, each implicated in different intracellular processes, such as endocytosis, exocytosis, membrane trafficking (for reviews see (Raynal & Pollard, 1994; Gerke *et al.*, 2005). The presence of the highly conserved amino acid sequence that categorises the members of the annexin family suggests these proteins have an important role in the intracellular mechanisms of most cells.

1.1.1.3. **The C2 domain**

The C2 domain is a calcium and phospholipid binding motif initially identified as the calcium regulated component of protein kinase C, which has one C2 domain (Inoue *et al.*, 1977; Coussens *et al.*, 1986; Parker *et al.*, 1986). Later identified as a regulatory domain shared by several intracellular proteins with possible implications in membrane binding (Perin *et al.*, 1990), the C2 domain was so named to account for its “bipartite” calcium-binding ability (Shao *et al.*, 1996). The domain is also described as ‘calcium dependent phospholipid binding’ owing to its ability to translocate to the membrane in the presence of Ca^{++} – first demonstrated in the double C2 domains of synaptotagmin (Davletov & Sudhof, 1993), each C2 domain – C2A and C2B –having calcium-dependent AND calcium independent interactions (Shao *et al.*, 1996; Südhof & Rizo, 1996) possibly giving rise to multiple intracellular functions.

The C2 domain structure consists of two, four-stranded anti-parallel β sheets, which form a β sandwich, in either a type I or type II topology (Nalefski & Falke, 1996), connected by three protein loops at the top of the domain, and four protein loops at the bottom. The chelation of calcium ions occurs exclusively in the top three protein loops, the calcium binding sites formed by aspartate and serine side chains and carbonyl groups. The protein loops differ in structural identity between family members, yet a high degree of identity exists in the core β sandwich which may suggest that this represents a protein scaffold sequence (Rizo & Sudhof, 1998).

The C2 domains vary in their phospholipid binding properties, in part due to the number of C2 domains present, and the number of calcium ions bound. The bound calcium ions are postulated to have ‘unsatisfied’ co-ordination sites, which, upon phospholipid binding of the C2 domain, can be filled by the phospholipids, which in turn increase the C2 domain affinity for calcium through co-operative binding (Rizo & Sudhof, 1998). Furthermore, C2 domains have been found to bind to other target proteins alongside the phospholipid, for example various isoforms of the two C2-domain protein synaptotagmin were demonstrated to bind syntaxin, a ‘SNARE’ protein (**s**oluble N-ethylmaleimide sensitive factor **a**ttachment protein **re**ceptor) associated with synaptic vesicular exocytosis (Li *et al.*, 1995; Rizo *et al*, 2008). C2 domains may therefore be implicated in processes such as secretory vesicle exocytosis and membrane fusion (for reviews see Nalefski *et al*, 1996; Duncan *et al.*, 2000; Friedrich *et al.*, 2010) , or fast neurotransmission by synchronised release of vesicles following increased intracellular calcium, as was found with synaptotagmin (Südhof *et al*, 1996; Rizo *et al*, 1998; Martens *et al.*, 2007; Rizo *et al*, 2008).

Several families of calcium binding proteins have been implicated in the secretion of neurotransmitters and membrane trafficking in the brain, and many of these have been characterised by the presence of two C2 domains at the carboxyl terminus. The **DOC2** proteins form a family of double C2 domain proteins discovered following a DNA screen of a human brain cDNA library using a C2 domain probe (Orita *et al.*, 1995), the family comprising of three isoforms, DOC2A, DOC2B and DOC2C. Each member consists of two conserved C2 domains (C2A and C2B) at the carboxyl terminus similar to those exhibited by synaptotagmin, and an amino terminus domain known as ‘Mid’, so named from **M**unc-**i**nteracting-**d**omain, which is unique to DOC2 proteins and is highly conserved between rat and human isoforms (Verhage *et al.*, 1997). The amino terminal sequence is followed by a variable spacer sequence with low levels of homology, and the two C2 domains – C2A and C2B – at the carboxyl terminus are separated by a variable inter-domain linker (Friedrich *et al.*, 2010).

All DOC2 family members are expressed in the brain; DOC2A is exclusively expressed in the central nervous system and isoforms DOC2B and DOC2C are ubiquitous (Verhage *et al.*, 1997). In the presence of calcium, DOC2A and DOCB have been found to reversibly translocate to the plasma membrane in neurons, which the authors suggest may be in response to, and possibly also modulating, synaptic transmission (Groffen *et al.*, 2006). Similarly, the C2A domain of the DOC2B protein has been demonstrated to bind the plasma membrane phospholipids phosphatidylcholine and phosphotidylserine in a calcium depended manner (Kojima *et al.*, 1996); and the C2B domain has been demonstrated to bind to other synaptic proteins such as the SNARE protein heterodimer syntaxin/SNAP-25 (Friedrich *et al.*, 2008) and the synaptic proteins Munc13 and Munc18, which are essential components of the synaptic vesicle fusion complex (Brose *et al.*, 1995; Verhage *et al.*, 1997; Groffen *et al.*, 2006; Friedrich *et al.*, 2010). These binding properties and membrane-linked interactions all point to the putative role of DOC proteins with C2-domains in membrane trafficking, vesicular transport, and regulation of secretion (Duncan *et al.*, 1999, 2000). Indeed it has recently been confirmed that DOC2 has the ability to mediate membrane fusion via synaptic SNARE proteins, in a calcium dependent manner implicated with asynchronous vesicular release (Yao *et al.*, 2011). Interestingly, in situ hybridisation and protein immuno-blotting illustrates that regions of the adult brain with high levels of DOC2A expression, such as the cortex and brain stem, show low levels of DOC2B; whereas regions of high DOC2B expression, such as the caudate putamen and cerebellum, show low levels of DOC2A (Verhage *et al.*, 1997). This expression of DOC2A and DOC2B has been described as “non-uniform and complementary”, initially suggesting that each isoform has a similar function in different subsets of neurons. Furthermore, in situ hybridisation demonstrates that the developmental expression of the DOC2A and DOC2B isoforms have temporal and spatial differences (Korteweg *et al.*, 2000) –

indicating a functional divergence –since DOC2B expression appears at embryonic stages of development whereas DOC2A did not, and during postnatal stages of brain development both isoforms were co-expressed prior to the adult brain. This alteration in expression suggests a different function for each isoform, perhaps during synaptogenesis or neuronal maturation.

1.1.2. The Copines are a novel double C2-domain calcium binding protein family

Recently, a novel family of double C2-domain calcium binding proteins named **Copine** were identified. The Copines are a nine member family of intracellular calcium binding proteins, first discovered following the isolation of phospholipid binding proteins in extracts of *Paramecium Tetraurelia* when investigating membrane trafficking processes in ciliates (Creutz *et al.*, 1998). The proteins present on immuno-blot with a single 55-kDa band, and were coined 'Copine' owing to their 'companionship' with lipid membranes.

1.1.3. Structure, sequence homology and function of the Copine family of proteins

<u>Structure:</u>

The Copine proteins are a two C2-domain protein family, with all nine members being structurally defined by the unique positioning of the conserved double C2-domain at the amino (N-) terminus, and a conserved protein binding "A-domain", structurally comparable to the von Willebrand factor A (vWA)-like-domain, at the carboxy (C-) terminus. The Copines are structurally different to the majority of other double C2 domains such as synaptotagmin and DOC2, since their C2 domains are located at the carboxyl terminal (see Figure 1-1.)

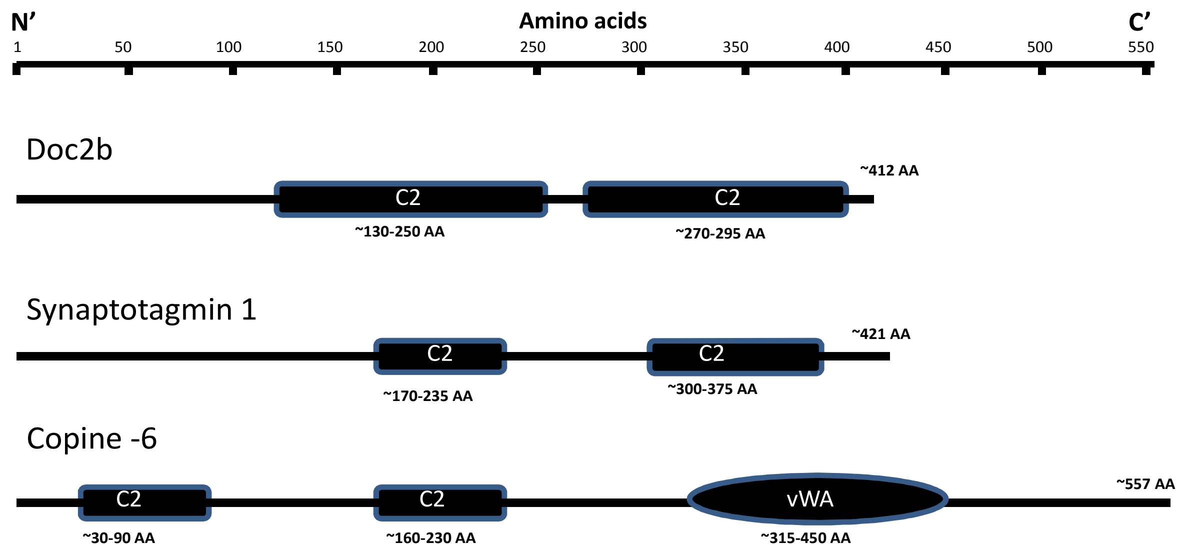

Figure 1-1 Schematic representation of rat proteins DOC2b, synaptotagmin 1, and Copine-6.

The C2 domains of the Copines are located at the amino terminus (N'), whereas in DOC2 and synaptogmin the C2 domains are at the carboxy (C') terminus. In addition, the Copine proteins also contain a vWA-like domain at the carboxy terminus. Protein accession numbers AAB47747.2, NP_001028852.2 and NP_001178042.1 for Doc2b, Synaptotagmin 1 and Copine-6, respectively, were obtained from Genbank, and were analysed by NCBI BLAST to show the conserved domains.

The von Willibrand A (vWA) portion of the Copine protein has a distant structural similarity to extracellular membrane proteins such as the integrins. Such proteins are known to be able to bind to other proteins when in the presence of magnesium, manganese or calcium via a 'metal-ion-dependent-adhesion site' (MIDAS), which is suggested to have a direct role in the control of protein ligand binding (Michishita *et al.*, 1993; Lee *et al.*, 1995) The vWA-like domain sequence exhibited by the Copines is predicted to bind divalent cations based on the presence of the critical residues required for such cationic binding (Creutz *et al.*, 1998). Indeed, it has been shown that native Copine has the ability to bind radioactive manganese, $^{54}Mn^{++}$, which can be outcompeted by Mn^{++} or Mg^{++}, and partially by Ca^{++}, suggesting the domain has greater selectivity for these divalent cations over calcium (Tomsig *et al*, 2000). The Copines consist of two putative divalent binding domains – the vWA-domain and the C2 domains – yet the properties of each can be distinguished since the C2 domain has greater affinity for Ca^{++} over Mg^{++}, Sr^{++} and Ba^{++} (Tomsig *et al*, 2000). Furthermore, in contrast to typical vWA-domains such as those exhibited by the majority of integrins, the Copines contain a conserved histidine within a 'sequence block' that is not found in any other A-domain to date (Creutz *et al.*, 1998), suggesting that the Copines may have additional, or modified function(s).

<u>Sequence homology:</u>

The Copine protein peptide sequence is conserved from plantae through to humans, with the highest degree of conservation in the C2-domains and the vWA domain.

Sequence alignment of the human Copine I peptide sequence with the Copine sequence from *Paramecium Tetraurelia* (ciliate), Caenorhabditis elegans (nematode), and Arabidopsis (green plant) give a degree of identity of 33%, 40%, and 40% respectively. (Creutz *et al.*, 1998) Furthermore, five human Copine genes were initially identified owing to similarities in cDNA sequence, and were referred to as human Copines I-V. Full length sequence alignment of human Copine I with the human Copines II, III, IV and V revealed a 60%, 78%, 53% and 56% degree of identity, respectively (see Figure 1-1) (Creutz *et al.*, 1998). This was later confirmed by sequence alignment of human Copine I with human Copine III, both extracted from the cytosol of neutrophils, which also revealed a 79% identical amino acid sequence (Cowland *et al.*, 2003). Following the discovery of an additional member of the Copine family, Copine -VI, or 'N-Copine', this was found to show a 49% identity with human Copine I (Nakayama *et al.*, 1998) More recently, Copine VII was discovered when scanning for candidate tumour suppressor genes associated with breast cancer, and shown to share 57%, 47% and 44% identity with Copine -VI, Copine III and Copine I, respectively (Savino *et al.*, 1999), while Copine VIII was discovered as a gene predominantly expressed in prostate and testis, and was found to be most homologous to Copine -VI (Maitra *et al.*, 2003). Six Copine genes, cpnA-cpnF, were later discovered in the eukaryotic single cell amoeba, *Dictyostelium* discoideum following cDNA sequencing, all with some homology to human Copine I (Damer *et al.*, 2005). Phylogenetic analysis using the nucleotide sequences of the nine rat Copines shows that every Copine member has a common ancestor, and small degrees of structural change have occurred during evolution (see Figure 1-2.)

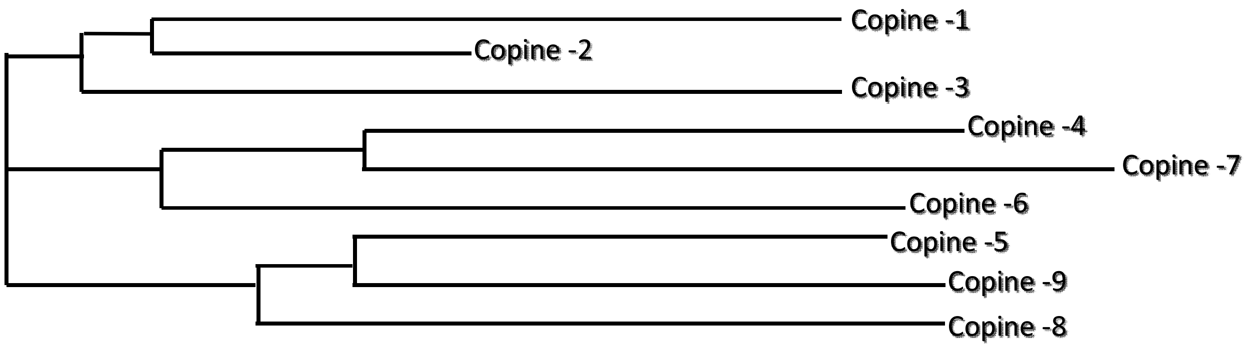

Figure 1-2 A phylogenetic tree of rat Copines -1 to -9.

Each Copine nucleotide sequence was subjected to multiple sequence aligment by CLustal W2 analysis, using EMBL-EBI tools. The phylogenetic tree illustrates the common relationships between certain Copine members, and the evolutionary change over time. The longer branches indicate a greater degree of structural change when compared to the common ancestor. Nucleotide sequences for the rat Copines were generated using Genbank, accession numbers NM_001256465.1, XM_001062196.2, NM_001107917.2, NM_001109003.1, NM_001107616.1, NM_001191113.1, NM_001108454.1, AM747284.1, NM_001024982.1.

Function:

The function of any of the Copines is unknown. However, the presence of an N-terminal double C2-domain in the Copines suggests a conserved function, which might be inferred from the functions of these domains in other proteins. However, whilst synaptotagmin and DOC2 proteins have both been implicated in processes of membrane trafficking and exocytosis including synchronised, and unsynchronised vesicular release, respectively (Geppert *et al*, 1998; Yao *et al.*, 2011), these are proteins which have C-terminal C2 domains. The C2 domain architecture of the Copines is more similar to the structure of protein kinase C, which has a single C2 domain at the amino terminus. Since this, and other double C2-domain containing proteins show calcium dependent binding to phospholipids with lipid selectivity (Rizo *et al*, 1998), the Copines might be expected to also do so.

The C2 domains of the Copines were predicted to bind calcium, based on the homology of these domains with other C2 domains, and the presence of the appropriate acidic residues in the same relative positions in the C2 domain sequences of human Copine I, and in the

Copine of Caenorhabditis elegans (a nematode) and *Paramecium Tetraurelia* (a ciliate) (Creutz *et al.*, 1998; Tomsig *et al*, 2000) . A putative non-calcium binding Copine was predicted to be present in Arabidopsis thaliana (plant) owing to the unusual start position of the protein sequence, part way through the first C2 domain (Creutz *et al.*, 1998). Indeed, until recently, the only evidence that the Copine proteins have the ability to bind phospholipids in a calcium dependent manner came from *in vitro* studies using lipid vesicles (Creutz *et al.*, 1998; Nakayama, Yaoi, & Kuwajima, 1999; Tomsig & Creutz, 2000a; Damer *et al.*, 2005). More recently, the translocation of the Copines to the plasma membrane in the presence of an increase in intracellular calcium has been shown *in vivo* in human embryonic kidney cells (HEK-293) (Perestenko *et al.*, 2010). The study also showed that Copine translocation in HEK-293 cells required calcium from both extracellular and intracellular stores, and that the sensitivity to calcium flux and the rate of translocation of each Copine family member differed in response to these changes in intracellular calcium (Perestenko *et al.*, 2010) This variation in intracellular response may indicate a variety of roles for each Copine family member. Interestingly, the DOC2 protein family members also differ in the speed of their response to increases in intracellular calcium, and this is postulated to work in a concerted manner for modulation of synaptic transmission (Groffen *et al.*, 2006) However, unique to the Copines, the calcium-dependent phospholipid binding of the C2 domain appears to be dependent on a conserved 22-amino acid 'linker' sequence immediately following on from the second C2 domain. In its absence, the C2 domains alone fail to associate with the plasma membrane following an influx of calcium suggesting that the linker sequence is critical for their membrane association *in vivo* (Perestenko *et al.*, 2010). This demonstrates that the C2 domains of the Copines appear to behave in a manner distinct from those of other C2 domain protein families. Furthermore, **t**he vWA-like domain at the carboxyl terminus, in addition to the double C2 domain, is unique to the Copines protein family. Interestingly, the vWA-like domain has been demonstrated to modulate the responsiveness of the Copine C2 domains to an increase in intracellular calcium. Indeed, domain swap experiments provide evidence to suggest that the vWA domain may contribute to the Copine ability to target different intracellular compartments (Perestenko *et al.*, 2010).

There are growing lines of genetic evidence to suggest that the Copines have important conserved intracellular roles. In the plant *Arabidopsis thaliana*, a mutation in the Copine gene BON1 results in a dwarf phenotype (Hua *et al.*, 2001); indeed, a mutation in the Arabidopsis gene CPN-1 was found to be responsible for morphological abnormality and aberrant regulation of cell death in the presence of pathogens (Jambunathan *et al.*, 2001). Together, this suggests that the BON-1/CPN-1 genes are associated with growth and disease resistance in plants, in stark contrast to the initially predicted un-functional Copine in Arabidopsis, based on sequencing (Creutz *et al.*, 1998). BON-1 is itself highly regulated, since the binding partner, BAP-1, is documented to be required for BON-1 function, and myristylation of the BON-1 gene is required for plasma membrane localisation (Li *et al.*, 2010).

In *Dictyostelium*, GFP-tagged CpnA is capable of localising with the plasma membrane, contractile vacuoles, and organelles of the endo-lysosomal pathway, possibly implicating the Copine in processes such as cell trafficking or membrane docking in a calcium dependent manner (Damer *et al.*, 2005). Furthermore, *Dictyostelium* CpnA mutations cause severe alterations in development particularly during the differentiation stages of cell development (Damer *et al.*, 2010), which associates the Copines in growth related processes, similar to those morphological abnormalities exhibited by Copine mutants in Arabidopsis.

In *C. Elegans*, the Copines have been associated with various receptor functions. The gene gem-4, which encodes a member of the Copine family of proteins, was identified as a putative regulator of the gonad division regulatory gene gon-2, a member of the TRPM (transient receptor potential ‘melastatin’) family. Although unable to suppress the effects on gonad division following a complete inactivation of gon-2, gem-4 was able suppress the adverse effects following a *reduction* in gon-2 activity(Church *et al*, 2003). The authors therefore suggest that the Copine gem-4 may be a physiological antagonist of gon-2, either directly or in parallel. In a proteomic study of proteins associated with the levamisole receptor, which is associated with the neuromuscular junction in *C.elegans*, a copine, NRA-1 (‘nicotinic receptor associated’) was co-purified with the receptor (Gottschalk *et al.*, 2005). Furthermore, in *C.elegans* expressing mutated NRA-1, the levamisole receptor had a reduced synaptic expression, and NRA-1:GFP constructs expressed in *C. elegans* were found to co-localise with the levamisole receptor at both neuronal and muscle plasma membranes. The authors suggested that NRA-1 might have a role in trafficking, or recruitment, of levamisole receptors at the plasma membrane (Gottschalk *et al.*, 2005). However the molecular mechanism underpinning the apparent trafficking of the levamisole receptor by the Copine is unclear.

Given the homology of the vWA-domain in the Copines with integrins, which can bind protein ligands, this domain in Copines has been suggested to act as an interaction domain for other proteins. Since the domain is coupled with the phospholipid binding C2-domains, it has been suggested that the Copines might act as trafficking proteins, carrying other proteins to the inner surface of the plasma membrane following increases in intracellular calcium (Tomsig *et al*, 2000) However, little firm evidence for the direct interaction of Copines with other proteins has so far been produced. Yeast Two-Hybrid screening of the Copines I, II and IV, using the vWA-domain as bait for a mouse embryo cDNA library identified several potential interactors, including protein phosphatase 5, NEDD8-conjugating enzyme UBC12 (involved in the regulation of the transcription factor ‘nuclear factor kB'), the single stranded RNA-binding octamer binding protein, and a variety of other proteins associated with intracellular signalling and the regulation of transcription and ubiquitination (Tomsig *et al.*, 2003). In the majority of cases these interactions varied between Copine family members and some were also confirmed by *in vitro* pull down assay. In addition, Copine I was also found to be the target of Copine IV, suggesting potential Copine-Copine oligomer interactions. In addition, full length Copine I was found to be able to recruit GST-fusion proteins of the identified target proteins and full length protein phosphatase 5 to immobilised phosphatidylserine in a calcium dependent manner, suggesting that the Copines might be able to recruit their binding partners to the plasma membrane following an influx of intracellular calcium.

Other interaction studies have suggested that Copine VI may interact with the osteosarcoma gene protein OS9, but here too there was no physiological role attributed to the interaction, which was with the C2B-domain rather than the vWA-domain (Nakayama *et al.*, 1999). mRNA transcripts of Copine III are described to be altered in post-mortem brain tissue analysis by microarray in patients with schizophrenia, implicating Copine III as a novel candidate gene in this disorder (Cohen *et al.*, 2012). In neuronal tissue, a potential, albeit weak, interaction between Copine VI and a novel neuronal calcium binding protein called NECAB-1 was established by Coomassie staining of an SDS gel, loaded with protein eluted from a column of immobilised NECAB and the sequential sequencing of the protein fragments. However, this interaction was rendered unlikely as the two proteins did not co-localise in the hippocampus, and it was suggested that the interaction was not real but due to NECAB and Copines being 'sticky' proteins (Sugita *et al.*, 2002). The physiological relevance of the majority of these interactions remains elusive. It should be noticed that the vWA-domain of Copine III has a sequence that is similar to other nucleotide binding pockets in kinases, and there is some evidence that Copine III has the ability to phosphorylate the exogenous substrate myelin basic protein in gel kinase assays, and following recombinant expression and purification of the human Copine III in yeast (Caudell *et al.*, 2000).

One of the Copine I interacting proteins identified by Tomsig and colleagues (Tomsig *et al*, 2000) was UC12, an enzyme regulator of nuclear factor- kB (NF-kB), and the role of Copine I in NF-kB has been examined further. The authors showed that expression of Copine I can also be enhanced by treating cells with tumor necrosis factor (TNFα), and that the responsiveness of the TNFα signalling pathway to muscarinic stimulation increased in parallel with the increased Copine I expression. These effects could be blocked by a dominant negative form of Copine I and this also inhibited the TNFα dependent degradation of IkB, a regulator of NF-kB (Tomsig *et al.*, 2004). The authors argued therefore that Copines may enhance NF-kB signalling by promoting IkB degradation via an activator effect on UBC12. However, in a follow up paper the same group showed that knockdown of Copine I by siRNA increases tumor necrosis factor and stimulated NF-kB transcription, whereas Copine I expression blocks endogenous transcription. They showed that p65, a member of the NF-kB family, binds directly to Copine I, and stimulates endoproteolysis of p65 within a conserved region that is required for base-specific contact with DNA. p65 proteins lacking the N- terminus fail to bind to DNA and act as dominant-negative molecules that inhibit NF-kB transcription. Thus Copine I appears to act as a novel repressor that physiologically interacts with p65 to inhibit NF-kB transcription. However, Copine I does not have any endogenous proteolytic activity and appears to act as an adapter molecular for an, as yet unidentified, enzyme (Ramsey *et al.*, 2008). The difference in their interpretation of the role of Copine I in NF-kB regulation between the two papers was suggested to be because in the first they used GFP-tagged Copine I, which could not enter the nucleus. It is interesting to note that in this study a myristoylated form of Copine I, which was constitutively membrane bound, showed a reduced ability to cause the cleavage of p65, and that the authors described the C2-domain mediated dimerization of Copine I.

In plants an interaction between the BAP-1 protein and the Arabidopsis Copine BON-1 vWA-domain was found using yeast two hybrid screening. Loss of BON1 function, caused by knockout of the gene, leads to miniature plants at ambient temperature due to a reduction in both cell expansion and division but has no obvious phenotype at high temperature. This dwarf phenotype can be reversed by overexpression of BAP-1, and this together with the finding that both BON1 and BAP1 expression are under temperature control, with both having elevated expression when plants were shifted from high to low temperature, has led to the suggestion that BON1 and BAP1 may have a direct role in regulating cell expansion and cell division at lower temperatures (Hua *et al.*, 2001). There is considerable genetic evidence that the Copine genes in plants such as Arabidopsis not only have roles in maintaining cell growth, they may also regulate plant disease resistance

(Hua *et al.*, 2001; Yang *el al*, 2004; Lee *et al*, 2009) but the molecular mechanisms by which they exert their functions has not been fully described. Recently, however, a yeast two hybrid study with the vWA-domain of BON1 identified two leucine rich repeat receptor-like kinases (LRRRKS), BIR1 and BAK1 as interacting partner for this Copine. Additionally BON1 and BIR1 could be phosphorylated by BAK1 *in vitro*, and bimolecular fluorescence complementation analysis showed that BON1 and BAK1 could be found at the membrane in Arabidopsis protoplasts. Null mutants of BON1 and BIR1 have phenotypes that are partially supressed by overexpression of BIR1 and BON1 respectively. Furthermore, the BIR1 phenotype is attenuated by a loss-of-function mutation in the Resistance (R) gene SNC1 (suppressor of npr1-1 constitutive -1) which mediates defence responses. Together, these results lead the authors to suggest a working model in which BON1 and two receptor like kinases, BIR1 and BAK1, mutually modulate one another's activity to negatively regulate multiple resistance genes (Wang *et al.*, 2011).

In mammalian cells, Copine III has also been identified to be an important component of ErbB2-mediated cell migration and signalling, following proteomic analysis of proteins associated with the ErbB2 receptors (Heinrich *et al.*, 2010). The binding of Copine III to the ErbB2 receptor requires it to be activated and depends on calcium release from internal stores. In addition to binding to the ErbB2 receptor, Copine III binds to Shc and RACK1, and appears to form a complex of these proteins at the cell membrane. Knockdown of Copine III results in a loss of ErbB2-dependent cell migration, and this together with the localisation of Copine III with phosphorylated focal adhesion kinase at the leading edge of migrating cells, suggest that it plays a significant role in cell motility. Since high ErbB2 levels correlate with aggressive forms of breast cancer, and there is a correlation of Copine III mRNA levels ad Erb2 gene amplification, Copine III is suggested to be an interesting therapeutic target for ErbB2 mediated cancers (Heinrich *et al.*, 2010).

Whilst a few protein partners of the Copines have been identified in plants and animals, with the possible exception of the interaction of ErbB2 with Copine III, there have been no direct demonstrations of Copines targeting proteins to the plasma membrane in response to rises in intracellular calcium. The main data to date suggests that Copines act as molecular adapters, which may function in the cytoplasm or the nucleus of cells, with the intriguing idea that whist the C2 domains may be able to bind to membranes in response to increased intracellular calcium, they may also function to dimerise the Copines (Ramsey *et al.*, 2008; Perestenko *et al.*, 2010)

1.1.4. Anatomical distribution of each Copine family member in mammals

The Copine proteins are expressed in many mammalian tissues, with some Copine family members having a more restricted tissue expression than others.

Western blot analysis of rat and bovine homogenates of various organs, probed with an antibody targeting the vWA domain of human Copine I detected Copine I expression in most tissue samples, including brain, heart, lung, liver and skeletal muscle, with higher levels of expression in rat spleen, large intestine and kidney. (Tomsig *et al*, 2000) This suggests that Copine I has a wide expression pattern in a variety of tissues

Copines I and III were isolated from human neutrophils using calcium affinity-chromatography, which provided the first example of two different Copine family members being co-expressed in the same cell type (Cowland *et al.*, 2003). Multiple Tissue expression (MTE) arrays containing a range of human mRNAs were probed, using the 3'-translated regions of different Copine transcripts as the probes. This method identified the following: high levels of Copine II expression in testis, lung and brain; Copine III expression in heart, kidney and lymph nodes; Copine IV expression in brain, heart and prostate; Copine V in brain and heart, Copine IV in brain only, and Copine VII in brain and stomach (Cowland *et al.*, 2003). Interestingly, all of the Copines were expressed in brain, but their expression levels differed dramatically in non-neuronal tissues.

Copine VI has been termed a “brain-specific” protein, also referred to as N-Copine (Nakayama *et al.*, 1998) owing to is its exclusive expression in the brain of mammals (Nakayama, Yaoi, & Kuwajima, 1999; Tomsig & Creutz, 2000a; Cowland *et al.*, 2003;

Bagley *et al.*, 2007) , with very small levels of expression in kidney and fetal heart (Cowland *et al.*, 2003).

This thesis focuses on the expression and distribution of Copine VI (here referred to as Copine-6) in the rodent brain.

1.2. Copine-VI (Copine-6)

The expression of Copine-6 in the brain has not been well characterised. Copine-6 cDNA was initially isolated from mouse hippocampal neurons and was designated N-Copine, or ‘neuronal’ Copine, since it was found in neurons, and not glia, of the hippocampus (Nakayama *et al*., 1998). Copine-6 mRNA was found to increase in the hippocampus following kainite injection into the hippocampus of mice, an increase that was dependent on the activation of N-methyl D-aspartate (NMDA) receptors (Nakayama *et al.*, 1998). Similarly the authors found that tetanic stimulation in acute hippocampal slices caused a rise in Copine-6 mRNA in the CA1 region. Northern blot analysis of Copine-6 mRNA in selected tissues of mouse and human (heart, brain, placenta, lung, liver, muscle, kidney and pancreas) suggested that Copine-6 was brain specific (Nakayama *et al*., 1998), a finding subsequently supported by other studies (Cowland *et al.*, 2003). Western blot analysis identified N-Copine in brain homogenates as a 62kDa protein ((Nakayama *et al.*, 1998).

Proteins containing the double C2 domain structure positioned at the carboxyl- terminus tend to be pre-synaptically located and several have been implicated in synaptic vesicle transportation and exocytosis, synaptotagmin being an example (Geppert & Südhof, 1998). In contrast, the double C2 domain of Copine-6 is positioned at the amino- terminus, which could suggest a different, or additional function of Copine-6. Consistent with this idea is the finding that in the hippocampus, Copine-6 has a very different regional distribution to typical synaptic vesicle-associated proteins, including synaptotagmin (Nakayama *et al*, 1999).

Rodent mRNA *in situ* hybridisation analysis and immunohistochemical analysis of Copine-6 show the protein to be most highly expressed in the main and accessory olfactory bulb, CA1 and CA3 pyramidal cells of the hippocampus, some granule cells of the dentate gyrus and the cerebral cortex (Nakayama *et al.* 1999). The former two of these regions are strongly associated with synaptic plasticity; the hippocampus having high levels of memory-associated plasticity, and the olfactory bulb being associated with plasticity and olfaction. Since Copine-6 mRNA has been documented to be much more strongly expressed in the olfactory bulb and the hippocampus when compared to other brain regions, then it could be postulated that Copine-6 may have specific functions(s) in these particular regions. Exactly what these function or functions are has yet to be discovered, and a more detailed account of Copine-6 expression and distribution in the brain, including the olfactory bulb and the hippocampus, will be investigated in this thesis.

1.3. Neocortex and the Hippocampus

<u>The Neocortex</u>

Based on structural and evolutionary grounds, the cerebral cortex can essentially be divided into two compartments: the **neocortex** (a six layered structure that is an evolutionary 'younger' region) and the **allocortex** (structures consisting of less than six layers, including the hippocampus, allegedly an evolutionary 'older' region). The neocortex ('new bark') is the outermost layer of the cerebral hemisphere, consisting of a layered, or laminar, structure of grey matter. The neocortical layers can be anatomically distinguished by their different cell populations, which are the excitatory output principle cells (predominantly consisting of pyramidal neurons, which constitute some 70-80% of the population (Sloper *et al.*, 1979) , and inhibitory non-principle cells (interneuron populations), which populate all layers.

The laminar structure of the neocortex is typically numbered using roman numerals I-VI, from superficial to deep layers (see Figure 1-3)

> **Layer I** is known as the 'molecular layer' – it contains very few neurons (no principle cells) and mainly consists of dendrites, axons and glial cells.

Layer II, the external granular layer, consisting mainly of soma of small principle pyramidal cells

Layer III, the external pyramidal layer, contains mainly small and medium sized principle pyramidal neurons.

Layer IV, the internal granular layer, contains several populations of stellate cells and principle pyramidal cells.

Layer V, the internal pyramidal layer, predominantly contains the largest pyramidal cells

Layer VI, the multiform, or fusiform layer, contains numerous cell types including large pyramidal cells.

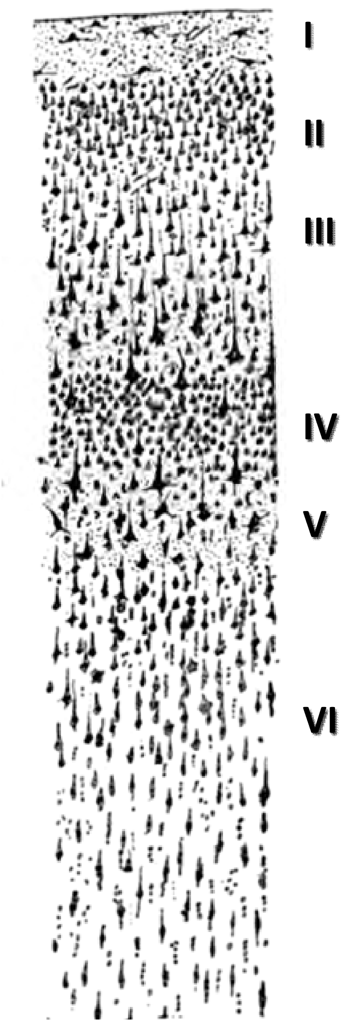

Figure 1-3 Ramon y Cajal's drawing of cortical layers in the motor cortex

Taken from his book "Comparative study of the sensory areas of the human cortex", page 361 (1899)

The excitatory pyramidal cells populate all layers of the neocortex except layer I, and have a typically triangular soma, often giving rise a single apical dendrite and to two or more basal dendrites (Sloper *et al.*, 1979). They use glutamate as their principle neurotransmitter. The largest of the pyramidal cells are Betz cells, which are characteristic of layer V of the motor neocortex and share many morphological features with smaller pyramidal cells other than proportionally having much smaller nucleus with respect to the cytoplasm (Kaiserman *et al*, 1972; Sloper *et al.*, 1979; Powell, 1981)

Amongst the glutamatergic principal cells within each cortical layer are numerous subpopulations of inhibitory interneurons. The interneuron populations primarily use the neurotransmitter GABA to facilitate inhibitory synaptic transmission, and vary greatly in morphology, molecular phenotype, cell density, neuronal connectivity and the organisation of their nerve fibres alongside the different afferent and efferent connectivity and network patterns. The cerebral cortex is synaptically integrated to numerous subcortical structures, such as the thalamus, basal ganglia and hippocampus, by both efferent and afferent connectivity; and the vast majority of connections are between cortical regions. The main three cortical regions are the motor (primary and secondary), sensory (visual, somatosensory, auditory) and association (parietal, temporal, occipital) cortex, each of which is connected to different cortical or subcortical regions to varying degrees. However, all of which receive afferent axons from a particular thalamic relay nucleus, or from a particular set of ipsi- or contra- lateral cortical area. The afferent connections, particularly to the sensory regions, are highly ordered and topographically organised sets of connections (Jones, 2004), demonstrating that the cortex, although complex, has intricate architecture. Indeed, the laminated appearance of the cortex is due to such differences in cell architecture, and more recently a complex organisational description of the neocortex has been advanced taking into account the complex cell connectivity and neuronal circuitry (Somogyi *et al.*, 1998). Interneurons constitute approximately 20% of the neocortex in layers II-VI, and 95% of the cell population in layer I (Gabbott *et al*, 1986), and the proportions of principal cells and interneurons are considered to be relatively constant in each layer throughout many species (Powell, 1981). However, the ever growing identification of interneuron subtypes in the cortex paired with the multiple experimental methods employed to investigate them highlights the complexity of the cortical system as a whole (Freund *et al.*, 1983, 1986; Gabbott *et al*, 1986; Somogyi *et al.*, 1998; Monyer *et al*, 2004; Ascoli *et al.*, 2008) although molecular protein markers have been used to delineate distinct subgroups of cortical GABAergic interneurons (Gonchar *et al.*, 2007) (Figure 1-4). In addition, it has long been recognised that a certain population of 'interstitial neurons', or 'neurons of the white matter', which are present in the white matter of the corpus callosum and often branch into the deepest layers of neocortex, constitute a neuronal population that likely differs from cortical interneurons (Kostovic & Rakic, 1980). These cells have been more recently identified to be remnants of the early subplate, and can exist as both glutamatergic projection neurons and GABAergic interneurons. The function of these cells, when their positioning at the cortical/white matter interface (a region dense in afferent connectivity entering the cortex) is considered, has been suggested to be auxiliary in nature perhaps through modulation of inputs to the cerebral cortex (Kostović *et al.*, 2011).

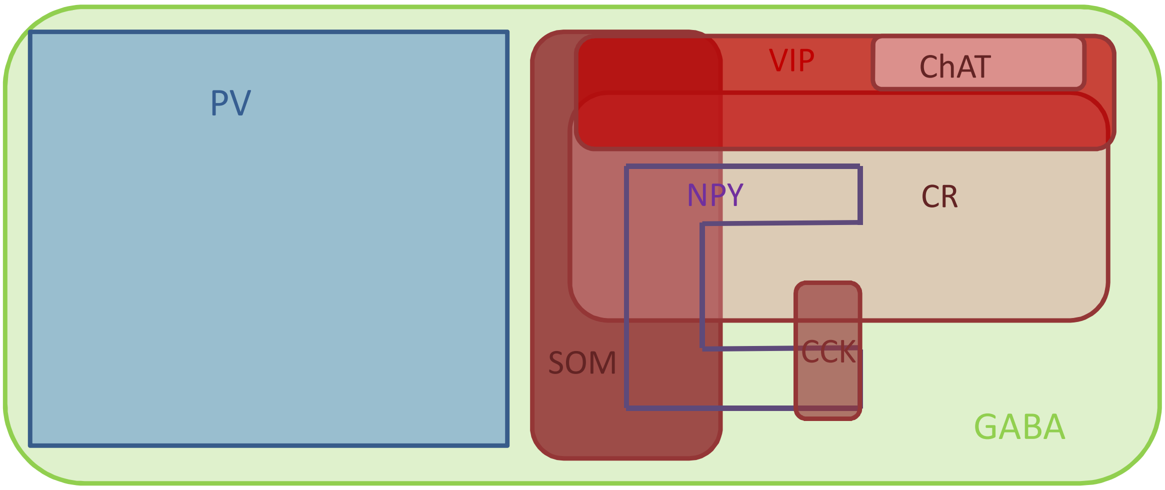

Figure 1-4 Distribution of cortical interneuron markers in adult mouse primary visual cortex (modified from Gonchar *et al.*, 2007).

Triple immunostaining with a panel of antibodies in the adult mouse visual cortex identifies distinct subgroups which constitute 90% GABAergic interneurons. There is some difference between mouse (above) and rat, which is documented to have no overlap between SOM and CR (Gonchar & Burkhalter, 1997). PV, parvalbumin; SOM, somatostatin; NPY, neuropeptide Y; VIP, vasointestinal polypeptide; ChAT, choline acetyltransferase; CR, calretinin; CCK, cholecystokinin.

The Hippocampal Formation

The hippocampal formation is a paired structure anatomically categorised as part of the allocortex, containing fewer cell layers than the neocortex (i.e. fewer than six layers). The hippocampus takes the form of a curved tube-like structure, initially likened to a seahorse (hence the latin name *hippocampus* taken from the Greek for “horse” and “sea monster”). Later, the hippocampus was likened to a ram’s horn-for which “Corni Ammonis” was derived - “horn of the Egyptian god Amun”- from which the anatomical regions CA1-4 regions still take their name.

The hippocampal formation comprises the subiculum, the hippocampus proper, and the dentate gyrus (see Figure 1-5). The two hippocampi sit opposite one another on both sides of the cerebral hemispheres -differing across species in size and position- in the rodent they join underneath the anterior corpus callosum. The hippocampi are anatomically distinguished as a narrowing of the cortex into a thin layer of densely arranged pyramidal cells which bend into a ‘U’ shape. The principal cells of the subiculum and hippocampus proper are pyramidal cells; those of the dentate gyrus are granule cells.

The hippocampal circuitry is complex, consisting of multiple afferent and efferent pathways linking the hippocampal formation to several brain regions such as the entorhinal cortex, the fornix, the thalamus and various regions of the neocortex. Intricate intrinsic neural pathways also exist within the hippocampal formation itself, between the granule cells of the fascia dentata and hilus (of the dentate gyrus) and the pyramidal cells of the cornu ammonis subfields. The most basic circuitry of the hippocampus was illustrated by Ramon y Cajal (See Figure 1-5) which demonstrates the entorhinal cortex as the main interface between the hippocampus and the neocortex, and the inputs and outputs between the hippocampus and the cortex and different regions of the hippocampus itself.

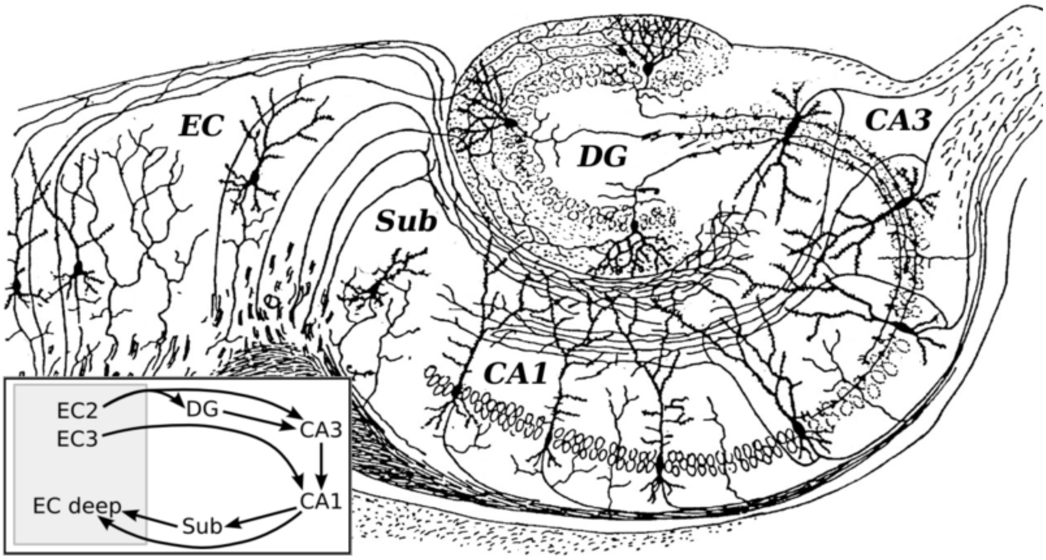

Figure 1-5 A sagittal view of the cellular architecture of the hippocampal formation

Drawn by Ramon y Cajal and displayed in his original works (Cajal, 1901a). The DG (dentate gyrus), and CA1-CA3 contain granule and pyramidal cell populations, respectively. The boxed image on the lower left depicts the basic network relationship between each region; The EC (entorhinal cortex) is the main interface between the hippocampus and the neocortex, with inputs and outputs between the EC, hippocampus, and the neocortex.

Ramon y Cajal (1901), with his student Lorente de Nó (1934), were the first neuroanatomists to suggest that the morphological differences and dendritic arbors of the various cell subpopulations in the hippocampus could be used to determine their functional significance. The 'laminar' structure of the hippocampus, as with the neocortex and olfactory bulb, may be a result of the afferent and efferent pathways and the subsequent pre- or post- synaptic connectivity (taken from (Freund *et al*, 1996) which references the original work of Lorente de Nó). This morphological characterisation is still used today, in addition to other more molecular phenotyping methods, such as monitoring the expression of different proteins in neuronal subpopulations using immunohistochemistry. Indeed, various techniques may be employed to investigate and analyse the neuronal structure and connectivity. Immunohistochemical analysis, alongside light or electron microscopy, can be used to visualise neurons and their dendritic or axonal processes, even visualising the fine structure of the synapse, by labelling and staining for neurotransmitters (or their synthesising enzymes), or other components of the cells such as cell surface markers, transcription factors, and signalling molecules such as calcium binding proteins or neuropeptides.

Both Copine-6 mRNA and protein expression has been identified in the cortex and hippocampus of the rodent brain (Nakayama *et al*, 1999), however the exact neuronal subpopulations expressing the protein are yet to be clarified. The study by the Nakayama group suggested that within the hippocampal formation, N-Copine (Copine-6) mRNA and protein expression was found in the pyramidal cells in the stratum radiatum CA1 and CA3, and granule cells of the dentate gyrus, particularly within the cell body and dendrites, and that Copine-6 had a weak expression in layer II of the cortex, which would suggest an immuno-positive distribution of Copine-6 in the small pyramidal cells of the external granule layer (for general cell distribution refer to Figure 1-3). A more extensive account of Copine-6 expression and distribution is examined in this thesis.

1.4. Olfactory bulb

The olfactory bulb is a paired protrusion that sits at the very front of the forebrain, and is the main neural system for olfaction in vertebrates. The olfactory bulb is synaptically integrated into the central nervous system both by output and input however it is unusual in the sense that the input and output pathways are anatomically separated.

The main olfactory bulb can be considered to be an extension of the cortex; it is phylogenetically conserved, consisting of a laminar cellular architecture, first depicted by Ramon y Cajal in his drawings of Golgi stained mouse olfactory bulbs (see Figure 1-6).

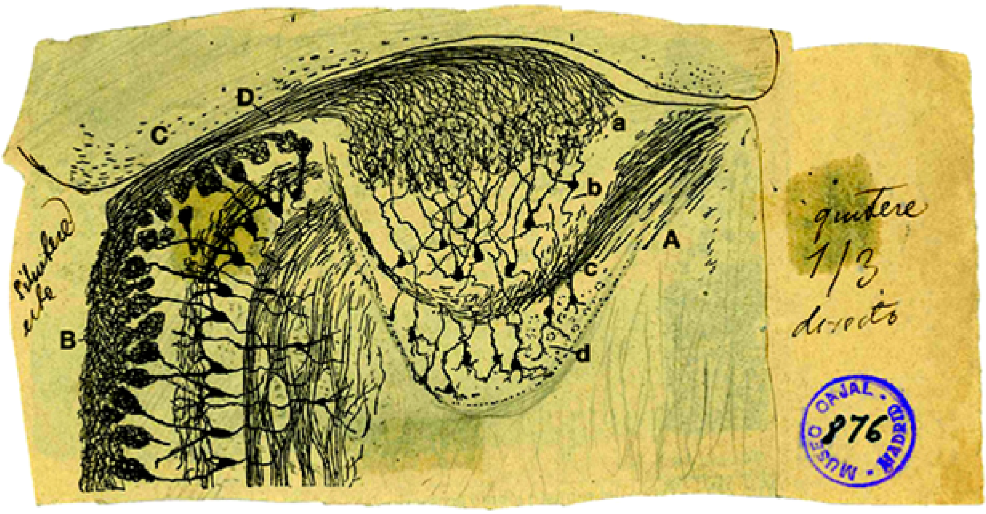

Figure 1-6 A reproduction of an original Cajal drawing from a Golgi stained horizontal section

The morphological features of a 20-day-old mouse accessory and main olfactory bulb. (Cajal, 1901b) taken from Martín-López *et al*, 2012 .

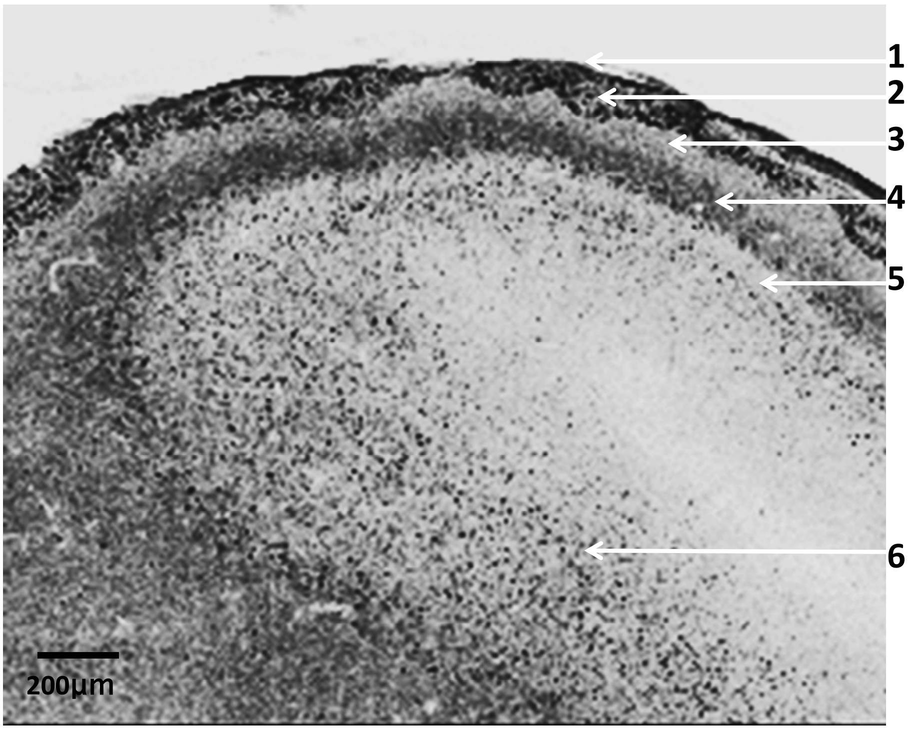

Figure 1-7 A calretinin labelled sagittal section of the main olfactory bulb outlining the different layers.

The layers are the superficial olfactory nerve layer (1), glomerular layer (2), external plexiform layer (3), mitral cell layer (4), internal plexiform layer (5) and the granule cell layer (6). The different layers are easily distinguished by the different densities of cell bodies, which are in abundance in the glomerular, mitral, and granule layers. Each layer is therefore anatomically distinct.

The main olfactory bulb consists of 6 layers, listed from superficial to innermost (refer to Figure 1-7)

1. The **superficial olfactory nerve layer**, consisting of incoming axons from receptor cells in the olfactory mucosa (nasal cavity)

2. The **glomerular cell layer**, consisting of bundles of spherical shaped structures of synapses and glial sheaths. The olfactory axons terminate in the glomeruli and are surrounded by periglomerular interneurons, a type of short axon cell whose axon distributes within the same histological region (Shepherd, 2004)

3. The **external plexiform layer** contains mainly dendrites of mitral cells;

4. The **mitral cell layer** contains mitral and tufted cells - the principal neurons- the long axons distributing outside of the histological region. The axons of the mitral cells are the main output of the olfactory bulb, and the soma of the mitral cells forms a thin layer below the glomerular layer.

5. The **inner plexiform layer** consists of granule cell dendrites

6. The innermost **granule-cell layer** consists mainly of granule interneurons. They have apical dendrites but no axon, and form dendro-dendritic synapses onto principal neuron dendrites (mitral cells) within the external plexiform layer. This is their only output. They receive synapses from the axons of mitral and tufted cells (Price & Powell, 1970a)

Each layer can be distinguished by differences in both structure and molecular composition. Not only are the input and output structures separated within the main olfactory bulb, but different cell types exist in each layer. Several types of interneurons can be identified in different layers (Price & Powell, 1970b; Pinching & Powell, 1971a), in part owing to their expression of different proteins, and it is these interneurons that have recently been identified as able to be newly generated in the adult brain. Following neurogenesis at the sub ventricular zone at the edge of the lateral ventricle, newborn neuroblasts have been found to migrate along a ‘rostral migratory pathway’ to the olfactory bulb, where they continue their maturation and differentiate into different types of interneurons: the granule cells, and the periglomerular cells (of which there are various subpopulations of both cell types) (Luskin, 1993; De Marchis *et al.*, 2007)

1.4.1. Adult Neurogenesis at the subventricular zone

In the 1960s, both the hippocampus and the olfactory bulb were identified by Joseph Altman as the only two sites in the adult brain associated with adult neurogenesis (Altman, 1963). Firstly, autoradiographic analysis identified the sub-granular zone (SGZ) of the dentate gyrus, a structure within the hippocampal formation, as the site of neurogenesis of hippocampal granule cells which continuously populate the granule cell layer of the dentate gyrus. Secondly, autoradiographic and immunohistochemical analysis later identified the sub-ventricular zone (SVZ), a layered structure on the wall of the lateral ventricle, as a site of neurogenesis of neurons that populate the olfactory bulb (Altman, 1969). The adult subventricular zone was considered a residual component of the embryonic lateral ganglionic eminence and the other embryonic germinal layers were suggested to disappear following birth (Bayer *et al.*, 1993). More recently, however, all parts of the telencephalic neuroepithelium including the medial and lateral ganglionic eminences and the cerebral cortex, have been shown by Cre-Lox fate mapping to contribute multipotent and self-renewing stem cells to the adult subventricular zone (Young *et al.*, 2007).

Analysis of a retroviral lineage tracer revealed that new-born neurons originating at the adult SVZ were able to migrate large distances along a specialised migratory pathway – the rostral migratory stream (RMS) – which anatomically follows the corpus callosum in a rostral direction over and above the striatum, where they eventually reach the olfactory bulb (Luskin, 1993) (See Figure 1-8). This was confirmed by injection of radioactive thymidine ^{3}H-Thymidine, a marker of cell division which incorporates into DNA, which following its injection into the wall of the lateral ventricle, was able to label new-born cells in the core of the olfactory bulb after 2 days (Lois *et al*, 1994), suggesting the cells had migrated from the SVZ over a long distance to the olfactory bulb. It is here, in the olfactory bulb, that the new-born neurons mature and integrate into existing neuronal circuitry; indeed, when SVZ cells from adult transgenic mice carrying a reporter gene for neuron-specific enolase (a marker of differentiated neurons) were grafted into adult mice, these cells could later be detected in the olfactory bulb, signifying that not only do the cells migrate, but they are able to mature and integrate into existing circuitry when they reach their destination (Luskin, 1993; Lois *et al*, 1994). Adult SVZ neurogenesis has been demonstrated as under the regulation of olfactory experience and learning in rodents, which implicated adult SVZ neurogenesis in olfactory learning (Lledo *et al.*, 2006), however the potential role in human is not elucidated. However, studies suggest that adult neurogenesis is up-regulated in rodent models of stroke, yet down-regulated in rodent models of neurodegenerative disease The regulation of SVZ neurogenesis by olfactory experience

and learning leads to the hypothesis that adult SVZ neurogenesis plays a role in olfactory learning

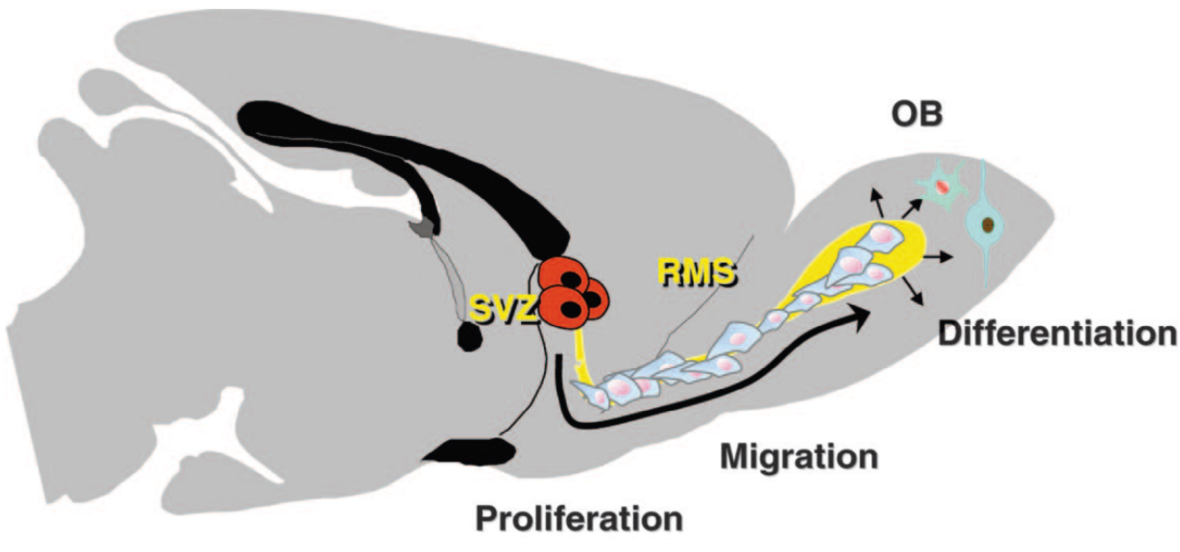

Figure 1-8 A sagittal view of an adult rodent brain, showing the main sites involved in adult neurogenesis.

Image taken from Abrous *et al* , 2005. The cells originate at the subventricular zone (SVZ) and migrate along the rostral migratory stream (RMS) to reach the olfactory bulb (OB), where they undergo radial migration and terminal differentiation into mature neuronal phenotypes.

Tangential homophilic chain migration is considered to be a hallmark of neuroblasts migration in the rostral migratory stream (RMS) (Wichterle *et al.*, 1997). Along the RMS, new-born cells change developmentally, which causes changes in their protein expression depending on their level of migration or maturation. Therefore, cells at the subventricular zone express some proteins whose expression may be down-regulated as they mature. Equally the process of maturation may cause the expression of proteins that were not initially present at the level of the subventricular zone but start to appear during or after radial migration in the olfactory bulb. Determining the presence of a 'chain' of migrating cells is in itself highly dependent on the ability to label them with specific cell markers, and a variety of cellular markers are therefore used to phenotype new-born, differentiating and mature cells by immunohistochemistry (see Figure 1-9). The cells are often categorised according to their level of maturation: they originate as **type B** cells, or stem cells, eventually becoming **type C** cells which are progenitors.

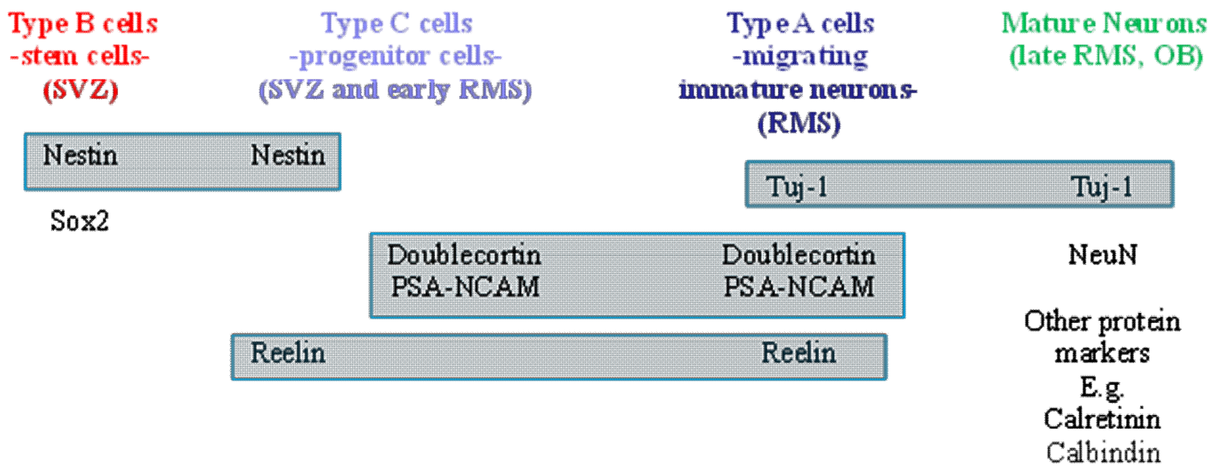

<u>Figure 1-9 A simplified sequence of marker expression during neurogenesis in the adult olfactory bulb.</u>

The different proteins can be detected immunohistochemically in order to identify different cell types and their levels of maturation. Some markers are expressed by more than one developmental stage (blue box outlines).

Following expansion, the cells become immature migrating neurons – **type A** cells, before completing differentiation and maturation as new neurons.The most commonly used cell marker for stem cells at the early stage of neural progenitor cell expansion (type B, to type C cells) is **nestin**, an intermediate filament protein first identified in stem cells of the rat central nervous system (Lendahl *et al.*, 1990). Nestin is expressed in the early stages of development by immature neurons. Neurons can be identified owing to their expression of certain intermediate filament proteins – most of which continue to be expressed through to maturation – yet nestin expression ceases following differentiation, making it a good candidate for the labelling of new-born, or progenitor, neural cells. **Reelin**, a glycoprotein implicated in cell migration and thought to act as a extracellular chemo-repellent 'detachment signal' for neuroblasts during radial and tangential migration (Hack *et al.*, 2002). It has been found in certain cell populations such as Cajal-Retzius cells during cell migration, particularly corticogenesis (D'Arcangelo *et al.*, 1995; Hack *et al.*, 2002), and disruption of the reelin allele results in the so-called '*reeler'* mutant (Falconer, 1951; D'Arcangelo *et al.*, 1995) which results in misdirected neuronal migration and structural abnormality in various regions of the brain including the cerebellum, cortex and olfactory bulb (Caviness *et al*, 1973; Wyss *et al.*, 1980; Hack *et al.*, 2002) Although the expression of reelin is greatest in the developing brain (possibly correlating with the higher levels of neurogenesis), it is still expressed in the adult rodent brain (D'Arcangelo *et al.*, 1995) and although the exact function of reelin is not known it can be used as a molecular marker for the rostral migratory stream, in addition to other immature cell, or migratory markers.

Early stages of neural cell maturation begin with the ability of the cell to migrate and differentiate. Identification of immature neurons with this ability to migrate is possible immunohistochemically, owing to their expression of the microtubule-associated protein **doublecortin** (Francis *et al.*, 1999; Gleeson *et al.*, 1999). This is expressed by immature, migrating neurons in the type C to type A stages of development, during both embryonic and postnatal development. Also, polysialic acid – neural cell adhesion molecule, **PSA-NCAM**, which is important for the migration of newborn cells from the SVZ to the olfactory bulb (Seki & Arai, 1993; Hu *et al.*, 1996; Bonfanti, 2006) can also be detected in type C and type A cells.

Once the neurons become more mature, they begin to lose their early developmental markers nestin and doublecortin, and begin to express post-mitotic proteins such as **TUJ-1**, a neuron specific beta-tubulin expressed exclusively by postmitotic neurons (Memberg *et al*, 1995), and **NeuN**, a neuronal nuclear protein, which is expressed by the majority of postmitotic neurons (Mullen *et al*, 1992). These markers are used to identify late stage type

A cells, and mature neurons. To further distinguish between neurons and other cells such as glia, glial cells can be immunohistochemically identified, using either glial fibrillary protein (**GFAP**) (Eng *et al.*, 1971) or **vimentin**, both of which are intermediate filament proteins that are <u>not</u> expressed by cells with a neuronal phenotype.

The final stages of neuronal maturation for the RMS cells occur in the olfactory bulb. However, the types of cells that repopulate the olfactory bulb of the adult brain are only now being discovered. Thus it is possible, using immunocytochemical identification of specific proteins, to differentiate cell phenotypes and thereby characterise the different cells involved in adult neurogenesis. Similarly, interneurons of the olfactory bulb can be immunohistochemically defined, in parallel with developmental tracing studies, to examine the migration and nature of the new-born cells. For example, different mature neuronal phenotypes can be identified by their expression of different markers, such as calcium binding proteins (Philpot *et al.*, 1997), and by developmental birth-dating studies (De Marchis *et al.*, 2007).

1.5. Aims of thesis

Given the interest in the laboratory in the function of the Copines, especially Copine-6, the aim of my work was to examine the developmental and regional distribution of the protein in the rodent brain, to see if this shed light on potential roles for the Copines during development ad in the brain. The main aim of this thesis is to give a detailed anatomical and molecular account of the expression of Copine-6 protein in the rodent brain.

<u>This required:</u>

1. The production and characterisation of a polyclonal antibody against Copine-6, and the application of this in immunohistochemical studies of different rodent brain preparations in order to describe Copine-6 expression and distribution at the light microscope level.

2. The classification and categorisation of Copine-6 immuno-positive cells based upon molecular and morphological phenotype. This includes analysis at a developmental level, in both dissociated cell culture and using rodent brain sections, and birth-dating analysis.

3. The fine structural analysis of Copine-6 protein expression in cells of the rat brain, using the electron microscope. This included the examination of pre- and post-synaptic localisation.

Chapter 2. **Characterising a rabbit polyclonal antibody against Copine-6**

2.1. Introduction

As noted in the introduction there is evidence to suggest that each member of the Copine protein family has a unique expression pattern in mammals, with some of the Copines being restricted only to certain tissues. It is striking that such a ubiquitous family of conserved calcium binding proteins are so little studied. Following their original identification as calcium-dependent phospholipid binding proteins in preparations of *Paramecium tetraurelia* (Creutz *et al.*, 1998), various small-scale studies have been conducted investigating the biology of individual Copine family members (see Chapter 1: Introduction). Copine mRNA expression profiles in a range of human tissues have been investigated and showed that every Copine family member is expressed in the brain, but each member differs substantially in their expression levels in non-neuronal tissues (Cowland *et al*. 2003). This study showed that Copine-6 mRNA expression was significant only in brain, thereby confirming the original work of Nakayama and co-workers (Nakayama *et al.*, 1998). Furthermore, not only did these authors report an increase in Copine-6 mRNA expression following hippocampal long term potentiation (LTP, but they also documented the anatomical expression pattern of both mRNA and protein in the rodent brain by in situ hybridisation and immunohistochemistry respectively, and noted that the protein appeared only to be expressed in neurons. This study also demonstrated the presence of Copine-6 in cells of the main and accessory olfactory bulb, CA1 and CA3 pyramidal cells of the hippocampus, and some cells of the cortex (Nakayama *et al*. 1999). The former two brain regions are heavily implicated in processes of synaptic plasticity, however no functional implication of Copine-6 could be predicted at this stage.

Following these original studies, no in-depth investigation into the expression of Copine-6 in brain has been carried out. Neither have the functional role(s), if any, of Copine-6 (indeed any of the Copine family members) been established.

This thesis therefore aims to more thoroughly investigate the expression profile of Copine-6 in brain, beginning with the production and subsequent characterisation of a suitably specific antibody for histochemical, molecular and anatomical investigation.

Previously in the McIlhinney laboratory (Medical Research Council, Anatomical Neuropharmacology), various different antibodies to different Copines had been produced following the identification of Copine family members in affinity isolates of the $GABA_B$ receptor from rat brain. The in house antibody production included antibodies to target Copine-6.

Two polyclonal antibodies were raised in two New Zealand white rabbits (termed 3 and 4) by subcutaneous immunization using purified mouse Copine-6. In this chapter, the two polyclonal antibodies are fully characterised, employing a variety of assays and immunohistochemical techniques. Each technique contributes to the final confirmation that we are working with an antibody that specifically targets Copine-6. This antibody was used for further immunohistochemical application.

2.2. Methods

2.2.1. Copine-6 protein production and production of the rabbit polyclonal antibody against Copine-6.

The production of the purified Copine-6 and the immunization process occurred prior to my arrival in the McIlhinney laboratory. The production of the Copine-6 protein was carried out by Dr Pavel Perestenko. Briefly, the shuttle vector pBackPAK9 was used to clone the histidine-6-tagged Copine 6 sequence into baculovirus The expression vector SF9 insect cell line was subsequently infected with the recombinant baculovirus and the recombinant Copine-6-histidine-tagged mouse protein was then purified from the cell lysates using a nickel column. The purified mouse Copine-6 was used to immunize two rabbits (named 3 and 4) in order to raise antibodies against Copine-6. One month following the initial inoculation, both rabbits were boosted 3 times, at 2 weekly intervals. Pre-immune antiserum was obtained prior to inoculation. The bleeds were taken 10 days after each boost, and the final bleed 10 days after the 4th injection. The serum from the final bleed was absorbed against Copine -2 to help to minimize Copine cross reactivity, and the sera was subsequently affinity purified using immobilized Copine-6 coupled to Affigel. The immunization of the rabbits, the sequential bleeds and the affinity purification of the sera from the final bleed were all carried out by Dr RAJ. McIlhinney.

A

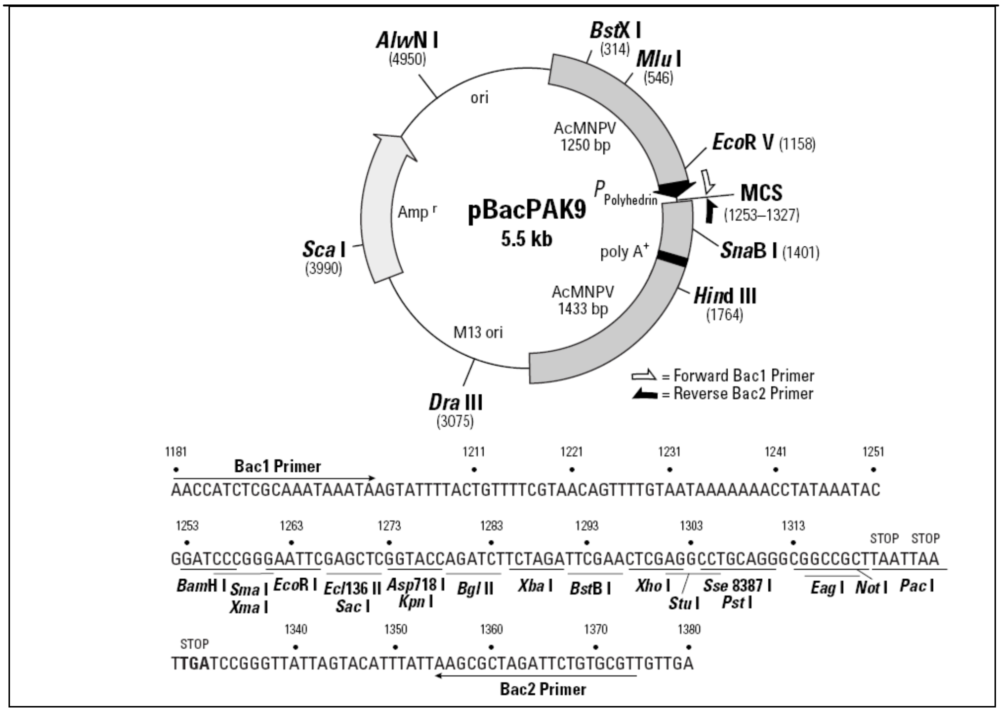

B

1 MGHHHHHHMS DPEMGWVPEP PAMTLGASRV ELRVSCHGLL DRDTLTKPHP CVLLKLYSDE
61 QWVEVERTEV LRSCSSPVFS RVLAIEYFFE EKQPLQFHVF DAEDGATSPS SDTFLGSTEC
121 TLGQIVSQTK VTKPLLLKNG KTAGKSTITI VAEEVSGTND YVQLTFRAHK LDNKDLFSKS
181 DPFMEIYKTN GDQSDQLVWR TEVVKNNLNP SWEPFRLSLH SLCSCDIHRP LKFLVYDYDS
241 SGKHDFIGEF TSTFQEMQEG TANPGQEMQW DCINPKYRDK KKNYKSSGTV VLAQCTVEKV
301 HTFLDYIMGG CQISFTVAID FTASNGDPRS SQSLHCLSPR QPNHYLQALR TVGGICQDYD
361 SDKRFPAFGF GARIPPNFEV SHDFAINFDP ENPECEEISG VIASYRRCLP QIQLYGPTNV
421 APIINRVAEP AQREQSTGQA TKYSVLLVLT DGVVSDMAET RTAIVRASRL PMSIIIVGVG
481 NADFSDMRLL DGDDGPLRCP KGVPAARDIV QFVPFRDFKD AAPSALAKCV LAEVPRQVVE
541 YYASQGISPG APRPSTPAMT PSPSP*

Figure 2-1 Cloning Copine-6.

A. Restriction Map and Multiple Cloning Site (MCS) of pBacPAK9 taken from Clontech GenBank Accession No.:U02440 as part of Cat. No. 631402. **B**. The amino acid sequence of Copine-6 with the histadine tag was cloned using the pBacPAK9 vector. The 6x histadine tag at the C-terminus is highlighted in red.

2.2.2. Indirect Fluorophore- Linked Immunosorbant Assay (FLISA)

Samples of the sera obtained at each bleed of the two rabbits (3 and 4) were here subjected to indirect fluorophore-linked immunosorbant assay (FLISA) to investigate the antibody titre and reactivity. . All sera samples were tested for both antibodies, which included pre-immune sera (control), antisera from bleeds 1, 2, the final bleed, and the affinity purified final bleed. Greiner Bio-One 96-well tissue culture polystyrene microplates (No. 655180, Greiner Bio-One, Gloucestershire) were initially coated with 20 µg/ml purified Copine-6 and left for 24 hours at 4^{o}C to absorb the protein. The plate was washed with PBS and then blocked using 1% BSA-PBS (Cat. no. 40-00-410, First Link UK, Birmingham) for 1 hour, followed by application of all sera samples to individual wells by serial dilution (1:100, 1:300 through to 1:100,000, 1:300,000) in BSA-PBS. Sera were left for 2 hours at room temperature. Wells were then washed in 1% BSA-PBS x3 times, followed by a 1 hour incubation with the secondary antibody, goat anti-rabbit (IgG (H+L) Alexa Fluor 680, Invitrogen UK, A-21076) at dilution of 1:1000 for 1 hour at room temperature. The plates were scanned and analysed using Odyssey Infrared Imaging System (LI-COR Biosciences, USA). The data was analysed based on arbitrary fluorescent units, which were then quantified using Microsoft Excel based on triplicate sampling of each dilution.

2.2.3. Production of HEK cells to constitutively express Copines –1, -2, -3, -6, -7

Cultured Human Embryonic Kidney cells (HEK) were transfected with Copines -1, -2, -3, -6 and -7 using polyethylenimine (PEI, JET-PEI™ DNA transfection reagent, Polyplus Transfection, USA). The Copine peptide constructs had previously been produced by P.Perestenko , and were C-terminally tagged with yellow fluorescent protein (YFP). Routinely (for each individual transfection), 12µl PEI was added to 125µl NaCl. 6µg DNA of the tagged Copine (either -1, -2, -3, -6 and -7) was added to 125µl NaCl. The two solutions were mixed and incubated for 30 minutes at room temperature. Each 250µl mixture was then applied to separate T25 flasks which were seeded with HEK cells at

$2x10^6$, 24 hours prior to transfection and incubated at 37°c . The transfected cells were left for a further 48 hours and were then washed with PBS, centrifuged, pelleted, and lysed with sample buffer (4% SDS, 20% glycerol, 40mM DTT, 125mM Tris-HCl; pH6.5) for analysis by Western Blot. The lysed cells were heated for 5 minutes at 90°c before being loaded onto a 10% polyacrylamide gel for electrophoresis. Precision Plus Protein Standards All Blue marker (No. 161-0373, Bio-Rad, Hertfordshire) was loaded into the first well for molecular weight quantification purposes. The proteins were then transferred onto a nitrocellulose membrane at 25V for 30minutes, and the membrane subsequently blocked using 5% non fat milk in PBS + 0.05% Tween-20. The affinity purified rabbit Copine-6 antibody was then applied to the membrane (diluted in blocking buffer to 1:1000, 0.5µg/ml). Following a 3 hour incubation at room temperature, membranes were washed in PBS-Tween-20 x4 times before applying the secondary antibody goat anti-rabbit (1:1000, IgG (H+L) Alexa Fluor 680, A-21076), Secondary antibody was diluted to 1:5000 and incubated for 1 hour at room temperature. Membranes were then visualized and analysed using the LI-COR Scanner. To check for the presence of YFP-tagged Copine in all wells, the membrane was stripped (using NewBlot™ PVDF 5X Stripping buffer, Odyssey® 928-40032, LI-COR UK according to the manufacturer's instructions), blocked in PBS-BSA and re-probed using rabbit anti-YFP (1:500, Living colours antibody, 632460, Clontech USA/Canada). The secondary antibody goat anti-rabbit (1:5000, IgG (H+L) Alexa Fluor 680, A-21076) was applied and again visualised on the LI-COR scanner. This basic protocol was used for all immunoblotting protocols. To check the specificity of the polyclonal antibody for Copine-6 alone, HEK cells transfected with the various Copine constructs were subjected to protein immunoblotting as described above and the membranes were probed with our rabbit polyclonal antibody in conjunction with one of the two commercially available monoclonal antibodies targeting Copine-6 (either anti-Copine-6 mouse clone 42, BD Biosciences, #612638, 1:200 or anti-Copine-6 mouse clone 6D11, Sigma Aldrich, #06272-6511, 1:200). The BD Biosciences antibody was raised to residues 4-125 of Copine-6, whereas the Sigma antibody was produced using a fusion protein encoding the whole Copine-6 sequence. The secondary antibodies goat anti-rabbit (1:5000, IgG (H+L) Alexa Fluor 680, A-21076, Invitrogen UK) and goat anti-mouse (1:5000, IgG (H+L) IRDye 800CW, 926-32210 LOT c#00816-03, Odyssey® LI-COR) were subsequently applied.

2.2.4. Protein immunoblotting of various rat tissues

In order to investigate the postulated exclusivity of Copine-6 in brain, dissociated hippocampal neurons were subjected to protein immunoblotting alongside the following rat tissues, which were dissected from adult animals (250g+): brain, heart, liver, lung, skeletal muscle, spleen, stomach and kidney. Purified Copine-6 was used as a positive control in the analysis of brain isolates. To investigate Copine-6 in brain membranes, the cerebellum was removed and the cortices were halved ensuring the meninges were removed prior to weighing. Routinely, either 5 volumes of SDS-PAGE (sodium dodecyl sulfate polyacrylamide gel electrophoresis) buffer was added containing 1µl of Benzonase® nuclease (9025-65-4, Sigma Aldrich UK) to brain, or brain tissue was homogenized in 5 volumes of 50mM Tris HCl pH 7.5 containing 0.15M NaCl, 5mM EGTA and 1:100 dilution of EDTA-free protease inhibitor (04693159001, Roche UK). Both the supernatant and pellet from brain tissue homogenised in the presence of EGTA was analysed, since the ability of Copine-6 to bind membranes would be reduced by calcium chelation and the protein should therefore remain in the supernatant fraction. Homogenisation was carried out by giving each sample 3x10 second bursts with a polytron homogenizer at half power. The resulting homogenates were centrifuged at 15,000 gav, at 4°C for 20 minutes and the supernatants carefully removed and saved. The brain pellets were resuspended in 0.05M Tris-Saline (TRIZMA® HCl and base, pH 7.5 at 25˚c, plus 0.01g/L sodium azide + 0.15M NaCl) + 1% Triton-X 100 (9002-93-1, Sigma Aldrich) to the same volume as the lysate, and the samples were frozen at -20°C.

To investigate the presence of Copine-6 in other tissues, rat tissue samples were dissected and homogenized at 4°C using a polytron homogenizer at half power in 10 volumes of 50mM Tris HCl pH 7.5 containing 0.15M NaCl, 5mM EGTA and 1:50 dilution of EDTA-free protease inhibitor (04693159001, Roche UK). Following centrifugation at 100,000gav for 40 minutes at 4^{o}C, the supernatants were removed and their protein content analysed using the BioRad dye binding assay (500-0001, Bio-Rad UK) and BSA as a protein standard. The samples were then stored in aliquots at -80^{o}C.

For electrophoresis, equal amounts of protein from all tissues (25µg) in sample buffer (62.5mM Tris HCl pH6.8, glycerol (10%) and 20mM dithiothreitol were heated to 90^{o}C for 5min and loaded into each gel track. After electrophoresis on a 10% gradient gel the proteins were transferred to nitrocellulose membranes using a BioRad semi-dry apparatus at 25V for 30 minutes. Membranes were blocked in Odyssey Blocking Buffer (diluted 1:1 in PBS) for 2 hours at room temperature, and primary antibodies rabbit anti-Copine-6 (1:1000) and mouse anti-Tubulin (1:2000, T-8203, Sigma Aldrich UK) were added to the blocking buffer, plus 0.1% Tween-20 (Sigma Aldrich UK, 9005-64-5) for 16 hours at 4˚c. Membranes were then washed in PBS+ 0.1% Tween-20, 4x 5 minutes, and secondary antibodies Alexa Fluor 680 goat anti-rabbit IgG (H+L), 1:5000, Invitrogen, A-21076) and IR Dye 800CW goat anti-mouse (926-32210 LOT c#00816-03 Odyssey® LI-COR) were applied at 1:5000 in Odyssey Blocking Buffer + 0.1% Tween-20, for 1 hour at room temperature. The membrane was then washed 4x5 minutes in PBS + 0.1% Tween-20, 2x5 minutes PBS alone to remove any residual Tween-20, and was scanned on the LI-COR Scanner.

2.2.5. Immunohistochemical analysis of tissue using polyclonal antibody against Copine-6

Dissociated tissue culture (rat hippocampal neurons) and sagittal 50µM sections of adult rat (250g+) brain tissue were employed to determine the histochemical specificity of our rabbit polyclonal Copine-6 in comparison to two commercially available mouse monoclonal Copine-6 antibodies. Rat hippocampal neurons were cultivated following hippocampal dissection either by Miss Kathryn Newton or Dr Pavel Perestenko. Routinely, cells were maintained for 21 days *in vitro*, on 13mm glass Coverslips (Menzel Glaser, No.1, 13mm, Cat No. CB00130RA1) in 500ml Neurobasal media supplemented with 10ml B27 (Invitrogen 17504-044), 1.25ml of 200mM glutamine and 5ml Penicillin Streptomycin at 37˚c incubation with 5 % CO_2. Before analysis, cells were fixed on the coverslip using 4% Paraformaldehyde for 10 minutes, followed by a 10 minute exposure to 50mM Tris HCl+0.15M NaCl, + 0.05% Triton X-100 . Bovine serum albumin (1% in phosphate buffer solution) containing 0.1% normal donkey serum was used to block the coverslips for 1 hour at room temperature. Antibodies were then applied as described below. Rabbit polyclonal antibody against Copine-6 was immunohistochemically applied to cells in culture alongside one of the mouse monoclonal anti-Copine-6 antibodies (either anti-Copine-6 mouse clone 42, BD Biosciences, #612638, 1:200 or anti-Copine-6 mouse clone 6D11, Sigma Aldrich, #06272-6511, 1:200). Coverslips were left with gentle rocking overnight at 4°C. Sections were washed in PBS four times, for 15 minutes, and secondary antibodies were applied for a minimum of 4 hours. Imaging was carried out using Zeiss Axiovert 100M confocal microscope, lasers HeNe1S43 and ArgonS14, reflectors 543Cy3 and FITC488, at objectives x10, x20, x40 and x60. Images were analysed using LSM Image Browser and Image J.

Rat brain histochemical procedures were carried out on Sprague–Dawley rats (200-350g; Charles River, Margate, Kent, UK). Environmental conditions and all procedures that were performed were in accordance with the Animals Scientific Procedures Act of 1986 (UK).) Rats were deeply anaesthetised using isofluorane (4% in O_2) plus pentobarbitone (200 mg/kg; i.p.; Sagatal; Rhône Mérieux, Tallaght, Dublin, Ireland), and transcardially perfused via the ascending aorta using 100mL 0.1M phosphate buffer (PB), followed by 300mL 4 % paraformaldehyde, 0.05 % glutaraldehyde and 0.2% picric acid in 0.1M PB (pH 7.4). Brains were immediately removed and postfixed in 4% paraformaldehyde in 0.1M PB for 24 hours before being sectioned at 50µM intervals in the sagittal plane on a Leica VT1000s vibrating microtome. Sections were collected in 5 vials, so each consecutive vial had every fifth section, and were stored in PBS containing 0.5% sodium azide until required. Sections were washed in PBS prior to antibody application to ensure fixative was completely removed. Rat brain sections were prepared for histochemical analysis by initial incubation in blocking solution containing PBS + 0.3% Triton X-100

(9002-93-1, Sigma Aldrich) + 10% normal donkey serum, either for 6 hours at room temperature or 24 hours at 4°C. Antibodies were added to 1ml PBS + 1% normal donkey serum with shaking overnight at 4°C. Rabbit polyclonal antibody against Copine-6 (1:1000) was applied together with one of the mouse monoclonal anti-Copine-6 antibodies (either anti-Copine-6 mouse clone 42, BD Biosciences, #612638, 1:200 or anti-Copine-6 mouse clone 6D11, Sigma Aldrich, #06272-6511, 1:200).Following incubation, sections were washed in PBS x4, 15 minutes. The secondary antibodies donkey anti- rabbit 488 (Alexa Fluor® 488, A-21206, Molecular Probes UK) and donkey anti-mouse CY3 (715-165-150, Jackson ImmunoResearch Labs, USA) were applied AT 1:1000 for a minimum of 4 hours at room temperature. Sections were finally washed x4, 15 minutes in PBS and sections were mounted on a slide using PBS and Vectashield Mouting Medium (H-1000, Vecta Labs UK). Imaging was carried out using Zeiss Axiovert 100M confocal microscope using lasers HeNe1S43 and ArgonS14, reflectors 543Cy3 and FITC488, at objectives x10, x20, x40 and x60. Images were analysed using LSM Image Browser and Image J.

2.2.6. Antigen retrieval

The mouse monoclonal anti-Copine-6 antibody from BD Biosciences required antigen retrieval methods in order for it to be immunohistochemically viable on rat brain sections. It worked without antigen retrieval methods on dissociated culture. Antigen retrieval involved the pre-heating of 10mM sodium citrate (pH 6.0) to 80°C. The 50µM sagittal rat brain sections were then incubated in the sodium citrate with continued heating at 80°C (in a water bath) for 25 minutes. Brain sections were then removed, washed x4 in PBS, and subjected to the normal blocking, permeabilising and antibody incubation procedures as described above (see 2.2.5)

2.3. Results

2.3.1. Indirect FLISA

The FLISA (Fluorescent-linked immunosorbant assay) data for rabbits 3 and 4 showed that both rabbits responded strongly to the immunizing purified Copine-6 (See Figure 2-2, A and B respectively). This was reflected in an improvement in titre of antibody following each subsequent boost. Serial dilution of all sera from the immunizing boosts showed the expected decrease in reaction with the immunogen, and the affinity purified final bleed remained reactive, and was able to produce a reaction at dilutions of 1:100,00 and 1:300,00. All the samples of serum from Rabbit 4 showed a stronger apparent reaction than those of Rabbit 3 (See Figure 2-2. B and A, respectively).

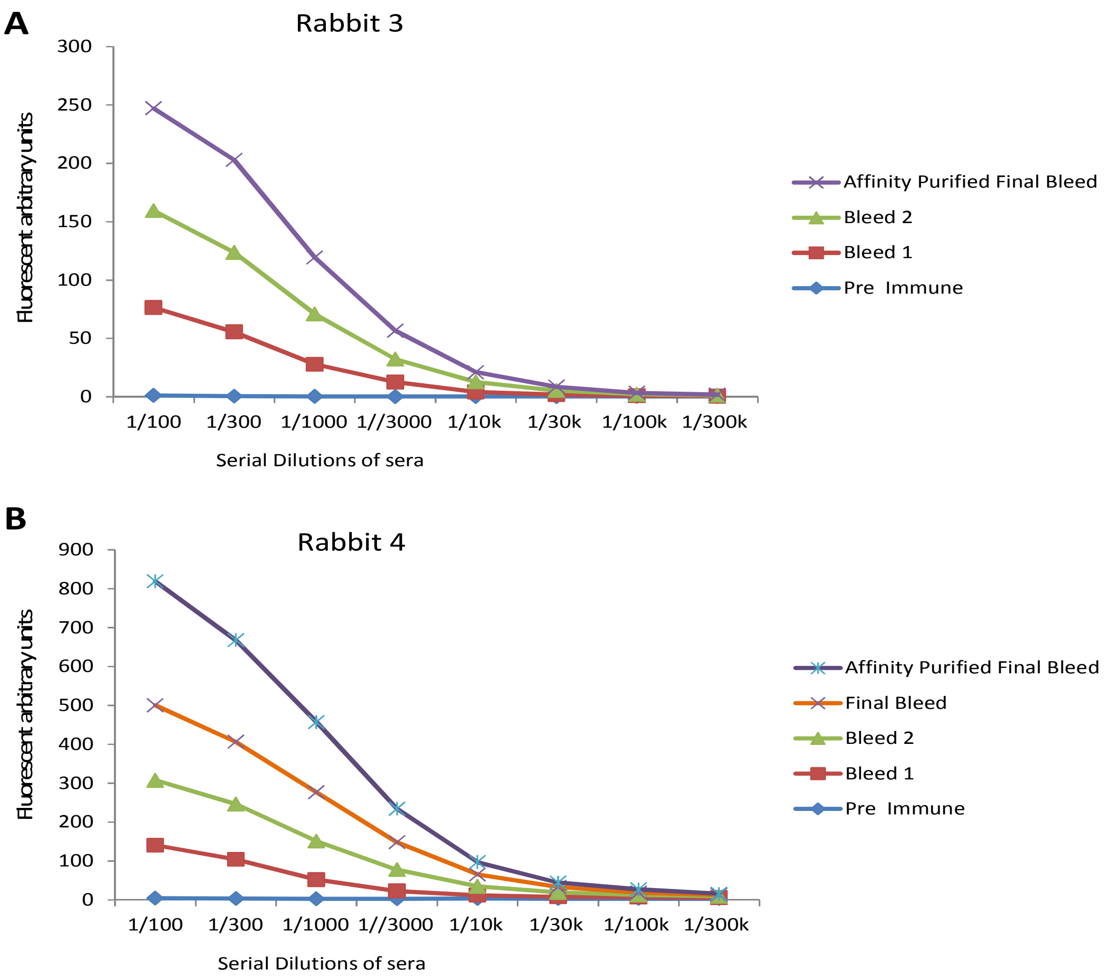

Figure 2-2 FLISA data for Rabbits 3 and 4.

Blood samples were taken from both rabbits at various intervals after the first immunization to quantify reactivity of the antibody following the immunising boosts. Both rabbits reacted strongly to the immunising peptide Copne -6, as demonstrated by the improvement in titre. Both rabbits showed an expected increase in reactivity between pre-immune and bleed 1, with a smaller increase in titre following subsequent boosts. The Y axis is defined in fluoresecence units, and the X axis shows the serial dilutions of the serum. The different serum samples are indicated by the appropriately coloured lines. (**A.** Rabbit 3**. B.** Rabbit 4)

2.3.2. One of the two rabbit polyclonal antibodies specifically targets Copine-6

HEK cells transfected with YFP tagged Copines -1, -2, -3, -6 and -7 were subjected to protein immunoblotting to investigate the specificity of both Copine-6 affinity purified antibodies 3 and 4. Both antibodies reacted strongly with the Copine-6 transfected cells and rat brain homogenates. The antibody from rabbit 3 did not show any cross reactivity with other Copines (see Figure 2-3, image A). However antibody 4 appeared to have a weak cross reaction with Copine -3 and Copine -7 (see Figure 2-3 image B). Following stripping and re-probing of the blot with a mouse anti-YFP, bands of different Copine-YFPs were detected, confirming successful transfection with the different Copine-YFP construct (see Figure 2-3 image C). These results were replicated on 2 separate attempts.

In order to further check the specificity of the Copine-6 rabbit polyclonal antibody from rabbit 3, the HEK cells transfected with the different Copine-YFP constructs described above were subjected to protein immunoblotting and subsequently probed alongside two commercially available monoclonal antibodies targeting Copine-6. The results showed clearly on both counts that the polyclonal rabbit and both monoclonal mouse anti-Copine-6 antibodies gave the same sized band at 80kDa, as expected of the Copine-6-YFP molecular weight.

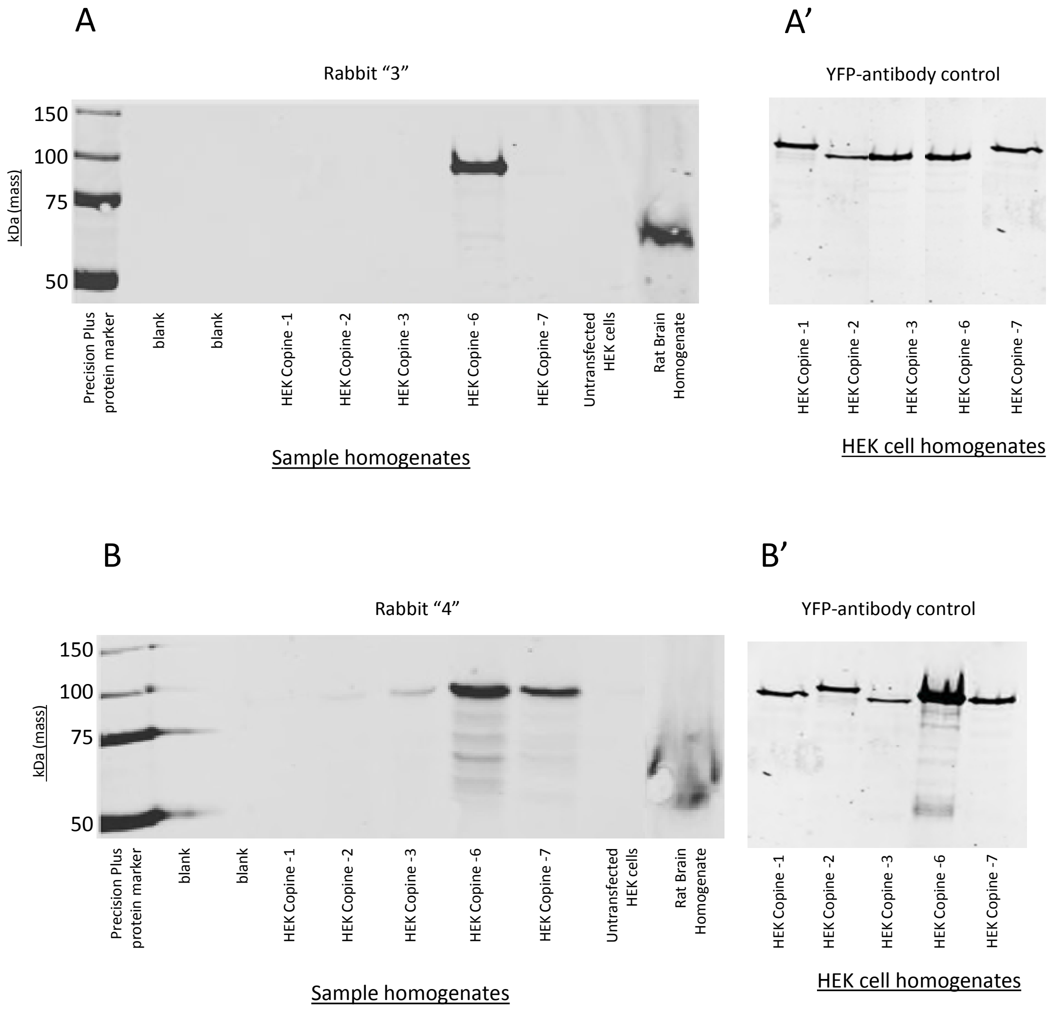

Figure 2-3 Protein immunoblotting of HEK cells with constitutive expression of Copines -1, -2, -3, -6 and -7, reacted with the affinity purified antibodies from rabbits 3 and 4.

HEK cells were transfected with the indicated Copine-YFP constructs and were analysed by protein immunoblotting. The membranes were reacted with the affinity purified antibodies from both rabbits 3 and 4. **A**. Rabbit 3 showed strong immuno-reactivity for *only* the HEK cells transfected with Copine-6-YFP. The immunoreactive band is visible at the expected molecular weight for Copine-6- YFP, approximately 80kDa, larger than the band for Copine-6 alone found in rat brain homogenate. The other lanes were blank showing that the antibody from rabbit 3 is reacting with Copine-6 alone. **A'**. All of the transfected HEK samples in blot A expressed the YFP-tagged Copine constructs, as demonstrated by YFP labelling following membrane strip and re-probe. **B**. Rabbit 4 showed some non-specific reactivity for Copine -3 and Copine -7. **B'**. All of the transfected HEK samples expressed the various YFP-tagged Copine constructs, as demonstrated by the identification of YFP in all samples using the anti-YFP antibody by membrane strip and re-probe.

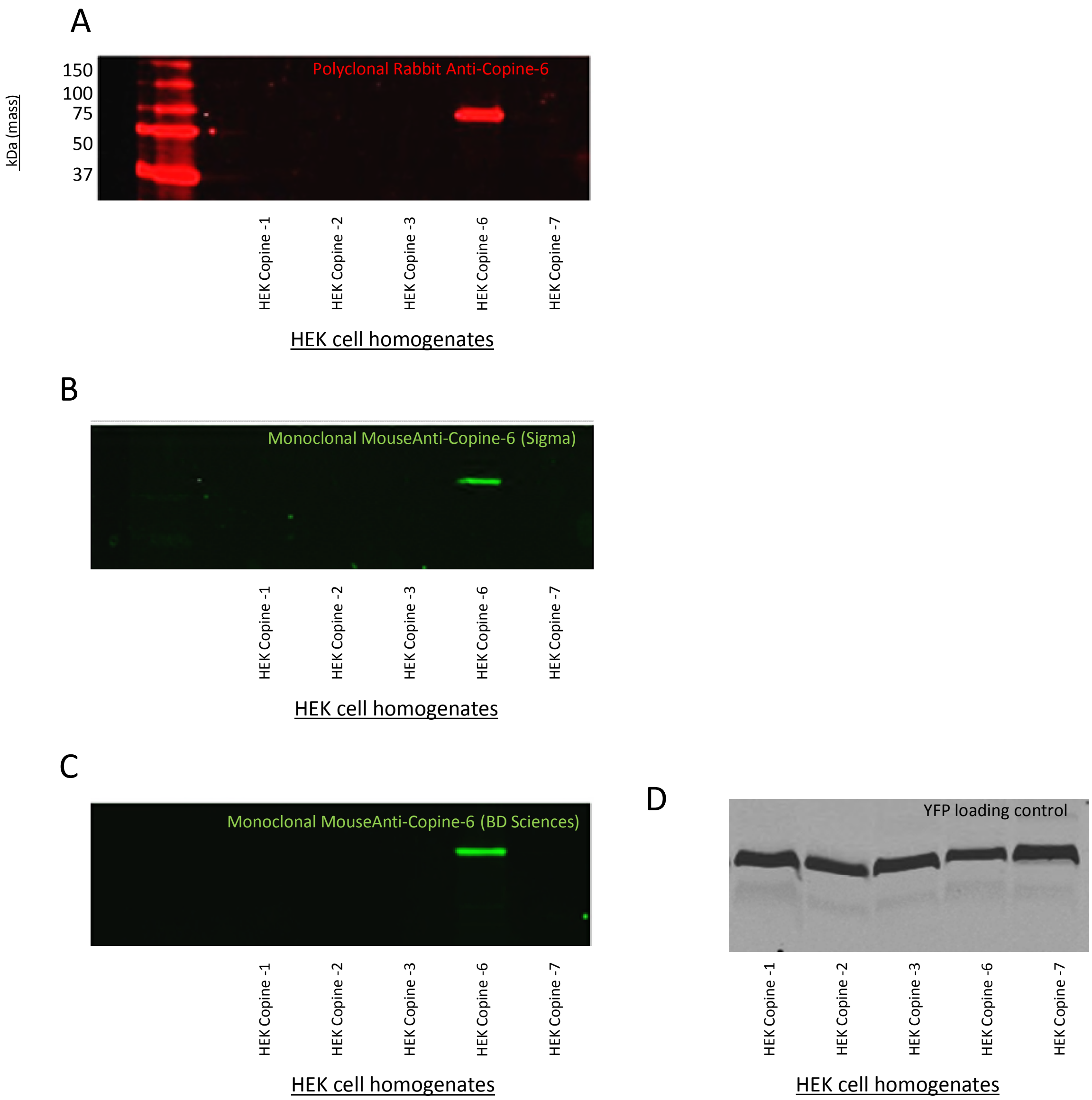

Figure 2-4 Protein Immunoblot analysis of the rabbit polyclonal anti Copine-6 from rabbit 3 compared to two commercially available monoclonal Copine-6 antibodies.

HEK cells with constitutive expression of Copine-YFP -1, -2, -3, -6 and -7 expression were subjected to gel electrophoresis and protein immunoblotting procedures. **A**. The membrane was reacted with the rabbit polyclonal targeting Copine-6 **B**. The membrane was reacted with mouse monoclonal anti-Copine-6 from Sigma Aldrich clone 6d11 **C**. The membrane was stripped and re-probed with mouse monoclonal anti- Copine-6 from BD Sciences clone 42. The band on all three images is identical in apparent molecular weight, and only visible in the HEK cell sample with Copine-6 expression. **D**. As before, the membranes were stripped and re-probed with mouse YFP antibody which confirmed successful sample loading on all gels and positive transfection as previously described (see Figure 2-3). The molecular markers were not visible in the channel wavelength used for the recognition of the mouse antibodies.

Since the antibody from rabbit 3 showed no reactivity with the other Copines available to test, and showed a similar immunoreactivity to these Copines as the two monoclonal antibodies raised to different immunogens, it was chosen as the preferred antibody for further characterization and from hereon will be referred to as the ‘Copine-6 antibody’.

2.3.3. The Copine-6 antibody from rabbit 3 identifies Copine-6 in brain

The expression of Copine-6 was investigated using rat brain homogenate and lysates from dissociated hippocampal cell cultures. When analysed by protein immunoblot, a 62kDa band could be seen in both brain and in the neuron culture samples, which were identical (but smaller in intensity) to the purified Copine-6 positive control (see Figure 2-5 Image A). This initial observation shows that Copine-6 can be identified in brain tissue using our polyclonal antibody. Protein immunoblotting and the subsequent application of the Copine-6 antibody to homogenised samples of rat brain, heart, liver, lung, muscle, spleen, stomach and kidney showed that the Copine-6 polyclonal antibody from rabbit 3 identified a protein band at approximately 62kDa in brain, again providing evidence for a strong and specific expression of Copine-6 in brain tissue (see Figure 2-5, Image B). All of the other rat tissue samples showed no reactivity with the antibody, and the simultaneous application of mouse anti-tubulin confirmed the equal protein loading and the presence of protein in every lane (see Figure 2-5, Image C)

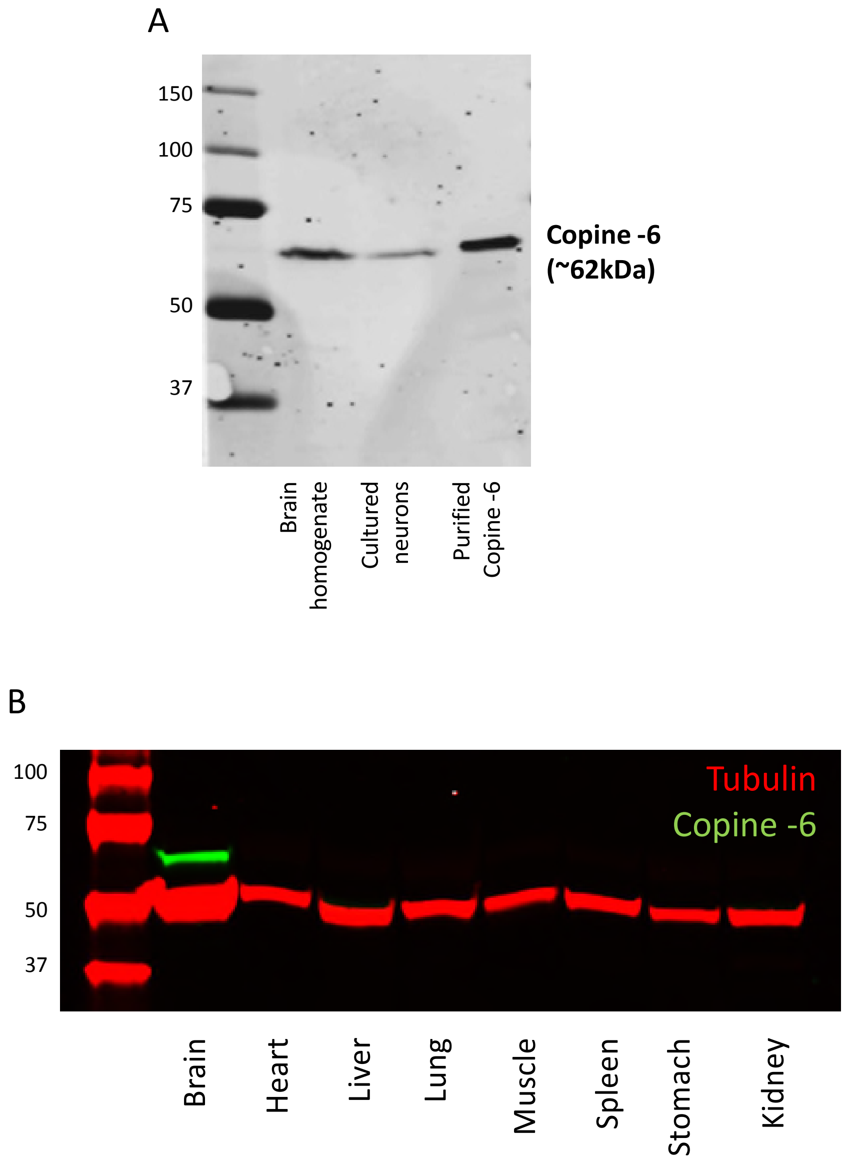

Figure 2-5 Rat tissue samples were subjected to protein immunoblotting to investigate the expression of Copine-6 in various tissues.

A. A Copine-6 reactive band is present in rat brain and dissociated neuronal culture loaded samples. Note the 62kDa band is identical to the positive purified Copine-6 control. **B**. When various different rat tissues were tested, Copine-6 was identified only in brain (Copine-6 shown in green at 62kDa) and was absent from the other tissues investigated. Mouse anti-tubulin (red) confirmed the presence of protein in every lane and that the same concentration of protein was loaded.

Brain tissue homogenised in the presence of the calcium chelator EGTA provided evidence for the calcium-depended membrane specific binding ability of Copine-6 (see Figure 2-6). In the presence of EGTA, a strong band at 62kDa was detected in the supernatant fraction. Very little Copine-6 was detected in the supernatant in the absence of EGTA. This suggests that the presence of calcium promotes membrane binding of Copine, whereas in the absence of calcium the Copine-6 is only weakly membrane associated. This behaviour is similar to that described for Copine-6 by Nakayama and co-workers (Nakayama *et al.*, 1998)

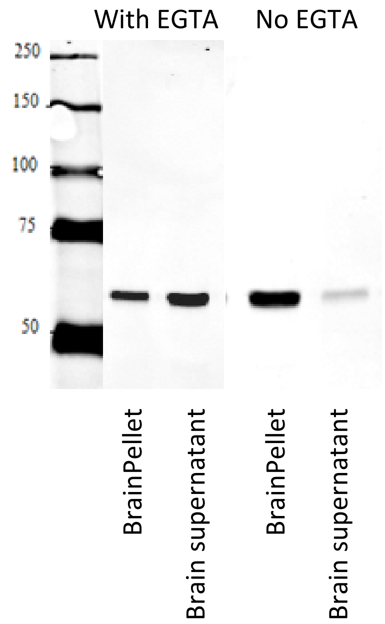

Figure 2-6 Protein immunoblot of adult rat brain pellet and supernatant in the presence and absence of EGTA.

In the presence of the calcium chelator EGTA, the membrane binding Copine-6 is reduced (blot on left hand side). In the presence of calcium (right hand side, no EGTA), Copine-6 binds to the brain membranes. Therefore in the presence of calcium, the majority of the Copine-6 is found bound to cell membranes and can be identified in the pellet.

The polyclonal antibody raised in rabbit 3 against the full length Copine-6 so far appears to be specific for Copine-6 alone, identifies Copine-6 in rat brain and neurons – but not other rat tissues – and exhibits calcium dependent binding similar to that previously described for Copine-6 (Nakayama *et al.*, 1998). The antibody also appears to give a strong immuno-reactive band in rat brain at an identical molecular weight to the two commercially available monoclonal anti-Copine-6 antibodies, and was therefore used to investigate the immunohistochemical distribution of Copine-6 in neurons and in brain.

2.3.4. The Copine-6 rabbit polyclonal antibody has an identical neuronal staining pattern as the commercial anti–Copine-6 monoclonal antibodies

In order to further characterise the specificity of the affinity purified anti Copine-6 described above, its immunoreactivity was compared to both the commercial monoclonal antibodies. Since our antibody was raised in rabbit and the monoclonal antibodies raised in mice, the cultures could be stained simultaneously with both reagents. Initially, dissociated hippocampal cell cultures, which contain neurons and glial cells, were employed to observe the expression pattern of Copine-6 in the culture. The immunohistochemical analysis shows that our polyclonal antibody indeed labelled a specific population of cells in the dissociated hippocampal cell culture, which had morphologies characteristic of neurons. This immunoreactive pattern was identical for both of the commercial monoclonal antibodies against Copine-6 (see Figure 2.7), with the same populations of cells reacting with the different antibodies. It was the case however that the polyclonal antibody gave a significantly stronger immunoreaction than the monoclonal antibodies. This meant that the extent of the immunolabelling for Copine-6 with the rabbit antibody tended to better delineate the dendritic arbour of the neurons, and picked out somatic and cytoplasmic labelling more clearly than the monoclonal antibodies.

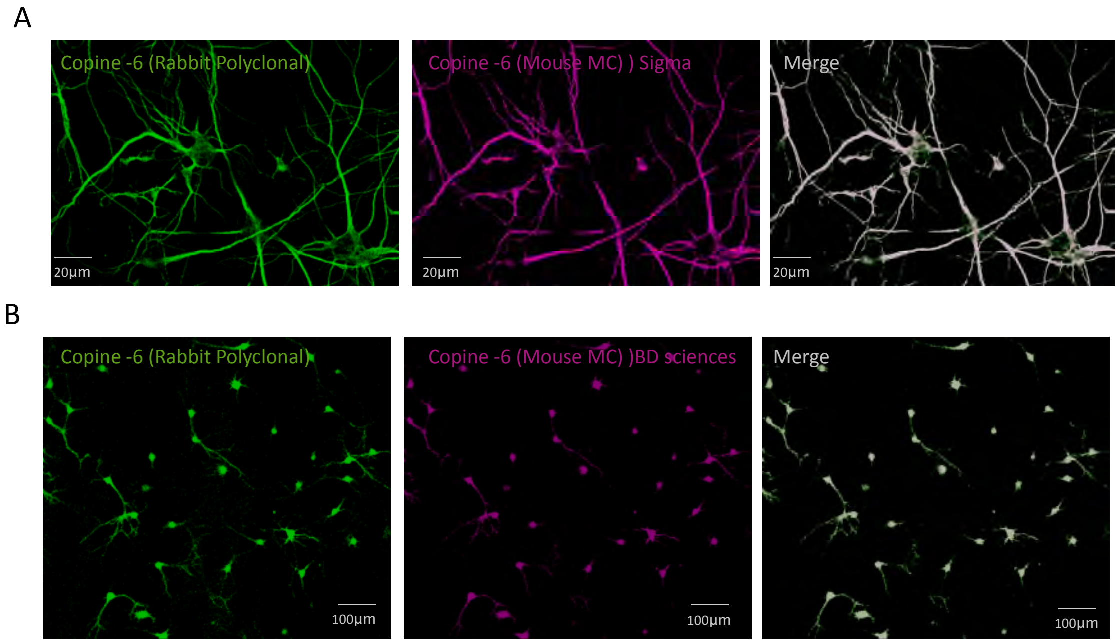

Figure 2-7 Immunohistochemical analysis of dissociated hippocampal culture comparing polyclonal rabbit anti-Copine-6 and two commercially available monoclonal anti-Copine-6

The immunocytochemical staining of cells in hippocampal culture confirmed that the characterised rabbit polyclonal antibody reacts with the same cells as two commercial monoclonal antibodies. **A**. Copine-6 staining using the polyclonal and Sigma monoclonal anti Copine-6. **B**. Copine-6 staining using the polyclonal and BD Sciences monoclonal anti Copine-6. The merge show co-reactivity (white) Note particularly in image B that the polyclonal antibody staining appears to be slightly stronger in comparison to the monoclonal antibody (purple). This may be a result of the antigen retrieval needed to optimise the BD Sciences monoclonal antibody.

In rat brain tissue sections, immunohistochemical staining of Copine-6 with our polyclonal antibody also yielded identical immunoreactivity as both commercial monoclonal Copine-6 antibodies. Without exception, all the same cells were labelled with all three antibodies. There was minimal background staining with all three antibodies in the tissue sections, and all immunopositive cells had well defined somatic and cytoplasmic immunostaining. Depending on location some cells also exhibited Copine-6 positive extensive dendritic arborisations. However, as mentioned earlier, the monoclonal antibodies gave a much weaker signal when expression intensity was compared to our polyclonal antibody. It is to be noted, however, that the monoclonal anti- Copine-6 from BD Biosciences did require antigen retrieval for optimal staining, and this was presumably necessary to expose the epitope recognised by this antibody. The antigen retrieval process slightly reduced the strength of the immunoreaction of our polyclonal antibody, but it did not alter its pattern of reactivity in the cells.

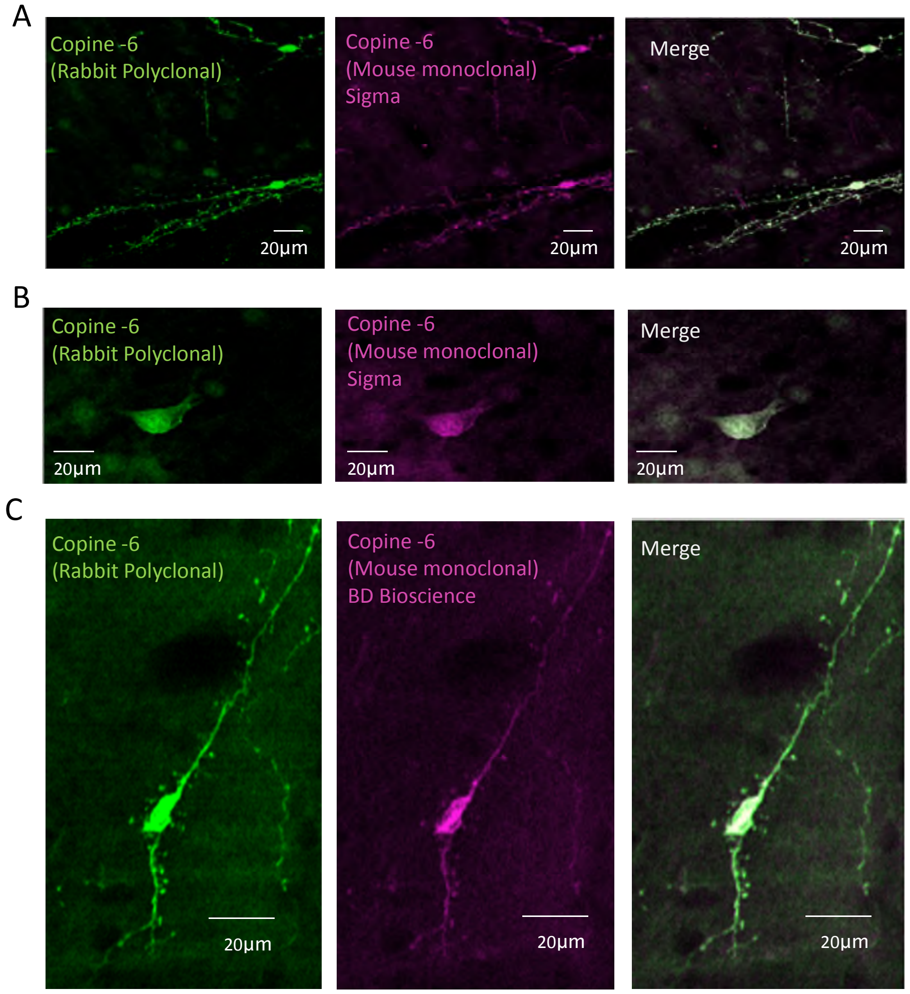

Figure 2-8 Immunohistochemical analysis of Copine-6 in adult rat brain sections using polyclonal rabbit Copine-6 and commercial monoclonal Copine-6 antibodies.

Rabbit anti-Copine-6 was applied histochemically to determine its applicability when compared to the commercially available monoclonal antibodies targeting Copine-6. Cells were identified in various regions of the brain and both commercial antibodies were used. **A**. The mouse anti Copine-6 from Sigma Aldrich co-labelled the same Copine-6 polyclonal labelled cells in the corpus callosum, and **B**. in the neocortex. **C**. The mouse anti-Copine-6 from BD Sciences also co-labelled cells in the deep corpus callosum where it meets the lateral ventricle. The location of these cells is noted as unusual (see 2.4 Discussion).

2.4. Discussion

The polyclonal antibodies of rabbits 3 and 4 were both raised to full length Copine-6 protein. In general, polyclonal antibodies have a higher risk of cross reactivity than monoclonal antibodies when employed for immunohistochemistry since they consist of different antibody immunoglobulin molecules which have specific binding sites that recognise different epitopes, or antigenic determinants, which make up the protein. In contrast, monoclonal antibodies are clones of a single immunoglobulin molecule targeting one single epitope with high affinity. Monoclonal antibodies have less scope for non-specific binding or cross reactivity with other proteins, particularly if the epitope is unique to the protein in question. In general, polyclonal antibodies – if specific – can give greater stronger immunoreactions, since they bind multiple epiptopes. This may however result in an increased risk of cross reactions with other proteins, particularly if these proteins contain conserved peptide sequences. The Copine family of proteins share conserved sequences, and they also share some common domains with other proteins such the C2 or vWA domains (See Chapter 1: Introduction, for detail). With this in mind, a full molecular characterisation of our polyclonal antibody was required – particularly in the absence of a knock out animal – in order to ensure that we were working with an antibody that identifies Copine-6 specifically. In order to minimise possible cross reactions with other Copines, the Copine-6 antiserum was first passed through a column containing purified Copine -2 before affinity purification. Following this, only one of the two polyclonal antibodies raised against Copine-6 was specific for Copine-6 alone, and, following protein immunoblotting, recognised a band at the appropriate molecular weight in cells transfected with Copine-6, and in homogenates of neuronal cultures and brain. A band with the same molecular weight was also identified, albeit more weakly, by two commercial monoclonal antibodies. The stronger immunoreactivity of the polyclonal antibody most probably reflects the greater number of epitopes being recognised by the Copine-6 antibody. The affinity purified anti Copine-6 from rabbit 3 did not react with Copines -1, -2, -3 or -7 when these were overexpressed in HEK 293 cells. It should be noted that polymerase chain reaction analysis of HEK 293 cells has shown the presence of mRNA for Copines -1, -2, -3, -7 and -8 in these cells, but not Copine-6 (McIlhinney, unpublished).

Protein immunoblotting of various rat tissue homogenates identified the presence of Copine-6 in brain, and its absence from heart, jejunum, thymus, kidney testis, and liver. This reflects the literature, which initially coined Copine-6 as the brain specific

'N'(neuronal)-Copine (Nakayama *et al*, 1999; Cowland *et al*. 2003; Creutz *et al*. 1998). However, based on the protein immunoblotting data, we cannot confidently state that Copine-6 is exclusive to brain. The 'neuron' specific status, suggested by the immunocytochemical analysis of neuronal cultures, may also apply to peripheral neurons.

In order to further characterise the specificity of the Copine-6 antibody, neuronal cultures and brain sections were reacted with it and with two different monoclonal antibodies, raised against different antigens. Whilst the monoclonal antibodies have not been epitope mapped, the fact that they were derived using different antigens increases the probability that they recognise different epitopes on Copine-6. Indeed, the fact that it was necessary to use antigen retrieval with the BD Sciences monoclonal antibody but not the Sigma supplied antibody suggests that this could be the case. The results from these studies were unequivocal, all of the cells identified as Copine-6 positive by the rabbit 3 antibody were also immuno-positive when either of the monoclonal antibodies were used. Indeed the major different in the immunoreaction patterns between these different antibodies lay principally in the stronger signal obtained with the polyclonal antibody. This tended to better delineate the cell axons and dendrites in culture and in the brain slices.

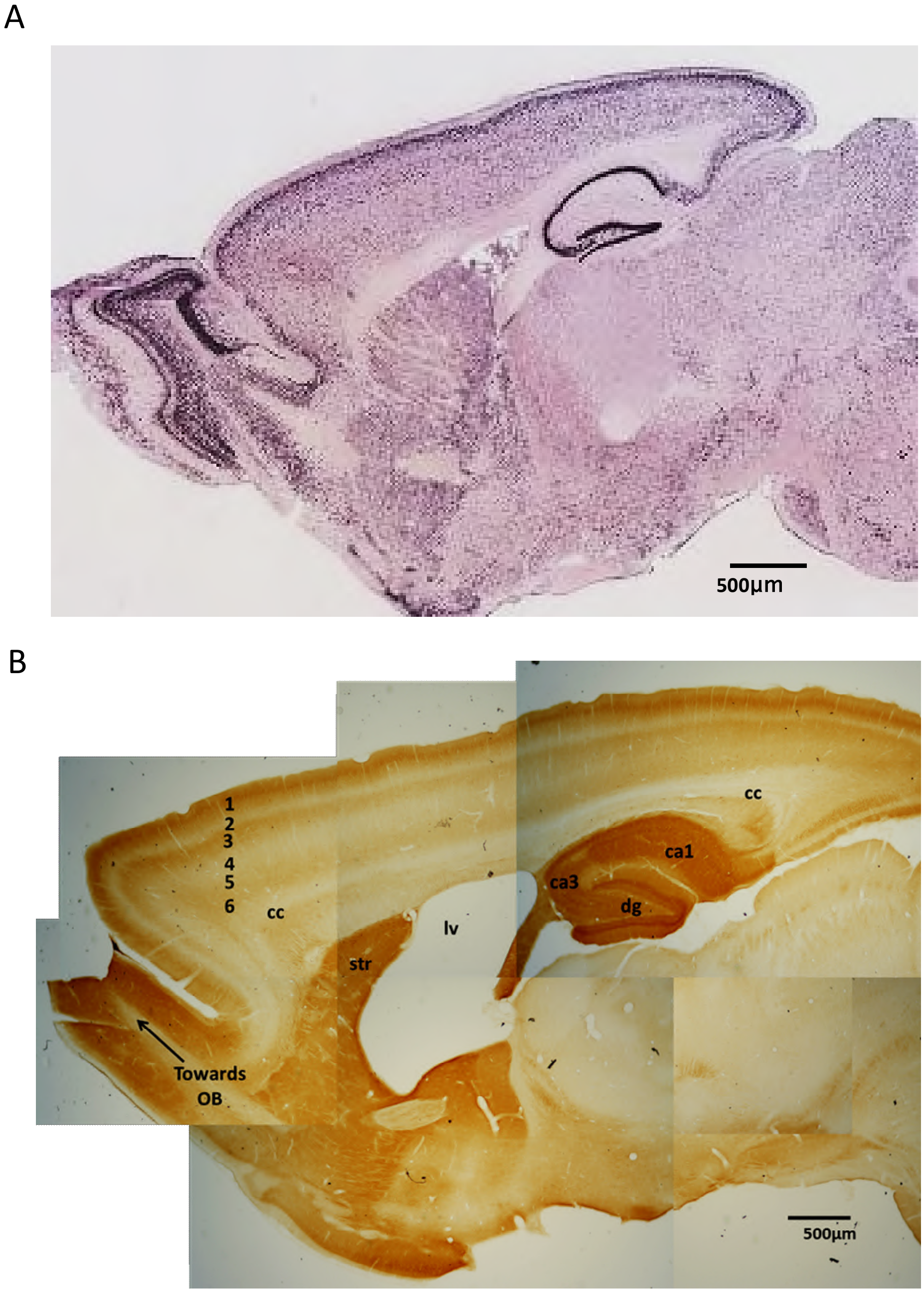

Figure 2-9 An overview of Copine-6 in the adult rat brain

Parasagittal sections ~3.90mm lateral of the midline. **A.** *In situ* hybridisation showing mRNA expression of CPNE6 in mouse, strain C57BL/6J, taken from mouse.brain-map.org. **B**. Protein expression of Copine-6 following immunohistochemical analysis, X20 magnification. Images were collated to show regional distribution. In both images, the Copine-6 staining shows a layered pattern in the neocortex, with stronger staining in layers 1, 2/3 and 6. The hippocampus shows strong staining throughout, with layered staining in different regions of the dentate gyrus, and CA1/CA3. The olfactory bulb was removed from the section in B; however a stronger staining pattern can be seen en route to the OB (arrow). The striatum is also strongly stained compared to other regions. OB, Olfactory bulb; CC corpus callosum; dg dentate gyrus; Str striatum, lv lateral ventricle.

In conclusion, I have shown that the rabbit 3 antibody following absorption and affinity purification reacts specifically with a 62kDa band in cells transfected with Copine-6, and not with other Copines. A similar band is found by protein immunoblot of brain tissue, and is also recognised by two different monoclonal antibodies raised to different fusion protein of Copine-6. Furthermore, the antibody identifies the same population of cells in neuronal culture and brain slices as the monoclonal antibodies. In addition, the antibody reacts with the same brain regions that had previously been documents as expressing high levels of both Copine-6 mRNA and protein in mouse brain (Nakayama *et al.*, 1998; Nakayama, Yaoi, & Kuwajima, 1999), namely the Olfactory bulb, hippocampus, and some cells of the cortex (see Figure 2-9). This antibody therefore seems suitable for use to examine the developmental and anatomical expression of Copine-6 in rat brain.

Chapter 3. **Immunohistochemical analysis of Copine-6 immuno-positive cells**

3.1. Introduction

Copine-6, or N-Copine, has been documented to be expressed in a neuron specific manner in the brain (Cowland *et al.*, 2003; Nakayama *et al*, 1999; Nakayama *et al*, 1998). In human and rodent brain, Copine-6 has been identified to be expressed in the hippocampal formation and the olfactory bulbs, with slightly lower expression in certain layers of the neocortex (Cowland *et al.*, 2003; Nakayama *et al.*, 1999; Nakayama *et al* , 1999, Nakayama *et al*, 1998). In Chapter 2 of this thesis, the histochemical application of our specific polyclonal antibody targeting Copine-6 confirmed the presence of Copine-6 in adult rodent brain, in the same regions documented previously. However, to date, the anatomical and cellular expression of Copine-6 protein in individual neurons has not been described in detail. Moreover, the intracellular distribution of Copine-6 has not been described.

Neurons are typically described and classified according to various morphological, physiological and molecular features within the region of the brain in which they are located. For the ideal classification of a neuronal population, all of these functional properties should be considered. However one or more of these properties might be sufficient to describe specific subpopulations of neurons within a brain region. As the techniques for the histochemical detection of cell molecules have improved, there has been developed a continuously expanding library of ‘cell markers’ that can be used to identify novel neuronal cell populations in defined regions of the brain. For example, cortical interneurons are often evaluated against a set of criteria known as Petilla terminology, which consider morphological, molecular and electrophysiological cell properties, all of which can be used to aid classification of other neuronal populations (Ascoli *et al.*, 2008). Furthermore, in an attempt to systematically classify GABAergic interneurons of the cerebral cortex, a taxonomical web-based method has recently been introduced based on agreed pre-determined criteria of interneurons (DeFelipe *et al.*, 2013).

The Copine-6 cells that have previously been identified in brain (Nakayama *et al.*, 1999) have been subsequently confirmed in this thesis (see Chapter 2). However, although the Copine-6 expressing cells are structurally typical of neurons, this does require histochemical confirmation. In this chapter, immunohistochemical analysis of rat brain using established cell markers alongside the polyclonal antibody against Copine-6 described in Chapter 2, confirmed that Copine-6 labels only neurons, as suggested by the Nakayama group (Nakayama *et al.*, 1999). In addition I have identified novel populations of neurons expressing Copine-6 in different rat brain regions. These neuronal populations can be identified consistently in dissociated neuronal cultures and in brain tissue sections, and have been subjected to a full immunohistochemical characterisation at the level of the light microscope.

3.2. Materials and Methods

3.2.1. Dissociated cell culture

Environmental conditions and all procedures that were performed were in accordance with the Animals Scientific Procedures Act of 1986 (UK).Female Sprague–Dawley rats (200-350g; Charles River, Margate, Kent, UK) were killed by schedule 1 methods and embryos were extracted at embryonic day 18. Hippocampus and olfactory bulb (including lower rostral migratory stream) were dissected by Dr Pavel Perestenko and were dissociated in HBSS and trypsin. Cells were plated and maintained on 13mm glass Coverslips (Menzel Glaser, No.1, 13mm, Cat No. CB00130RA1) in 500µl Neurobasal media supplemented with B27 (1X, diluted 1:50, Invitrogen 17504-044), 1.25ml of 200mM glutamine and 5ml Penicillin Streptomycin at 37˚c in an atmospheric incubator with 5% CO_2. The standard age of culture used for immunohistochemical analysis was 21 days *in vitro*, since at this time the neurons were considered to be at their most stable, healthy and reasonably mature.

3.2.1.1. **Cell Culture Immunocytochemistry by Indirect Immunofluorescence.**

When required for analysis, the cells were fixed on the coverslip using 4% Paraformaldehyde for 10 minutes, and permabilised by 10 minute exposure to Tris-buffered saline (0.05M Tris HCl + 0.15M NaCl. pH 7.6) , + 0.05% Triton X-100 in ddH_20. Bovine serum albumin (1% in phosphate buffer solution) containing 0.1% normal donkey serum was used to block the coverslips for 1 hour at room temperature. Antibodies were then applied as described below. Rabbit polyclonal antibody against Copine-6 was applied to cells in culture together with different primary antibodies (for dilutions and details, see Table 1. Coverslips were left with gentle rocking overnight at 4°C. Sections were washed in PBS four times, for 15 minutes, and fluorophore conjugated secondary antibodies were applied as described in Table 1 for a minimum of 4 hours. Imaging was carried out using Zeiss Axiovert 100M confocal microscope, lasers HeNe1S43 and ArgonS14, wavelengths 543Cy3 and 488FITC, with objectives x10, x20, x40 and x60. Images were analysed using LSM Image Browser and Image J.

Table 1 Primary antibodies for immunocytochemistry (dissociated cell cultures)

Antigen	Marker	Species	Supplier	Product Code	Dilution	Secondary Fluorophore
Copine-6	--	Rabbit	McIlhinney Lab	--	1:1000	Alexa Fluor 488 donkey anti rabbit IgG(H+L) A21206, Invitrogen, 1:1000
MAP-2	Dendrites of Neurons	Chicken	Aves Labs, US	#MAP	1:500	CY3 donkey anti Chicken IgG (H+L) 703-165-155, Jackson's Labs, 1:500
		Mouse	Sigma Aldrich, UK	M4403	1:500	Cy3 donkey anti mouse IgG (H+L) 715-165-150, Jackson's Labs, 1:500
Synaptophysin (clone SVP-38)	Neuronal spines	Mouse	Sigma Aldrich, UK	S5768	1:20	Cy3 donkey anti mouse IgG (H+L) 715-165-150, Jackson's Labs, 1:500
Ankyrin-G	Axon initial segment	Goat	Santa Cruz, US	Sc-31778	1:1000	Cy3 donkey anti goat IgG (H+L) 705-165-003, Jackson's Labs, 1:500
GAD67	GABAergic neurons	Goat	Chemicon (Millipore), US	MAB5406	1:500	Cy3 donkey anti goat IgG (H+L) 705-165-003, Jackson's Labs, 1:500
Calretinin	Calcium Binding protein Calretinin	Goat	Swant, Switzerland	CG1	1:500	Cy3 donkey anti goat IgG (H+L) 705-165-003, Jackson's Labs, 1:500
Tuj1, Neuron Specific Beta III Tubulin	Neuronal tubulin	Mouse	R & D Systems, US	MAB1195	1:200	Cy3 donkey anti mouse IgG (H+L) 715-165-150, Jackson's Labs, 1:500

3.2.2. Section preparation of adult rat brain in the parasagittal plane

Procedures were carried out on Sprague–Dawley rats (200-350g; Charles River, Margate, Kent, UK, n=10). Environmental conditions and all procedures that were performed were in accordance with the Animals Scientific Procedures Act of 1986 (UK).) Rats were deeply anaesthetised using isofluorane (4% in O_2) and euthanized with pentobarbitone (200 mg/kg; i.p.; Sagatal; Rhône Mérieux, Tallaght, Dublin, Ireland), and transcardially perfused via the ascending aorta with 100mL 0.1M PBS, followed by 300mL 4 % paraformaldehyde, 0.05 % glutaraldehyde. In some cases 0.2% picric acid in 0.1M PB (pH 7.4) was also used. Brains were immediately removed and postfixed in 4% paraformaldehyde in 0.1M PB for 24 hours before being sectioned at 50μM intervals in the sagittal plane on a Leica VT1000s vibrating microtome. Sections were collected in 5 vials, so each vial contained every fifth section which were stored in PBS containing 0.5% sodium azide until required. Sections were washed in PBS prior to antibody application to ensure fixative was completely removed.

3.2.2.1. **Immunohistochemical analysis of adult rat brain**

Rabbit polyclonal antibody against Copine-6 was immunohistochemically applied to parasagittal sections of rat brain, alongside several different antibodies targeting different antigens, in order to characterise different Copine-6 neuronal populations. All antibodies and their antigens, including marker details, are listed in Table 2. Imaging was carried out using Zeiss Axiovert 100M confocal microscope, lasers HeNe1S43 and ArgonS14, wavelengths 543Cy3 and 488FITC, with objectives x10, x20, x40 and x60. All images are single scans unless otherwise stated to be z-stacks. Images were analysed using LSM Image Browser, Image J and cell distribution was analysed using MBF Stereoinvestigator.

Table 2 Primary antibodies for immunohistochemistry (rat brain sections)

Antigen	Marker	Species	Supplier	Product Code	Dilution	Secondary Fluorophore
Copine-6	Calcium Binding protein	Rabbit	McIlhinney Lab	--	1:1000	Alexa-Fluor 488 Donkey anti rabbit A21206, Invitrogen, 1:1000
						CY3 Donkey anti-rabbit 711-165-152, Jackson's labs, 1:1000
Copine-6	Calcium Binding protein	Mouse (clone 42)	BD Biosciences, UK	612638	1:200	Cy3 donkey anti-mouse IgG (H+L) 715-165-150, Jackson's Labs, 1:500
Copine-6	Calcium Binding protein	Mouse Clone 6d11	Sigma Aldrich, UK	06272-6511	1:200	Cy3 donkey anti-mouse IgG (H+L) 715-165-150, Jackson's Labs, 1:500
NeuN	Neuronal nuclei	Mouse (clone A60)	Millipore, US	MAB377	1:1000	Cy3 donkey anti-mouse IgG (H+L) 715-165-150, Jackson's Labs, 1:500
						Alexa-Flour 647 donkey anti-mouse IgG (H+L) 715-605-150, Jackson's labs, 1:1000
Calretinin	Calcium Binding protein calretinin	Goat	Swant, Switzerland	CG1	1:1000	Cy3 donkey anti-goat IgG (H+L) 705-165-003, Jackson's Labs, 1:500
						Alexa-Flour 647 donkey anti-goat IgG (H+L) 705-605-003, Jackson's labs, 1:1000
Calretinin		Mouse	Millipore, US	MAB1568	1:500	Cy3 donkey anti-mouse IgG (H+L) 715-165-150, Jackson's Labs, 1:500
Calbindin D29K (Calretinin)		Rabbit	Synaptic Systems, Germany	214 102	1:500	CY3 Donkey anti-rabbit 711-165-152, Jackson's labs, 1:1000
Tuj1, Neuron Specific Beta III Tubulin	Neuronal tubulin	Mouse	R & D Systems, US	MAB1195	1:200	Cy3 donkey anti-mouse IgG (H+L) 715-165-150, Jackson's Labs, 1:500
GFAP (glial fibrillary acidic protein)	Mature Glial intermediate filament	Mouse	Sigma Aldrich, UK	G3893	1:400	Cy3 donkey anti-mouse IgG (H+L) 715-165-150, Jackson's Labs, 1:500
Vimentin	Immature Glia intermediate filament	Mouse	Sigma Aldrich, UK	V6630	1:200	Cy3 donkey anti-mouse IgG (H+L) 715-165-150, Jackson's Labs, 1:500
Doublecortin	Migrating (immature) Neuroblast	Goat	Santa Cruz, US	SC-8066	1:500	Cy3 donkey anti-goat IgG (H+L) 705-165-003, Jackson's Labs, 1:500

Immunohistochemical analysis of Copine-6 immunoreactive cells

Antigen	Marker	Species	Supplier	Product Code	Dilution	Secondary Fluorophore
Nestin	Immature neuron intermediate filament	Mouse	Abcam, UK	Ab6142	1:500	Cy3 donkey anti-mouse IgG (H+L) 715-165-150, Jackson's Labs, 1:500
Reelin	Neuronal glycoprotein	Mouse	Abcam, UK	Ab18570	1:1000	Cy3 donkey anti-mouse IgG (H+L) 715-165-150, Jackson's Labs, 1:500
PSA-NCAM	Neuronal cell adhesion molecule (glycoprotein)	Mouse	Millipore, US	MAB5324	1:200	Cy3 donkey anti-mouse IgG (H+L) 715-165-150, Jackson's Labs, 1:500
GAD67	GABAergic neuron	Goat	Chemicon (Millipore), US	Mab5406	1:500	Cy3 donkey anti-goat IgG (H+L) 705-165-003, Jackson's Labs, 1:500
						Alexa-Flour 647 donkey anti-goat IgG (H+L) 705-605-003, Jackson's labs, 1:1000
VGAT	Pre-synaptic vesicular GABA-amino acid transporter	Guinea Pig	Synaptic Systems, Germany	131 004	1:500	Cy3 donkey anti-goat IgG (H+L) 705-165-003, Jackson's Labs, 1:500
						Alexa-Flour 647 donkey anti-goat IgG (H+L) 705-605-003, Jackson's labs, 1:1000
Gephyrin	Inhibitory post-synaptoc	Mouse	Synaptic Systems, Germany	147 011	1:500	Cy3 donkey anti-mouse IgG (H+L) 715-165-150, Jackson's Labs, 1:500
Ankyrin -G	Axon Initial Segment	Goat	Santa Cruz, US	Sc-31778	1:1000	Cy3 donkey anti goat IgG (H+L) 705-165-003, Jackson's Labs, 1:500
Enkephalin	Peptide transmitter	Mouse	Chemicon, US	MAB350	1:500	Alexa-Flour 647 donkey anti-goat IgG (H+L) 705-605-003, Jackson's labs, 1:1000
Calbindin D28K	Calcium Binding protein Calbindin	Mouse	Swant, Switzerland	CB300	1:1000	Cy3 donkey anti-mouse IgG (H+L) 715-165-150, Jackson's Labs, 1:500
GABABR1 GABA-B receptor	GABA receptor	Mouse	NeuroMab, US	N93A/49	1:500	Cy3 donkey anti-mouse IgG (H+L) 715-165-150, Jackson's Labs, 1:500
NECAB1	Neuron calcium signalling protein	Mouse	Abnova, US	H00064168-B01P	1:500	Cy3 donkey anti-mouse IgG (H+L) 715-165-150, Jackson's Labs, 1:500
Parvalbumin	Calcium Binding protein	Guinea Pig	Synaptic Systems	195004	1:500	Alexa-Flour 647 donkey anti-goat IgG (H+L) 705-605-

Immunohistochemical analysis of Copine-6 immunoreactive cells

Antigen	Marker	Species	Supplier	Product Code	Dilution	Secondary Fluorophore
Somatostatin	Hormone transmitter	Mouse	Genetex	GTX71935	1:500	Cy3 donkey anti-mouse IgG (H+L) 715-165-150, Jackson's Labs, 1:500

3.3. Results

3.3.1. A general overview of Copine-6 histochemistry

The Copine-6 polyclonal antibody labelled several different neuronal populations in both dissociated neuronal cell cultures of hippocampus and olfactory bulb and in rat brain sections.

In rat brain sections, Copine-6 immunoreactive cells were identified in the following areas.

In the **hippocampus**, Copine-6 expression was strong in a majority if CA1 – CA3 pyramidal cells, and in some granule cells of the dentate gyrus (see Section 3.3.4).

In the **olfactory bulb** Copine-6 expression allowed clear distinction to be made between each layer of the main bulb, with strong expression of the protein in the granule and glomerular layers. Individual cells were well defined by the Copine-6 antibody with the granule cell layer showing heterogeneity in the immmunoreactivity for Copine-6 (see section 3.3.5).

These results are in accordance with a previous study in rat brain using *in situ* hybridisation for Copine-6 mRNA and antibodies to detect the protein (Nakayama *et al*, 1999).

In the **cortex**, three morphologically distinct populations of cells were identified. Firstly, a weakly expressing 'band' of very tightly packed cells (~15-20µm) could be seen throughout layer II-III of the neocortex (see section 3.3.6). Secondly, a sparse population of cells with a faintly stained, larger soma (~25µm) could be seen through most layers, particularly in layers III-IV of the neocortex (see section 3.3.6). Thirdly, in layer VI of the neocortex and often branching into and on the periphery of the white matter of the corpus callosum, a novel population of cells with intense immunoreactivity for Copine-6 were distributed in a 'chain-like' manner. They have small soma (~10-20µm) with long ornamented arborisations. These cells appear to border the rostral-caudal axis in the most medial of parasagittal-cut sections, following the rostral migratory stream (RMS) and the anterior hippocampal continuation (AHC) running above the striatum and hippocampus, respectively. (Figure 3-1, section 3.3.7).

Each of these Copine-6 immunopositive cell populations described above were further characterised using different molecular markers, and the novel Copine-6 cells in the corpus callosum and RMS cells are described in more detail in section 3.3.7.

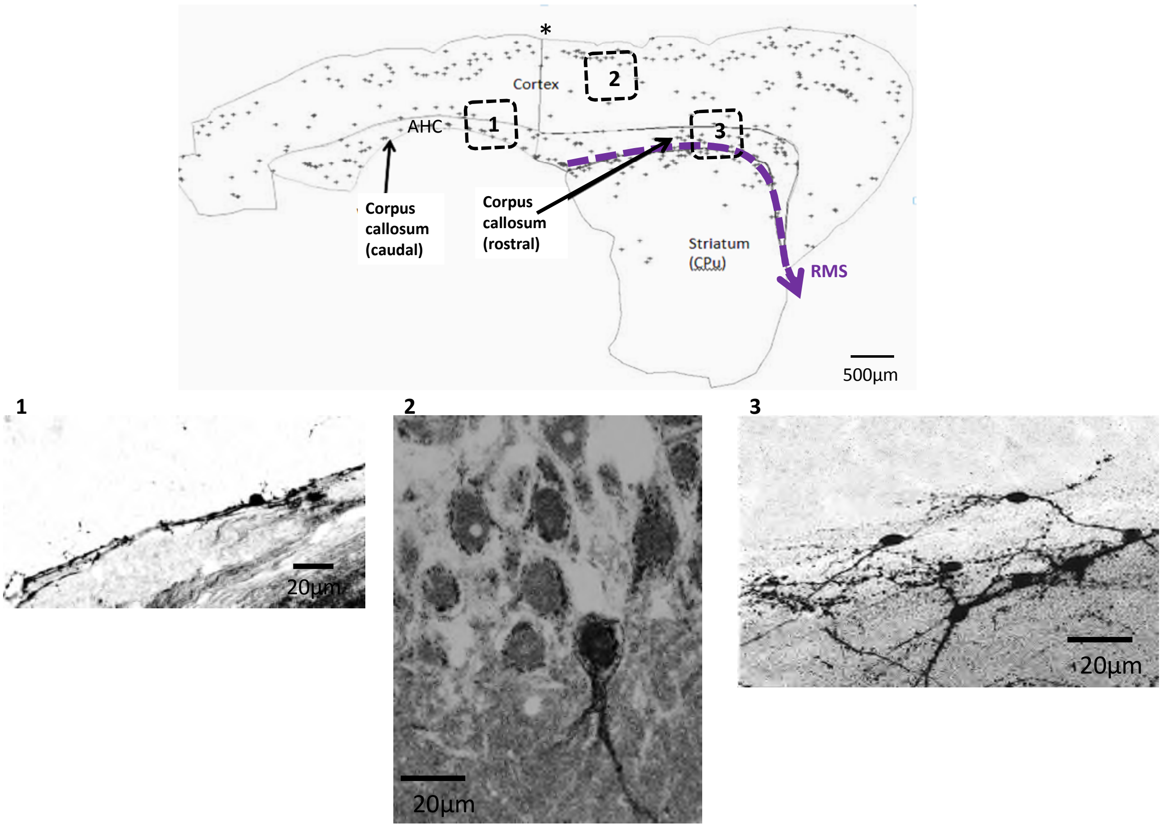

Figure 3-1 Mapping the distribution of Copine-6 immunoreactive cells in the rat brain using MBF Stereoinvestigator

A medial parasagittal section ~2.90mm lateral of the midline. Different populations of Copine-6 cells are present, which populate the cortex and white matter of the corpus callosum, following the anterior hippocampal continuation (AHC) and the rostral migratory stream (RMS). A few Copine-6 reactive cells were seen branching into the dorsal striatum (CPu, caudate putamen). * indicates the mid-point line where the section had to be analysed in two halves. The Copine-6 cells found in three regions (1. Caudal corpus callosum, 2. Cortex, 3.rostral corpus callosum) are shown in images 1-3.

3.3.2. Immunohistochemical analysis of cultured dissociated hippocampal neurons.

Dissociated hippocampal neurons were used in the first instance to study the intracellular distribution of Copine-6 in neurons. Dissociated hippocampal cultures at 21d.i.v. were used as standard, since the cells were well established and were consistently healthy and relatively mature. Copine-6 expression was heterogeneous with ~85% of all neurons labelling for Copine-6 and of those that were immunopositive for Copine-6, some were more intensely stained than others. [The number of neurons immuno-positive for Copine-6 throughout development is analysed in detail in Chapter 4]. The heterogeneity of Copine-6 expression was evident in the different intensities of immmunoreactivity seen in the soma and dendritic arbors of different cells. Immunoreactivity for Copine-6 was found in both axons and dendrites, though not all of the cells showed strong axonal staining. Plasma membrane staining for the protein could be seen as well as cytoplasmic staining in most of the cells. The nucleus was not particularly immunopositive in any of the hippocampal cells. (See Figure 3-2).

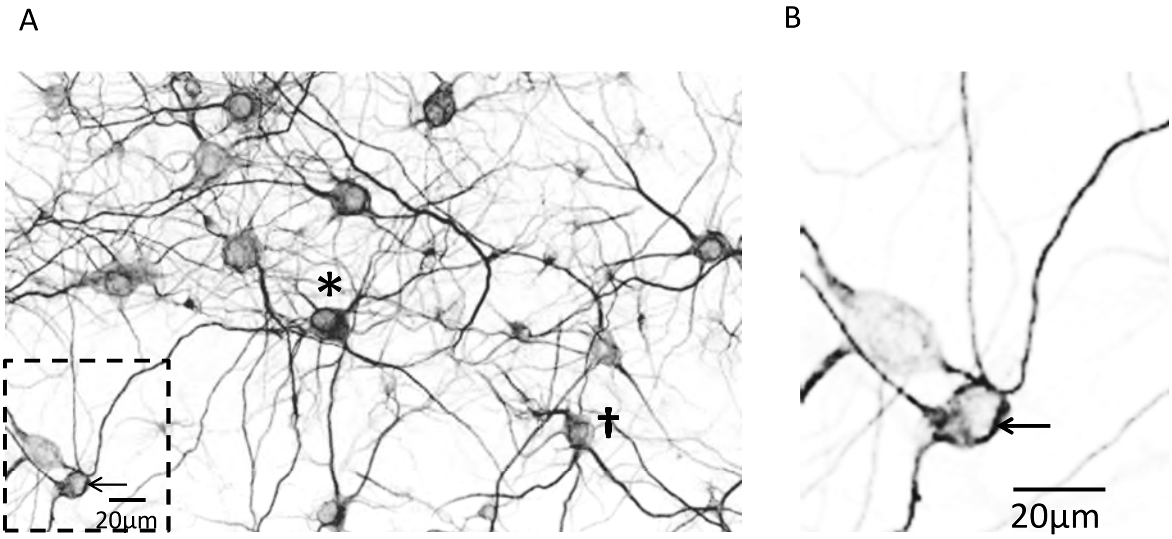

Figure 3-2 Immunohistochemical analysis of dissociated hippocampal cultures following 21 days *in vitro* show a heterogeneous immunoreactivity for Copine-6.

Cells were immunostained for Copine-6 to investigate the general expression pattern of Copine-6 in a 21 day *in vitro* culture. Some neurons were more intensely immunopositive than others. **A**. The different staining pattern of Copine-6 in different neurons. Some cells labelled for Copine-6 in the soma and dendrites with little nuclear staining (*), whereas some cells have a weakly expressing soma but strongly expressing dendritic arbor (†). Some cells exhibited strong plasma membrane reactivity (arrow). **B**. Enlarged image of the Copine-6 +ve cells in the dotted box (Image A) which emphasises the apparent plasma membrane localisation of the protein (Arrow). All images are single scans using x20 and x40 objective, respectively.

To confirm that the Copine-6 cells in the dissociated hippocampal culture were indeed neuronal, immunohistochemistry was carried out using the Copine-6 antibody alongside markers for NeuN (neuronal nuclei), TUJ-1 (neuron specific class III Beta tubulin), MAP2 (neuronal microtubule associated protein 2) , GFAP (Glial fibrillary acidic protein), and Ankyrin –G (a scaffolding protein associated with voltage gated sodium channels that are dense at the site of the axon initial segment of all neurons with an axon). All of the Copine-6 immunopositive cells in the dissociated hippocampal culture were immunopositive for NeuN, TUJ-1, MAP2, and Ankyrin –G, confirming that they are neuronal. The cells were repeatedly immunonegative for GFAP, confirming that they are not astrocytes or other glial cells labelled by these markers. (Figure 3-3).

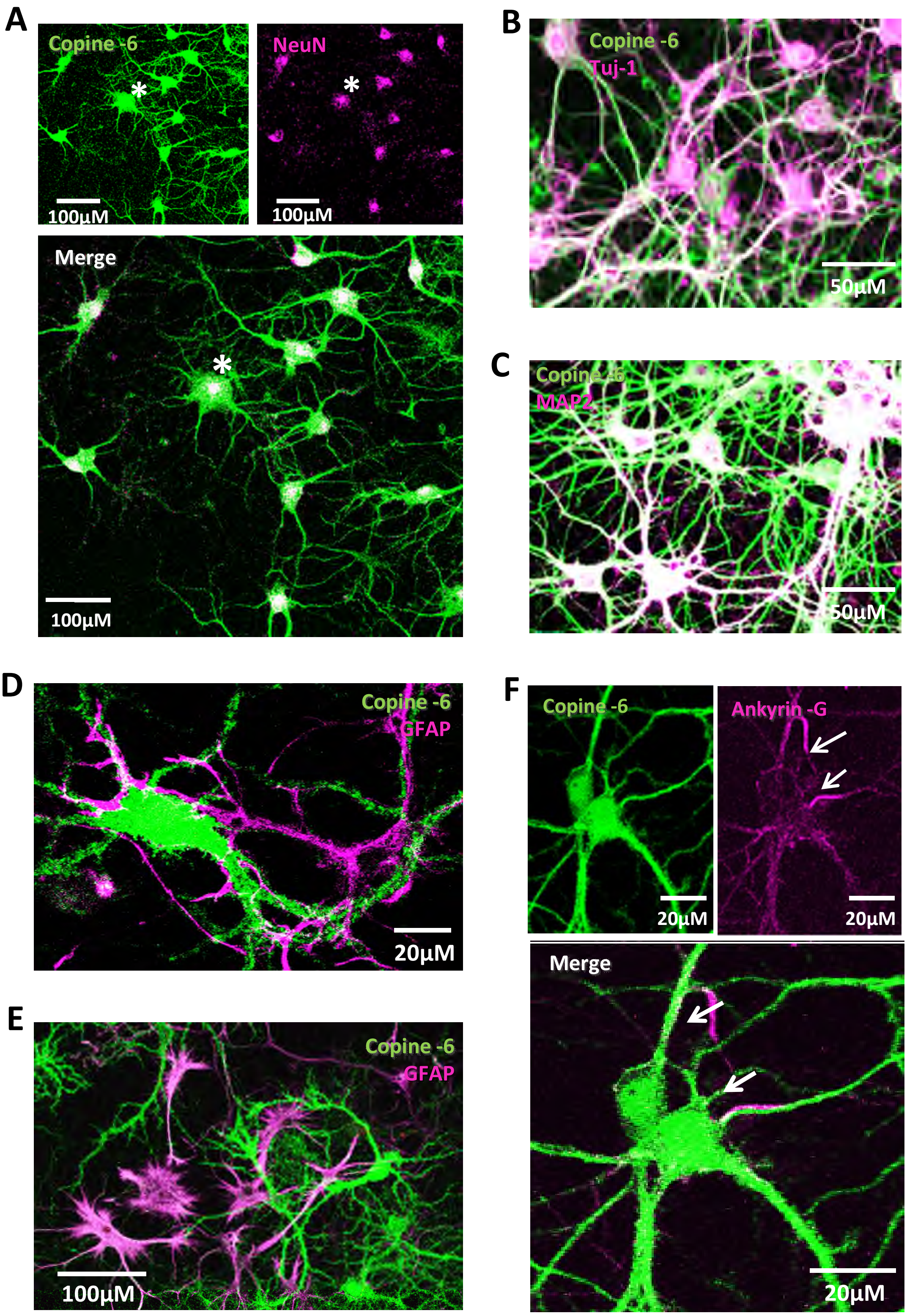

Figure 3-3 Immunohistochemical protein expression analysis of dissociated hippocampal cultures following 21 days *in vitro*.

(Fig. 3-3) Cells were probed for Copine-6 alongside antibodies targeting different neuronal or glial proteins. **A**. All of the Copine-6 neurons in the hippocampal culture were immunopositive for NeuN, the neuronal nuclei marker. The * indicates one example of co-localisation. Images were taken at x20 objective. **B**. All of the Copine-6 neurons were immunopositive for TUJ-1, x40 and **C**. co-positive for MAP2, x40. . **D** and **E**. All Copine-6 neurons were repeatedly immunonegative for the glial marker GFAP (glial fibrillary acidic protein, x40 and x 20 objective respectively). Note how the glial cells are in close proximity to, and often intertwined with neuronal processes suggesting a mature cellular network consisting of multiple cell types. **F**. All Copine-6 neurons in the hippocampal culture displayed an Ankyrin –G immunopositive axon initial segment, x40 objective, arrows point to axonal labelling. The Ankyrin –G also weakly labels the entire cell soma and dendritic arbor, this is not due to overexposure rather the expression of voltage gated sodium channels throughout the cell membrane, which also requires Ankyrin –G for scaffolding but in lower concentration. The striking axon initial segment shows the dense recruitment of Ankyrin -G and a subsequent increase in sodium channel expression, required for action potential initiation at this site.

The heterogeneity of the expression of Copine-6 has been investigated further in Chapter 4 and also investigates the developmental profile of Copine-6 expression levels.

3.3.3. Immunohistochemical analysis of cultured dissociated olfactory bulb neurons.

The expression of Copine-6 in the olfactory bulb was initially investigated using dissociated culture, since different cell populations can be identified using a variety of histochemical markers. The olfactory bulb dissection was taken to contain part of the tangential rostral migratory stream as defined in the literature (Rakic, 1995; Peretto *et al.*, 1997; Fasolo *et al.*, 2002), in the hope to include any migratory cells during their later stages of migration and maturation (See Figure 3-4)

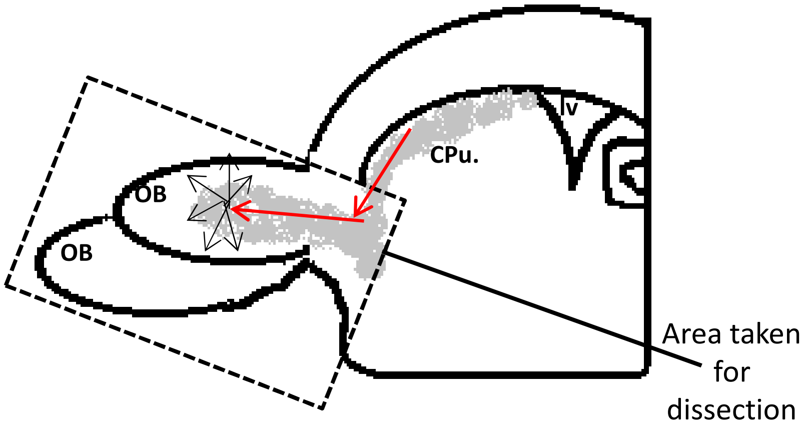

Figure 3-4 A schematic figure of the anatomical areas isolated for the Olfactory bulb (OB) cultures.

The dissected region of the embryonic brain taken for tissue culture is indicated by the dotted box. The rostral migratory stream is indicated in grey, which originates at the edge of the lateral ventricle and progresses over the top of the Caudate Putamen (CPu. i.e. the striatum). The red arrows indicate the tangential mode of migration, and the black arrows in the OB indicate radial migration where the cells travel to their final destination. By this age of embryonic development (E18) the ganglionic eminences have disappeared and the basal ganglia (which includes the CPu) are developing.

A striking heterogeneity was observed in the dissociated olfactory bulb culture. Of those cells that were immunopositive for Copine-6, the majority had low Copine-6 expression intensity in the cytoplasm. These weakly Copine-6 reactive cells had a medium sized round soma(~20-25µm), and very few arborisations were visible with the Copine-6 labelling (see * in Figure 3-5). However, in addition to these weakly expressing cells were a sparse population of intensely immunopositive cells which were instantly identified owing to their brightly stained, small rounded soma (<15-20µM). The nucleus is intensely labelled, and the cells exhibit long, extensively branched proximal dendritic arborisations with multiple 'spine-like' protrusions. These cells were referred to as 'Copine-6 spiny cells' (Figure 3-5)

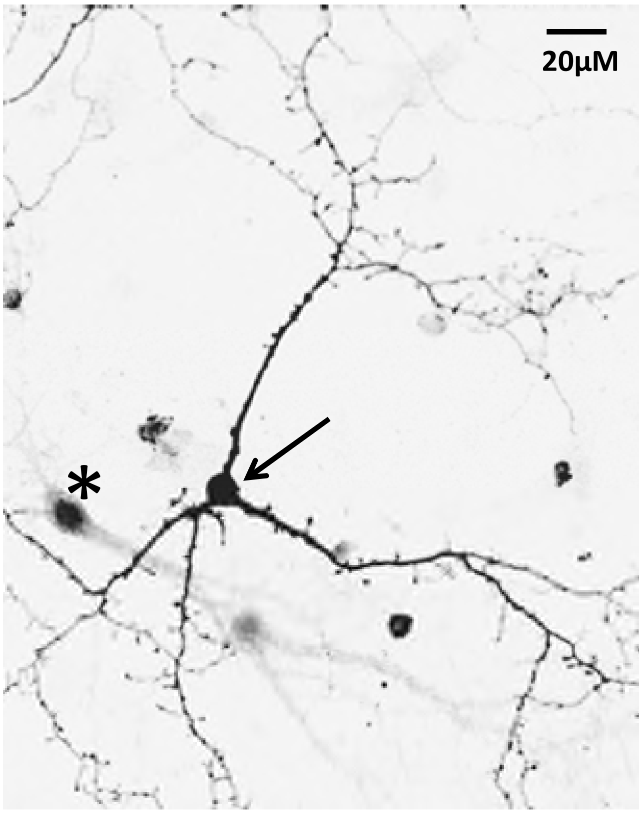

Figure 3-5 A Copine-6 ‘spiny cell’ in dissociated olfactory bulb cell culture.

The spiny cell, identified by Copine-6 immunoreactivity using the rabbit polyclonal antibody, shows strong expression of Copine-6 in the soma (arrow). These cells with strong expression of Copine-6 are distributed sparsely in the cultures, yet are easily identifiable due to their ‘spiny’ dendritic arbor. They exhibit bi- or multi-polar proximal dendrites, with multiple branched secondary dendrites. Intense Copine-6 immunoreactivity can be seen throughout the soma, dendrites, and ‘spine-like’ protrusions. This can be contrasted to the weakly labelled Copine-6 neuron in the same culture (*), which lacks the Copine-6 staining intensity in the cytoplasm and dendrites but does have stronger nuclear staining. The image is a single scan using x40 objective.

In the olfactory bulb cultures, Copine-6 reactivity was neuron specific, congruent with the neuron specific labelling in the hippocampal cultures. Again, all Copine-6 cells in the olfactory bulb cultures were immunonegative for glial cell markers (see Figure 3-6), and they were repeatedly and undoubtedly immunopositive for NeuN, TUJ-1 and MAP2, all of which are typical neuronal markers (see Figure 3-7, images A, B, D, E).

The Copine-6 immunoreactivity in the cultured ‘spiny cells’ was investigated in detail. The Copine-6 labelling, at the level of the light microscope, appeared to be intense throughout the soma and the processes. The nucleus and cytoplasm were indistinguishable owing to the intensity of the staining. The spiny cells were all bi- or multi- polar, and all carried a GABAergic phenotype identified by their co-expression of GAD67, typical of olfactory interneurons (Figure 3-7 C). Some (but not all) of these spiny cells were also immunoreactive for calretinin, the calcium-binding protein expressed by certain subpopulations of interneurons including those in the olfactory bulb (Résibois & Rogers, 1992) – (Figure 3-7 F). Interestingly, all of these intensely immunopositive Copine-6 small spiny cells lacked immunoreactivity for Ankyrin –G, a scaffolding protein required for the recruitment of sodium channels, which are densely populated in the axonal initial segment (Angelides *et al.*, 1988; Kordeli *et al.*, 1990). This was not due to a failure of the staining for Ankyrin –G as other neurons in the culture showed immunoreactivity for it (Figure 3-7 G).

The intensely stained ‘spiny’ Copine-6 cells accounted for a very small proportion (<10%) of the neuronal population and were practically absent when the dissection did not include a section of the rostral migratory stream (see Discussion 3.4.2). The majority of the olfactory bulb dissociated culture cell population consisted of either immunonegative, or very weakly positive Copine-6 neurons, most of which were immunopositive for Ankyrin –G. This together with the fact that these cells did not stain for GAD67 meant that these neurons were easily distinguishable from the spiny Copine-6 immunoreactive neurons.

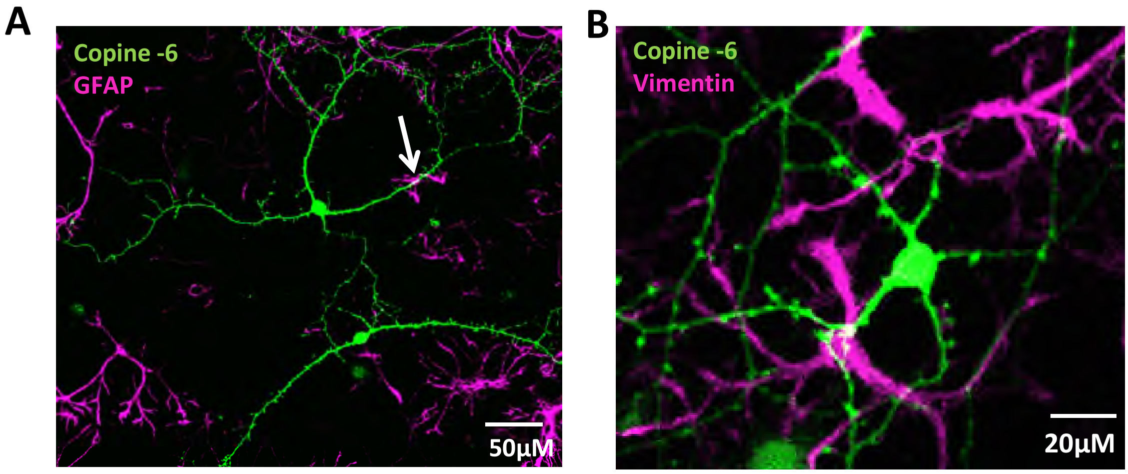

Figure 3-6 Copine-6 cells in dissociated olfactory bulb culture are not glia.

A. Immunohistochemical staining for Copine-6 alongside glial fibrillary protein (GFAP). The arrow points to an example of close contact between the GFAP cells and Copine-6 neurons but a lack of co-reactivity. **B**. Labelling for vimentin also shows a lack of co-immunoreactivity with Copine-6. Both images are z-stacks of 1-µm optical slice thickness, 10 z-sections collected at 0.5-µm intervals

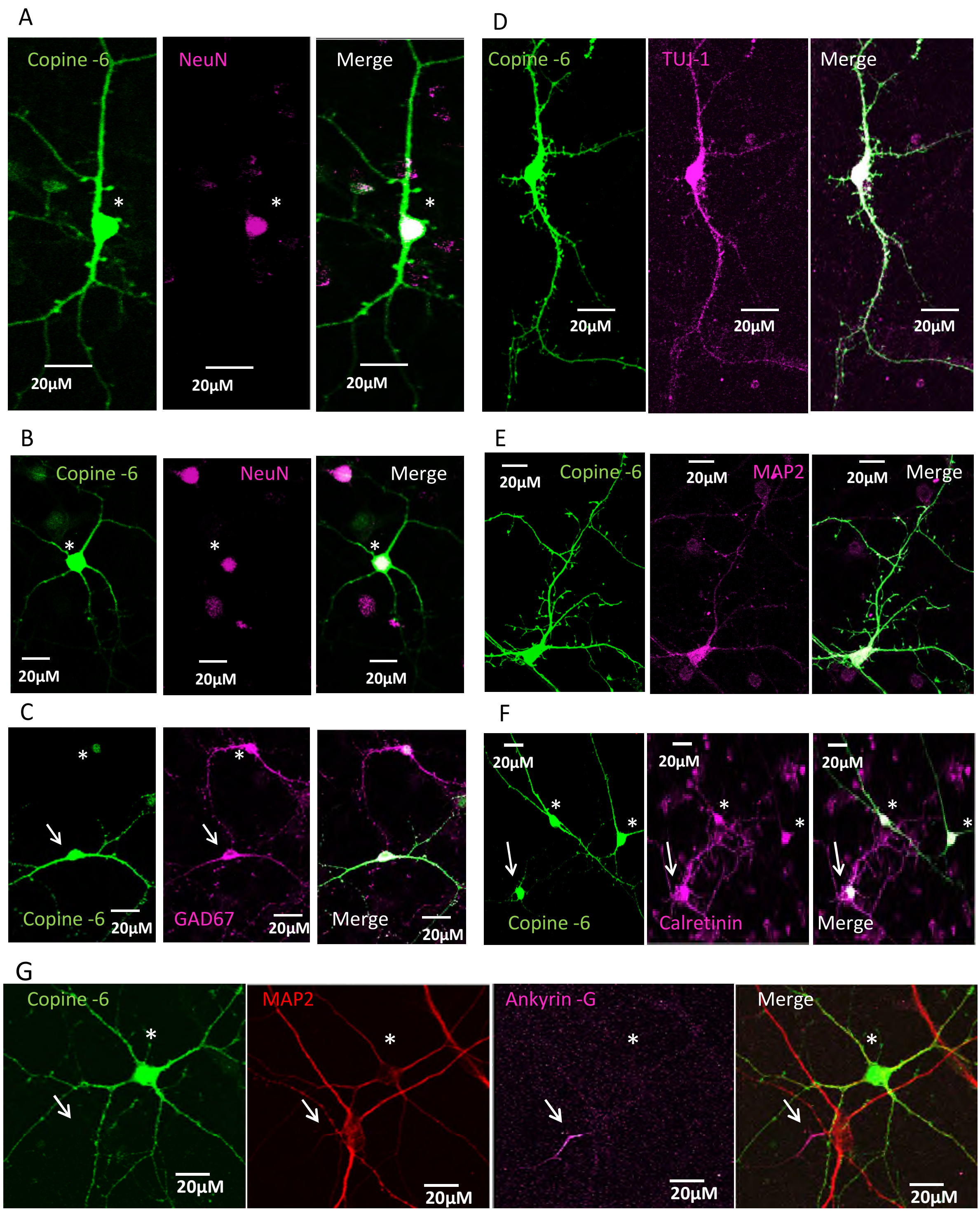

Figure 3-7 Copine-6 immunoreactive 'spiny' neurons in olfactory bulb cultures after 21 days *in vitro*.

Olfactory bulb cultures were maintained for 21 days to allow for cell maturation. The cultures were stained for Copine-6 and NeuN, GAD67, TUJ-1, MAP2 and calretinin. All Copine-6 cells were confirmed to be neuronal. A and B. All Copine-6 cells were co-immunopositive for NeuN, the neuronal nuclei marker (*). C.The Copine-6 spiny cells were GAD67 immunoreactive, suggesting a GABAergic phenotype (arrow). Note the GAD67 immunoreactive cell (*) that lacks Copine-6 immunoreactivity other than nuclear background staining, suggesting that not all GABAergic cells express Copine-6 protein. D. All Copine-6 cells – 'spiny' and not spiny – were co-immunoreactive for TUJ-1 and E. MAP2, again indicating a neuronal phenotype. F. 55% of 'spiny' cells were co-immunoreactive for calretinin, a calcium binding protein exclusively expressed in some GABAergic neuronal populations. The (*) indicates two strongly immunopositive Copine-6, calretinin cells; The (arrow) points to a strong calretinin cell with weaker Copine-6 suggesting a variable protein content between cells of the same culture. G.The Copine-6 spiny cells appear to be immunonegative for

Ankyrin –G, a marker of the initial axon segment, suggesting that these cells do not have an axon (*). Other neurons in the culture, which were immunopositive for MAP2 (see arrow) did have an axon. The images were either single scans or z-stacks of 1-µm optical slice thickness, 10 z-sections collected at 0.5-µm intervals.

3.3.4. Copine-6 in the adult rat hippocampus

Copine-6 expression within the hippocampal formation is generally very strong. At x10 objective using the light microscope, the Copine-6 staining appeared to be layered through the hippocampus, and the neuronal staining of the soma comparable to that of mRNA expression in the mouse hippocampus (Figure 3-8). Protein expression of Copine-6 using immunohistochemistry was somatic, dendritic and axonal. Most intense neuronal staining could be seen in the Stratum Pyramidales of CA1-CA3, and the Stratum Granulosum of the dentate gyrus. A few cells are labelled for Copine-6 in the hilus of the dentate gyrus. An apparently non-specific increase in staining intensity was noted in Stratum Radiatum and Stratum Moleculare, and very little labelling in Stratum Lacunosum, which contributed to the layered expression pattern. Furthermore, a closer look at individual neuron staining revealed that some (but not all) cells of the CA1, CA2 and CA3 pyramidal cell layer are immunoreactive for Copine-6 (Figure 3-9). Some cells within the granular layer of the dentate gyrus are also immunopositive for Copine-6.

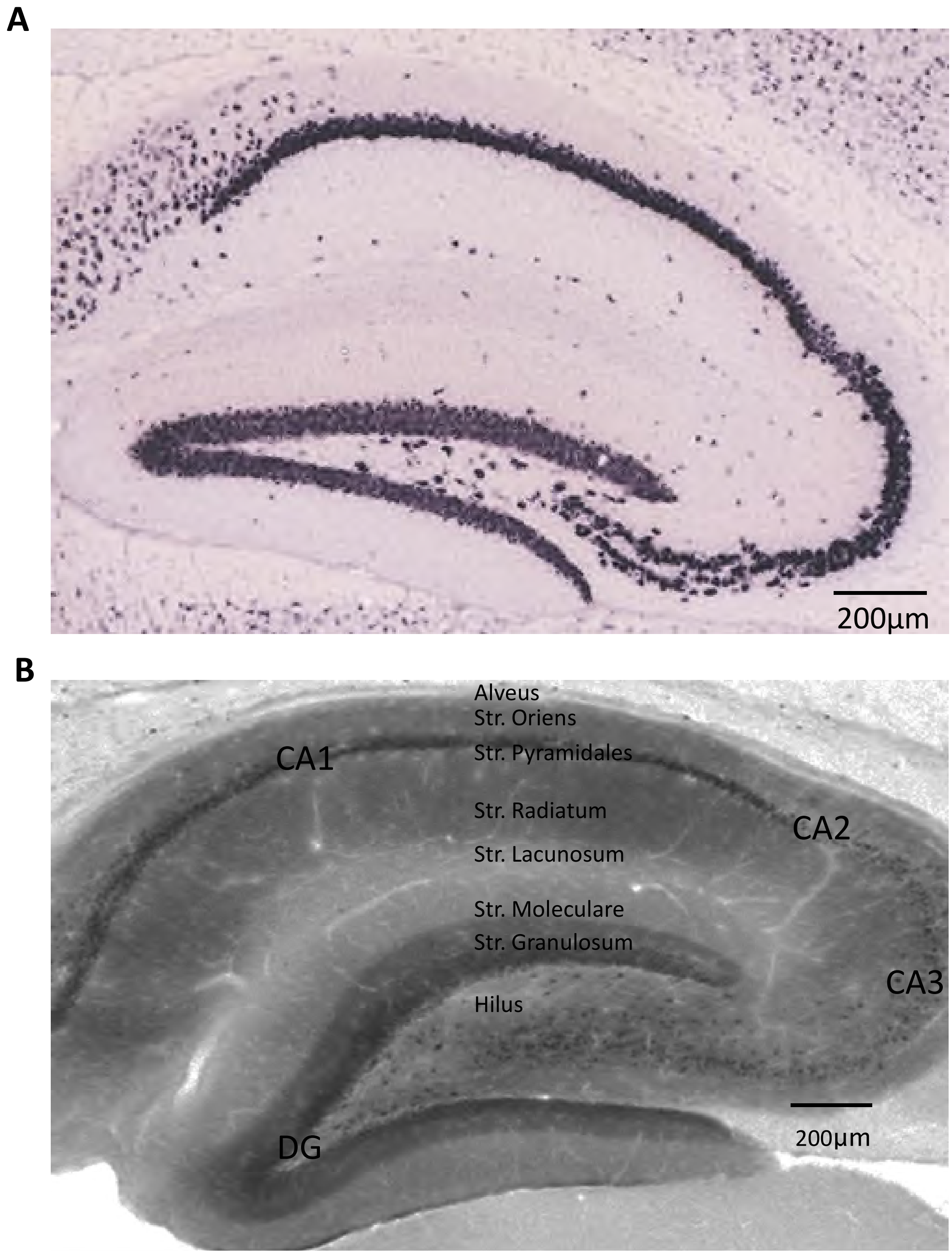

Figure 3-8 Copine-6 mRNA and protein expression in the hippocampus.

A. mRNA Copine-6 in the mouse hippocampus, taken from Allen Brain atlas. Copine-6 mRNA is present in cells of the dentate gyrus, and pyramidal cell layer, as demonstrated also by the Copine-6 protein expression. **B**. A single scan showing Copine-6 protein immunohistochemistry. Copine-6 labels the hippocampus in a layered manner. Note how pyramidal cells within the Stratum Pyramidales of CA1 and some cells within CA3 are intensely stained by the antibody. The layered appearance is due to a difference in expression intensity; Stratum Radiatum and Stratum Moleculare are more strongly labelled than Stratum Lacunosum. Also, the Stratum Granulosum (granule cell layer) of the dentate gyrus (DG) have strong labelling. This perhaps indicates that Copine-6 is staining particular cell populations in these regions. In general, the overall Copine-6 staining in the hippocampus was strong in comparison to other brain regions examined, and is accurate based on the mRNA expression.

Each region of the hippocampus was examined independently. In the cornu ammonis, all of the Copine-6 immunoreactive cells were within the pyramidal cell layer. The apparent layered staining pattern throughout the entire hippocampus could not be attributed to any particular cell reactivity other than within the Stratum Pyramidales and the Stratum Granulosum/DG hilus. This labelling could be neuropil and will therefore not be examined further here. The neuronal reactivity was most dense in CA1 (see Figure 3-8), and very sparse in CA3 with only a few neurons labelled in the CA2 region. All of the Copine-6 cells in the cornu ammonis were co-immunopositive for NeuN, and in CA1 the majority of cells were also immunoreactive for the markers CAMKII (Erondu & Kennedy, 1985) and Ctip2 (COUP TF1-interacting protein 2), a marker of some cells within the adult hippocampus(Leid *et al.*, 2004; Arlotta *et al.*, 2005; Britanova *et al.*, 2008; Nielsen *et al.*, 2010) (Figure 3-9.Images A, C and E). In the dentate gyrus, the majority of Copine-6 reactive cells were also co-immunoreactive for NeuN and Ctip2 (Figure 3-9.Images B and D respectively). Reacting hippocampal slices for Copine-6 and the interneuron markers GAD67, Somatostatin and Parvalbumin showed that the Copine-6 positive cells did not stain for these markers, suggesting that Copine-6 does not delineate these types of interneurons in the hippocampus (Figure 3-10, Figure 3-11).

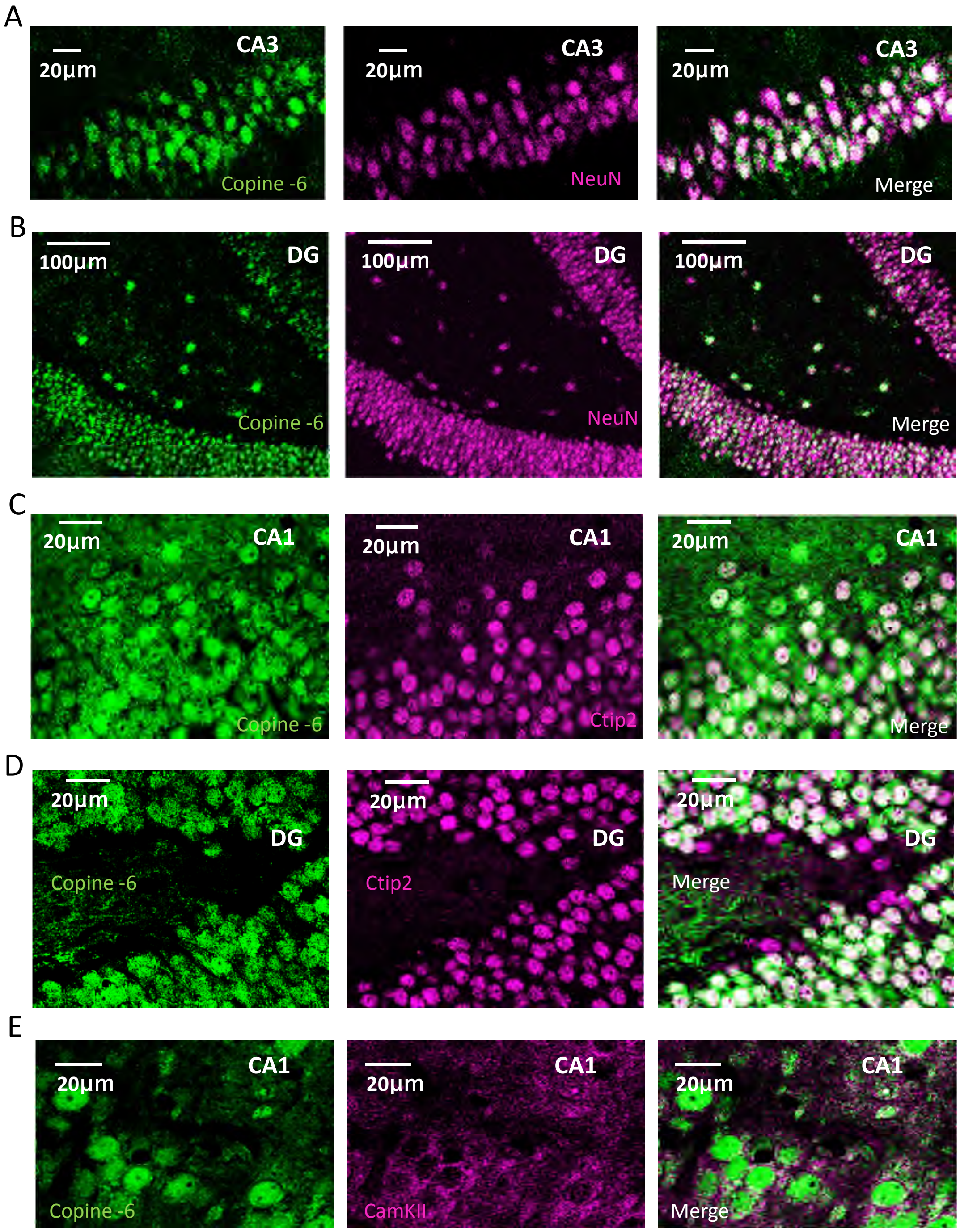

Figure 3-9 Copine-6 labelling in the hippocampus of the adult rat.

A. Copine-6 co labels NeuN reactive neurons in the stratum pyramidales of CA3 and **B.** in granule cell layer of the dentate gyrus. Note the presence of some sparse Copine-6 neurons within the hilus of the DG, which may be interneurons. **C.**The majority of Copine-6 pyramidal cells in CA1 were co-immunoreactive for Ctip2 **D.** The majority of granule cells in the dentate gyrus were also Ctip2 positive. **E.** Most pyramidal cells of cornu ammonis were CAMKII immunopositive. All images are single scans.

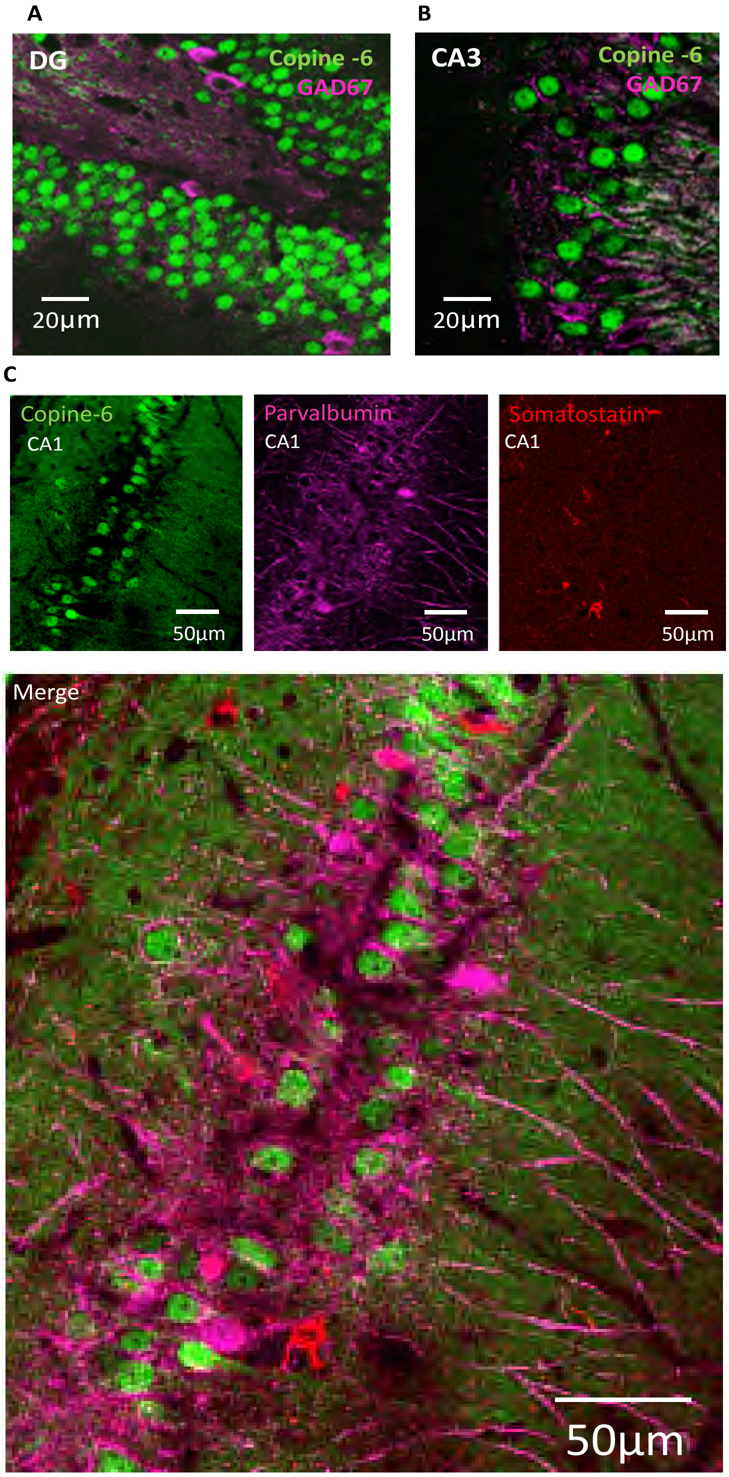

__Figure 3-10 Copine-6 does not label GAD67/PV/SOM interneurons.__

A Copine-6 labelled cells were immunonegative for GAD67 in the dentate gyrus granule cell layer and **B**.in the cornu ammonis. **C**. The Copine-6 cells were also immunonegative for calcium binding proteins parvalbumin and somatostatin in both regions, here shown in CA1. This image also demonstrates that some Copine-6 reactivity is also neuropil. All images are single scans.

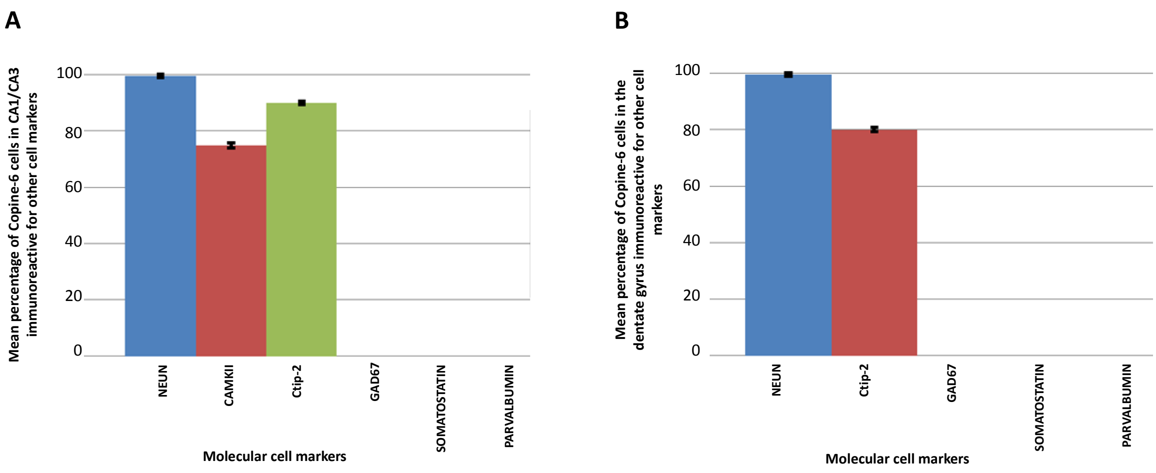

Figure 3-11 Co-reactivity of Copine -6 cells in the hippocampus with other cell markers

A. Copine -6 cells in the cornu ammonis (CA1+CA3) were counted for co-localisation with other cell protein markers. The Copine -6 cells were neuronal (~100% NeuN +ve) with heterogenous CAMKII (~74%) and Ctip2 (~87%) reactivity. B. In the dentate gyrus, Copine -6 labelled cells were neuronal (~100% NeuN +ve) with heterogenous Ctip2 (~79%) reactivity. All cells were immunonegative for interneuron markers GAD67, Somatostatin and Parvalbumin. For each reaction 400-600 cells were counted, using every fifth section of a total of 4 adult rat brains.

3.3.5. Copine-6 in the Olfactory Bulb

The Copine-6 immunoreactivity in the olfactory bulb is strong, and the laminated structure of the main olfactory bulb can clearly be seen. This is as suggested by the mRNA expression profile of CPNE6 (on the Allen Brain Atlas, See Figure 3-12A). The most reactive region of Copine-6 immunoreactivity appears to be within the internal granule cell layer, which was found to have strong immunoreactivity in both the soma and the cell processes. Some Copine-6 immunoreactive soma can be seen within the mitral cell layer, and surrounding the glomeruli within the glomerular cell layer (see Figure 3-12). The granule and glomerular cell regions were explored in detail, since they are populated by GABAergic interneurons.

A

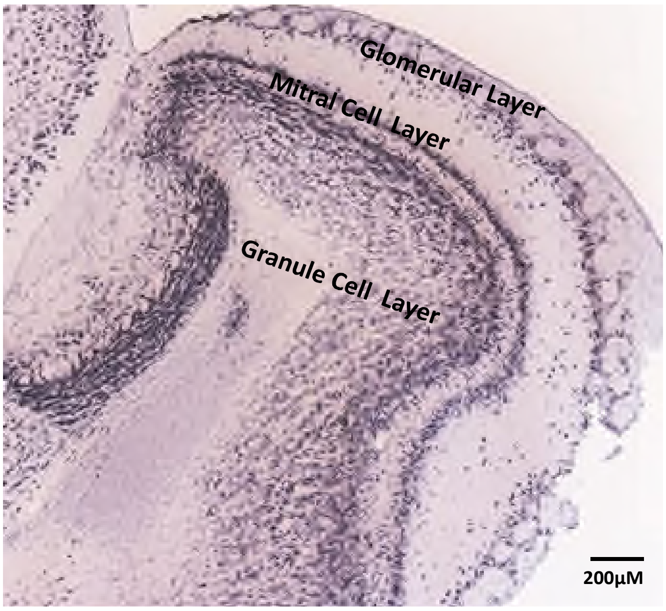

B

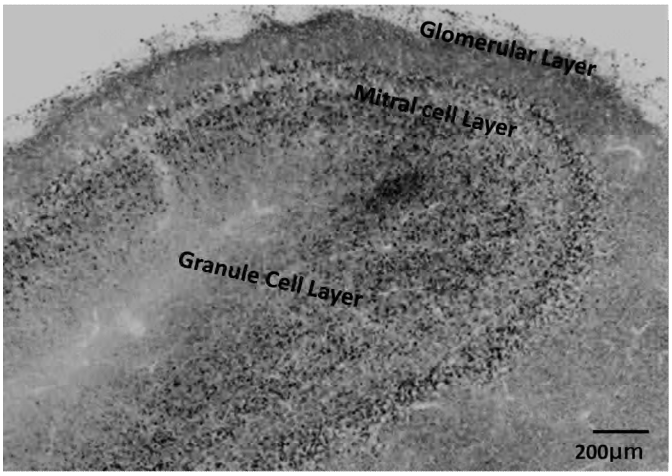

Figure 3-12 Copine-6 labelling in the adult rat main olfactory bulb.

A. Copine-6 mRNA profile taken from Allen Brain Atlas. **B**. Copine-6 protein labelling is strong in the granule cell layer, and some cells in the mitral and glomerular cell layer. Copine-6 cells in the glomerular layers were sparse and distributed around the spherical glomeruli, which themselves were not labelled by the Copine-6. Single scan, x20 objective. The protein and mRNA expression profiles are the same. See below for area descriptions.

Granule cell layer:

In the internal granule layer, positive Copine-6 granule cell soma and dendrites are strongly labelled, and are scattered amongst many negative cells. The soma is rounded and are ~10-15µm in diameter, both of which are typical of granule cells (Price *et al*, 1970; Shepherd, 1979). The Copine-6 staining is membranous with diffuse cytoplasmic staining. The processes of the Copine-6 cells are well labelled, and can be seen intertwined with one another and appear to be densely populated, making it difficult to trace individual processes back to any specific soma. Some of the Copine-6 immunoreactive cell processes are decorated with spine-like protrusions. The fluorescence of the cytoplasm varies greatly between each Copine-6 expressing cell, with no obvious morphological or distribution-related cause for this heterogeneity (Figure 3-13).

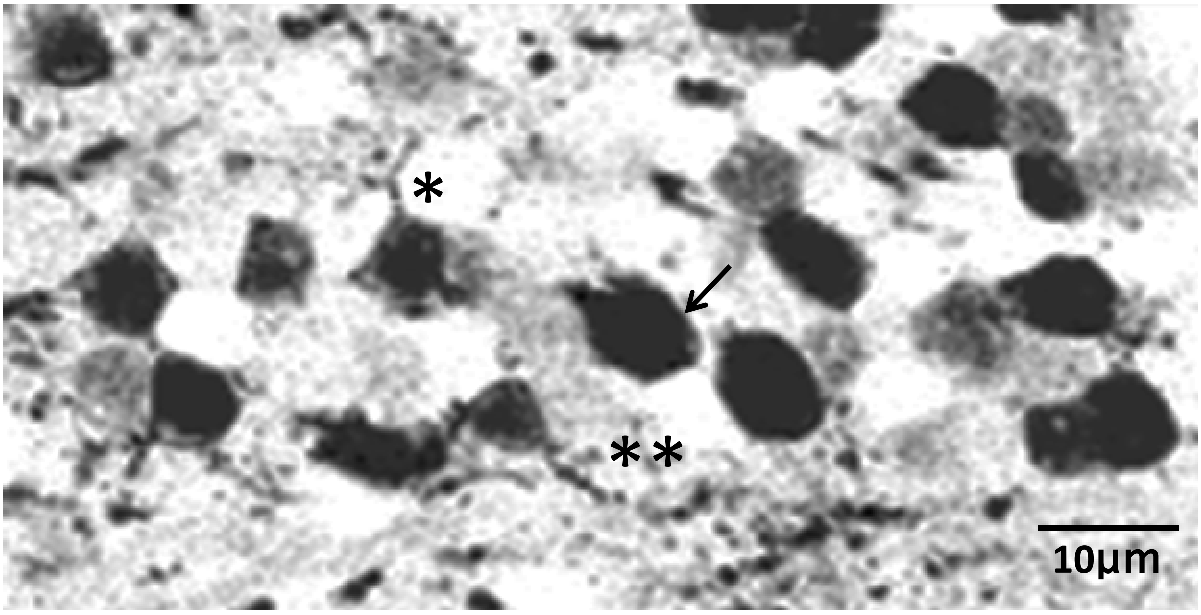

Figure 3-13 An example of heterogenic Copine-6 labelling in granule cells of the main olfactory bulb.

Some cells were intensely labelled throughout the soma (arrow), whereas other cells had weaker staining which appeared to be nuclear and membrane (*). The processes of some cells were also stained by the Copine-6 antibody (see **) and many of these had characteristic spiny protrusions decorating the dendrites. The image shows a single scan at x40 objective.

All (>94%) of the Copine-6 immunoreactive cells in the granule cell layer are co-immunopositive for GAD67 and NeuN (Figure 3-14A and B, Figure 3-18). They are therefore GABAergic neurons, a phenotype typical of olfactory granule cells which are the interneurons of the internal granule cell layer of the main olfactory bulb (Price *et al*, 1970) .

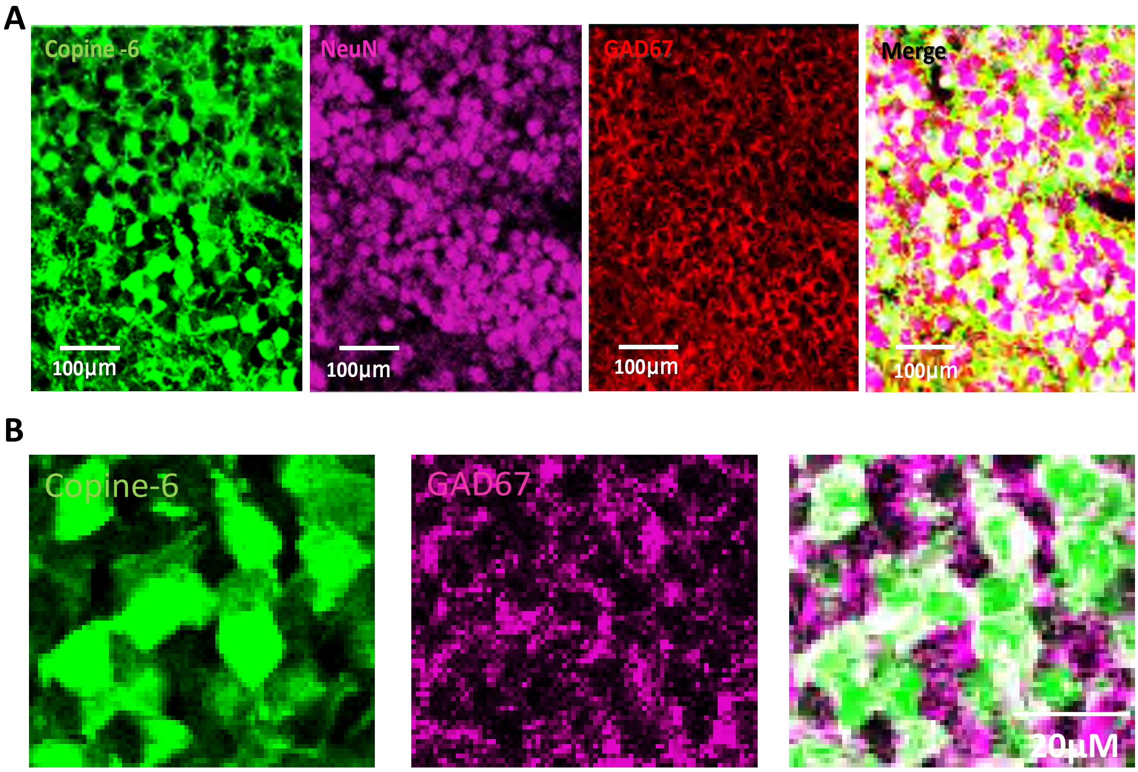

Figure 3-14 Copine-6 labelling of Olfactory granule cells.

A. A low resolution image to show the neuron specific labelling of all Copine-6 granule cells. The cells are labelled by Copine-6 (green), NeuN (purple), GAD67 (red). The final image merge illustrates that all of the Copine-6 cells are immunopositive for both markers of neurons with a GABAergic phenotype, respectively (white indicates their co-reactivity). Some Copine-6 negative neurons can be seen in the image merge which show up pink) **B**. A higher magnification of some Copine-6 cells in the granule cell layer to show their co-reactivity for GAD67. All images are single scans, x20 and x40 objective, respectively.

~50% of the Copine-6 immunoreactive cells in the granule layers are also immunopositive for calretinin (Figure 3-15, Figure 3-18), which has previously been documented to be expressed by many – but not all – granule cells (Résibois & Rogers, 1992). Furthermore, following the staining here, it was identified that there were also Copine-6 +ve/calretinin –ve cells, and calretinin +ve/Copine-6 –ve cells. Therefore there were some cells present that contained only one of either Copine-6 or calretinin, and neither marker could predict the presence of the other. The two cell populations were distributed similarly and some of the Copine-6 +ve/calretinin –ve processes could be seen close to the calretinin +ve/Copine-6 –ve processes (Figure 3-15 Image C).

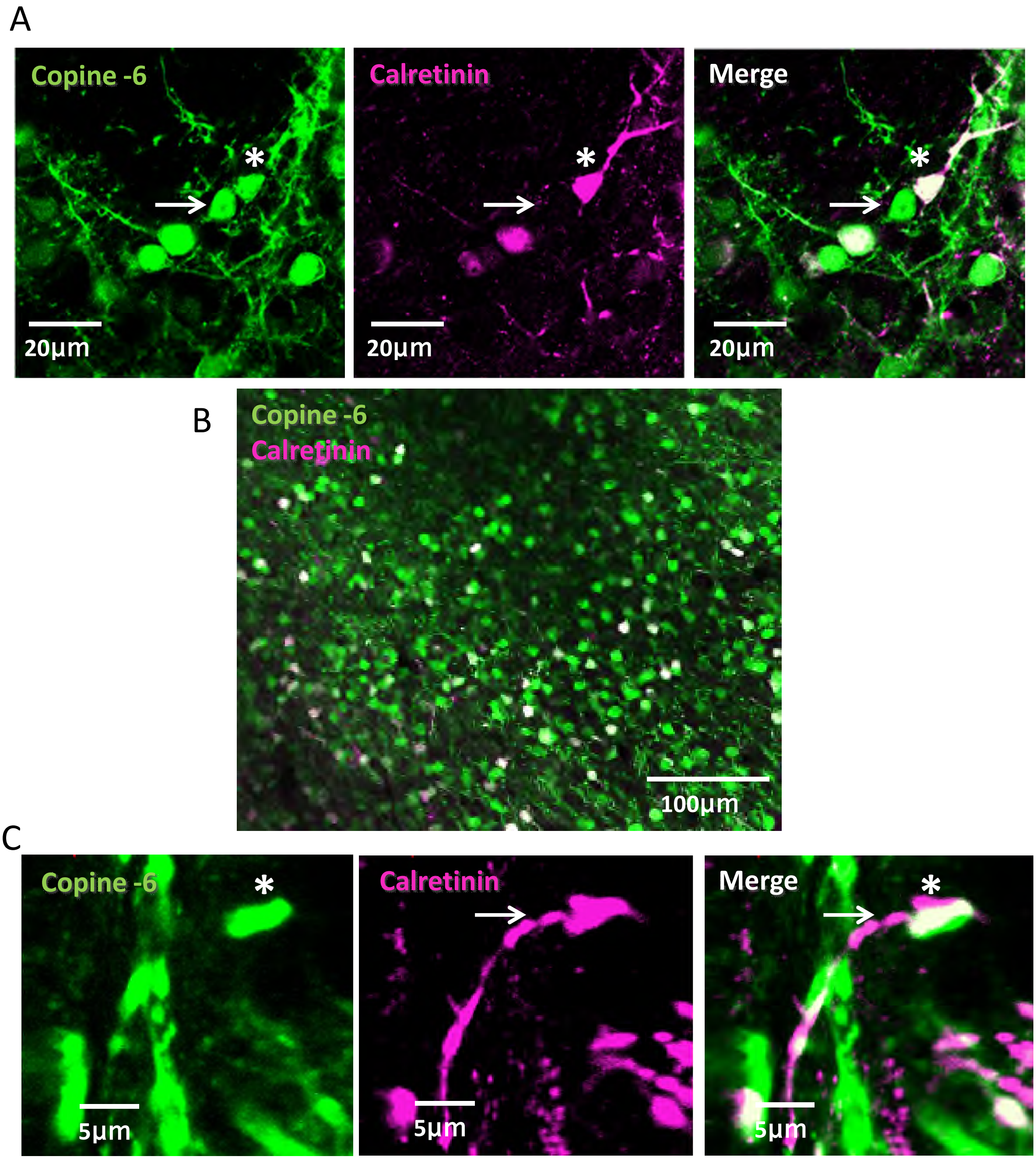

Figure 3-15 Copine-6 Olfactory granule cells have a heterogenic calretinin expression.

A. The arrow points to a Copine-6 +ve, calretinin –ve cell, and co-expression indicated by (*). Note that some of the Copine-6 cells in the OB are 'spiny', similar to those observed in the olfactory cultures. The images are single scan. **B**. A x20 objective single scan image to show the heterogenic expression of calretinin and Copine-6. Co-reactive cells appear white. Note that there are many Copine-6 only, and some calretinin only neurons, in addition to their co-expression. **C**. A calretinin process lacking Copine-6 reactivity (arrow), but in close apposition to a Copine-6 appendage (*) which may indicate a putative synapse. The image is a z-stack of 1-µm optical slice thickness, 20 z-sections collected at 0.5-µm intervals.

All of the Copine-6 immunoreactive neurons in the granule cell layer were immunonegative for other olfactory cell markers: calbindin, doublecortin, tyrosine hydroxylase and enkephalin (see Figure 3-16, Figure 3-18).

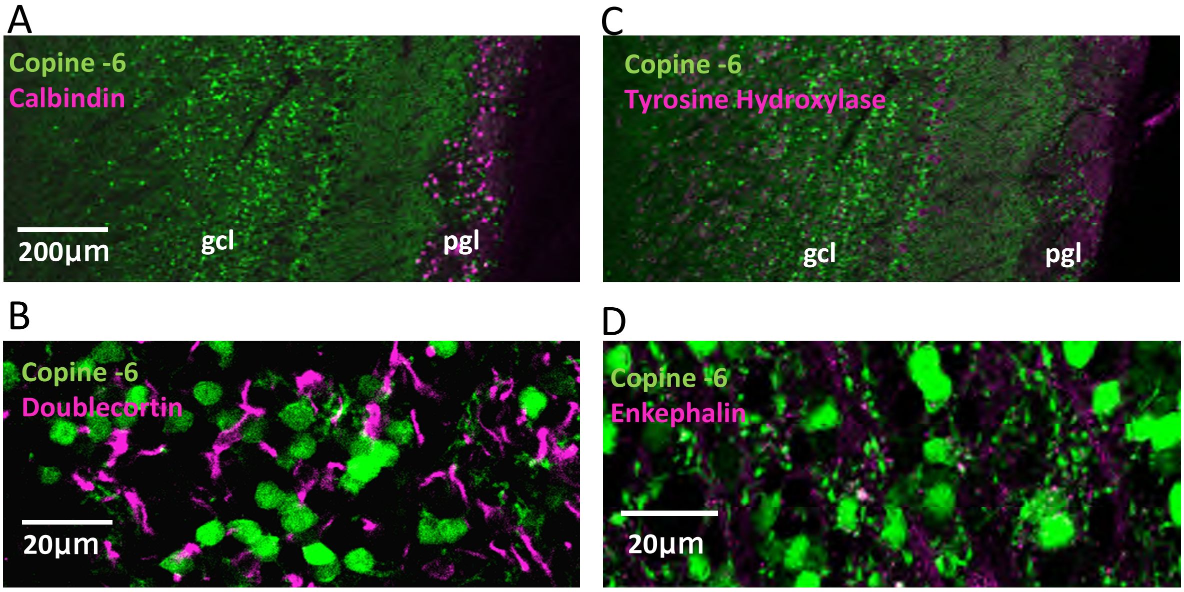

__**Figure 3-16 Copine-6 granule cells are negative for other olfactory granule cells markers.**__

A. Copine-6 cells in all layers of the olfactory bulb are immunonegative for calbindin. **B**. Copine-6 cells are not labelled by doublecortin, here shown in the granule cell layer. **C**. Copine-6 cells are immunonegative for tyrosine hydroxylase in all olfactory layers. **D**. The Copine-6 cells are not labelled by enkephalin in the granule cell layer of the olfactory bulb. All images are single scans at x20 and x40 objective.

Furthermore, some of the 'spine-like' protrusions exhibited by the granule Copine-6 immunopositive cells in the olfactory bulb also contained VGAT in the main body of the 'spine-like' protrusion (Figure 3-17, Figure 3-18). This suggests the presence of GABAergic vesicles. When co-stained with gephyrin, a post-synaptic marker of GABAergic synapses (Craig *et al*, 1996; Kirsch *et al*, 1993; Langosch *et al*, 1992) which is important for postsynaptic GABAA receptor clustering (Betz, 1998; Essrich *et al.*, 1998), immunoreactive puncta could be seen on both Copine-6 immunopositive and immunonegative cells (Figure 3-17). This gephyrin staining may therefore indicate that the Copine-6 cells themselves are postsynaptic to other neurons. It was also noted that the gephyrin puncta were not always apposed to any VGAT +ve terminal (Figure 3-17, merge), and since gephyrin is considered to be exclusively postsynaptic which suggests that it is not recruited prior to the formation of a synapse (Fritschy *et al.*, 2008) this might indicate either its presence at glycine receptor clustering, or simply reflects the focal plane of the tissue.

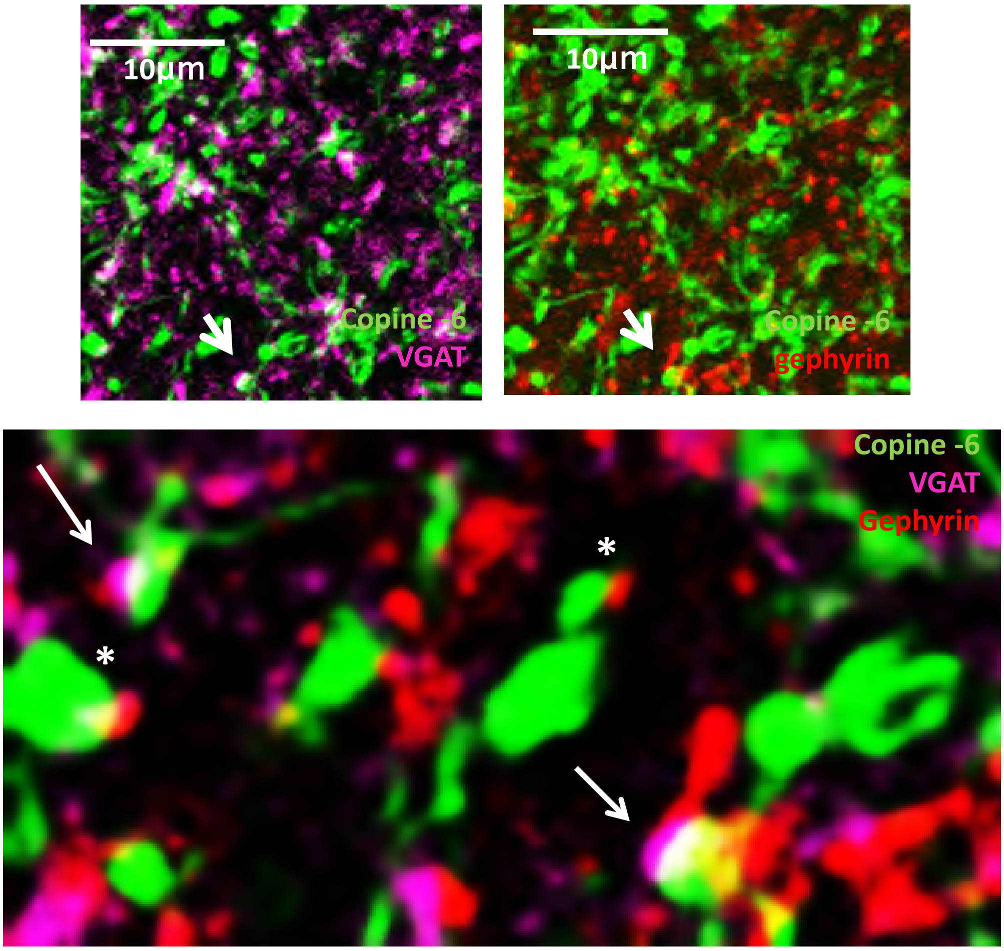

Figure 3-17 VGAT and gephyrin reactivity in the processes of Copine-6 olfactory granule cells.

The granule cell layer of the olfactory bulb has strong immunoreactivity with VGAT (purple) and co-reactivity with Copine-6 is evident by the white staining in some of the cell varicosities. Gephyrin (red) can be identified both in close apposition to, and within, some of the Copine-6 processes. The merged image is expanded to demonstrate co-reactivity. The arrows point to putative Copine-6 +ve/VGAT +ve spines, in close apposition to gephyrin +ve puncta. Some Copine-6 appendages are identified to be lacking VGAT, but have gephyrin puncta in close apposition (*) making it difficult to assess if they are themselves postsynaptic or that they are presynaptic to gephyrin puncta on other cells. Note how some gephyrin puncta are not apposed to VGAT +ve terminals which might reflect the clustering of glycinergic receptors. The images are single scans at x40 and x60 objective.

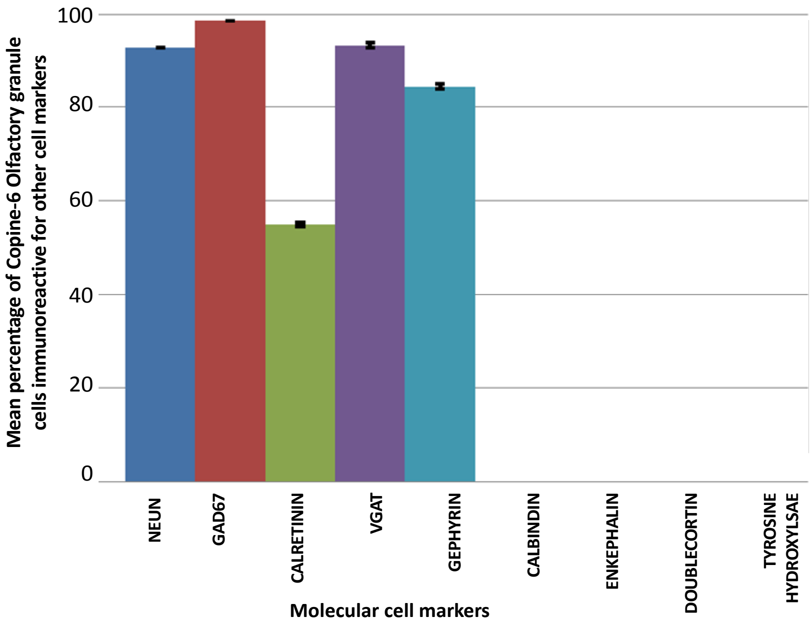

Figure 3-18 Co-localisation of Copine-6 olfactory granule cells with other olfactory cell markers

Copine-6 granule cells in the olfactory bulb were statistically analysed for co-reactivity with other established olfactory cell markers. The majority were immunoreactive for NeuN, GAD67, VGAT and Gephyrin, suggesting a neuronal GABAergic phenotype with pre- and post-synaptic proteins (~94%, 99%, 92% and 83% respectively). The granule cells had a heterogeneous co-expression of calretinin (~50%) and were immunonegative for calbindin, enkephalin, doublecortin and tyrosine hydroxylase. For each reaction 400-600 cells were counted, using every fifth section of a total of 4 adult rat brains.

Glomerular cell layer:

In sagittal rat brain sections of the olfactory bulb, Copine-6 intensely labels some small neurons surrounding the spheroid-shaped glomeruli (Figure 3-19 A). These Copine-6 immunoreactive cells have a remarkably small soma (~8-10µm) and are stained throughout the soma and processes with strong Copine-6 immunoreactivity. The cell processes appear to run in parallel to the edge of each glomeruli. The cells (~97%) are co-immunoreactive for GAD67. (See Figure 3-19 B, Figure 3-21)

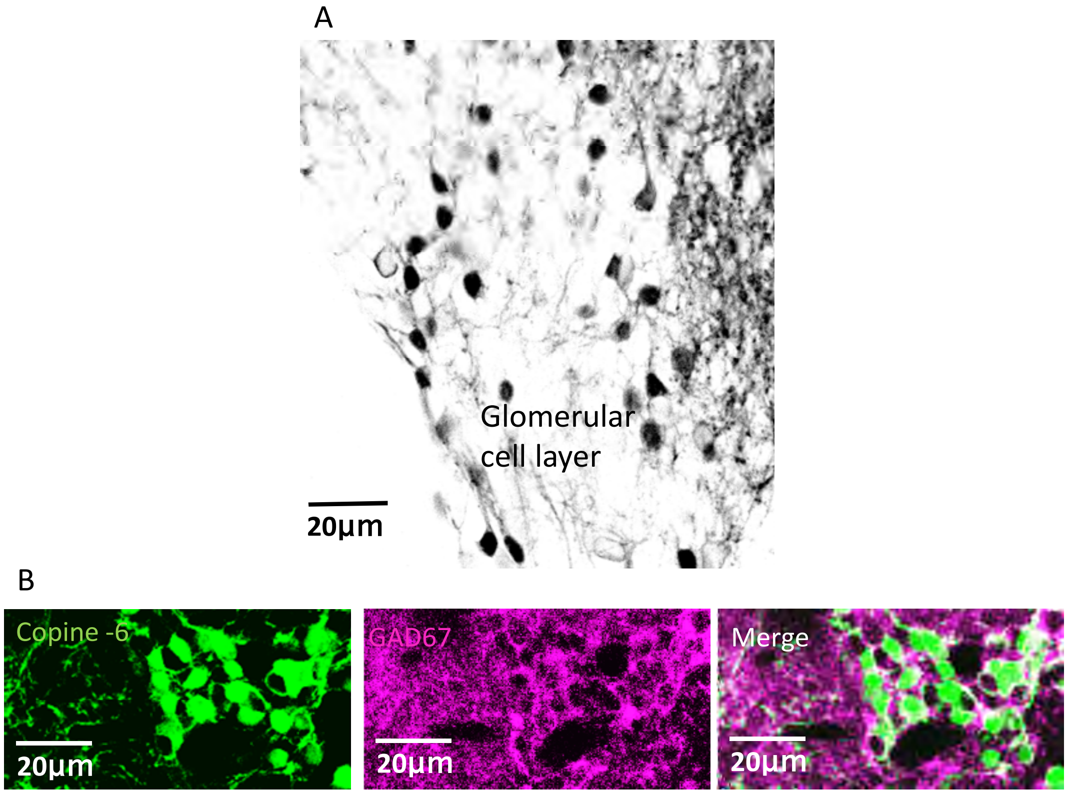

<u>Figure 3-19 Copine-6 labels cells surrounding the olfactory glomeruli.</u>

A. Copine-6 reactivity labels cells surrounding the glomeruli of the glomerular cell layer **B**. The Copine-6 neurons are co-immunoreactive for GAD67 appearing white in the merged image. Both images are single scans, x20 objective.

The small soma (<15µm), GABAergic phenotype and the location of the neurons on the periphery of each glomeruli is characteristic of periglomerular inhibitory intrinsic neurons (Kosaka *et al*, 2005; Kosaka *et al*, 1998; Pinching *et al*, 1971; Shepherd, 1979).

Some ~67% of the Copine-6 immunopositive neurons are co-immunoreactive for calretinin (Figure 3-20 C, Figure 3-21), and ~44% positive for enkephalin (Figure 3-20 A+B, Figure 3-21). All of the Copine-6 labelled cells were consistently immunonegative for calbindin and tyrosine hydroxylase, which also identify certain subpopulations of periglomerular neurons (Kosaka *et al.*, 1998) (refer back to Figure 3-16 Images A and B, Figure 3-21)

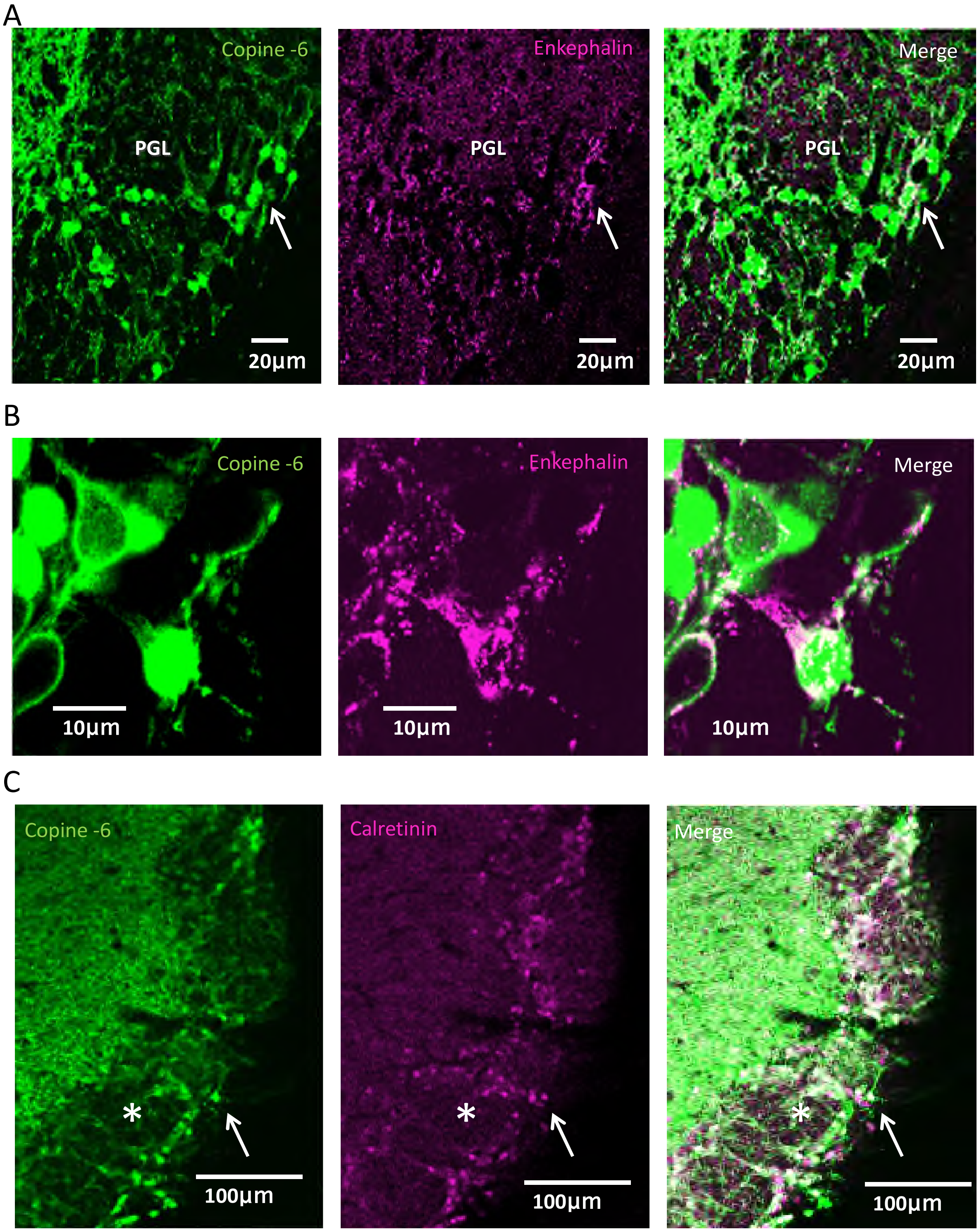

Figure 3-20 Some Copine-6 labelled cells in the olfactory glomerular layer co-express enkephalin and calretinin.

A and **B**. A small number of Copine-6 cells are co-labelled by enkephalin in the periglomerular layer The images are z-stacks of 1µm optical slice thickness, 20 z-sections collected at 0.5-µm intervals, x20 and x40 objective respectively. **C.** Some of the periglomerular Copine-6 cells are also co-reactive for calretinin although there are more calretinin reactive neurons than Copine-6 neurons surrounding the glomeruli (*). Image c is a single scan using x20 onjective.

In the olfactory bulb, the morphological (spiny, axonless - based on the lack of Ankyrin G -) and molecular (GAD67, calretinin and/or enkephalin) phenotype of the Copine-6 reactive granule and periglomerular cells are similar, to different degrees, to the spiny Copine-6 neurons in dissociated olfactory bulb cell culture.

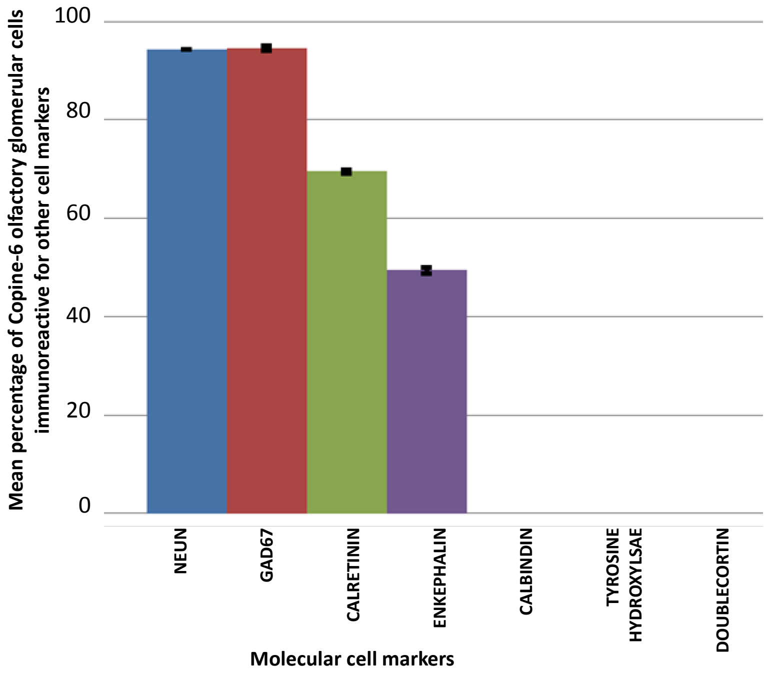

Figure 3-21 Co-localisation of Copine-6 olfactory glomerular cells with other olfactory cell markers

Copine-6 glomerular cells in the olfactory bulb were statistically analysed for co-reactivity with other established olfactory cell markers. The majority were immunoreactive for NeuN and GAD67 suggesting a neuronal GABAergic phenotype (~94%, 95% respectively). The glomerular cells had a heterogeneous co-expression of calretinin (~67%) and enkephalin (~44%) and were immunonegative for calbindin, doublecortin and tyrosine hydroxylase. For each reaction 400-600 cells were counted, using every fifth section of a total of 4 adult rat brains.

3.3.6. Copine-6 in the neocortex

Histochemical analysis of Copine-6 in rat brain identifies three different populations of Copine-6 immunopositive neurons in the neocortex. There is a general ‘layered’ staining throughout the cortex.

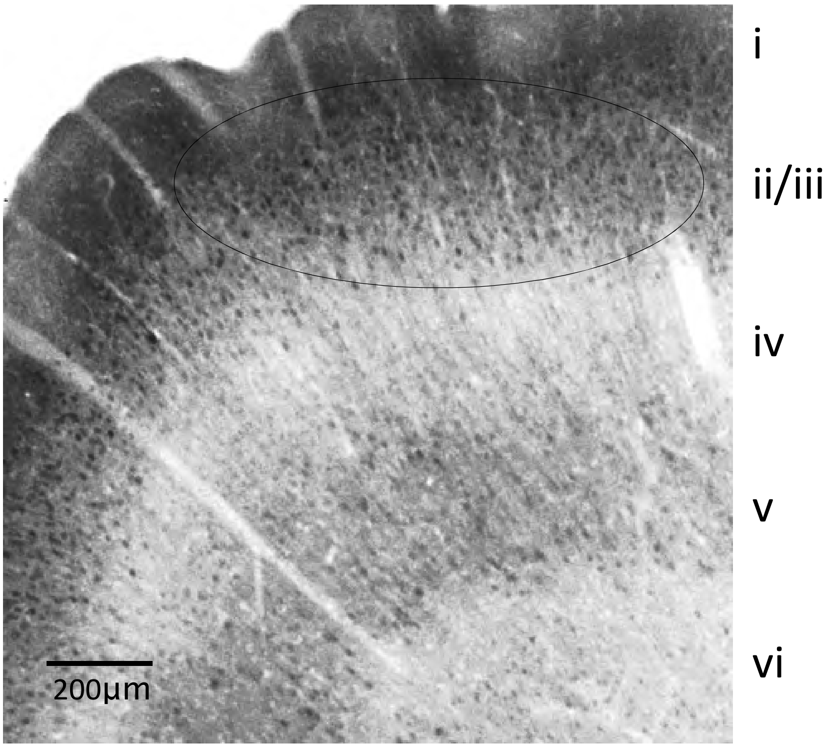

Figure 3-22 Copine-6 labelling in the adult rat neocortex.

The image shows a region of the frontal cortex, in a parsagittal section (~3.90mm lateral of the midline). Copine-6 labelling outlines the layers of the cortex. In particular, a band of cells in layer II/III (indicated by the circle) can be identified, alongside stronger staining in layer v. Throughout all layers, some larger but sparsely distributed cells are labelled for Copine-6 (not visible on this low resolution image, see Figure 3-25 and Figure 3-26). The image is a single scan using x20 objective.

The first cell population can be seen throughout layer II/III of the cortex (see Figure 3-22, indicated by the circle). At first considered weak or possible background staining, closer inspection confirmed that the Copine-6 antibody is weakly labelling some tightly packed cells, with small round soma. There is diffuse and weak Copine-6 reactivity throughout the cytoplasm and nucleus of these cells, and the nucleolus lacks reactivity (Figure 3-23A). There is no obvious Copine-6 reactive dendritic arbor to these cells. Based on location and morphology, these cells appear to be small pyramidal neurons of layer ii/iii. 83% of these cells are co-immunoreactive for CAMKII and 40% are also labelled with Ctip2 (Figure 3-23, A and B respectively, Figure 3-24).

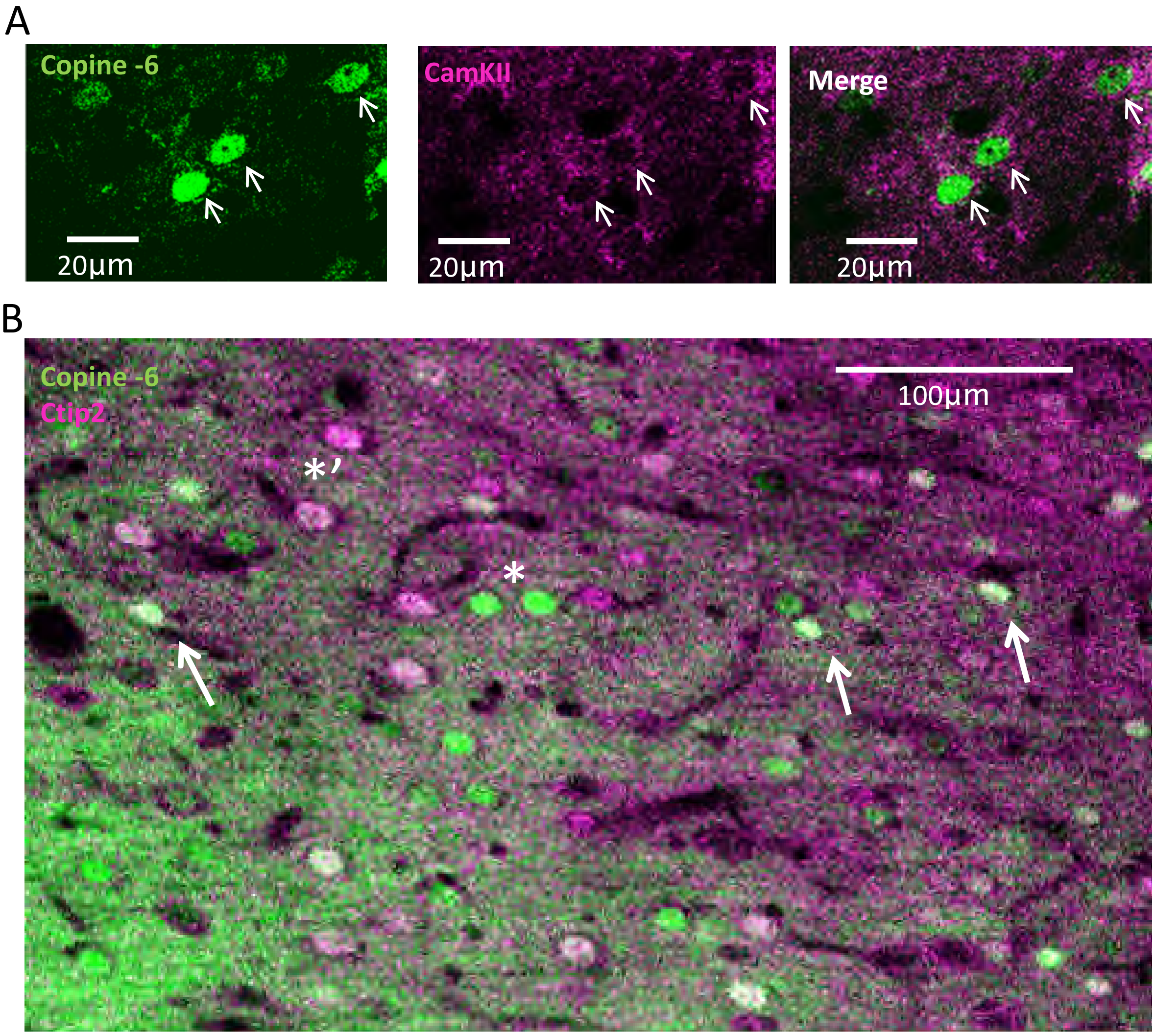

Figure 3-23 Copine-6 labels small pyramidal neurons in layer II/III of the adult rat neocortex.

A. Copine-6 labelling of small pyramidal neurons is weak, but co-reactive with CamKII. Not all CamKII cells are labelled by Copine-6. **B**. The Copine-6 reactive cells are co-reactive for Ctip2, a nuclei transcription factor Not all Ctip2 pyramidal cells are labelled by Copine-6 (*') and vice versa (*). Co-reactivity is indicated by the arrows. The cells were also examined at a higher magnification to ensure true immunoreaction (not shown). All images are single scans using x40 and c20 objective, respectively.

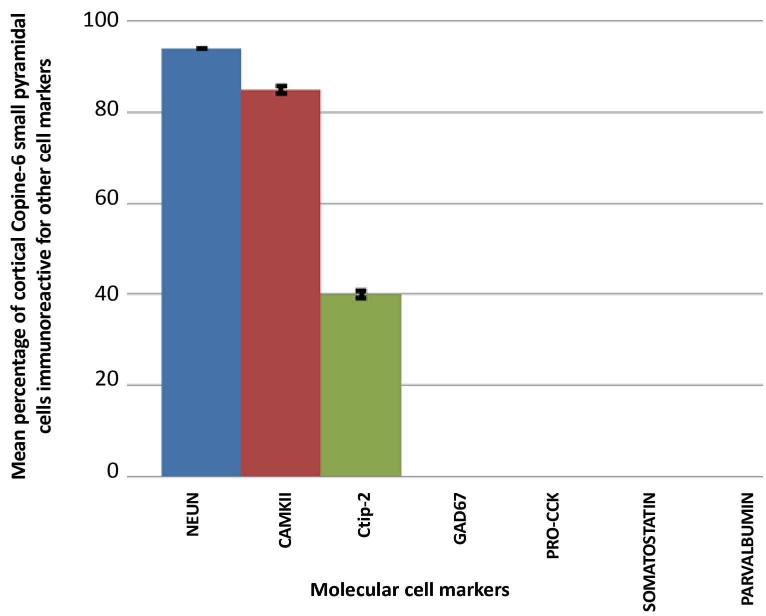

<u>Figure 3-24 Co-localisation of Copine-6 cortical small pyramidal cells with other cell markers</u>

Copine-6 small pyramidal cells were statistically analysed for co-reactivity with other established cell markers. The majority were immunoreactive for NeuN and CAMKII suggesting a neuronal and pyramidal cell phenotype (~96%, 83% respectively). Some cells had co-expression of Ctip2 (~40%) but were immunonegative for GAD67, PRO-CCK, Somatostatin and Parvalbumin. For each reaction 400-600 cells were counted, using every fifth section of a total of 4 adult rat brains.

A second population of cells immunoreactive for Copine-6 are seen scattered sparsely throughout layers II-IV of the entire neocortex (Figure 3-25). The cells present with a large, fusiform perikaryon and intensely stained plasma membrane, the cytoplasm having very weak Copine-6 immunoreactivity. The Copine-6 staining of these cells is described here as 'ghost-like' owing to this outlined staining. The nucleus of these cells is strongly immunoreactive for Copine-6. The 'ghost cells' appear to possess a short bipolar somatodendritic morphology based on the Copine-6 labelling.

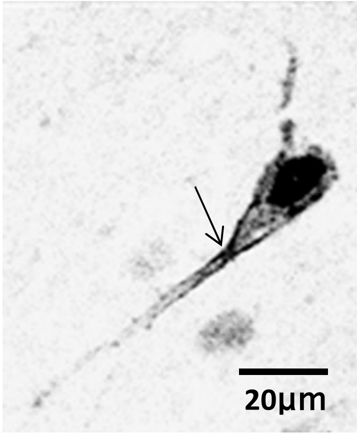

Figure 3-25 A typical Copine-6 "ghost cell" in the neocortex of the adult rat brain.

Copine-6 intensely stains the nucleus, and the cytoplasm and processes are weakly labelled creating a ghost-like appearance. The cell was imaged as a single scan using x40 objective.

Immunohistochemical analysis of these 'ghost-like' cortical cells expressing Copine-6 reveal that the cells are co-immunopositive for NeuN, GAD67 and calretinin (see Figure 3-26, Images A B and C, respectively, and Figure 3-29). This GABAergic phenotype is supported by co-reactivity for the $GABA_B$ receptor 1 subunit and the peptide precursor pro-cholosystokinin (pro-CCK) (Figure 3-27 A and B and Figure 3-29). All of the Copine-6 labelled ghost cells are immunoreactive for NECAB1, the neuronal calcium binding protein which is documented to label scattered cells throughout the neocortex and has been found to be a putative binding partner for N-Copine (Sugita *et al.*, 2002)(Figure 3-27C). Moreover, the ghost cells exhibit an axon as defined by the presence of an Ankyrin –G labelled axon initial segment (see Figure 3-27 D). The 'ghost cells' were repeatedly immunonegative for the markers parvalbumin and somatostatin (Figure 3-28).

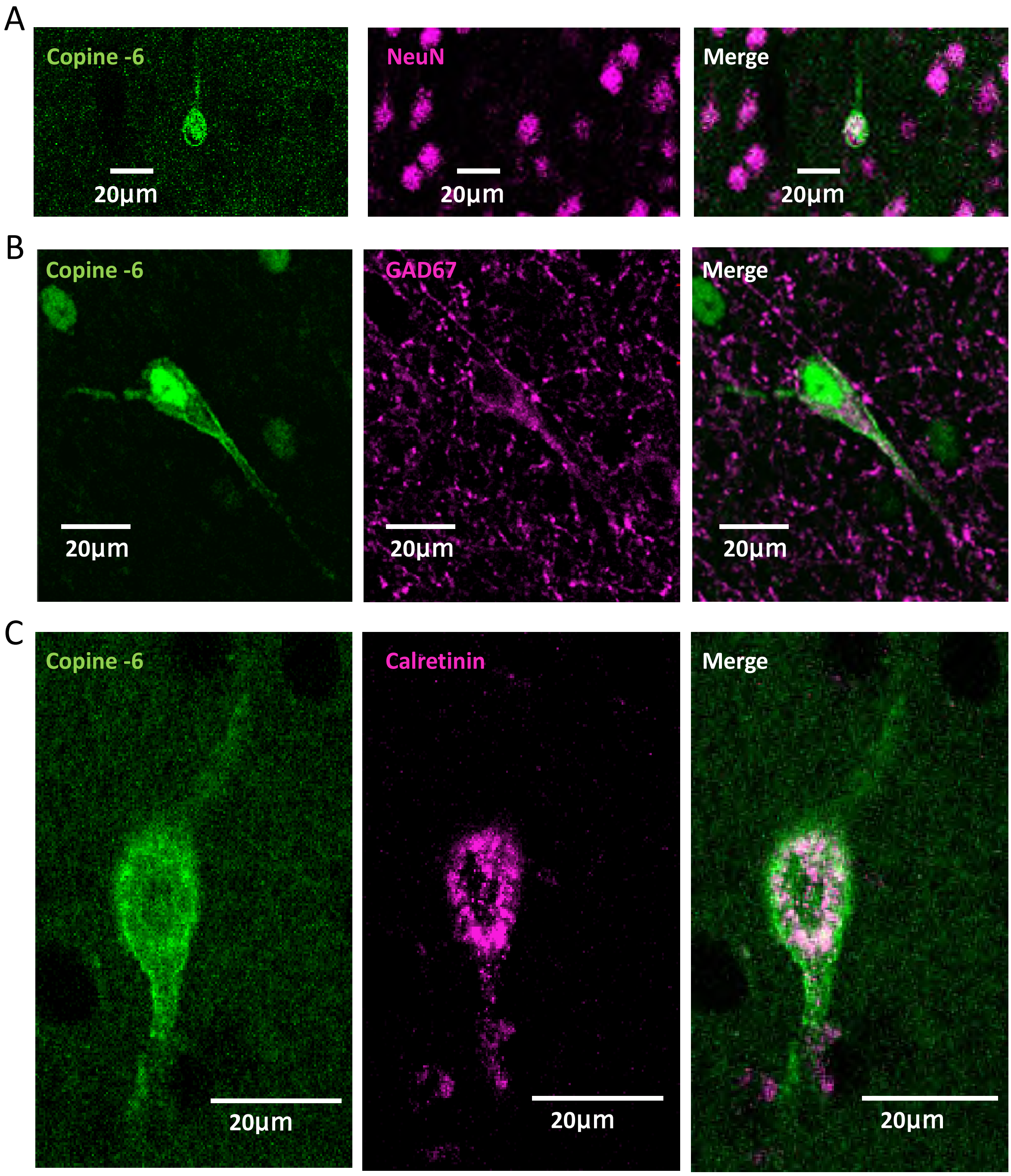

<u>Figure 3-26 Copine-6 labelling of 'ghost cells' in the neocortex.</u>

A. All Copine-6 ghost cells are co-immunoreactive for NeuN, **B**. Co-reactivity with GAD67 and **C**. Co-reactivity with calretinin. All were taken as single scans at x20 and x40 objectives.

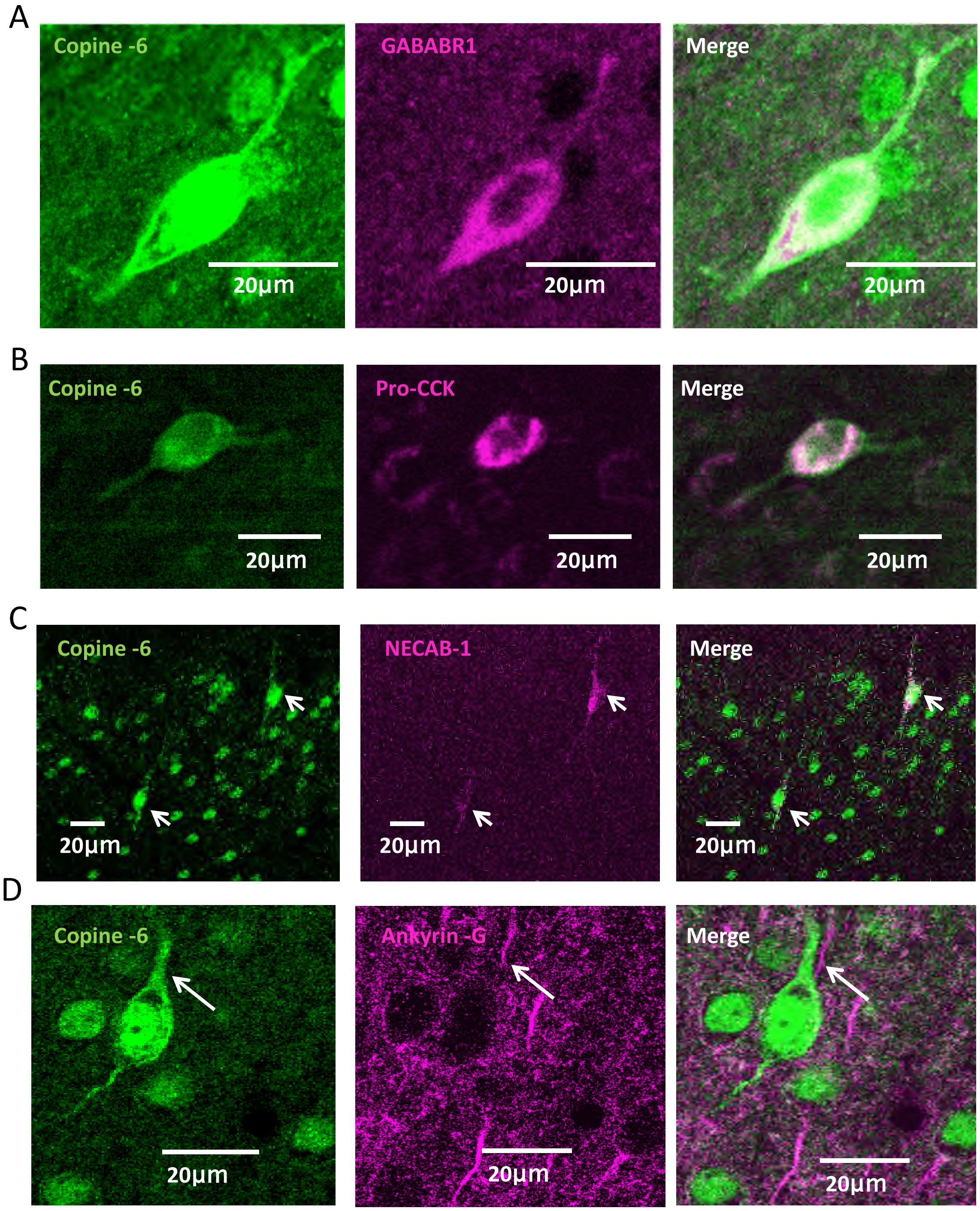

<u>Figure 3-27 Copine-6 labelling of "ghost cells" in the neocortex (continued).</u>

A. Copine-6 labelled cells are co-immunoreactive for the $GABA_B$ receptor 1 subunit, **B**. Co-reactivity with pro-CCK **C**. Co-labelling with NECAB1. **D**. An Ankyrin –G reactive axon initial segment (arrow) can be seen branching off the soma, or a primary dendrite, of the majority of Copine-6 ghost cells. Note also the presence of some small pyramidal cells labelled by Copine-6 in the image field. All images are single scans at x20 and x40 objective.

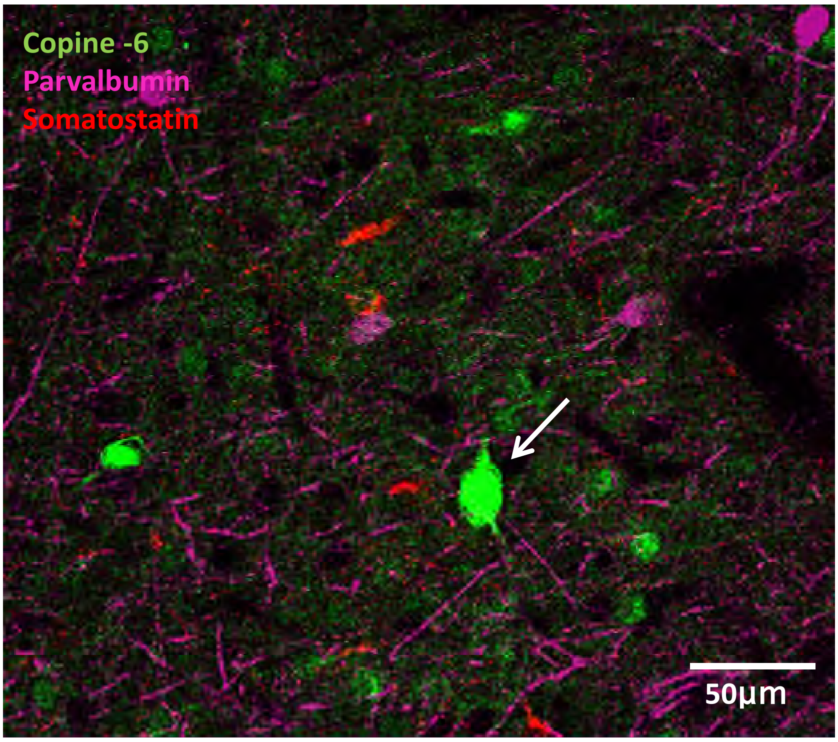

Figure 3-28 Copine-6 "ghost cells" do not express the interneuron markers parvalbumin or somatostatin.

Copine-6 does not colocalise with the markers parvalbumin or somatostatin in the frontal cortex of the adult rat. The image shows a single scan, x20 objective.

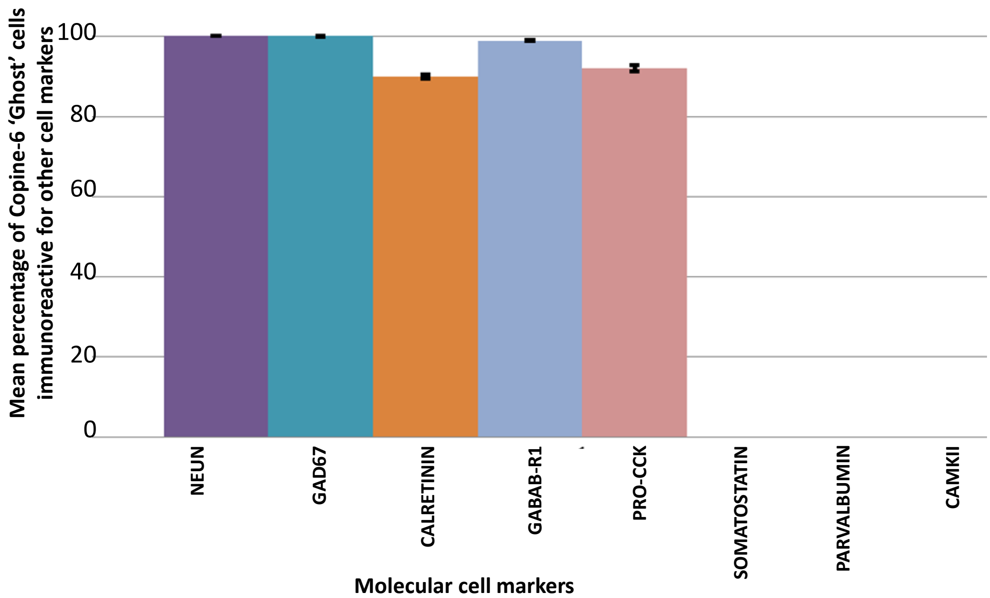

Figure 3-29 Co-localisation of Copine-6 cortical 'ghost' cells with other interneuron cell markers

Copine-6 reactive 'ghost' cells throughout the neocortex are GABAergic interneurons (<98% NeuN, GAD67, GABAB-R1), the majority with Calretinin and Pro-CCK (88%, 91% respectively). The cells were not immunoreactive for somatostatin, parvalbumin or CAMKII. For each reaction 400-600 cells were counted, using every fifth section of a total of 4 adult rat brains.

A third population of neocortical Copine-6 immunoreactive cells can be seen in layer VI of the neocortex, on the periphery and intertwined with the white matter of the corpus callosum. These cells appear to be unusual in location, morphology and orientation, and have been studied in great detail. (See below, 3.3.7)

3.3.7. Copine-6 in layer VI of the neocortex and the corpus callosum

The Copine-6 antibody labels an isolated, intensely stained population of small neurons in layer VI of the cortex and the corpus callosum. The cells can be seen bordering and within the white matter of the corpus callosum in both a rostral and caudal direction in parasagittal brain sections (see Figure 3-30). These Copine-6 neurons present with a small round soma, between 10-18µm. The somata of these cells are intensely labelled, and the nucleus and cytoplasm often cannot be distinguished owing to the sheer intensity of this staining. The Copine-6 neurons all display bipolar processes, some of which have more extensive secondary (possibly dendritic) branching which also appears to follow the direction of the white matter in a rostral-caudal plane. The Copine-6 labelled processes are very long and are often intertwined with processes of other Copine-6 labelled cells with the same morphology, in a 'chain-like' distribution. The arborisations of the Copine-6 cells are consistently ornamented with 'spine-like' protrusions along their entire length, in a non-uniform manner identical to those 'spiny' cells identified in the dissociated olfactory culture (Figure 3-31). For ease of description and owing to their similarly to the 'spiny' cells of the dissociated olfactory culture, these Copine-6 neurons will be referred to as 'Copine-6 spiny cells' in the corpus callosum.

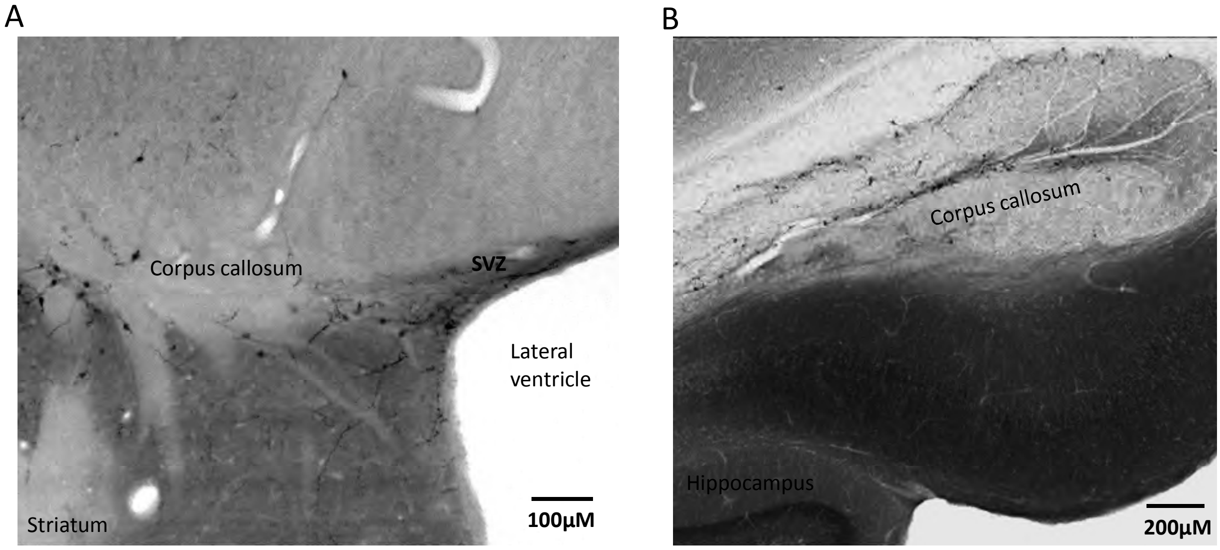

Figure 3-30 Copine-6 spiny cells in the rostral and caudal corpus callosum.

A. Copine-6 cells in the rostral corpus callosum. The Copine-6 spiny cells can be seen bordering the lateral ventricle, branching into the subventricular zone (SVZ) and also into the striatum proper. The cells border the corpus callosum, some soma located in the body of the corpus callosum itself. **B**. The caudal corpus callosum, part of the anterior hippocampal continuation, over and above the hippocampus. Copine-6 spiny cells can be seen within the splenium of the corpus callosum. Both images are single scans using x20 objective.

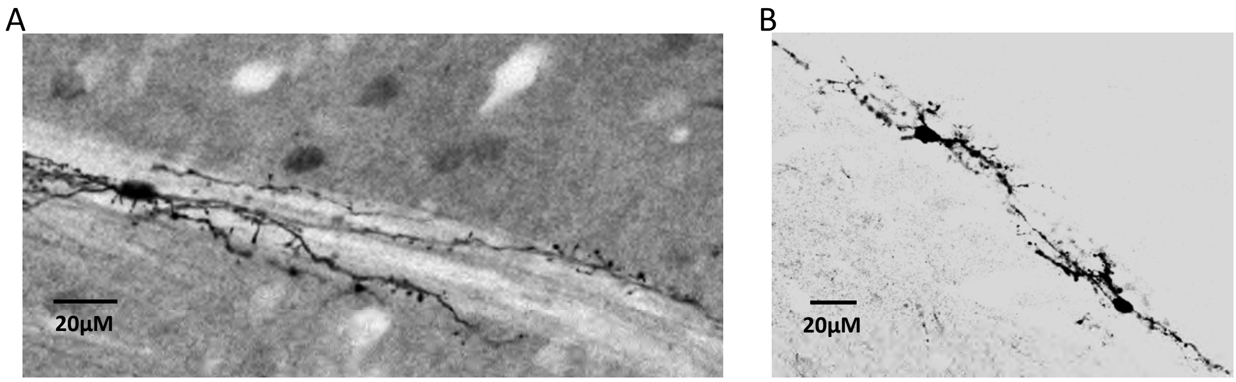

Figure 3-31. Typical Copine-6 spiny cells in the corpus callosum of the adult rat brain.

The 'spiny' processes appear to run in parallel with the white matter tracts. **A**. The cell is located at the top corner of the striatum, where it meets the lateral ventricle and layer VI of the neocortex. **B**. The 'chain like' distribution of the Copine-6 spiny cells that is seen in the rostral and caudal corpus callosum. Both images are z-stacks using 1-μm optical slice thickness, 25 z-sections collected at 0.5-μm intervals

The Copine-6 spiny cells in the rostral portion of the sagittal brain sections appear to be within, or peripheral to, the rostral migratory stream (RMS) which is the migratory pathway of newborn and migrating neuroblasts. The migrating cells undergo tangential migration to the olfactory bulb, where they then undergo radial migration to their final destination within the granule or periglomerular cell layer (see Introduction). The Copine-6 cells are distributed in a uniform chain-like manner along the edge of the nestin-defined RMS, often branching into the white matter itself with some soma being located in the body of the corpus callosum(Figure 3-32 A). This is true of the cells in both a rostral and caudal direction from the lateral ventricle. Some Copine-6 cells are found 'clustered' close to one another at the subventricular zone border, where it meets the lateral ventricle (see Figure 3-32 B) and often the cells can be seen branching into the striatum proper. The processes of these Copine-6 reactive cells appear to be branching into the subventricular zone, the soma appearing to point towards the ventricle itself.

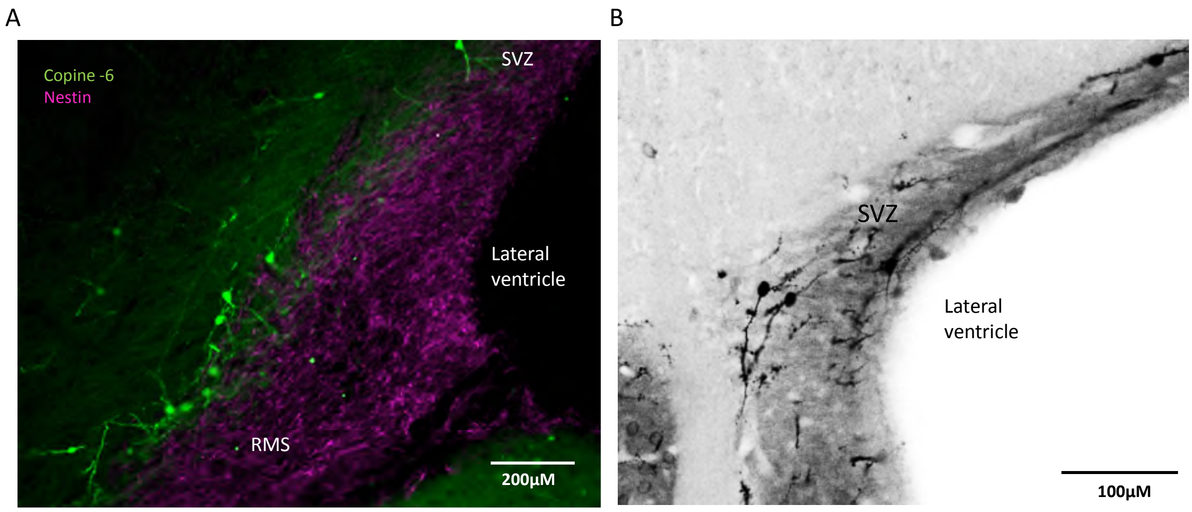

Figure 3-32 Copine-6 spiny cells bordering the rostral migratory stream (RMS) and the subventricular zone (SVZ).

A. Copine-6 cells can be seen to border the nestin-labelled RMS. Some Copine-6 cells branch into the corpus callosum and subventricular zone. Single scan image at x20 objective. **B**. Copine-6 spiny cells can also be seen bordering and the processes branching into the SVZ itself. Z-stack of 1-µm optical slice thickness, 20 z-sections collected at 0.5-µm intervals.

The Copine-6 cells, although small in population, are not in a neuron-rich environment. Co-immunostaining for NeuN revealed that the Copine-6 spiny cells were indeed immunopositive for NeuN (Figure 3-40) , but there were very few other neurons labelled in the corpus callosum (see Figure 3-33). Therefore, in order to better characterise these unusual Copine-6 positive spiny cells, a variety of established protein markers were applied in conjunction with the Copine-6 antibody.

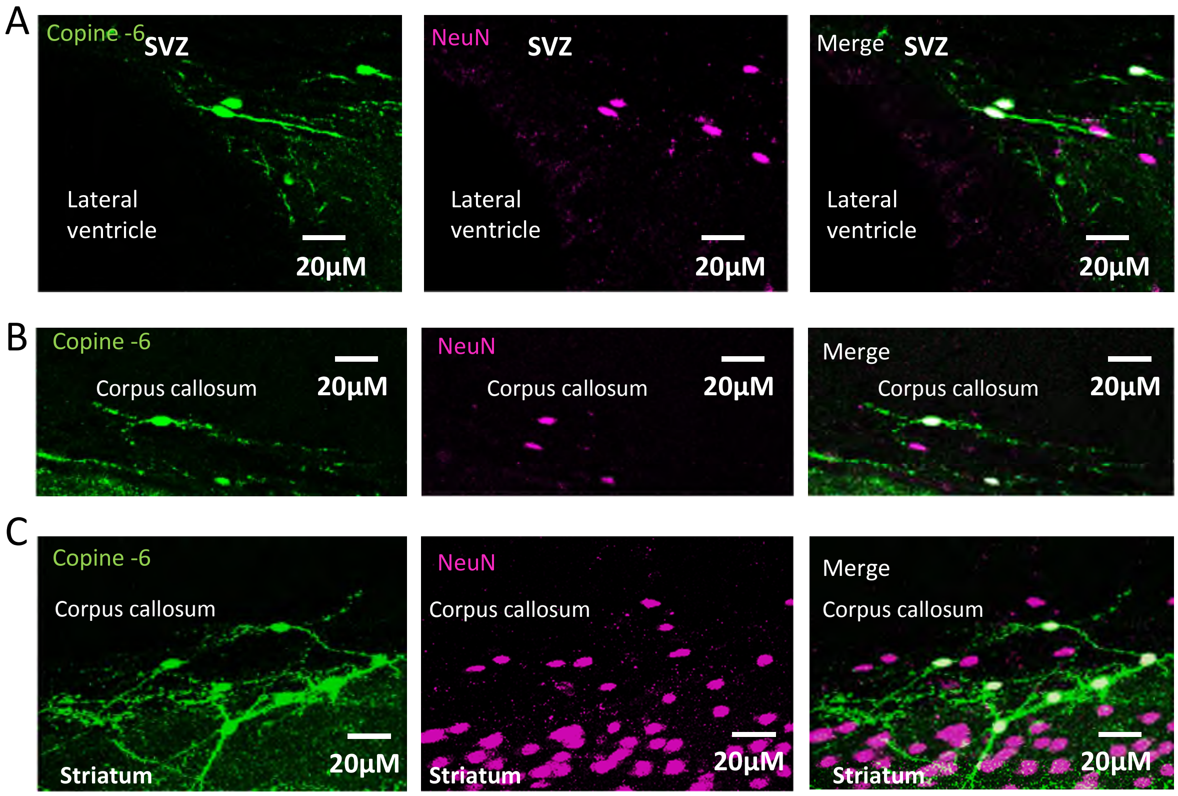

Figure 3-33 The Copine-6 spiny cells in the corpus callosum of the adult rat are immunopositive for the neuronal marker NeuN.

A. Copine-6 cells at the border of the lateral ventricle and in the subventricular zone are all immunopositive for NeuN. **B**. A Copine-6 spiny cell in the corpus callosum itself is reactive for NeuN. There are very few other NeuN +ve cells in the corpus callosum. **C**. The Copine-6 spiny cells branching into the corpus callosum above the striatum are NeuN immunoreactive. Note how few NeuN +ve cells are in the corpus callosum compared to their abundance in the striatum proper. All images are z-stacks of1-µm optical slice thickness, 20 z-sections collected at 0.5-µm intervals

Histochemical analysis revealed that the Copine-6 labelled cells did not co-localise with GFAP (Figure 3-34 A) or vimentin (Figure 3-34 B) (also, see Figure 3-40), which label immature glial cells and astrocytes. This is in line with the previous analysis of the spiny cells in the dissociated olfactory cultures and also confirms the neuronal reactivity with NeuN. Furthermore, Copine-6 cell labelling did not co-localise with nestin, the stem cell and progenitor cell marker (see Figure 3-34 C, and Figure 3-40). The nestin antibody labelled the subventricular zone and the entire rostral migratory stream.

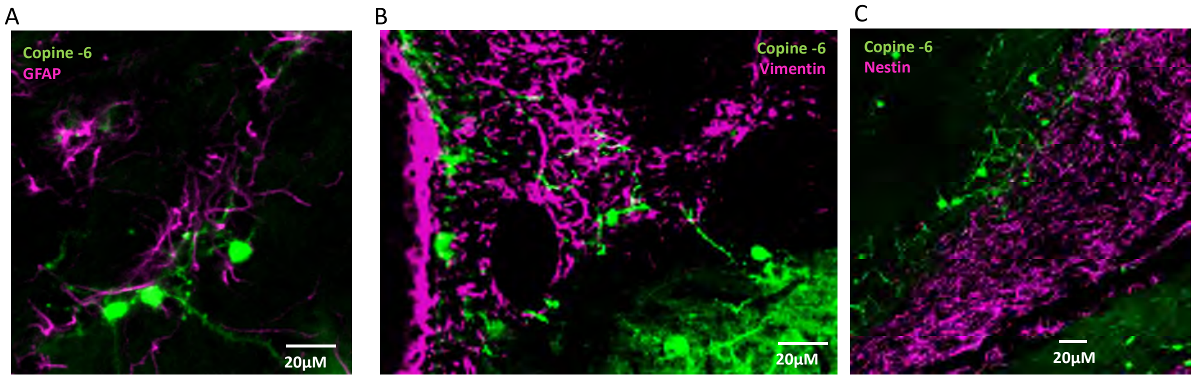

Figure 3-34 Copine-6 spiny cells are not glia or newborn neuroblasts.

A. Copine-6 spiny cells are not GFAP labelled glial cells. **B**. Copine-6 spiny cells are not vimentin labelled glial cells. **C**. Copine-6 cells were not labelled by the neuroblasts marker nestin. In all cases, note how the Copine-6 cells are closely located to the glial and newborn cells. All images are single scans at x20 objective.

At a higher magnification, individual nestin immunopositive cells could be seen in the RMS, which were small and varied in their number of processes. The Copine-6 labelled cells were morphologically distinct to these immature migrating cells, both by soma shape and size and the dendritic arbors that the Copine-6 neurons possess. Although the Copine-6 cells do exhibit long processes orientated in the direction of the RMS – similar to those of the immature neuroblasts – there were clear morphological differences observed between the two cell populations. However, rather strikingly, some of the Copine-6 histochemical labelling appeared to be peripheral, but in very close proximity, to some of the nestin immunopositive cell processes (see Figure 3-34, Image C). The most numerous of the Copine-6 cells were located on the cortical side of the RMS, some branching into the corpus callosum and others within layer VI of the neocortex. The distribution of the Copine-6 cells could be described as a 'boundary', with no nestin cell processes extending beyond the Copine-6 reactive soma and processes (Figure 3-34 C). Indeed, the Copine-6 cells in the corpus callosum were identified throughout the corpus callosum, in both the rostral and caudal direction which suggests that these cells are not exclusive to the migratory pathways in the adult rat brain.

Histochemical analysis revealed that there was no co-localisation between Copine-6 and the migratory markers PSA-NCAM (Figure 3-35 A) and doublecortin (Figure 3-35 B and C) (also see Figure 3-40). Both markers labelled migrating cells within the rostral migratory stream in its entirety, and individual migrating cells could be visualised at higher objectives. The doublecortin and PSA-NCAM immunopositive cells were similar to those previously labelled nestin-positive cells, although the cells appeared to be labelled more heavily in the long processes which wrapped around other cells along the migratory pathway. It was also noted that some of the Copine-6 spiny cell processes appeared to be in close contact with some of the doublecortin migrating cell processes, as though each cell population was intertwined (Figure 3-35 C).

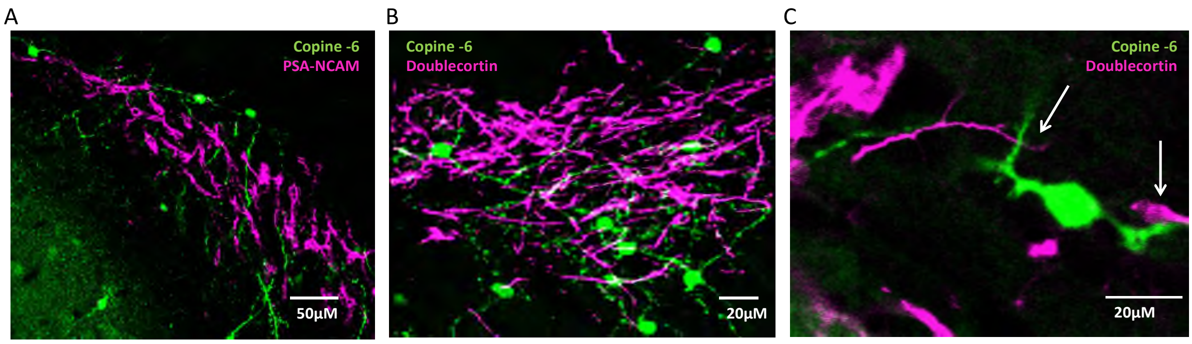

Figure 3-35 Copine-6 spiny cells in the corpus callosum are not PSA-NCAM or doublecortin postive.

A. Copine-6 labels a different cell population to PSA-NCAM **B**. Copine-6 cells are not labelled by doublecortin **C**. The Copine-6 cell processes appear to be very closely positioned to doublecortin labelled processes (arrows). All images are Z-stacks at 1-µm optical slice thickness, 20 z-sections collected at 0.5-µm intervals

Since the Copine-6 spiny cells in the corpus callosum appear to share morphological characteristics of the small spiny cells identified in the dissociated cultures of the olfactory bulb (see section 3.3.3), identical histochemical tests were conducted to molecularly classify these apparently mature neurons as evidenced by their co-immunoreactivity with NeuN. In line with the results of the dissociated olfactory bulb culture, the spiny cells in the white matter were all strongly immunopositive for GAD67 (see Figure 3-36 A, B, Figure 3-40) and lacked immunoreactivity for Ankyrin –G, suggesting an axonless phenotype as defined by this scaffolding protein (Figure 3-36 C). In the corpus callosum and including the subventricular zone, ~69% of the Copine-6 cells spiny cells were also immunopositive for calretinin (see Figure 3-37, Figure 3-40).

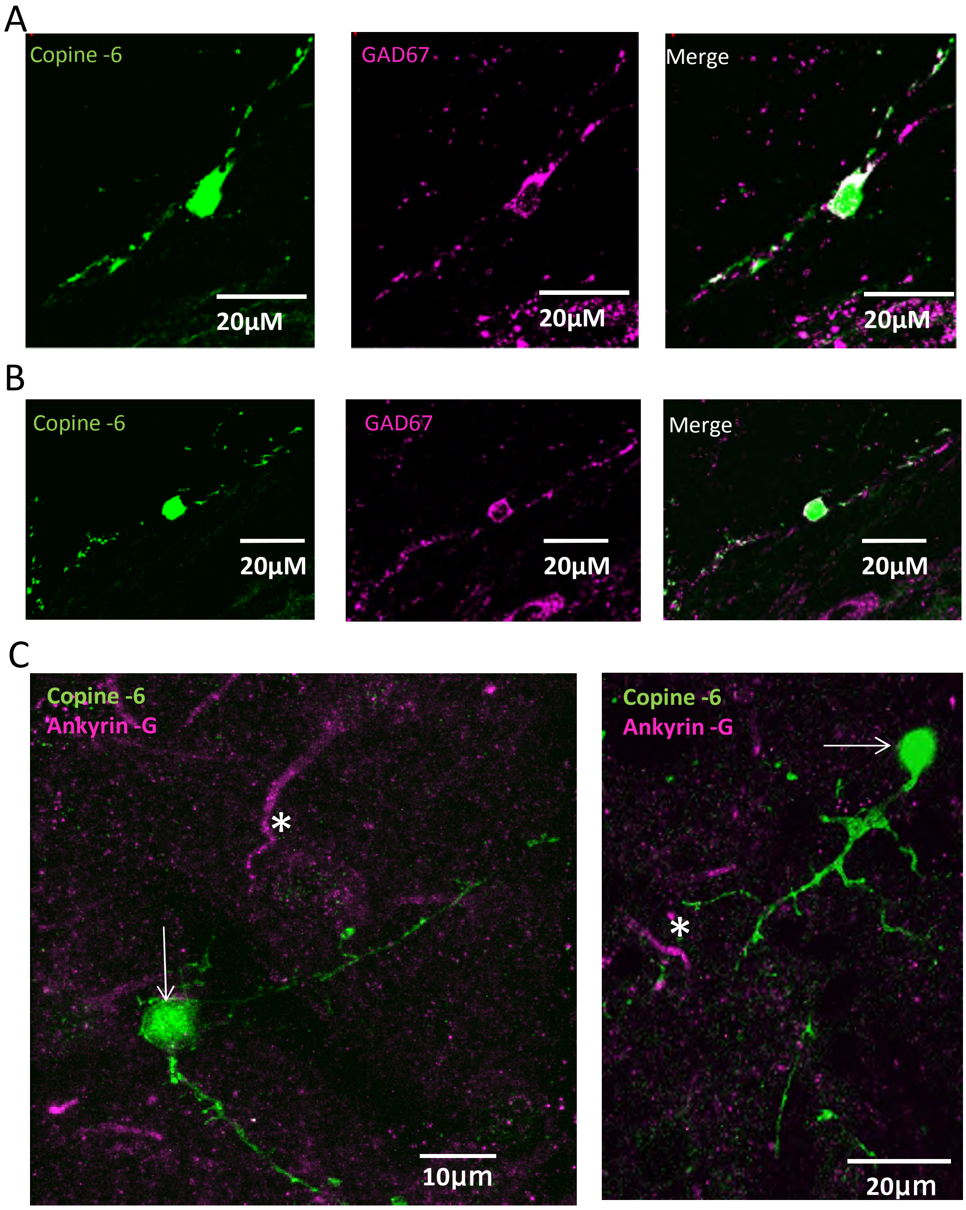

Figure 3-36 Copine-6 spiny cells in the corpus callosum are immunoreactive for GAD67 and lack an Ankyrin –G defined axon.

Copine-6 cells are GAD67 positive in **A**.the rostral corpus callosum and **B**.the caudal corpus callosum. **C**. Two images to show two different Copine-6 spiny cells that lack Ankyrin =G expression (arrows). Other Ankyrin –G positive axon initial segments can be identified (* in both images). All images are z-stacks of 1-µm optical slice thickness, 20 z-sections collected at 0.5-µm intervals

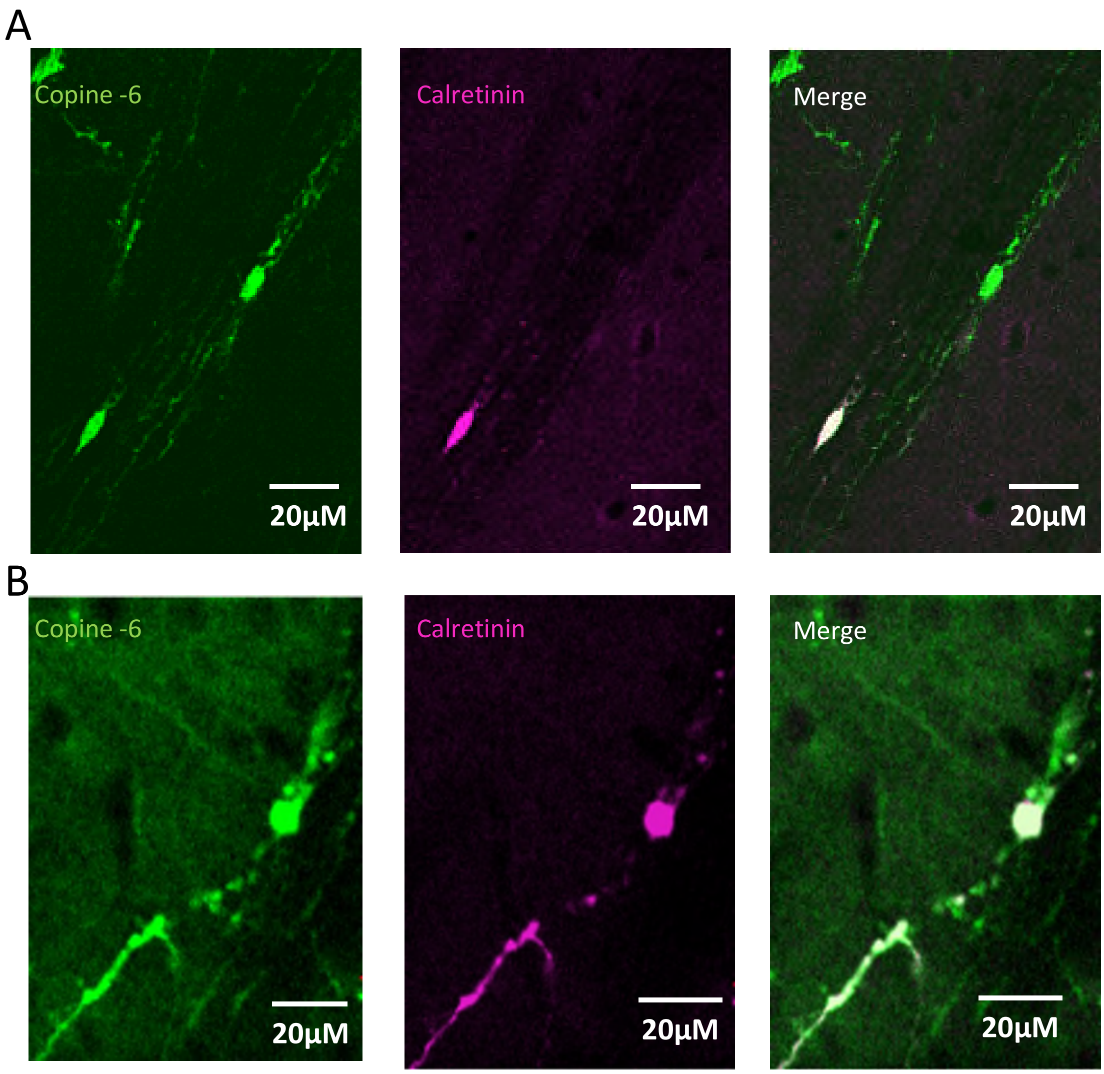

Figure 3-37 Some Copine-6 spiny cells are co-immunoreactive for calretinin.

A. Two Copine-6 cells, one co-immunoreactive for calretinin and one immunonegative. **B**. Co-reactivity, when present for both calretinin and Copine-6 was evident in the soma, processes and spine-like protrusions. All images are single scans at x40 objective.

Since the co-immmunoreactivity for calretinin suggests the Copine-6 cells may be an interneuron population, rat brain sections were subsequently co-stained for other interneuron markers. All of the Copine-6 spiny cells were immunonegative for parvalbumin and somatostatin (Figure 3-38 A, Figure 3-40). Cell markers which are known to identify neurons in the corpus callosum were therefore investigated by co-staining Copine-6 cells with neuropeptide Y (NPY), and neuronal nitric oxide synthase (nNOS). Small numbers of NPY +ve/nNOS +ve neurons could be identified in a rostral and caudal direction within the corpus callosum, but all of the Copine-6 spiny cells were immunonegative for both markers (Figure 3-38, Image B, Figure 3-40).

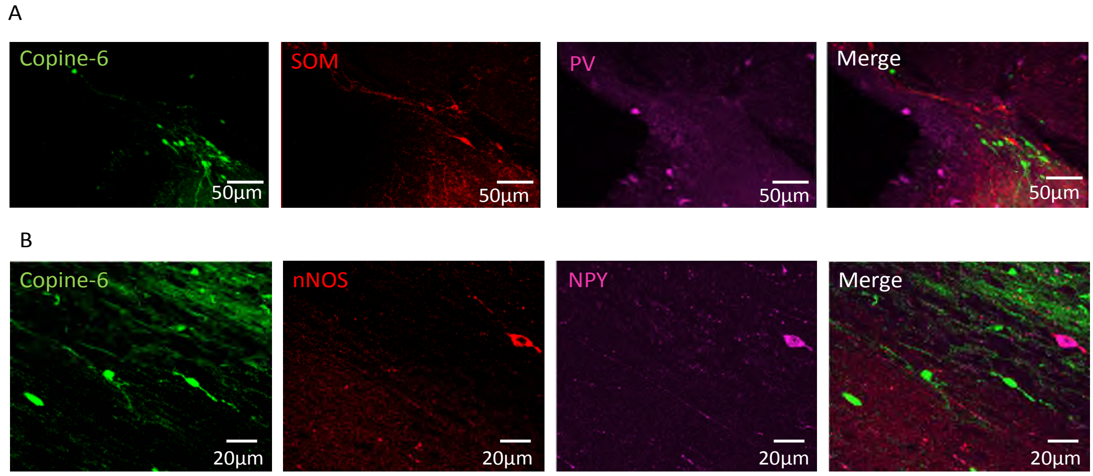

Figure 3-38 Copine-6 spiny cells are not labelled by other interneuron markers.

A. Copine-6 cells bordering the subventricular zone (SVZ) are immunonegative for somatostatin (SOM) and parvalbumin (PV). **B**. Copine-6 cells are also immunonegative for nNOS and NPY. An nNOS/NPY +ve neuron is present in the corpus callosum, although they are not in abundance. All images are single scans at x20 objective.

Some ~42% of the Copine-6 spiny cells, however, are immunoreactive for enkephalin.(see Figure 3-39, Figure 3-40) In most cases, this immunoreactivity was only visible in some of the processes and in the spine-like appendages; only ~10% of the cells identified had reactivity in the soma. This suggests that enkephalin is restricted to the boutons in those cells in which it was identified.

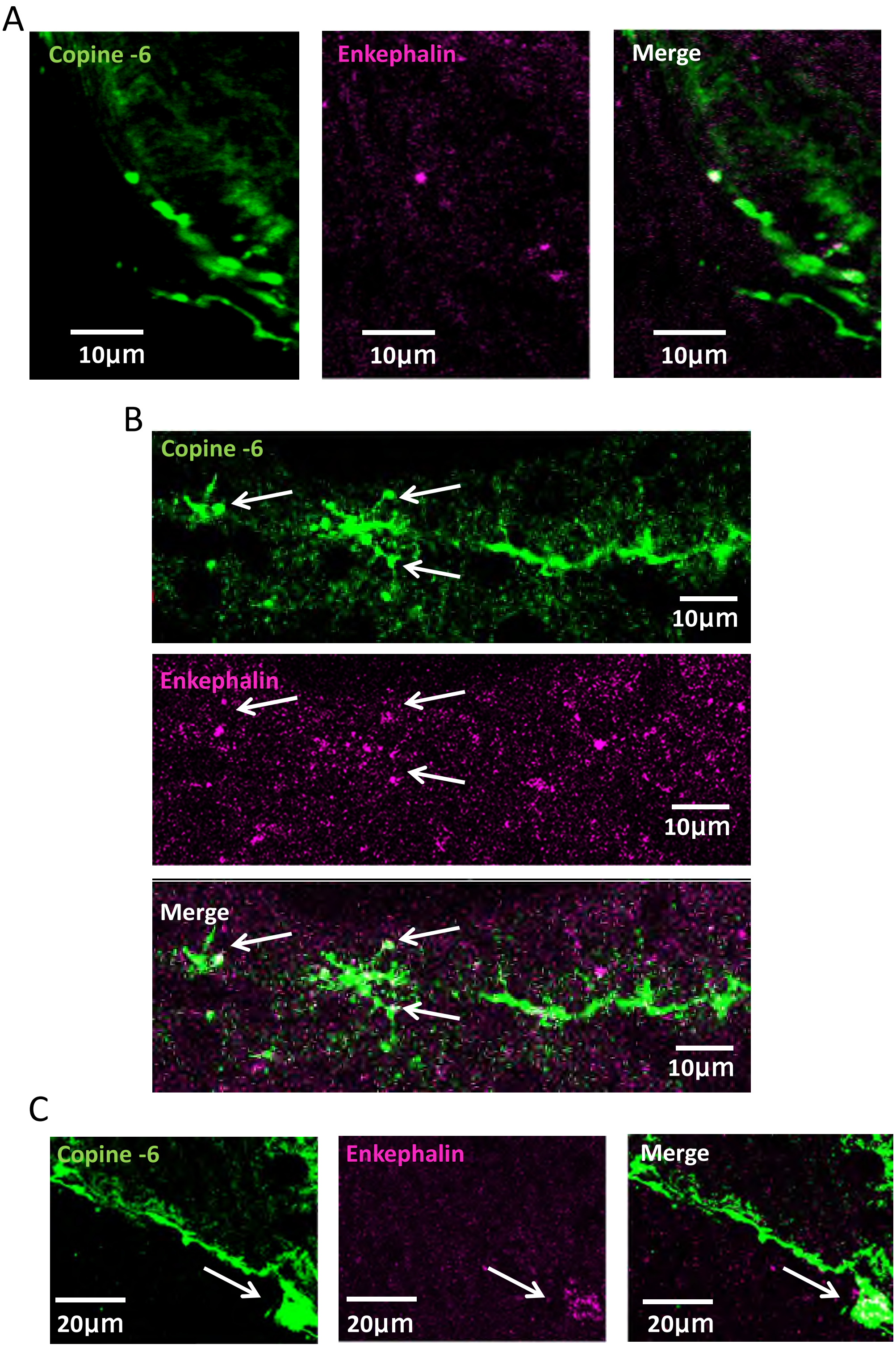

Figure 3-39 Some Copine-6 spiny cells in the corpus callosum are immunoreactive for enkephalin.

A and **B** Copine-6 processes and spine-like protrusions had some enkephalin reactivity **C**. Some of these cells also had a soma reactive for enkephalin. All images are z-stacks of 1-µm optical slice thickness, 20 z-sections collected at 0.5-µm intervals.

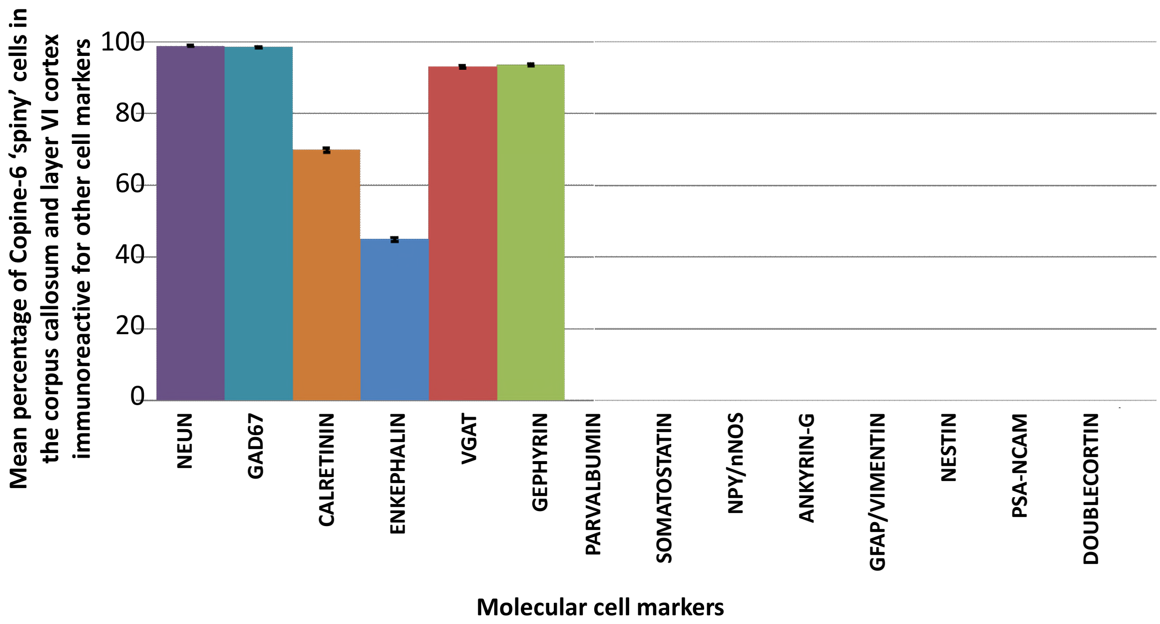

Figure 3-40 Co-localisation of Copine-6 'spiny' cells in the corpus callosum with other cell markers representative of cells in the neurogenic location.

Copine-6 spiny cells were compared to known interneuron and immature cell markers in order to characterise the cell population in the neurogenic region and in the corpus callosum. The Copine-6 cells are NeuN, GAD67 immunoreactive (~99%) and exhibit pre-and post-synaptic proteins VGAT (~94%) and Gephyrin (~95%), respectively. The cells have heterogeneous calretinin (~69%) and enkephalin (~42%) expression indicating an interneuronal phenotype. The cells were immunonegative for other interneuron markers (PV, SOM, NPY, nNOS), immature cell markers (nestin, PSA-NCAM, Doublecortin), glial cells (GFAP, Vimentin) and negative for the axon initial segment marker Ankyrin-G. For each reaction at least 600 cells were counted, using every fifth section of a total of 6 adult rat brains.

The data thus far indicates that the Copine-6 spiny cells are mature GABAergic interneurons (>97% NeuN +ve and GAD67 +ve, ~70% calretinin +ve), with no molecular properties indicating they are in migration, immature development or of a glial cell phenotype (doublecortin -ve, PSA-NCAM-ve, nestin -ve, reelin -ve, GFAP -ve /vimentin -ve, respectively). To summarise, all of the immunohistochemical imaging with markers of the rostral migratory stream (nestin, reelin, doublecortin), and with markers of other neuronal populations in the corpus callosum (NPY +ve/nNOS +ve) indicated that the Copine-6 cells were in very close proximity to the rostral migratory stream and to other recognised neuronal populations within the corpus callosum but were not included in them. In some cases the 'spine-like' protrusions of the Copine-6 cells were opposite, and almost overlapping with NPY +ve dendrites or spines.

Immunohistochemical staining for VGAT revealed that some of the larger spine-like protrusions of the Copine-6 spiny cells were co-immunoreactive for VGAT (See Figure 3-41 A, Figure 3-40). Not all of the spine-like protrusions were labelled with the VGAT antibody, however those that were labelled were intensely so. The cell soma and dendritic arbor were free of VGAT immunoreactivity which indicated that the marker was specific for a component present within these spine-like protrusions, most likely to be GABA-filled vesicles. Since VGAT labelling revealed replicable co-localisation, the post-synaptic marker gephyrin was also histochemically investigated. Copine-6, VGAT and gephyrin applied as triple labelling revealed that the Copine-6 +ve/VGAT +ve immunopositive terminals were often closely apposed to one (or sometimes multiple) gephyrin immunopositive puncta (See Figure 3-41 B, C and D, Figure 3-40). Some gephyrin puncta with no obvious VGAT +ve terminal in close apposition were also identified, which may reflect the presence of gephyrin at glycinergic receptor clustering or the focal plane of the tissue.

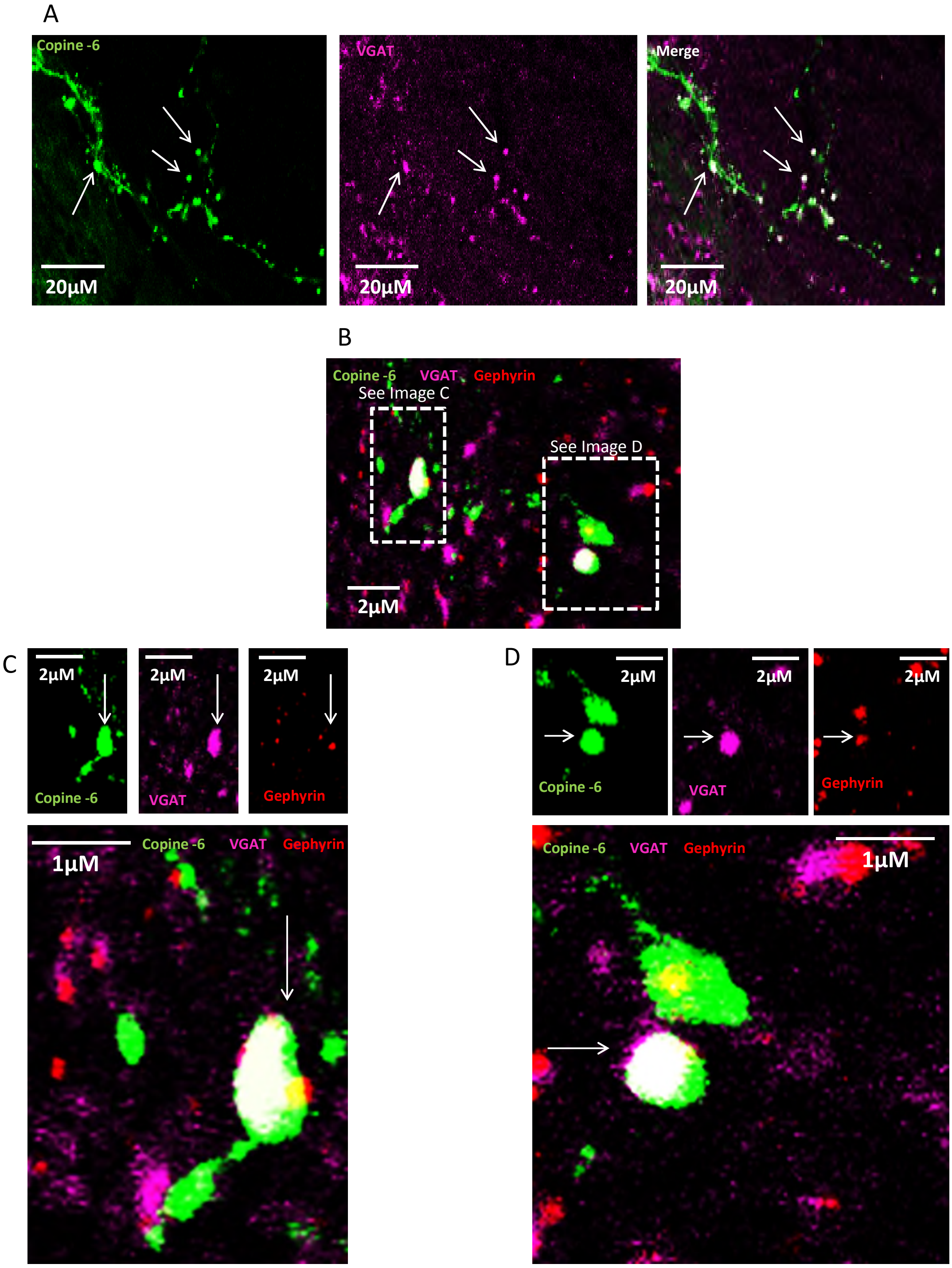

<u>Figure 3-41 Copine-6 spiny cells are co-immunoreactive with presynaptic VGAT and form appositions with postsynaptic gephyrin.</u>

A. Copine-6 processes are immunoreactive for VGAT in some of the spine like protrusions. **B**. Copine-6 +ve/VGAT +ve terminals that are in close apposition to gephyrin puncta. The boxes show two regions which are subsequently shown in images C and D. **C**.An enlarged image from image B of a Copine-6 +ve terminal containing VGAT with a gephyrin reactive puncta in close apposition (arrow). VGAT fills the Copine-6 terminal. **D**. An enlarged image again from image B showing another Copine-6 +ve/VGAT +ve terminal with gephyrin puncta. Both cases of Copine-6+/VGAT +ve appendages apposed to gephyrin puncta are typical of a putative synapse. All images are z-stacks of 1-µm optical slice thickness, 20z-sections collected at 0.5-µm intervals

The apposition of the Copine-6 appendage, with the pre-synaptic VGAT and postsynaptic gephyrin, suggests that the Copine-6 positive spiny cells can form dendro-dendritic synapses. However, given the limited resolution of even confocal light microscopy, firm conclusions cannot be drawn from the data presented here.

3.4. Discussion

The histochemical analysis of Copine-6 expression in rat brain has led to the identification of selective and neuron specific cell populations. Each of these neuronal populations has, to varying degrees, been molecularly categorised as belonging to particular subtypes of neurons. Briefly, Copine-6 is here documented to label the following subpopulations of cells: Pyramidal cells of the hippocampus, particularly within the CA1-CA3 regions, and granule cells of the dentate gyrus; certain calretinin immunopositive olfactory granule cells and calretinin +ve/enkephalin +ve periglomerular cells of the olfactory bulb (identified in rat brain sections and in dissociated olfactory culture); Small pyramidal cells within layers ii/iii of the adult rat neocortex; certain CCK +ve/calretinin +ve interneurons of the rat neocortex (Figure 3-42); and finally an unusual population of GABAergic (putative) interneurons within the corpus callosum and layer VI of the neocortex with striking molecular and morphological similarity to some olfactory granule and periglomerular cells (Figure 3-42). Each of these Copine-6 reactive subpopulations are discussed in detail below.

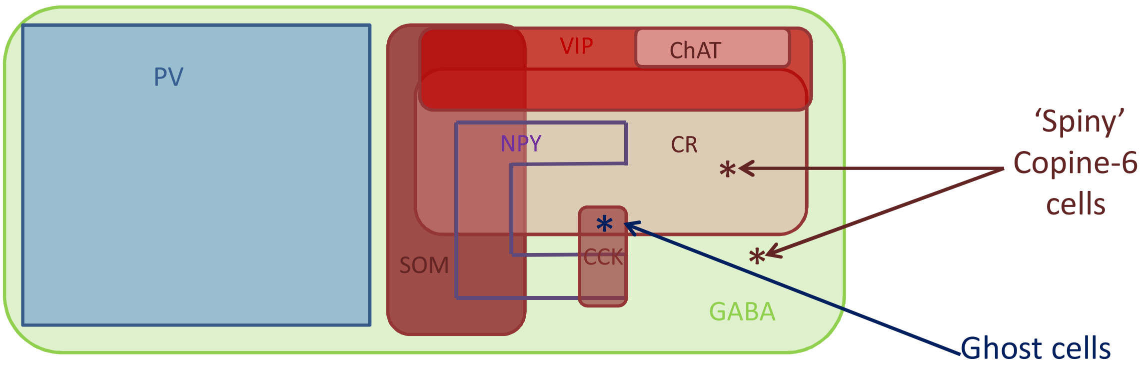

Figure 3-42 Where the Copine-6 'spiny' and 'ghost' cells fit into the distribution of cortical interneuron markers (image modified from Gonchar *et al*., 2007).

The Copine-6 GABAergic cells have here been identified as belonging to two different subpopulations of interneurons and can be categorised based on their marker expression (see also Figure 1-4). The Copine-6 'ghost cells' of the neocortex (*) fit into the small population of Calretinin +ve, CCK +ve intrinsic interneurons (see 3.4.4 for discussion), and the Copine-6 'spiny' cells of the layer VI neocortex and corpus callosum(*) fit within the Calretinin +ve interneurons, and the Calretinin –ve (some encephalin +ve) interneuron population (see 3.4.5 for discussion).

3.4.1. Copine-6 immunolabelling of some pyramidal cells and granule cells in the rat hippocampus

Immunohistochemical analysis of Copine-6 in the hippocampus identifies that the Copine-6 antibody labels pyramidal and granule cells of cornu ammonis, and the dentate gyrus, respectively.

These cell types were concluded based on the co-expression of the established protein markers NeuN, CAMKII, and Ctip2 (Arlotta *et al.*, 2005; Britanova *et al.*, 2008; Nielsen *et al.*, 2010). However, in addition, it has been noted that although these cells were analysed, there was a unique pattern of Copine-6 expression intensity throughout the hippocampus. A 'layered' pattern of immunoreactivity was visible, with very strong labelling within Stratum Pyramidale and Stratum Granulosum, a neuropil-like labelling in Stratum Radiatum and Stratum Moleculare, and very little labelling could be identified in Stratum Lacunosum. These different expression intensities contribute to the layered pattern visible at low magnification, which could be indicative of different pre- or –post- synaptic expression of the protein within different hippocampal regions, or it may be associated with the different input and output connections to each region. Although this could not be explored in detail in this thesis, it would certainly be worth further investigation.

3.4.2. Copine-6 immunolabelling identifies an 'axonless' spiny interneuron subpopulation in dissociated olfactory culture, with similarities to olfactory granule and/or periglomerular cells

Copine-6 labels a certain 'spiny' neuron population in olfactory bulb dissociated culture, which initially appears to be morphologically and molecularly similar to the GABAergic granule and periglomerular interneurons of the olfactory bulb. The molecular conclusion was drawn owing to a full co-expression between Copine-6 and GAD67 in these spiny cells and a partial co-expression with calretinin, in addition to a consistent lack of labelling for the axon initial segment marker Ankyrin –G. Within the olfactory bulb, the former two markers are expressed only by intrinsic neurons (i.e. granule or periglomerular interneurons) (Shepherd, 2004), and the lack of an axon as defined by a lack of labelling with Ankyrin –G would initially suggest that these cells belong to an axonless granule cell subpopulation (first identified by Golgi and Cajal, see reviews by Pinching & Powell, 1971; Price & Powell, 1970; Gordon M Shepherd *et al.*, 2007), although an axonless phenotype has also been suggested of certain periglomerular cells (Pinching & Powell, 1971a; Shepherd, 2004). Morphologically, the Copine-6 spiny cells in culture present with a small soma, lack of an axon, and dendritic arborisations decorated with spine-like protrusions, or putative 'gemmules' (Rall *et al*, 1966) as described for granule and periglomerular cell populations (Price & Powell, 1970c; Pinching & Powell, 1971a). Accurate characterisation of these putative Copine-6 reactive interneuron populations could not be carried out in dissociated olfactory culture alone for the following reasons. The dissected cells are no longer *in situ*, instead being isolated from their usual homeostatic environment of the rat brain which could lead to alterations in cell phenotype, molecular expression, or morphological disturbance. The majority of the dissociated culture actually consisted of cells that were very weakly reactive for Copine-6. In the intact olfactory bulb, however, Copine-6 reactivity is very strong in the majority of cells therefore there is some discrepancy between the immunohistochemical analysis of sections and tissue culture. It is not clear exactly why the bright Copine-6 reactive cells that fill the olfactory bulb (particularly of the granule cell layer) are not also strongly reactive for Copine-6 in the tissue culture, but it may reflect the embryonic developmental stage at which the cultures were prepared (day E17-18) since the neurogenesis of the majority of granule and periglomerular cells occurs during postnatal development (Bayer, 1983). It is therefore highly possible that their genesis has not yet occurred at the time of tissue collection, or may be in the process of occurring, at the subventricular zone away from the dissected site, thus resulting in them being excluded from the cultures. The tissue culture conditions may also be insufficient to promote optimal cell growth, particularly if the cells are immature. Despite this, and perhaps most importantly for this study, the Copine-6 spiny interneurons that are to be focussed on in subsequent chapters of this thesis were present in the culture – though only when the dissection was taken to include part of the RMS – and the weakly labelled cells (that may represent other olfactory neurons) failed to exhibit any morphological or molecular similarity to these spiny Copine-6 cells. It was presumed on the ground that the weak Copine-6 cells were lacking any GABAergic molecular markers that they are likely to be principal excitatory neurons, probably the mitral cells of the olfactory bulb mitral cell layer (for an overview of the topic, see Shephard, 1979).

3.4.3. Copine-6 is expressed by certain olfactory granule and periglomerular cell populations in the rat olfactory bulb

Copine-6 indeed labels numerous cells in the granule cell layer of the rodent brain, and a subpopulation of periglomerular cells in the glomerular layers.

As seen in the dissociated olfactory bulb cultures, all of the Copine-6 cells in the granule and periglomerular cell layers were GABAergic, as expected of intrinsic olfactory interneurons (Rall *et al.*, 1966; Lledo *et al.*, 2004; Shepherd, 2004; Shepherd *et al.*, 2007) . The co-expression of the calcium-binding protein calretinin in some, but not all, Copine-6 cells is typical of the heterogeneous calretinin-positive GABAergic granule and periglomerular interneuron populations (Résibois & Rogers, 1992; Kosaka *et al.*, 1998; Kato *et al.*, 1999; Kohwi *et al.*, 2007; Batista-Brito *et al.*, 2008). This would be consistent with the widely held view that the interneuron populations of the olfactory bulb are certainly not homogeneous (Pinching & Powell, 1971a; Fritschy & Mohler, 1995; Kosaka *et al.*, 1998; Lledo *et al.*, 2004; O'Connor & Jacob, 2008).

The Copine-6 cells in the olfactory granule cell layer lack immunoreactivity for Ankyrin – G, a marker of the axon initial segment, as do some of the Copine-6 reactive periglomerular cells which is also typical of some periglomerular subpopulations lacking a morphological axon(Pinching & Powell, 1971b; for a review see Shepherd, 2004). The Copine-6 spiny cells in the olfactory culture also lacked the Ankryin - G reactivity which helped to distinguish these cell populations alongside their characteristic spiny arborisations. In both the Copine-6 reactive granule and periglomerular cells in brain sections, and the 'spiny' Copine-6 reactive cells in dissociated culture, the numerous, unevenly distributed spines could be classified as 'gemmules'. First described by Rall and collegues (Rall *et al*, 1966), such gemmule-like varicosities are typically presynaptic spines to postsynaptic principal cells within the olfactory bulb and are typical of the granule and periglomerular cell populations. 'Spine-like' structures resembling gemmules were visible on the majority of Copine-6 'spiny cell' processes (hence their descriptive name) and this, together with their axonless phenotype, may indicate that the spiny Copine-6 cells are a similar subpopulation to olfactory interneurons. Furthermore, histochemical analysis revealed the presence of VGAT in selected Copine-6 reactive gemmules of the Copine-6 granule cells in the olfactory bulb, pointing towards putative GABAergic signalling (McIntire *et al.*, 1997). VGAT was the first of a novel family of neurotransmitter transporters to be identified to co-localise with synaptic vesicles containing GABA, and has been widely used as a presynaptic marker since its identification (McIntire *et al*., 1997). This GABAergic signalling, or VGAT reactivity, is particularly expected of both granule and periglomerular cell phenotypes (Rall *et al.*, 1966;

Pinching & Powell, 1971a; Ribak *et al.*, 1977; Kosaka *et al.*, 1998; Kosaka & Kosaka, 2005; Shepherd *et al.*, 2007) .

Olfactory Granule cells: Copine-6 labels some – but not all- calretinin immunopositive granule cells within the olfactory granule cell layer. Furthermore some Copine-6 cells within the granule cell layer do not co-label with any of the subpopulation markers (tyrosine hydroxylase, calbindin, enkephalin, somatostatin, parvalbumin, NOS, NPY) described for these cells. Together this suggests that Copine-6 immunoreactivity identifies additional subpopulations of olfactory granule cells. Interestingly, Copine-6 (or, as cited as 'N-Copine'), has recently been itself employed as a olfactory granule cell marker owing to its strong expression in the mouse olfactory bulb (Bagley *et al.*, 2007). Bagley and co-workers describe Copine-6 labelling as cytoplasmic, with some labelling of proximal dendrites in cells of the granule cell layer with less intense, sparse labelling in the glomerular layers, in good agreement with our findings.

It is not possible to exclude the possibility that the unclassified Copine-6 granule cells described above are at a particular, perhaps a mid-mature, stage of development or integration into the olfactory bulb as part of its ongoing and constant plasticity. It is difficult to assign a time-point at which Copine-6 expression begins, particularly because *all* of the neurons immunoreactive for Copine-6 express NeuN. This indicates that either the cells mature prior to Copine-6 expression, which would explain why no immature cells are immunoreactive for Copine-6, or it may indicate that the cells are born during an earlier developmental time-point and all labelled cells are therefore mature by the time histochemical analysis is carried out. This issue will be addressed in Chapter 4.

Olfactory Periglomerular cells: As with the granule cell populations of the olfactory bulb, it is well established that periglomerular cells are a heterogenous GABAergic interneuron population expressing different calcium binding proteins and/or different neuropeptides, with small degrees of overlap between each group (Kosaka *et al.*, 1998). According to the molecular profiles of these cells reported by Kosaka and collegues, it would appear that Copine-6 labels some of the enkephalin +ve/calretinin +ve / GAD67 +ve periglomerular subpopulation(s). However, as was found with the granule cells, the Copine-6 expression overlapped only to a certain degree with calretinin. Unlike the granule cells, some of the periglomerular cells were enkephalin immunopositive. A few of the Copine-6 labelled cells were negative for both enkephalin and calretinin, which could indicate the identification of a novel cell population. However, this may also be a reflection of developmental protein marker expression (Kosaka *et al.*, 1998).

3.4.4. Copine-6 labels neocortical small pyramidal principal neurons, and a discrete population of calretinin +ve/CCK +ve GABAergic interneuron (the 'ghost' cell)

Small pyramidal cells: The Copine-6 labelled cells in layer ii/iii of the neocortex are concluded to be small pyramidal cells following their co-reactivity with CAMKII, a marker of glutamatergic neurons in the cortex, and some co-reactivity for the nuclear transcription factor Ctip2 which also labels some glutamatergic neurons in the neocortex particularly within layers v/vi (Arlotta *et al.*, 2005; Molyneaux *et al.*, 2007a; Britanova *et al.*, 2008; Nielsen *et al.*, 2010). This labelling of excitatory pyramidal cells is further evidence that Copine-6, alongside its expression in pyramidal cells of the hippocampus, is not exclusive to inhibitory neurons, as found in other cells of the cortex and olfactory bulb.

Copine-6 labelled 'Ghost' cells: Copine-6 labels a population of calretinin-expressing GABAergic intrinsic interneurons (Condé *et al*,1994; Gonchar *et al*, 1997; Kawaguchi *et al*, 1997; Kubota *et al* , 1994; Ribak, 1978, Somogyi *et al*, 1985; Somogyi *et al*., 1984. For a review see Barinka *et al*, 2010) (Figure 3-42). The morphological appearance of the Copine-6 'ghost cells', with a fusiform/oval-shaped soma and bipolar dendrites is also in accordance with previously described morphologies of these calretinin-expressing non-pyramidal cortical neurons (Jacobowitz *et al*, 1991; Résibois *et al*, 1992). The lack of immunoreactivity with other neocortical interneuron markers such as calbindin, parvalbumin or somatostatin contributes to this classification, and also suggests that Copine-6 reactivity may be unique to these particular calretinin- expressing non-pyramidal cortical interneurons in rodent neocortex (Gonchar *et al*, 1997; Gonchar *et al*, 2007; Jacobowitz *et al*, 1991; Kubota *et al*., 1994; Résibois *et al*, 1992). The presence of pro-

CCK in the Copine-6 immunopositive ‘ghost cells’ is also in accordance with previously described subpopulations of GABAergic calretinin +ve interneurons of the neocortex (Demeulemeester *et al*, 1988; Peters *et al*, 1983; Somogyi *et al*., 1985). However, since Copine-6 did not label *all* pro-CCK immunopositive cells in the neocortex, Copine-6 may be specific to only a certain subpopulation(s) of CCK interneurons. Currently, two populations of CCK +ve/calretinin +ve neurons are documented to exist, and the co-expression of pro-CCK, calretinin and Copine-6 may therefore indicate that Copine-6 labels only cortical interneurons belonging to one of these groups. These are the CCK +ve/calretinin +ve subpopulation identified by Cauli and co-workers as ‘irregular spiking’ fusiform non-pyramidal cells (Cauli *et al*., 2000), or the small population CCK +ve/calretinin +ve cells that belong to the regular-spiking non-pyramidal cell population of the neocortex (Cauli *et al*., 1997; Kawaguchi, 1995). The detailed classification of these Copine-6 ‘ghost cells’ would therefore require electrophysiological analysis. In addition, it is documented here that the ghost cells are co-immunoreactive for NECAB1, a neuronal calcium binding protein that also shows a restricted expression to subsets of neurons, which is in line with the finding by Sudhof and co-workers that N-Copine is a putative protein interactor of the NECABs (Sugita *et al*., 2002) but this requires further molecular analysis.

The presence of the $GABA_B$ receptor subunit 1 in the ‘ghost’-like interneurons also suggests that they are part of a functional GABAergic signalling network. The ability of GABAergic interneurons to take part in a two-way inhibitory network, by releasing and being a target for GABA, has been documented to be part of an organised network throughout all layers of the neocortex. This is controlled by dense communications between dendritic and synaptic branching, originally identified by Somogyi and co-workers (Somogyi *et al*, 1986, for a review see Somogyi, 1989). Therefore, the immunohistochemical results suggest that Copine-6 labelled ‘ghost cells’ may release GABA (evident by their being positive for GAD67) and be a target for GABA (evident by their reaction for $GABA_BR$), thus contributing to such essential inhibitory cortical networks. Indeed, the $GABA_B$ receptor has been described in 90-98% of calretinin immunopositive interneurons in the visual cortex of the rat (Gonchar *et al*, 2001) and the co-expression of pro-CCK, the precursor of the neuroactive peptide cholesystokinin (CCK) in GABAergic non-pyramidal cells is well established (Peters *et al*, 1983). The Copine-6 labelling of some cells with these molecular phenotypes therefore points towards our identification of a subpopulation of cortical interneuron, particularly since the Copine-6 'ghost-like' cells were consistently immunonegative for other interneuron cell markers. Therefore, some of the Copine-6 immunoreactive 'ghost' cells are probably a subpopulation of cholesystokinin +ve/calretinin +ve cortical interneurons, (Demeulemeestcr *et al*., 1991; Demeulemeester *et al*, 1988; Gonchar *et al*, 1997; Kawaguchi *et al*, 1998).

3.4.5. Copine-6 labels a novel 'spiny' interneuron subpopulation in the corpus callosum of the rat with striking similarities to olfactory intrinsic interneurons

The histochemical analysis of Copine-6 in rat brain identified an unusually distributed population of 'spiny' interneurons in the corpus callosum and layer VI of the neocortex. The location of these spiny cells in white matter is here considered unusual, for reasons that will be discussed below.

An original paper documenting the identification of NeuN as a neuronal specific marker did not identify any NeuN positive neurons in the white matter (Mullen *et al*, 1992). However since then, some sparse populations of neurons expressing NeuN and other mature neuronal markers such as GABA, neuropeptide Y and calretinin have been documented in the corpus callosum of the postnatal and adult brain of various species (Riederer *et al.*, 2004; Yoshimura *et al.*, 2009; Jovanov-Milošević *et al.*, 2010). Here, I report the labelling of certain NeuN +ve/GAD67 +ve possible interneuronal subpopulations with the Copine-6 antibody in the corpus callosum of the rodent brain. The cells have a spiny morphology, and are located on the periphery of and within the corpus callosum, with some cells branching into layer VI of the neocortex. The cells are seen in both a rostral and caudal direction, following the corpus callosum in its entirety. Most unusually, the cells appear to have the molecular phenotype of certain axonless olfactory interneurons, namely the granule and/or periglomerular cells.

Firstly, the NeuN co-labelling of these spiny interneurons indicates that these cells are mature, or at least post-mitotic neurons, however the location of some of these Copine-6 labelled cells in the rostral corpus callosum (almost within the neurogenic rostral migratory stream and surrounding subventricular area) could suggest otherwise. It is understood that the expression of NeuN is up-regulated at around the same developmental time-point as other markers of immature migration, such as doublecortin and PSA-NCAM, are down-regulated, with a small degree of overlap between the expression periods (Mullen *et al.*, 1992). The expression of doublecortin and PSA-NCAM therefore captures a particular transient stage of neuronal maturation, which can essentially categorise cells in between the immature and mature stage of cell development. Although all of the Copine-6 spiny cells are immunoreactive for NeuN, their unusual location spanning the white matter is not typical of any other neuron population, particularly when the Copine-6 spiny cells bordering the neurogenic subventricular zone are taken into account. It would therefore be plausible to consider that the Copine-6 spiny cells may express markers for *both* a mature and migrating/immature developmental state, particularly since there is no strict transition from the molecular expression of one marker to another and the cells may be mid-transition. However, since it was clear following further histochemical analysis that the Copine-6 spiny neurons are indeed mature and they do not co-express any markers of migration which would have otherwise overlapped developmentally, this leaves open the question of why the Copine-6 cells are located in these neurogenic regions, with very few other neighbouring neurons. One possibility is that the cells are born in the adult rat brain, and Copine-6 expression occurs once the cells are of a certain maturity level. However, this still does not account for their unusual location where so few mature neurons are identified. Another possibility is that the Copine-6 spiny interneurons are born during an early stage of development, and remain in these neurogenic regions throughout the life of the rat, perhaps with a functional purpose. Since the cells share the molecular phenotype of some granule and/or periglomerular cells of the olfactory bulb which are generated in the subventricular zone during neurogenesis, it would be plausible if the Copine-6 spiny cells were born either in the same location as the olfactory intrinsic cells, or were once programmed to develop or migrate to the olfactory regions. Although determining the exact function of the Copine-6 spiny cells in the corpus callosum is beyond the scope of this thesis, a full developmental analysis of these cells is achievable and would help to elucidate when they are born with respect to the adult born olfactory neurons. With this in mind, BrdU birthdating analysis of the Copine-6 spiny cells was carried out, see Chapter 4.

Again focusing on the location of the Copine-6 spiny interneurons in the corpus callosum, their mature neuronal morphology at first seems unusual, perhaps more so for those spiny cells positioned in the subventricular zone which is a neurogenic region. The location of the SVZ is home to progenitor cells and neuroblasts, which are histochemically distinct nestin +ve/reelin +ve/PSA-NCAM +ve cells, which clearly do not share any morphological or molecular similarity to the Copine-6 spiny interneurons. Interestingly, however, the Copine-6 spiny neurons were not completely isolated from these immature cells within the RMS or SVZ, neither were they isolated from other small populations of neurons in the rostral or caudal corpus callosum. The Copine-6 spiny cells in the rostral corpus callosum might be described as “tunnel-like”, since the spiny Copine-6 interneurons are orientated on the periphery of the immature cells, wrapping around the migratory stream. Since there are no immature cells present in the caudal corpus callosum this distribution was not true of the Copine-6 spiny interneurons within the anterior hippocampal continuation where these Copine-6 spiny cells were a more isolated cell population. Although the function of the Copine-6 cells is unknown, the rostral and caudal distribution of these interneurons suggests that they may have more than one function, perhaps related to cell migration or neurogenesis, or perhaps associated with the maintenance of the corpus callosum itself. Putative communication between the Copine-6 cells and other neurons may be possible since in *all* histochemical investigations (of a rostral and caudal direction) it was noted that the Copine-6 spiny cell processes were often in close proximity to other cell processes.

This was true of the cell processes rostrally, which included immature nestin +ve/doublecortin +ve/PSA-NCAM +ve cells and mature NPY +ve/nNOS +ve neurons, and caudally true of some NPY +ve/nNOS +ve neurons.

Morphologically, and by the presence of NeuN, the Copine-6 spiny cells in the corpus callosum appear to be mature neurons. Their lack of Ankyrin –G immunoreactivity suggests they may form dendro-dendritic synapses on their long bipolar processes. Recently Monyer and co-workers described 'post-natally generated small axonless neurons' in the white matter of the mouse brain and the cells were identified by their unipolar axonless calretinin-positive phenotype (Le Magueresse *et al.*, 2011). In my study, similar unipolar calretinin positive axonless neurons immunoreactive for Copine-6 could be found, however they were few in number. Additionally, they were morphologically distinct from the Copine-6 *bipolar* spiny interneurons that are visible on the periphery of the corpus callosum, and they do not have the long dendritic bipolar arborisations characteristic of the Copine-6 spiny interneurons. Although electron microscopic analysis did suggest that these unipolar axonless calretinin positive neurons could form dendro-dendritic synapses (Le Magueresse *et al.*, 2011), they do not have the ornamented dendritic varicosities that are exhibited by the Copine-6 interneurons. Whilst *some* of the unipolar axonless calretinin cells identified by Monyer and colleagues do express Copine-6 which suggests some Copine-6 subpopulations are born in the postnatal brain, the Copine-6 spiny interneurons identified in this thesis are almost certainly a different population of neurons. The subsequent birth-dating of the Copine-6 spiny interneurons reported in Chapter 4 also supports this conclusion. .

The morphology of the Copine-6 spiny interneurons clearly requires further structural investigation. The putative spiny varicosities on the dendrites of the Copine-6 spiny interneurons may be true spines, possibly gemmules if the cells indeed belong to some olfactory granule or periglomerular lineage (Rall *et al.*, 1966). If so, these spines may form dendro-dendritic synapses. Furthermore, the heterogenic co-staining with enkephalin, which has been described in neuronal subpopulations of the striatum (Hong *et al*, 1977), neocortex (Somogyi *et al*, 1982) and olfactory bulb (Bogan *et al*, 1982), could point towards peptidergic signalling, and the apparent restriction of the majority of this staining to the spine-like appendages leads to the assumption that enkephalin is restricted to the boutons. Whether or not the spines are synaptically active cannot be concluded until ultra-structural studies and/or electrophysiological studies are carried out. The strong VGAT co-reactivity in some of these spiny protrusions would also support this presumption by indicating the presence of the necessary vesicular machinery required of a pre-synaptic structure (Gray, 1959), however it should be noted that the presence of vesicles within a dendrite or dendritic spine is not itself evidence enough of a pre-synaptic structure (Gray, 1959; Pinching & Powell, 1971). The presence of a true synapse requires ultra-structural evidence of both pre- and post- synaptic architecture. Although the histochemical analysis with gephyrin would be consistent with the presence of several post- synaptic appositions to the VGAT varicosities, the resolution at the level of the light microscope does not permit this conclusion.

The electron microscope was therefore employed to analyse any putative communication between Copine-6 spiny cells and/or other cell populations within the corpus callosum, and to investigate if the Copine-6 cells do indeed have the structural ability to integrate into a neuronal network as the histochemical analysis suggests. (See Chapter 5).

Chapter 4. **Developmental expression of Copine-6 in mouse and rat brain**

4.1. Introduction

During embryonic development of the brain, neuroepithelial cells within the neural tube undergo massive spatial and temporal structural changes particularly during embryonic days e11-e17 (Angevine & Sidman, 1961; Caviness & Sidman, 1973; Caviness & Takahashi, 1995). The neuroepithelium begins as a single layer of pseudostratified epithelial cells which rapidly proliferate to form the forebrain, midbrain and hindbrain. The forebrain consists of the diencephalon and telencephalon, and the telencephalon gives rise to the embryonic neocortex/hippocampus and basal ganglia from its two structural divisions, the pallium and subpallium, respectively (see Figure 4-1).

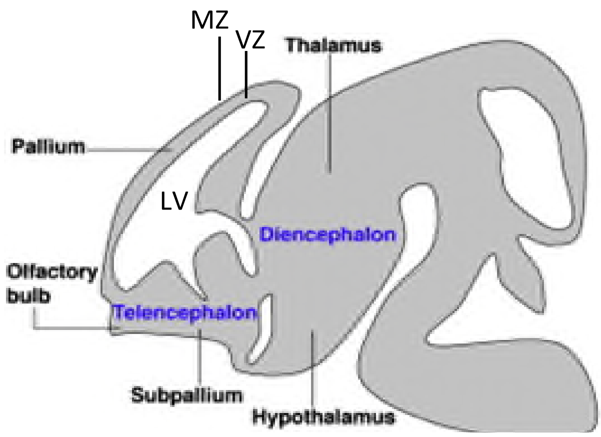

Figure 4-1 Schema of a sagittal section through the brain of an embryonic day e12 mouse.

The main subdivisions of the telencephalon are shown (pallium and subpallium) The lateral ventricles (LV) are surrounded by the ventricular zone (VZ) of the developing telencephalon. The marginal zone (MZ) is at the pial surface of the developing neocortex.. The olfactory bulbs (OB) can be seen at the front on the developing telencephalon. Image modified from (Goulburn *et al.*, 2012)

The ventricular zone (VZ) of the embryonic telencephalon contains most of the neuroepithelial cells that eventually form the six layers of the neocortex. Neural progenitor and stem cells originating at the VZ undergo proliferation, migration and differentiation to generate various types of glial cells and neurons (for a review see Temple, 2001). Initially the immature neurons migrate radially from the ventricular zone to the marginal zone (MZ) at the pial surface of the cortical plate, and as the cortical plate expands these cells form the six layered neocortex in an “inside –out” manner, with younger neurons migrating past the mature cells (Rogers & Berry, 1965; Parnavelas, 2000; Olson & Walsh, 2002; Kriegstein & Noctor, 2004; Kriegstein *et al.*, 2006). The newborn neurons therefore have to migrate long distances to their destination (for a review, see Molyneaux *et al.*, 2007). In general, newborn neurons originating in the dorsal (pallium) ventricular zones migrate radially and differentiate within the cortical plate to form the layered neocortex, which is typically expected of glutamatergic projection neurons (for a review see Marín *et al*, 2003a; Khodosevich *et al*, 2011). In contrast, it is generally considered that GABAergic interneuron precursor cells such as those that populate the olfactory bulb primarily originate in the ventral ventricular zones (subpallium). The subpallium is structurally divided into the medial, caudal and lateral ganglionic eminences (MGE, CGE and LGE, respectively), the preoptic area (POA), and the septum anlage (Brazel *et al.*, 2003; Marín, 2013). Cells originating in these areas undergo tangential migration to their final destinations in various regions of the brain including the olfactory bulb and neocortex (Corbin *et al.*, 2001; Gelman & Marín, 2010; Anastasiades & Butt, 2011; Marín, 2013). Furthermore, cells originating in the medial and lateral ganglionic eminences are considered to take different migratory routes, thus populating different final regions in the developing brain (Wichterle *et al.*, 2001; Marín & Rubenstein, 2003; Kriegstein & Noctor, 2004; Gelman & Marín, 2010; Khodosevich & Monyer, 2011; Marín, 2013). Indeed, it has been suggested that the precursor cells originating in these different regions may give rise to different subtypes of interneuron (for reviews, see Anderson *et al.*, 2001; Wonders & Anderson, 2006; Molyneaux *et al.*, 2007b; Gelman & Marín, 2010). This follows from the observations that the different ventricular zones are comprised of differentially specified precursor cells which may later progress through further specification stages under the control of specific genes (Parnavelas, 2000; Brazel *et al.*, 2003; Molyneaux *et al.*, 2007b; Young *et al.*, 2007; Gelman & Marín, 2010; Marín, 2013). The diversity of these precursor cells is recognised due to a continuously expanding library of molecular and genetic cell markers that enables different cell populations in the neurogenic regions of the developing and adult brain to be identified. Tuj-1, to give one example, is a neuron specific class III beta tubulin expressed by immature neurons throughout development and which continues to be expressed in the adult brain. Therefore it can be used to distinguish neuronal cells from undifferentiated neuroepithelial cells in the regions of cell division. Proliferative neuronal progenitor cells at the ventricular zone of the embryonic neocortex have been shown to be immunoreactive for Tuj-1 (Luskin & Menezes, 1994), which at first appear as a single layer of immature neurons at the VZ. Later in embryonic development Tuj-1 labels cells throughout the neocortex and marginal zone of the cortical plate, reflecting their developmental expansion (Luskin & Menezes, 1994; Pencea & Luskin, 2003).

Olfactory bulb interneurons initially originate in the embryonic ventral telencephalon, or subpallium, and although the exact location is still a matter of debate there is suggestion that they are generated in the dorsal region of the lateral ganglionic eminences (for reviews and discussions see Anderson *et al.*, 2001; Corbin *et al.*, 2001; Marín *et al*, 2003). Interestingly, neurogenesis of olfactory interneurons continues into adulthood in the adult subventricular zone, which is at the edge of the lateral ventricle (Altman, 1962, 1963, 1969; Lois & Alvarez-Buylla, 1994; Doetsch *et al.*, 1999; Lledo *et al.*, 2006; Zhao *et al.*, 2008). Although the foetal subventricular zone forms during early embryogenesis adjacent to the ventricular zone and is structurally prominent in the embryonic ganglionic eminences, it is not known which structural or anatomical properties are retained in the subventricular zone of the adult brain. During the later stages of development, however, the prolific ganglionic eminences disappear leaving behind the subventricular zone. Since the adult subventricular zone is known to retain some of the proliferative behaviour of the embryonic brain and also repopulates the olfactory bulb interneurons, it has been suggested that it may comprise of remnants from the embryonic lateral ganglionic eminence (García-Verdugo *et al.*, 1998; Alvarez-Buylla *et al.*, 2001; Lledo *et al.*, 2008). In postnatal and adult brain, Tuj-1 can also be used to label immature neurons in the rostral migratory stream and subventricular zone (Luskin & Menezes, 1994; Doetsch & Alvarez-Buylla, 1996).

During adult neurogenesis, newborn neurons originating at the adult subventricular zone migrate along the rostral migratory stream to the olfactory bulb (García-Verdugo *et al.*, 1998; Alvarez-buylla & Garcıa-Verdugo, 2002; Lledo *et al.*, 2006; Zhao *et al.*, 2008). Neuroblasts and immature neurons undergo homophilic tangential migration in a chain-like manner through the mesh of glial cells that constitute the underlying structure of the RMS, and which has remained from embryonic and postnatal development. Following arrival at the olfactory bulb, the immature neurons integrate into established neuronal circuitry and complete the final stages of maturation. Cells at each stage of migration in the rostral migratory stream, and in the olfactory bulb of the adult rodent brain can be molecularly characterised (see Chapter 1 and Chapter 3 for detailed descriptions).

Immunohistochemical analysis of Copine-6 protein expression in the adult rat brain (see Chapter 3) identified a spiny interneuron population in the corpus callosum, bordering the lateral ventricle and adjacent to the adult subventricular zone, following the rostral migratory stream towards the olfactory bulbs. In Chapter 3 the spiny interneurons were molecularly characterised as mature GABAergic neurons, with putative inhibitory synaptic communication (VGAT+/Gephyrin+ immmunoreactivity). A striking feature of this population of Copine-6 spiny interneurons is their position in the corpus callosum – not only due to the scarcity of mature neuronal populations in this region – but also due to how close the Copine-6 cells are to the immature migrating neuroblasts within the rostral migratory stream. The Copine-6 spiny interneurons are on the periphery of doublecortin, nestin, PSA-NCAM immunoreactive migrating cells in the adult brain, yet do not share any molecular phenotype to these or to glia. Since the Copine-6 spiny interneurons are so close to the neurogenic subventricular zone and rostral migratory stream in the adult rat brain, it raises the question of when they are born.

In order to carry out a full developmental analysis of Copine-6 in neurons of the rodent brain, the following studies were conducted:

1. The amount of Copine-6 protein in brain was analysed in different stages of development

2. Dissociated hippocampal neurons were analysed at various different stages of maturation to investigate the cellular expression of Copine-6

3. Copine-6 expression was analysed in the brain of rat embryos (E12, E18), and postnatal rats aged 2 and 8 days (p2, p8).

4. Birthdating analysis of the Copine-6 spiny interneurons was carried out using BrdU in embryonic (mice) and adult (rats).

4.2. Materials and Methods

4.2.1. Protein immunoblotting of developing rat brain from embryo to adult

To investigate the developmental expression of Copine-6 in developing rat brain, brain tissue from various different developmental timepoints (E18, p1, p4, p8, p21, p28, adult) were dissected, homogenised and prepared for electrophoresis following the protocol described in Chapter 2, Methods section 2.2.4. The protein content of each cytosolic and membrane supernatant fraction was determined using the Bio-Rad protein assay kit according to the manufacturer’s instructions (Bio-Rad UK, #500-0001). Equal amounts of the total protein were loaded onto a 10% polyacrylamide gel and the subsequent electrophoresis and transfer of the proteins to the nitrocellulose membrane were carried out as previously described in Chapter 2, Methods 2.2.4 Primary antibodies rabbit anti-Copine-6 (1:1000) and mouse anti-GAPDH(1:500, Abcam ab9485) were added to the blocking buffer, plus 0.1% Tween-20 (Sigma Aldrich UK, 9005-64-5) for 24 hours at 4˚c. Membranes were then washed in PBS+ 0.1% Tween-20, 4x 5 minutes, and secondary antibodies Alexa Fluor 680 goat anti-rabbit IgG (H+L) (Invitrogen, A21109), and IR Dye 800CW goat anti-mouse (Odyssey, 926-32210 LOT c#00816-03) were applied at 1:500 in Odyssey Blocking Buffer + 0.1% Tween-20, for 1 hour at room temperature. The membrane was washed 4 x5 minutes in PBS + 0.1% Tween-20, then 2 x5 minutes in PBS alone to remove any residual Tween-20. The membrane was scanned on the LI-COR Scanner and the Copine- 6 signal was quantified in relation to the control GAPDH fluorescence intensity using LI-COR Image Studio Western Analysis. The results from 3 separate experiments were pooled.

4.2.2. Developmental immunocytochemical analysis of dissociated hippocampal culture

Dissociatied rat hippocampal neurons were cultivated and plated as described in Chapter 3, section 3.2.1. Cultures were maintained and matured to a variety of time-points; 2, 4, 6, 8, 10, 12, 21 and 28 days *in vitro.* Cells were then fixed on the coverslip using 4% Paraformaldehyde for 10 minutes, followed by a 10 minute exposure to 50mM Tris HCl+0.15M NaCl, + 0.05% Triton X-100. Bovine serum albumin (1% in phosphate buffer solution) containing 0.1% normal donkey serum was used to block the coverslips for 1 hour at room temperature. Antibodies mouse anti-Tuj-1 (1:500) and rabbit anti- Copine-6 (1:1000) were then applied to the blocking solution. Coverslips were left with gentle rocking overnight at 4°C. Coverslips were washed in PBS four times, for 15 minutes, and secondary antibodies Cy3 conjugated donkey anti mouse IgG (H+L) (715-165-150, Jackson's Labs, 1:500) and Alexa Fluor 488 donkey anti rabbit IgG(H+L) (A21206, Invitrogen, 1:1000) were applied in PBS-BSA. Imaging was carried out using Zeiss Axiovert 100M confocal microscope, lasers HeNe1S43 and ArgonS14, wavelengths

543Cy3 and 488FITC, with objectives x10, x20, and x40. Images were analysed using LSM Image Browser and Image J. At least 2 coverslips were used for each developmental stage, of which at least 6 different random fields of view were taken using the x10 or x20 objective. Data was calculated based on the percentage of neurons that were immunopositive for Copine-6 at each stage of culture maturation, out of a total number of neurons to allow for discrepancies in cell plating and distribution on the coverslips. The numerical data was pooled.

4.2.3. Immunohistochemical analysis of Copine-6 in embryonic and postnatal rat brain

Procedures were carried out on Sprague–Dawley rats (200-350g; Charles River, Margate, Kent, UK). Environmental conditions and all procedures that were performed were in accordance with the Animals Scientific Procedures Act of 1986 (UK). For embryo extraction, impregnated female rats were killed by Schedule 1 methods and embryos extracted from the uterus. Embryos were immediately placed in 4% paraformaldehyde for fixation, for 48 hours at 4ºc. Embryos were then embedded in 4% agar solution, allowed to set, and then sectioned at 60µm using the vibrotome.

For postnatal analysis, female rats were left to give birth naturally and offspring were killed by Schedule 1 methods at day p2 and p8 of development. Brains were removed and placed in 4% PFA for 48 hours, embedded in 4% agar solution, and sectioned using the vibrotome.

4.2.4. (BrdU) analysis of Copine-6 cells in the white matter of the adult rat brain

Male Sprague–Dawley rats (200-350g) were treated with either one dose of 200mg/kg BrdU and perfused after 24 hours, or with x2 100mg/kg dose over 5 days (total 10 injections) and maintained for 21 and 28 days before perfusion.

Brains were isolated as previously described (see Chapter 3, Methods 3.2.2) and were postfixed in 4% PFA before sectioning on the vibrotome at 50µm.

Before immunohistochemical analysis, tissue was processed by incubating in 37% HCl at 37ºc for 30 minutes for antigen retrieval (a requirement for visualisation of BrdU) and once cool was incubated in 0.1M borate buffer, pH 8.2 for 5 minutes. Sections were washed x3 times in PBS and were then blocked in 0.3% w/v Triton x-100 for at least 4 hours. Primary antibodies rabbit anti Copine- 6 (1:1000) and biotinylated sheep anti- BrdU (1:200, ab2284, Abcam UK) were applied to the blocking solution for 48 hours at 4ºc. Sections were washed and incubated in donkey anti sheep-biotin SP (long spacer, 1:500, 713-066-147, Jackson Immunoresearch USA) to enhance the biotin signal. Secondary antibodies Alexa Fluor 488 donkey anti rabbit IgG(H+L) (1:1000, A21206, Invitrogen) and streptavidin-CY3 (1:1000, 43-4315, Molecular Probes UK) were applied for 12 hours at 4ºc. Sections were then washed x4 times in PBS and were mounted on slides using Vectashield.

4.2.5. Embryonic BrdU birthdating analysis of Copine-6 cells in the white matter of mouse brain

Between 12-15 adult female impregnated mice were used during the course of this study each producing a litter of which 2-6 pups were analysed. Pregnant mice were injected i.p with 200mg/kg BrdU when the pups were in different stages of embryonic development (days e10.5-e15.5, see Table 3). The mice delivered the litters normally and the pups were allowed to develop to a range of different ages (p4-p67). See Table 3 for details of postnatal ages. For licencing reasons the injections and procedures were carried out by Dr Louise Kay, Oxford. Pups were sacrificed by Schedule 1 methods and brains immediately removed, sectioned at 300µm on the vibrotome with oxygenation and immediately incubated in 4% PFA for 48 hours. The fixed 300µm sections were then embedded in agar and were further sectioned using a vibrotome into 75µm sections for immunohistochemical analysis, as described above (See section 4.3.4)

Embryonic Inj.	Slice Age
10.5	p4
	p10
	p12
	p14
	p16
	p24
	p26
12.5	p4
	p9
13.5	p4
	p7
	p14
	p18
	p26
	p29
	p67
14.5	p4
	p29
	p67
15.5	p4
	p7
	p9
	p14
	p15
	p22
	p26

Table 3 The embryonic injection days and subsequent postnatal tissue processing ages of mice used for BrdU analysis.

Embryonic age indicates the age of the embryo at which the pregnant dam was injected with BrdU. The slice age indicates the day at which the pups were sacrificed for analysis.

4.3. Results

4.3.1. Copine-6 expression increases during brain development

Protein immunoblotting of rat brain at E18, p1, p4, p8, p21, p28 and adult showed that Copine-6 expression increases during brain development, with the greatest increase in

Copine-6 occurring between embryonic day 18 and postnatal day 8. From postnatal day 8, the expression of Copine-6 appears to remain relatively stable (Figure 4-2).

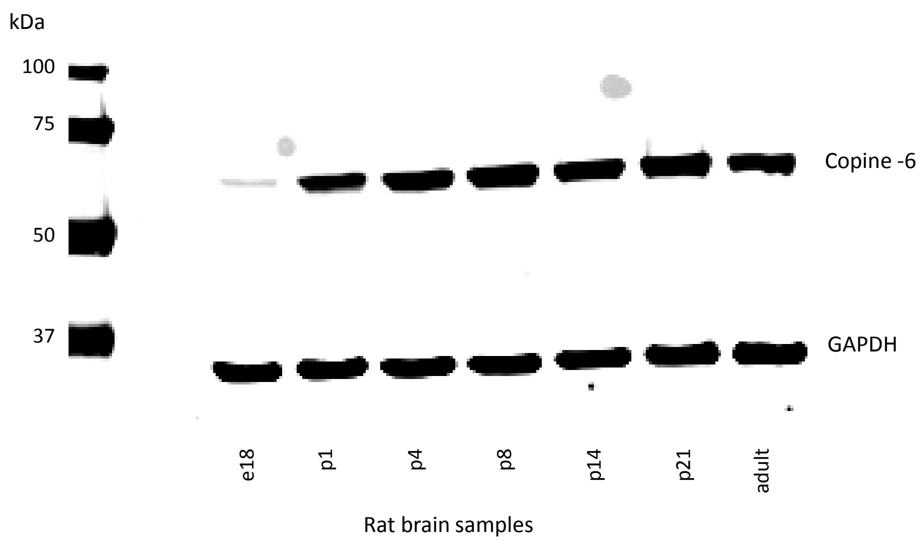

Figure 4-2 Protein immunoblot of rat brain at different developmental stages.

Total protein concentration was measured using a BioRad protein assay, and equal quantities of protein (100µg) were added to each well. The Copine-6 band at ~65kDa, as expected, shows a very small amount of Copine-6 in embryonic brain (e18) which increases during p1 and p8, and then remains at the same level to adulthood. The GAPDH tracks (35kDa.) show that all lanes had a similar loading of lysate protein.

4.3.2. Developmental analysis of Copine-6 expression in dissociated hippocampal culture

To investigate the possibility that Copine-6 expression may alter during maturation, dissociated hippocampal cultures were maintained for 2, 4, 6, 8, 10, 12, 21 and 28 days *in vitro* and then analysed by immunohistochemistry. Tuj-1 (neuron specific class III Beta tubulin) and MAP2 (neuronal microtubule associated protein 2) both labelled all neurons in the cultures at all ages. The neuronal markers were used interchangeably.

The data illustrates that the total number of neurons immuno-positive for Copine-6 increases during maturation of the dissociated hippocampal cell culture (See Figure 4-3). At day 2, approximately 60% of the neurons within the culture were immuno-reactive for the Copine-6 antibody when counted against those cells immuno-positive for MAP2 or TUJ-1. The percentage of Copine-6 positive cells increases to almost 70%, and by day 8 almost 80% of all neurons express Copine-6. From day 8 onward, the percentage of total neurons that are immuno-positive for Copine-6 plateaus and remains fairly constant at around 80-85%, suggesting that this represents the maximum percentage of Copine-6 cells.

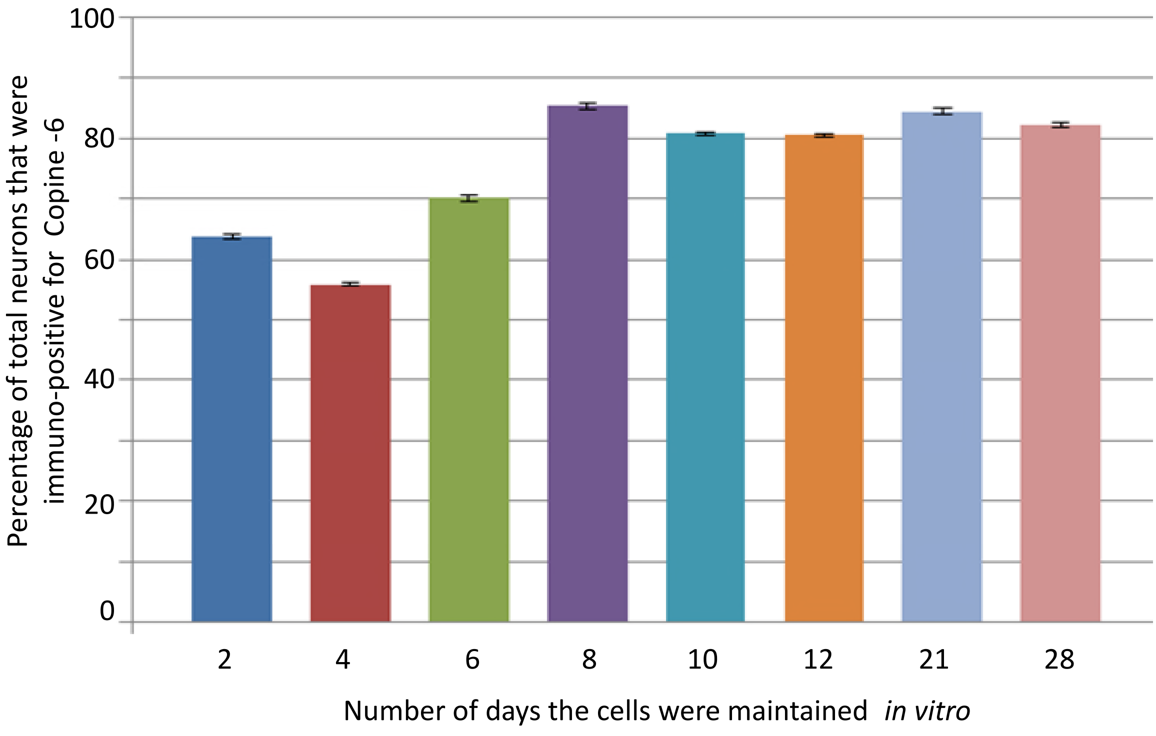

Figure 4-3 The developmental expression of Copine-6 in dissociated hippocampal cell cultures at 2, 4, 6, 8, 10, 12, 21 and 28 days *in vitro*.

Cells were maintained for the various time periods and were immunohistochemically analysed. Anti-Copine-6 was applied alongside either MAP2 or TUJ-1 antibodies which labelled all neurons within the culture. The neurons that were immuno-positive for Copine-6 were calculated as a percentage of the total number of cells. The data is pooled from 4 separate experiments with a minimum of 500 cells per developmental timepoint. The standard error of the mean is shown by the error bars (±SE).

Differences in the neuronal arborisations and branching patterns of Copine-6 immuno-positive cells could be seen between all ages of culture (see Figure 4-4). At day 2, the soma of some neurons was labelled with Copine-6, but these younger cultures had short stubby dendrites. As the cultures matured, they displayed significantly more, longer and spinier neurites, forming a much denser network on surface of the coverslip, and the intensity of Copine-6 immunoreactivity increased. This suggests that although the total number of Copine-6 neurons plateaus and remains stable from day 8 onward, the cultures are still undergoing visible morphological changes as they mature further. Indeed, the changes in morphology associated with maturation is true of *all* neurons i.e. the same morphological changes could be seen in neurons that were immuno-negative for Copine-6, therefore this is likely to be a reflection of the normal healthy growth of neurons in dissociated culture.

4.3.3. Copine-6 expression in the embryonic and postnatal rat brain

Immunohistochemical analysis of Copine-6 in embryonic (e12, e18) and postnatal (day p2 and p8) rat brain showed that Copine-6 is expressed in the embryo from as early as e12.

In the embryonic day 12 rat brain, Copine-6 immunoreactive cells can be seen lined up along the neuronal marginal zone of the embryonic neocortex (see Figure 4-5 and Figure 4-7). Copine-6 reactive cells are absent from the nestin, To-Pro, and ki67 labelled ventricular zone at the border of the lateral ventricle (see Figure 4-6, Figure 4-7, Figure 4-8 respectively) at e12 and e18, although Copine-6 cells are present throughout the developing neocortex. The majority of Copine-6 cells in the location of the marginal zone are immunopositive for Tuj-1 (see Figure 4-5 and Figure 4-7) indicating a neuronal phenotype as early as day e12.

.

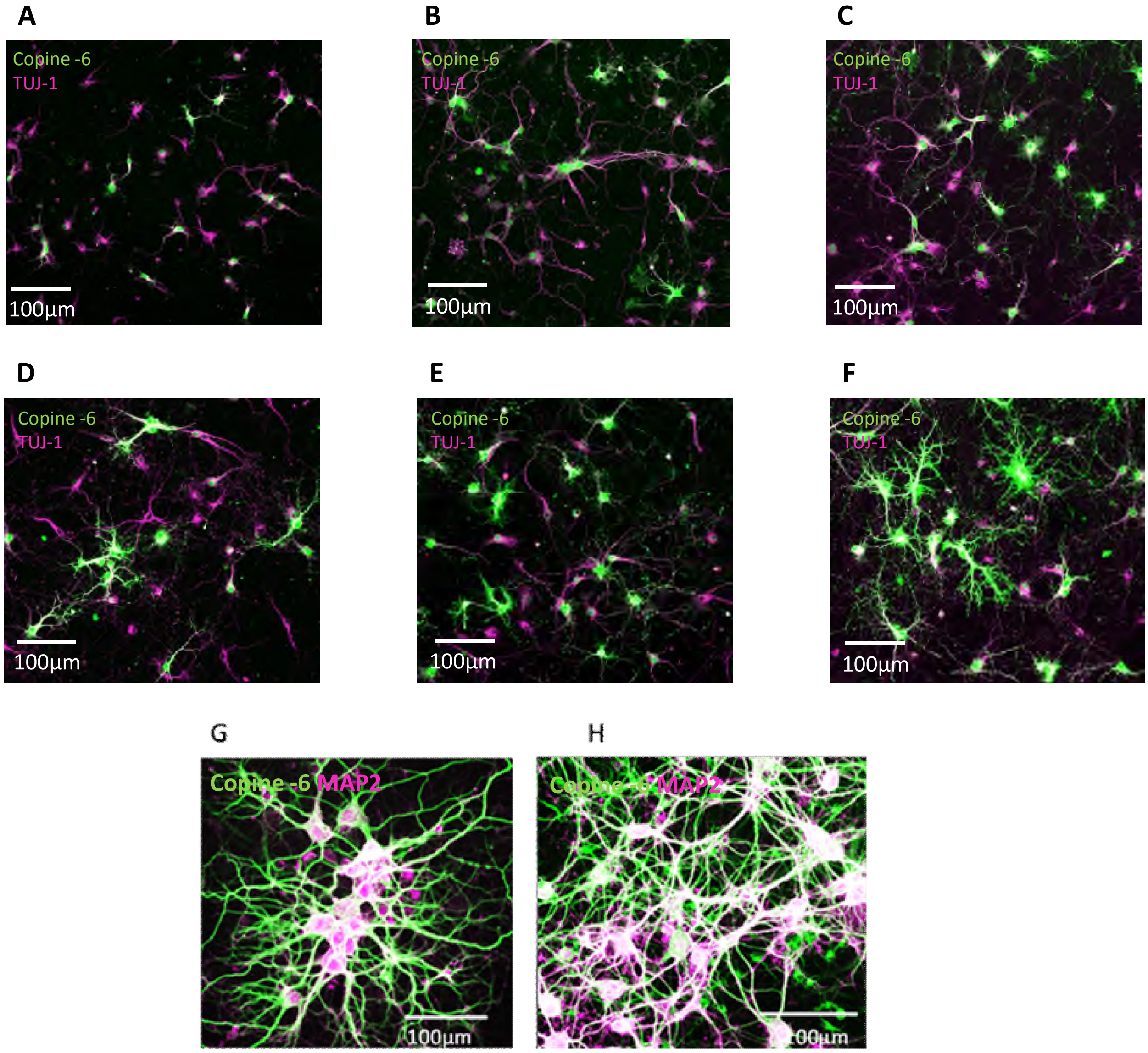

Figure 4-4 A general overview of the developmental expression of Copine-6 and Tuj-1 in dissociated hippocampal tissue cultures.

Dissociated cultures were maintained *in vitro* and immunohistochemically analysed for Copine-6 and the neuronal markers Tuj-1 and MAP2 between 2 to 28 days maturation. **A**. at 2 div, the neurons are immature, with minimal dendritic branching and the Copine-6 expression in some neurons is visible only in the soma. **B**. 4 div, the neurons are becoming more established and the Copine-6 expression can be seen in the soma and dendrites of some Tuj-1 positive neurons. **C**. 6 div, the neurons are branched and the coverslip is beginning to look less sparse. **D**. 8 div, **E**. 10 div, and **F**. 12 div, show that the neurons are becoming much more branched and the Copine-6 immunoreactivity increases and spreads to the branched dendritic arborisations. The number of neurons that express Copine-6 remains fairly constant from here on, although the intensity of Copine-6 expression continues to increase, particularly as the neurons become more branched. **G**. 21div and **H**. 28 div. Copine-6 immuno-positive fibres can be seen across the coverslip forming a dense network. All Copine-6 cells were found to have a neuronal phenotype. Where there is co-localisation the cell appears white. Images were taken of random fields using the x10 (A-F), x20 (G-H) objective on each cover slip to get a general idea of neuron distribution and morphology at each developmental stage. All Copine-6 neurons are co-immunoreactive for either Tuj-1 or MAP2, but some neurons at all time-points examined do not express Copine-6, which suggests that Copine-6 is expressed by certain populations of neurons. Although the expression intensity appears reduced on the low power images, the microscope settings for size of optical slice and laser were kept the same for all conditions.

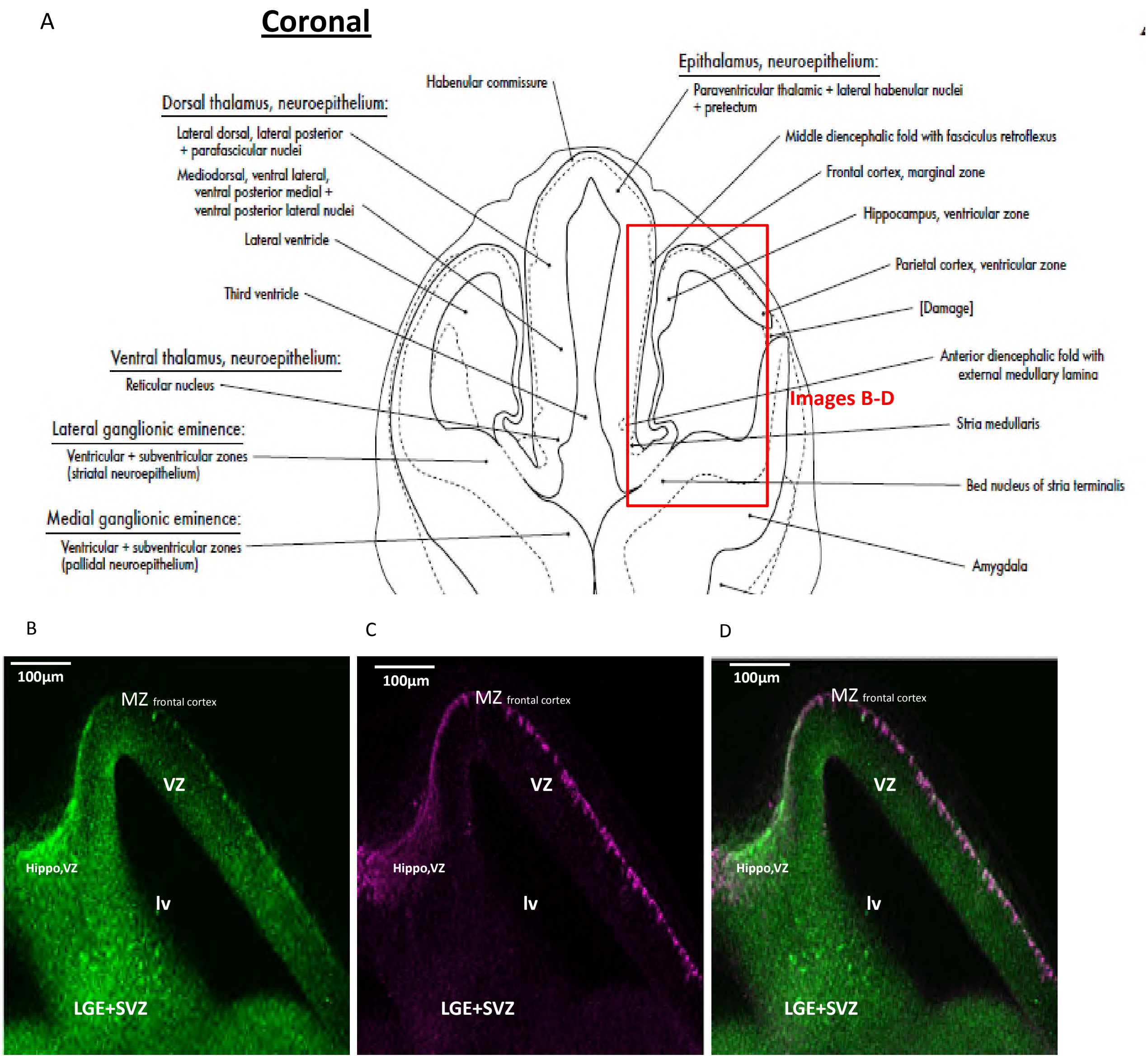

Figure 4-5 Copine-6 in the e12 rodent brain (part 1).

A. A coronal section of the e12 developing mouse brain taken from the online version of Prenatal Mouse Brain Atlas, Uta Schambra representing the region of the brain analysed in images B-D. **B**.In these sections, Copine-6 is expressed weakly throughout the neocortex with more intensely stained cells in the hippocampal ventricular zone (Hippo,VZ), throughout the hippocampus, and along the marginal zone (MZ). **C**. The marginal zone is labelled by Tuj-1. **D**. Copine-6 expression is more intense at the marginal zone with some apparent co-reactivity with TUJ-1. A cluster of Copine-6 reactive cells can also be seen in the developing lateral ganglionic eminence (LGE) and subventricular zone (SVZ)

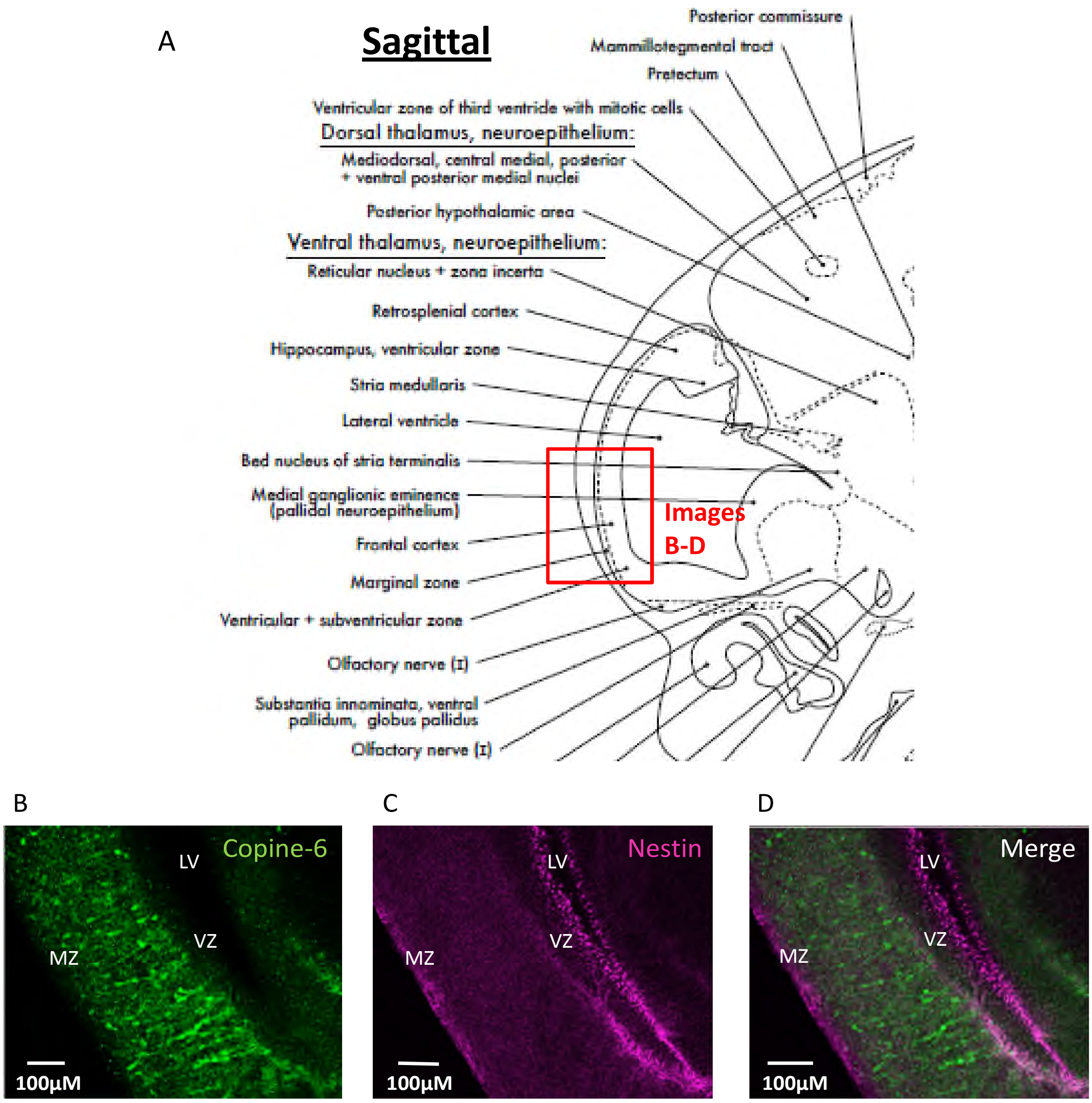

Figure 4-6 Copine-6 in the e12 rodent brain (Part 2)

A. A sagittal section of the e12 developing mouse brain taken from the online version of Prenatal Mouse Brain Atlas, Uta Schambra representing the region of the brain analysed in images B-D. **B**. Copine-6 labelling shows reactive cells throughout the developing neorcortex with some cells within the marginal zone (MZ). Copine-6 labelling is absent from the ventricular zone (VZ). **C**. The proliferative regions lining the lateral ventrical (LV) are labelled by nestin (ventricular zone, VZ). Nestin can also be seen throughout the neocortex and marginal zone since it is labelling immature migrating cells and radial glia processes. **D**. Copine-6 doesn't seem to label as many cells as nestin but can be seen in the same locations with the exception of the ventricular zone.

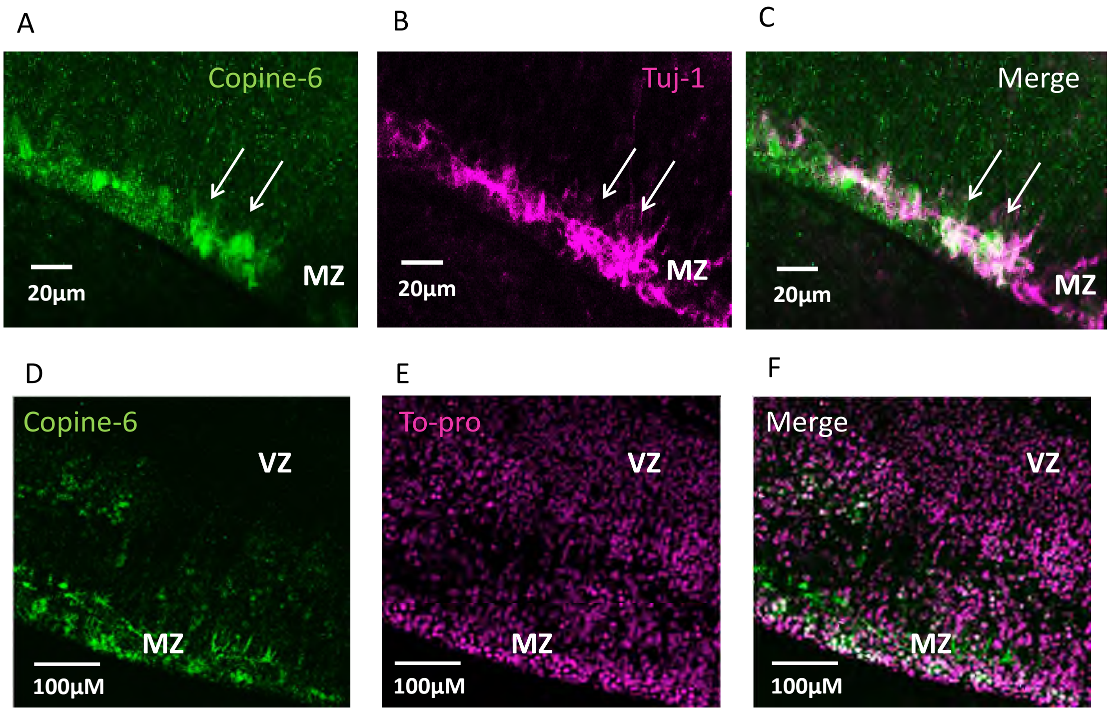

<u>**Figure 4-7 Copine-6 cells in the marginal zone (MZ) appear to be immunopositive for Tuj-1 and are absent from the ventricular zone (VZ)**</u>

A. Copine-6 cells weakly label the neocortex with a line of intensely stained cells along the marginal zone in some regions. **B**. Tuj-1 labels immature neurons throughout the marginal zone region. **C**. Some of the Copine-6 +ve cells have apparent co-reactivity with Tuj-1. This might suggest that the Copine-6 cells have a neuronal phenotype as early as e12. NB some technical problems with sectioning and embryonic tissue integrity had to be overcome by embedding sections in agar prior to processing. **D**. Copine-6 cells at the marginal zone and within the developing neocortex. **E**. To-pro was used to stain cell nuclei, this shows the presence of cells with the ventricular zone (VZ) which Copine-6 is absent from. **F**. Image merge showing that Copine-6 cells are present at the marginal zone but not the ventricular zone.

By embryonic day 18 the number of Copine-6 cells appear to be more numerous in the developing neocortex, and cell soma could be identified throughout the neocortical layers with the exception of the proliferative cell layer (ventricular zone) which was labelled by Ki67 (Figure 4-8 Images A-C). There is an apparent discrepancy between this immunohistochemical data and the protein immunoblot (Figure 4-2) which shows very little Copine-6 in the e18 brain. However, the quantity of Copine-6 in the embryo may be a relatively small proportion of total protein compared to the adult brain, and this Copine-6 expression intensity increases as the cells develop.

In the e18 brain, the rostral migratory stream is also identifiable, with Copine-6 immunoreactive cells on the border of nestin reactive immature/migrating cells (Figure 4-8 Images D-F). A small number of Copine-6 cell processes appear to be immunoreactive for nestin and this may reflect their immature stage of development. Molecular analysis of the Copine-6 cells show that they are immunoreactive for both GAD67 and Tuj-1, indicating a GABAergic neuronal phenotype (Figure 4-9).

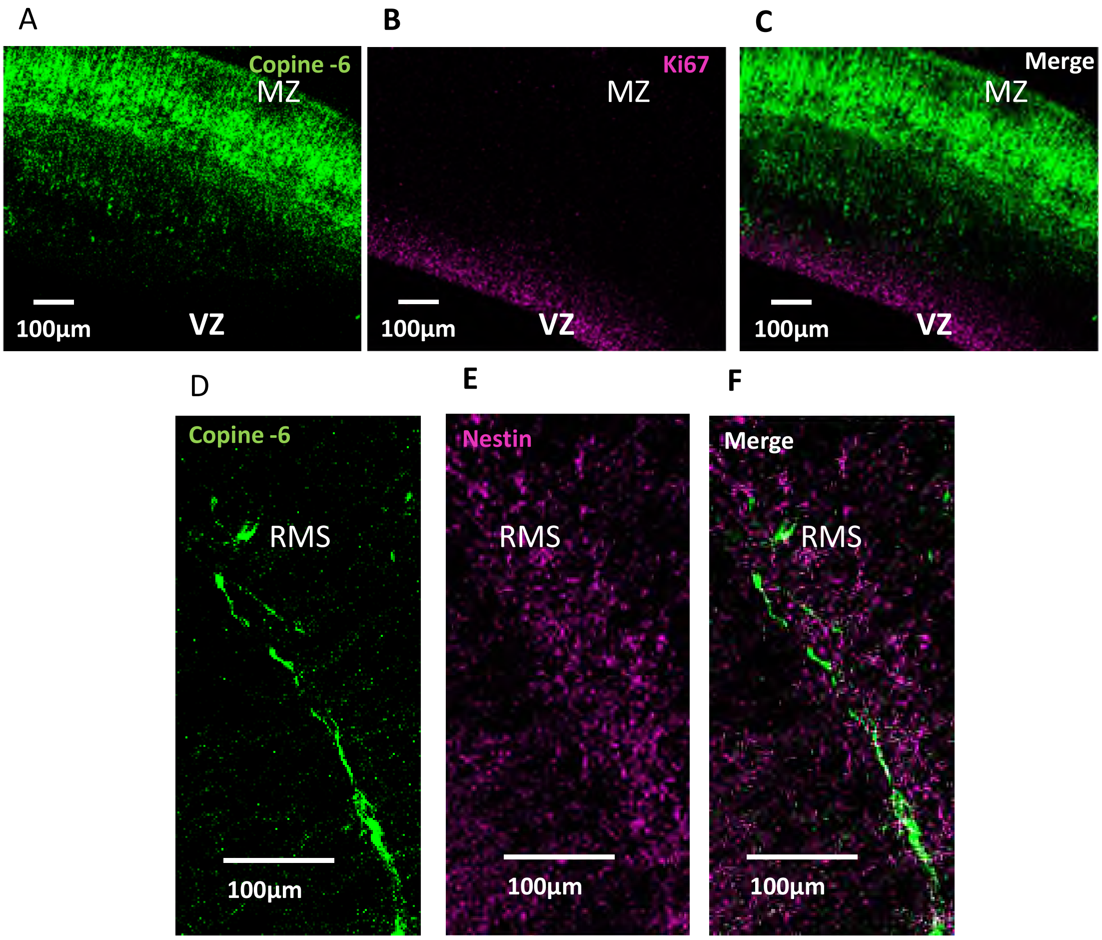

Figure 4-8 Copine-6 in the e18 developing neocortex and rostral migratory stream.

A. At e18, Copine-6 labels cell soma and processes throughout the body of the developing neocortex **B**. Ki67 labels proliferating cells on the border of the ventricular zone(VZ). **C**. The cells on the ventricular zone are not immunoreactive for Copine-6 at e18. **D**. At e18 a Copine-6 stream of cells can be seen bordering the rostral migratory stream. **E**. The rostral migratory stream is developing and is labelled by nestin **F**. The Copine-6 cells can be seen along the edge of the nestin defined RMS.

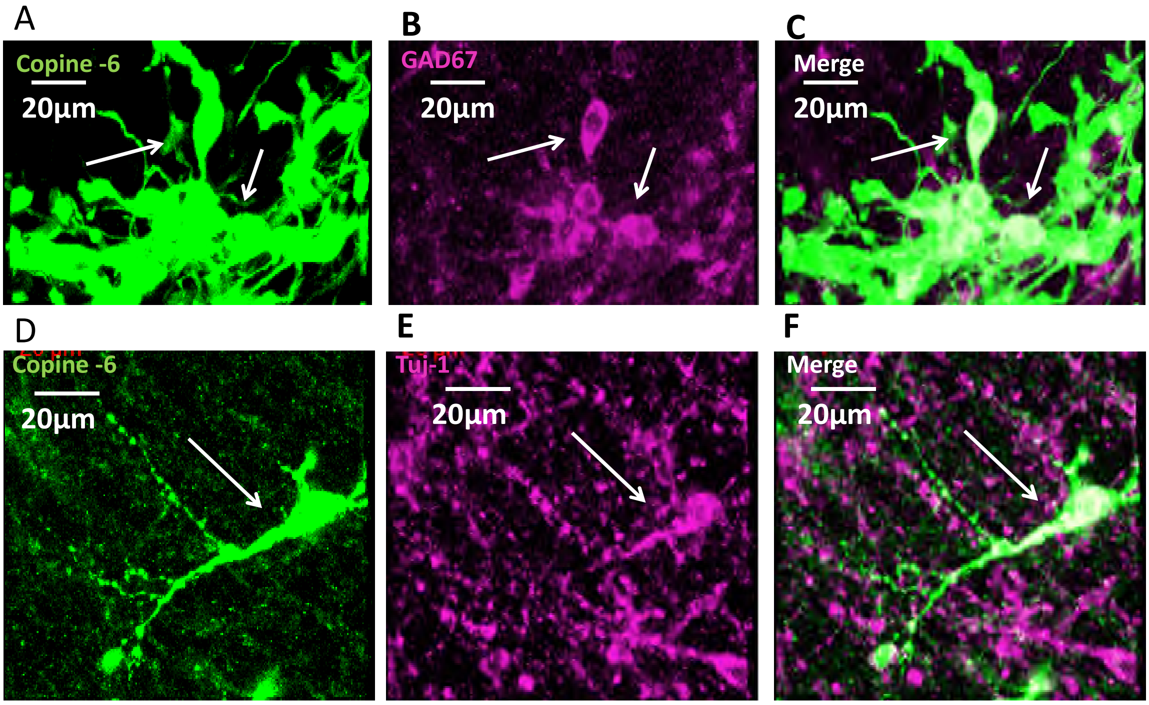

Figure 4-9 Copine-6 cells in the e18 brain neocortex and neighbouring rostral migratory stream are GABAergic neurons.

A. Copine-6 cells on the border of the e18 RMS **B**. GAD67 cells bordering the e18 RMS. **C**. Co-immunoreactivity of Copine-6 and GAD67 indicates a GABAergic phenotype. **D**. A Copine-6 cell near the RMS of the e18 brain. **E**. Tuj-1 labelling of the RMS. **F**. The Copine-6 cells are Tuj-1 +ve further confirming a neuronal phenotype.

Copine-6 immunoreactive cells can also be seen in the e18 developing hippocampus, where they take a migratory-like appearance with long cell processes (Figure 4-10). In the developing olfactory bulbs (see Figure 4-11) of the e18 rat, Copine-6 expression is strong in the granule and glomerular cell layer, almost identical to what is observed in the adult rat brain. Although the olfactory bulb of the e18 rat is much smaller than that of the adult, Copine-6 reactivity still labels each layer of the bulb. The Copine-6 labelling of the granule and glomerular cell layers were most distinguishable in medial sagittal and lateral sagittal sections, respectively. This may also reflect the ongoing development and growth of the olfactory bulb at e18, since in the adult brain all layers can be labelled by Copine-6 in most section planes. The majority of the Copine-6 cells in the olfactory bulb are immunoreactive for TUJ-1 (see Figure 4-11, Image B-D) and GAD67 (see Figure 4-11 E-G). Some but not all of the cells in the olfactory bulb were nestin immmunoreactive in the processes (see Figure 4-11 Images H-J).

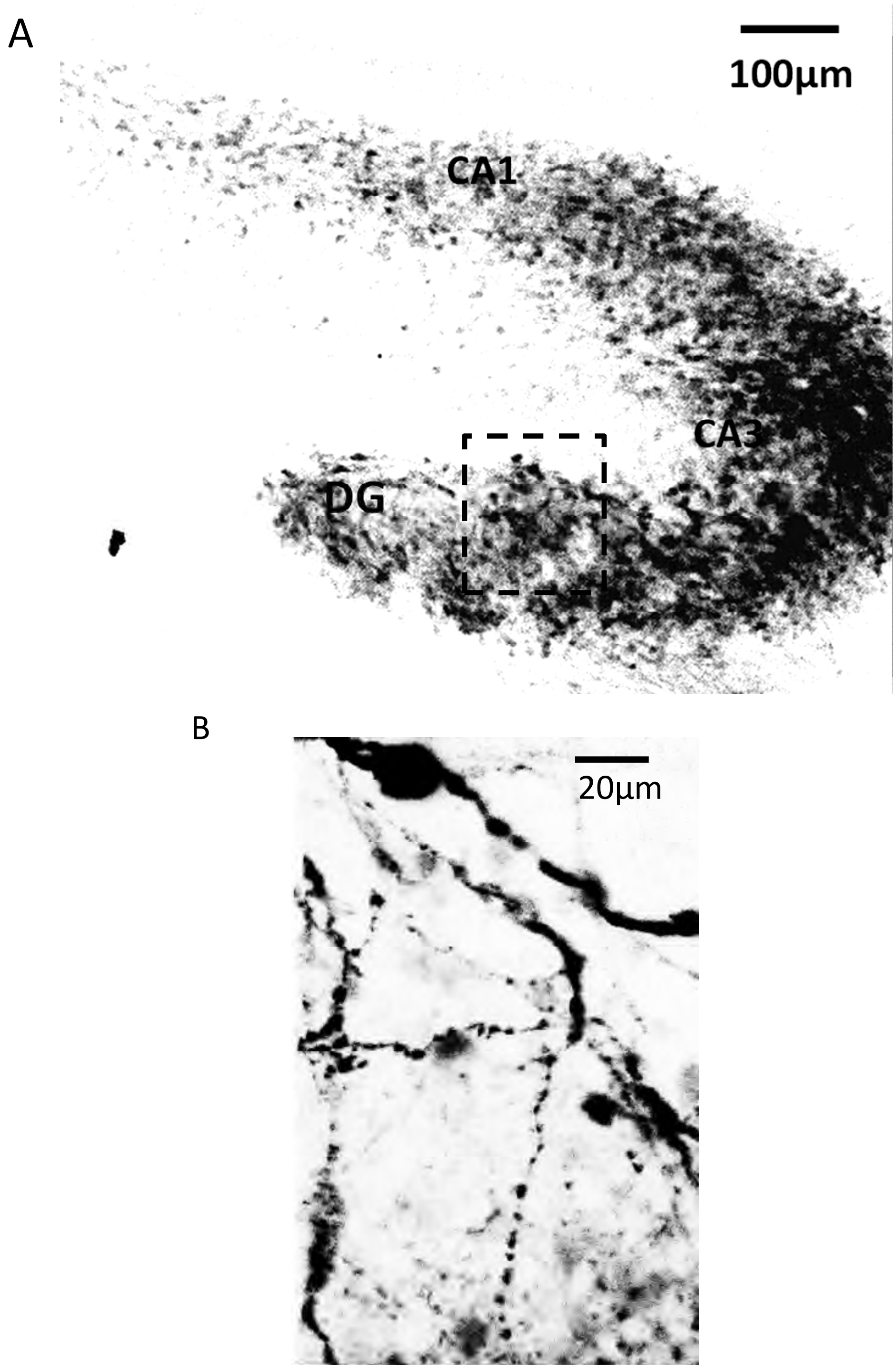

Figure 4-10 Copine-6 in the e18 developing hippocampus.

A.Copine-6 labelling can be seen throughout the cornu ammonis (CA1-CA3) and the dentate gyrus (DG). Some cells exhibit long processes typical of migration(boxed area, enlarged in Image **B**). The main structural regions of the hippocampus that are present in the adult are undergoing development and the Copine-6 reactivity is strong yet less organised than that observed in the adult brain (see Chapter 3).

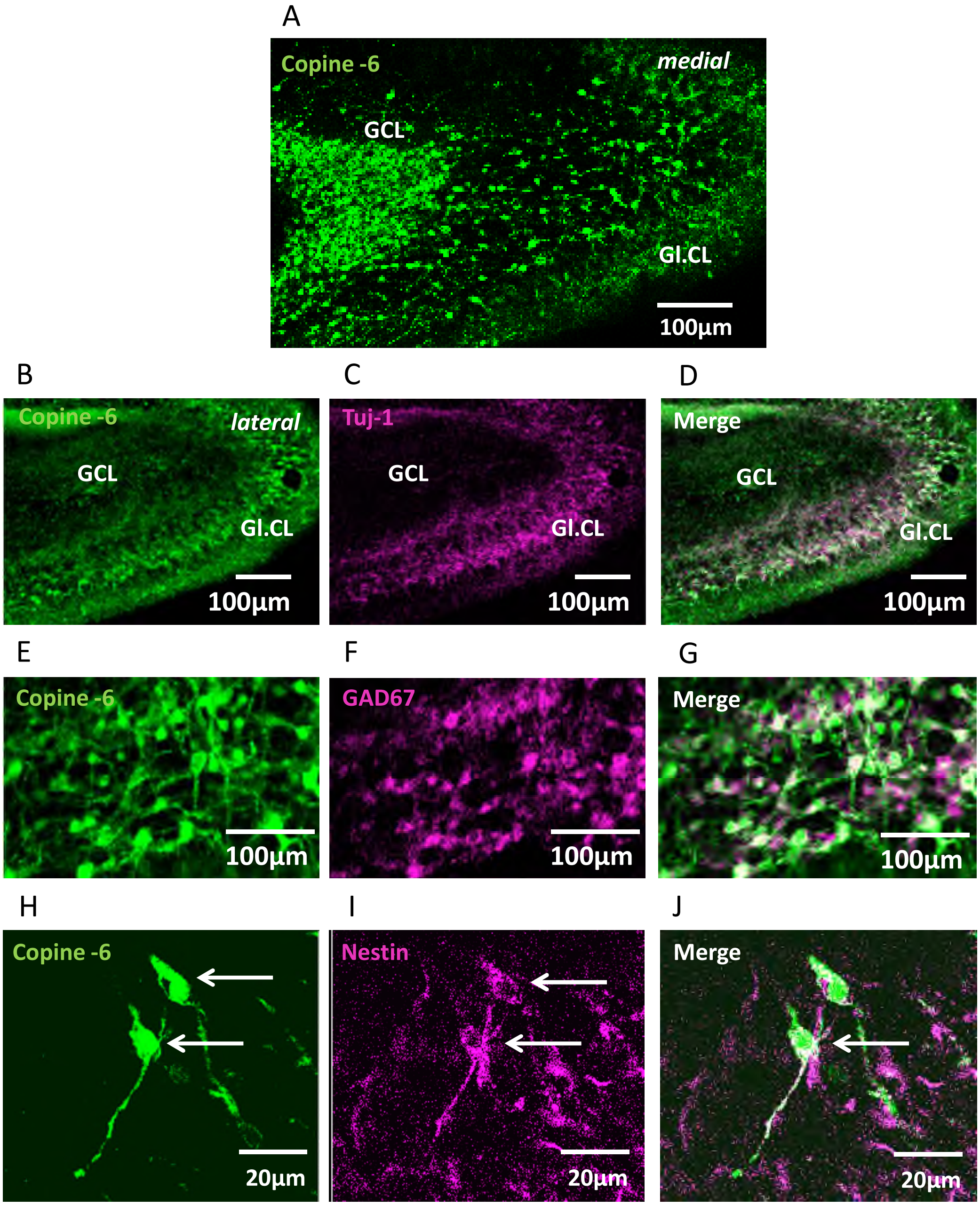

Figure 4-11 Copine-6 immunolabelling in the e18 developing olfactory bulb.

A. Copine-6 staining is strong in the granule (GCL) and glomerular cell layers (Gl.Cl), medial section. **B**. Copine-6 labeling of glomerular cell layer is more prominent in lateral sagittal sections. **C**. Tuj-1 reactivity in the e18 OB. **D**. There is apparent co-immunoreactivity between Tuj-1 and Copine-6 in the main OB indicating a neuronal phenotype of some of these cells. The low resolution images are shown to illustrate the overall expression pattern of the markers and not to prove co-labelling. **E**. Copine-6 cells in the granule cell layer **F**. GAD67 labelling in the granule cell layer. **G**. Copine-6 cells in the granule cell layer (and the glomerular cell layer, not shown) are immunoreactive for GAD67 **H**. Two Copine-6 cells entering the olfactory bulb at the lowermost RMS. **I**. Nestin staining in the lower RMS near to the OB. **J**. The Copine-6 cells have nestin reactivity at e18 which indicates a relatively immature phenotype in the e18 olfactory bulb.

In the postnatal brain, Copine-6 expression is strong and confined to specific structural locations. In the post natal day 2 brain, Copine-6 labels neurons in the CA1-CA3 pyramidal cell layer of the hippocampus and some sparse cells in the dentate gyrus (see Figure 4-12 Image A). In the cortex, several cells can be seen throughout all layers of the cortex which take a migratory-like morphology with long processes aligned towards the pial surface of the cortex (see Figure 4-12, Image B). In the p2 olfactory bulb, Copine-6 expression is very strong throughout the granule and glomerular layers (see Figure 4-12 Image C), and a stream of Copine-6 cells are visible in the white matter of the corpus callosum over the hippocampus, which is continuous towards the olfactory bulb following the rostral migratory stream(see Figure 4-12 Images A and C).

The expression of Copine-6 in the p2 rat brain is identical in anatomical location to what is observed in the adult rat brain, however it is clear that the brain is still undergoing cell growth and migration since the morphological appearance of the Copine-6 cells in the cortex and corpus callosum do differ. A small number of the Copine-6 cells in the p2 corpus callosum exhibit the long dendritic arborisations that are observed in the adult (See Figure 4-13) and these cells now lack nestin reactivity which labels immature and migrating cells with the rostral migratory pathway.

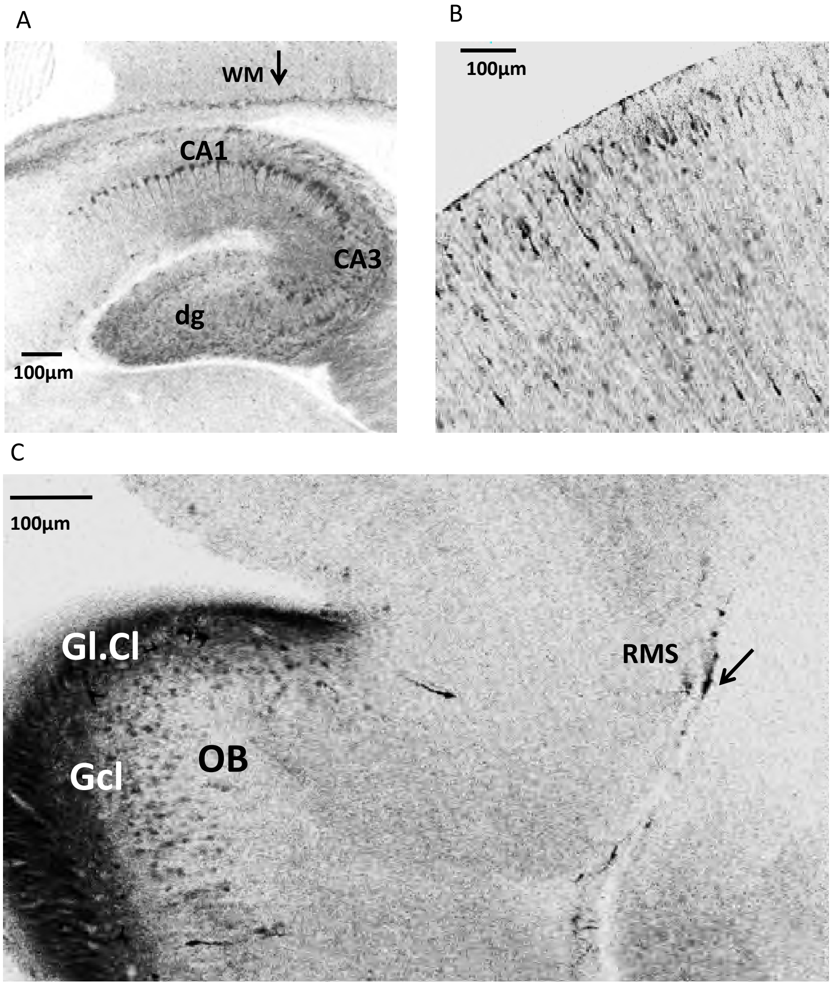

Figure 4-12 Copine-6 in the post natal day 2 rat brain.

A. Copine-6 labels cells in the pyramidal cells layers of CA1-CA3 of the hippocampus, and some sparse cells in the dentate gyrus (dg). The white matter (WM) above the hippocampus contains a chain of Copine-6 reactive cells (arrow), identical to that observed in the adult rat (See Chapter 3). **B**. In the cortex, Copine-6 labels cells that exhibit a migratory morphology with long processes pointing towards the surface of the cortex. These cells can be seen in all cortical layers. **C**. In the olfactory bulb Copine-6 expression is intense at the developing glomerular cell layer (Gl.Cl) and granule cell layer (Gcl). Some individual cells are labelled by Copine-6 on the periphery of the granule cell layer which may be en route to the OB. The 'stream' of cells that were identified in the e18 brain (refer back to Figure 4-8 D-F) are retained in the postnatal brain in the location of the rostral migratory stream (RMS, see arrow) and this is becoming similar to that observed in the adult rat brain (Chapter 3).

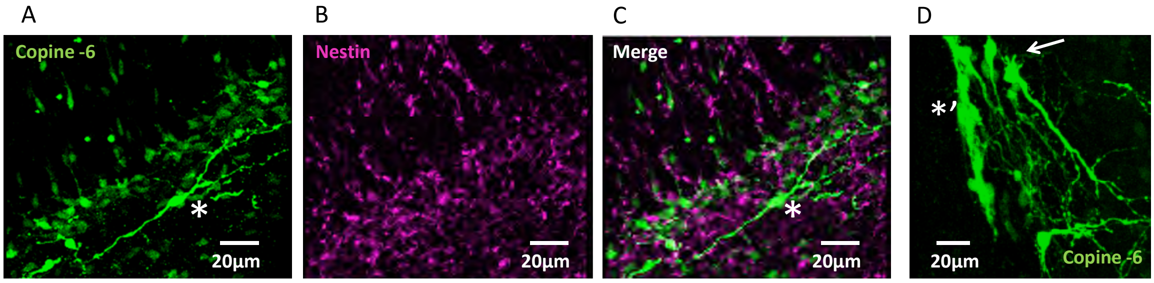

Figure 4-13 Copine-6 cells bordering the corpus callosum in the p2 brain.

A. Copine-6 labels cells peripheral to the rostral migratory stream, bordering the corpus callosum. (*) indicates a Copine-6 cell with a neuronal appearance with dendritic processes aligned with the white matter and the RMS. This cell is morphologically distinct to the Copine-6 cells undergoing possible migration, which are peeling away from the RMS. **B**. Nestin staining in the rostral migratory stream of the p2 brain. **C.** Copine-6 cells lack nestin reactivity. **D**. Copine-6 reactive cells in the corpus callosum of the p2 rat brain, some of which exhibit long arborisations and filipodia-like protrusions which may be indicative of growth (arrow). The Copine-6 cells in the corpus callosum of the p2 rat brain are in the same location to the Copine-6 spiny interneurons of the adult rat brain, but have a morphology typical of immature neurons with thickened, short and filopodia like processes (*').

In the post natal day 8 neocortex and olfactory bulb, Copine-6 labelling of cells is restricted to the same anatomical locations that are observed in the adult brain, and the number of cells exhibiting a migratory-like morphology is reduced. The neocortical layers are now more defined by the Copine-6 labelling (see Figure 4-14 Image A). In the hippocampus, the pyramidal cell layer of the cornu ammonis is labelled by Copine-6 immunostaining which is also becoming architecturally organised (see Figure 4-14 Image B). By post natal day 8, the Copine-6 cells bordering the corpus callosum and rostral migratory stream are almost identical in location and morphology to the Copine-6 spiny interneurons observed in the adult rat brain in Chapter 3 (see Figure 4-14 Images C, D and E-G). The Copine-6 cells bordering the corpus callosum exhibit a mature neuronal phenotype with several processes, which give rise to numerous spiny protrusions along the entire length of the process (see Figure 4-14 Image D, arrows). This is again identical to the Copine-6 spiny interneurons identified in the adult corpus callosum in Chapter 3 and suggests that the cells exist from postnatal, if not embryonic, stages of development. The Copine-6 cells border, but are not co-immunoreactive, for nestin positive immature neuroblasts in the rostral migratory stream (see Figure 4-14 Images E-G) which is also identical to the Copine-6 cells observed in the adult corpus callosu, and suggests that the cells are not immature or migrating.

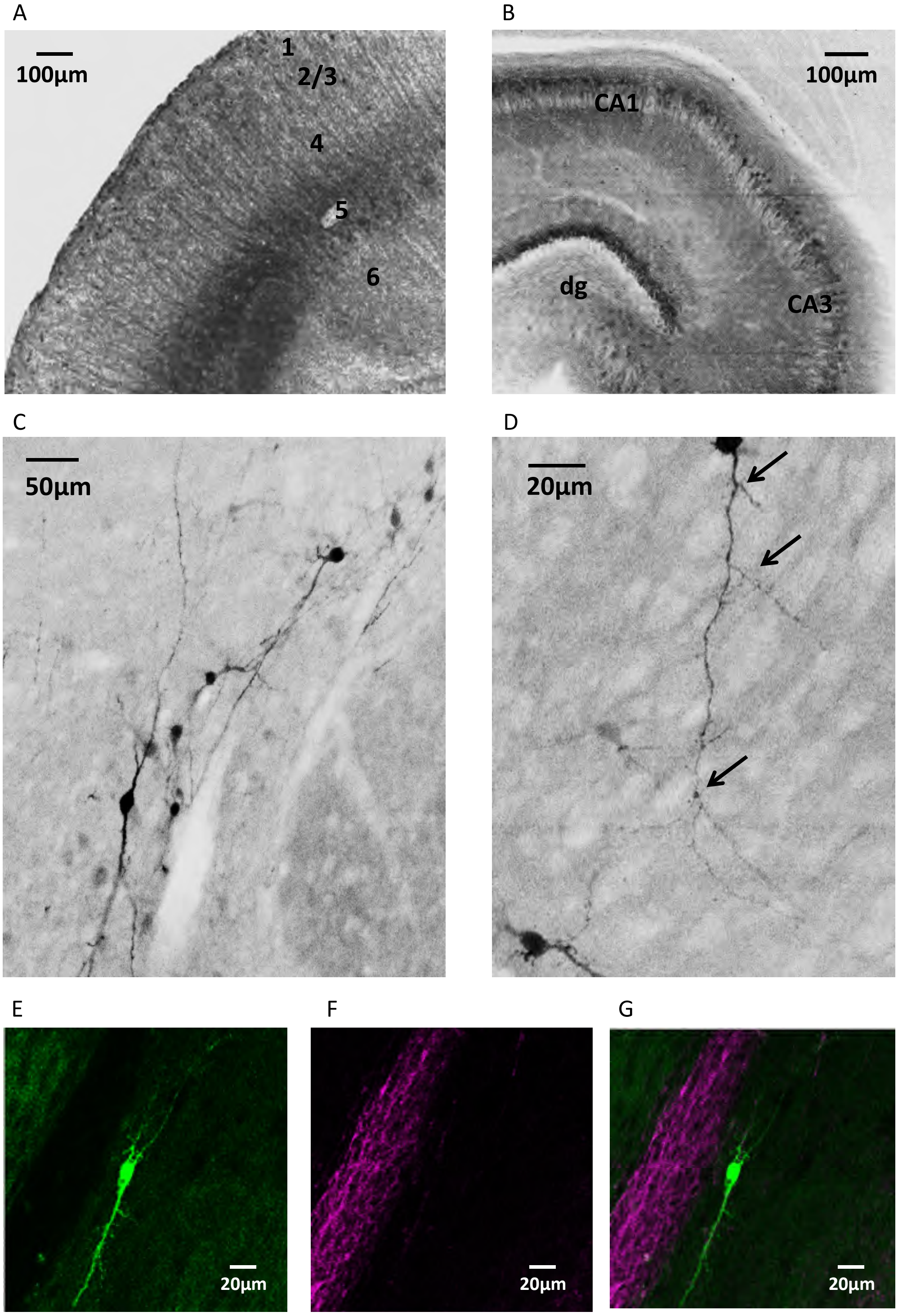

Figure 4-14 Copine-6 expression in the p8 rat brain.

A. Copine-6 labels cells and processes throughout the p8 cortex. An intense band of reactivity in layer 5 of the neocortex can be seen, alongside sparse Copine-6 reactive soma in the layer 2/3. **B**. In the hippocampus, Copine-6 reactivity has a more restricted profile to that observed in the p2 brain. Copine-6 reactive cells are visible in the cornu ammonis CA3 and CA1 pyramidal cells layer, and the granule cell layer of the dentate gyrus (dg), similar to that observed in the adult rat brain. **C**. and **D**. In the white matter of the corpus callosum, in a rostral and caudal direction over the striatum and hippocampus respectively, spiny Copine-6 cells can be seen that are identical in location and morphology to the Copine-6 spiny interneurons in the adult rat brain. The spine-like protrusions are distributed along the entire length of the cell processes (arrows, Image D). **E**. A Copine-6 cell on the border of the RMS. **F**. Nestin labelling defines the RMS in the p8 brain. **G**. The Copine-6 cell is clearly peripheral to the nestin-labelled rostral migratory stream. The Copine-6 spiny cells are themselves immunonegative for nestin, therefore are not immature or migrating.

4.3.4. BrdU analysis: Copine-6 spiny interneurons are not born in the adult rat brain

The location of the Copine-6 spiny interneurons in the corpus callosum of the adult rat brain at the site of adult neurogenesis in the rostral portion (subventricular zone and RMS, see Chapter 3) initially led us to question if these cells are themselves born in the adult brain. The evidence in support of this is the location of the cells at the neurogenic subventricular zone, in contrast the evidence against is their lack of any protein markers that are typical of immature or migrating cells within the RMS. BrdU analysis of newborn cells in the adult rat brain was therefore carried out, both as a single pulse when the rat was sacrificed after 24 hours, and as a course of pulses over 5 days which were maintained for 21 and 28 days. This was important to cover a range of possible birth dates of cells in the adult brain, and to also give time for any subsequent migration of newborn cells should this be occurring. The results showed that in both experimental conditions, no Copine-6 spiny interneurons in the subventricular zone or rostral migratory stream were labelled by the BrdU in the adult brain. The BrdU, which was visible only after the acid antigen retrieval, gave strong labelling in the nucleus of cells lining the lateral ventricle in the subventricular zone area following the 24 hour pulse (see Figure 4-15 Image A) and the 21/28 day pulse (see Figure 4-15 Image B), and within the rostral migratory stream itself following the 21/28 day pulses only (see Figure 4-15 Images B and C). In all cases the Copine-6 cells were adjacent to many of the BrdU labelled cells. The acid antigen retrieval process reduced the intensity of Copine-6 immunohistochemical labelling, but the cells were still labelled by the Copine-6 antibody and it was clear that these cells were different to those labelled by BrdU.

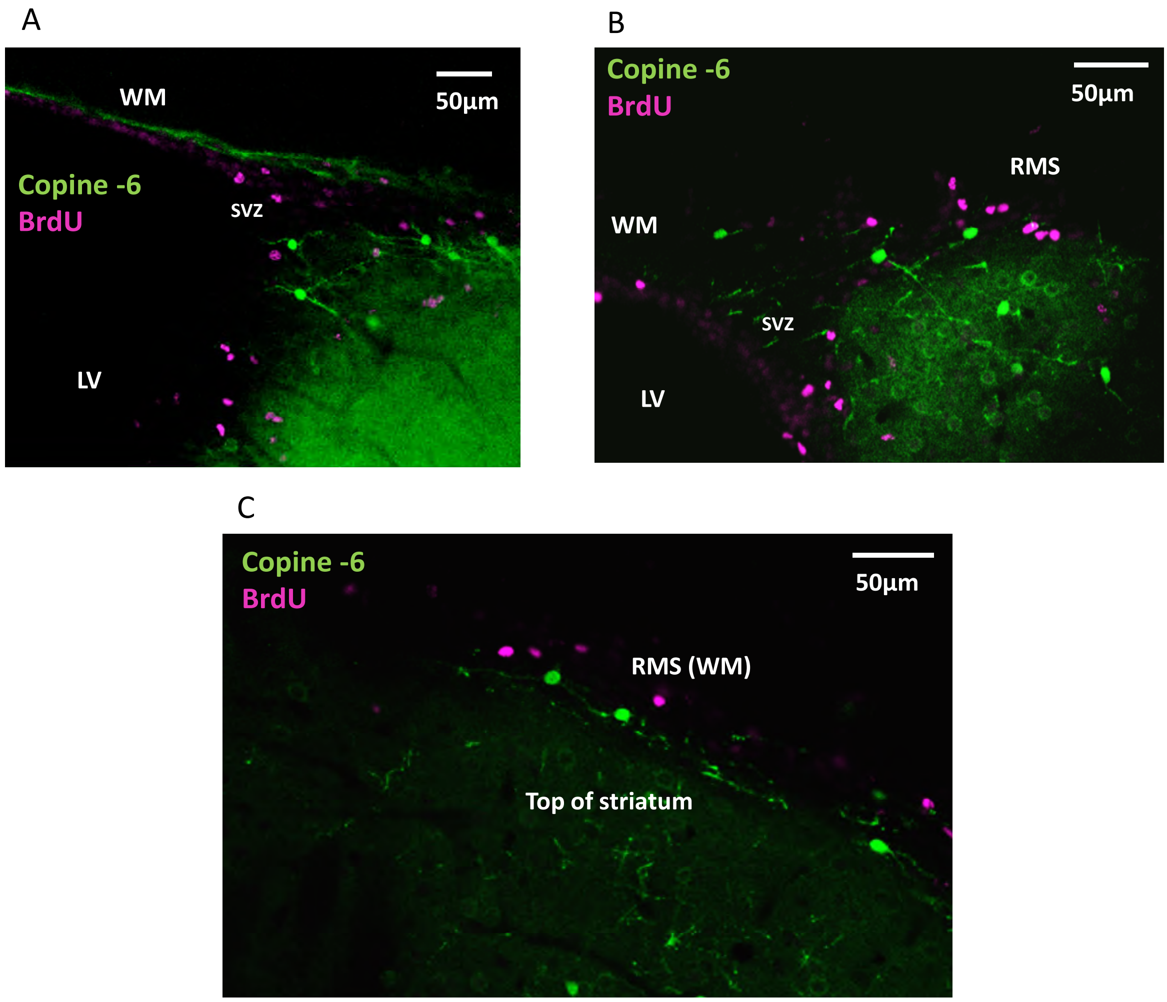

Figure 4-15 Copine-6 spiny interneurons in the adult rat brain are not born during adult neurogenesis.

A. BrdU labels cells at the subventricular zone (SVZ) at the edge of the lateral ventricle (LV) after a 24 hour BrdU pulse and these cells are not co-immunoreactive for Copine-6 after 24 hours. **B**. Following a 21 day incubation with BrdU in adult rats, again no Copine-6 cells have incorporated the BrdU compound and no co-reactivity can be seen at in the white matter (WM), subventricular zone or the rostral migratory stream (RMS). **C**. Following a 28 day incubation with BrdU, no Copine-6 cells were labelled.

BrdU labelling could be seen, as expected, in the dentate gyrus granule cell layer (see Figure 4-16). Since neurogenesis occurs only at the subventricular zone and the dentate gyrus of the adult rat, this labelling could be used as a positive control for the BrdU uptake into cells and for the subsequent immunohistochemistry. BrdU labelling was also confirmed using Ki67, a proliferation cell marker, which showed co-immunoreactivity with BrdU but not with any Copine-6 spiny interneurons (Figure 4-17). Some unidentified cells were labelled with Ki67 but not BrdU which reflects the time limiting ability of BrdU to integrate into DNA only during S-phase of the cell cycle.

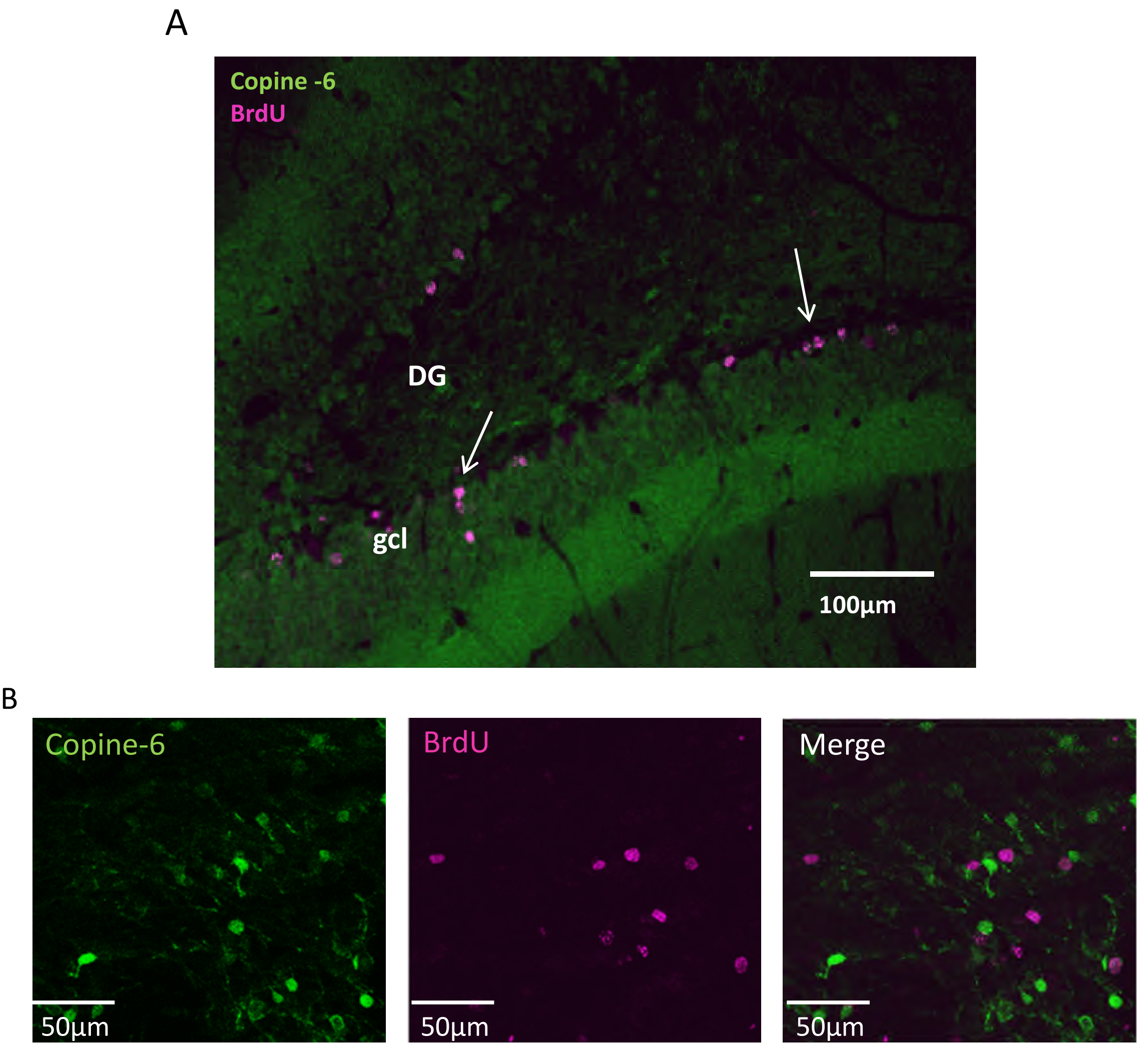

Figure 4-16 BrdU labelling in the adult rat hippocampus following x5 days of BrdU dosing and 28 day incubation prior to sectioning.

A.BrdU labelling can be seen in some cells within the granule cell layer (gcl) of the dentate gyrus (DG), see arrows, x10 objective. The Copine-6 labelling is not co-immunoreactive with BrdU. This labelling of some granule cells in the dentate gyrus shows that the BrdU has been successfully administered and the immunohistochemical conditions are sufficient for its detection. The same result was achieved following the 24 hour and 21 day BrdU pulse (not shown). B. A x20 objective to show at higher power that there is no co-immunoreactivity between the BrdU labelled cells and Copine-6 immunoreactive cells in the dentate gyrus of the adult rat following 28 day incubation period. All images are single scans.

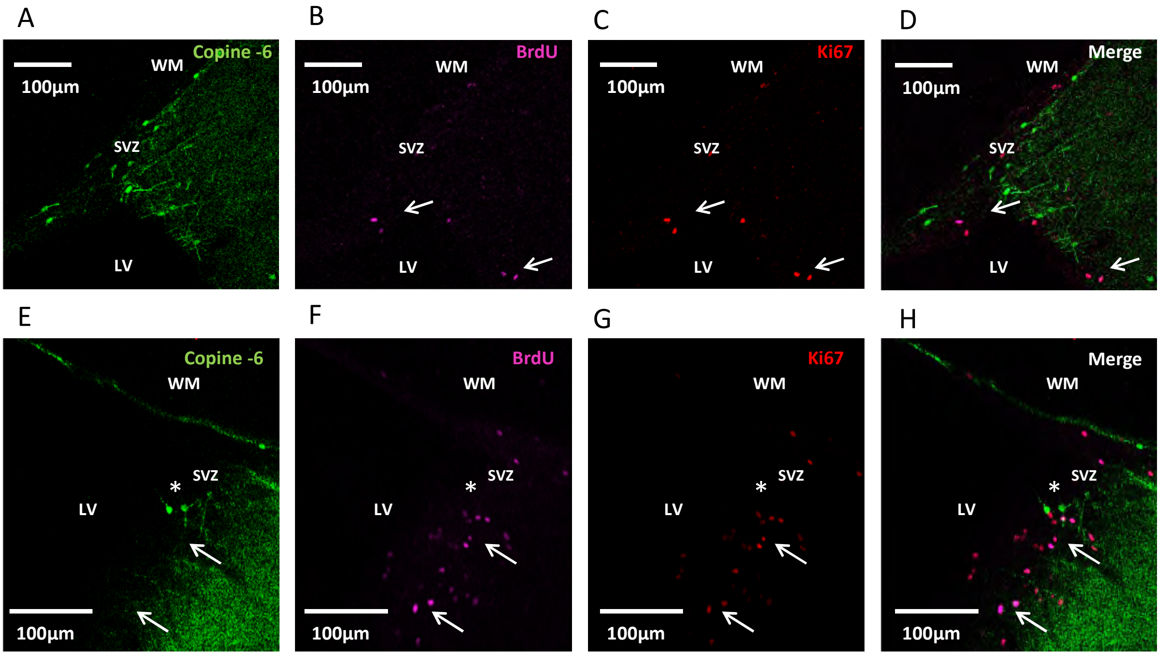

Figure 4-17 Copine-6 spiny interneurons in the subventricular zone (SVZ) and white matter(WM) are not co-labelled by BrdU or Ki67.

A. Copine-6 spiny interneurons at the SVZ and bordering the lateral ventricle (LV).**B**. BrdU labelling following 21 day incubation. **C**. Ki67 labelling of proliferating cells. **D**. Copine-6 cells are not labelled by BrdU or Ki67. BrdU and Ki67 co-label the same cells (arrows) which shows successful administration of the BrdU compound. **E**. Copine-6 at the SVZ. **F.** BrdU at the SVZ following 28 days incubation. **G**. Ki67 labelling at the SVZ. **H**. Copine-6 cells are not labelled by either marker but the Ki67 again confirms the incorporation of BrdU into proliferating cells. Co-labelling of proliferating cells is identified by pink nuclei. Note: more cells are labelled by Ki67 than BrdU owing to the restricted integration of BrdU during only S-Phase of the cell cycle. Some Copine-6 neurons are positioned close to the proliferating cells (Images E - H (*)) but it is clear that they are not themselves immunoreactive for either proliferative cell marker.

BrdU was also examined in the olfactory bulb of rats maintained for 21 and 28 days following the BrdU 5 day pulse, with the assumption that any cells destined for the OB would have time to migrate there during the designated incubation period. Indeed, following both 21 and 28 days incubation, BrdU cells were present in the granule and glomerular cell layers of the olfactory bulb. The majority of BrdU cells were immunonegative for Copine-6, and the majority of Copine-6 cells in these layers lacked BrdU in the nucleus. However, a small number of cells (on average between 10-20 cells per animal) were co-labelled for Copine-6 and BrdU in the granule cell layer (see Figure 4-18 Images A-C and D-F) and (less so) in the glomerular cell layer (see Figure 4-18 Images G and H). This indicates that some olfactory bulb cells that are born during adult neurogenesis express Copine-6. However, it is not clear if the Copine-6 expression occurs during cell migration, or if Copine-6 expression is turned on once the cells are within the olfactory bulbs. The latter hypothesis is supported by the finding that no co-labelled Copine-6+ BrdU+ cells are seen at all in the SVZ or rostral migratory stream. The Copine-6 spiny interneurons within the corpus callosum certainly were not labelled by BrdU following administration in the adult rat, therefore it is unlikely that these spiny cells are destined for the olfactory bulb at these later stages of development. Furthermore, the embryonic and postnatal identification of Copine-6 spiny interneurons bordering the rostral migratory stream from early developmental stages also points towards a younger birthdate of this particular cell population which is likely to be very different to those few BrdU reactive Copine-6 cells in the olfactory bulbs.

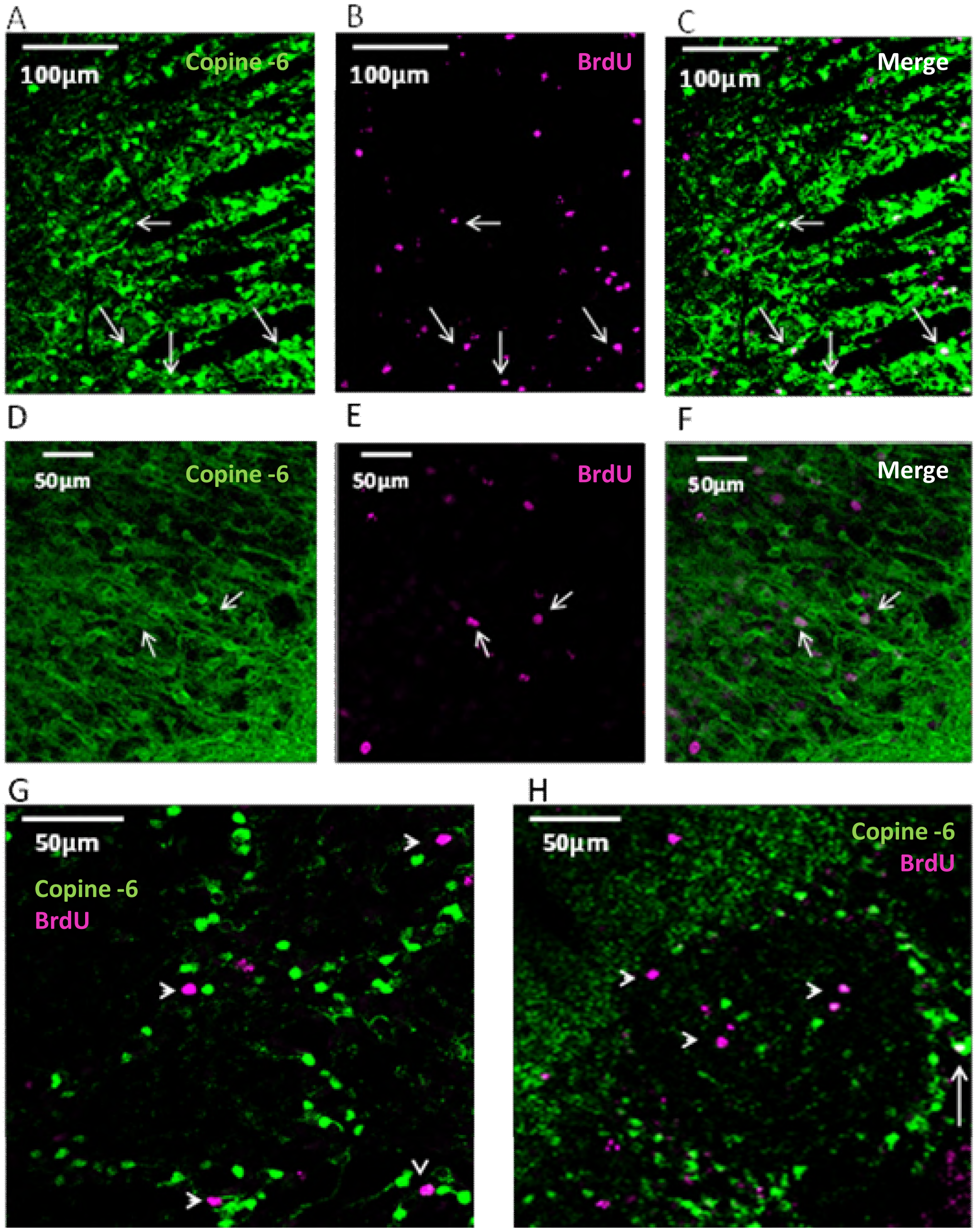

Figure 4-18 A small number of Copine-6 cells co-label for BrdU in the granule and glomerular cell layers of the olfactory bulbs.

A. Copine-6 in the granule cell layer, x10. **B**. BrdU in the granule cell layer following a 28 day incubation period. **C**. Some Copine-6 +ve granule cells had incorporated the BrdU. **D**. Copine-6 in the granule cell layer, x20 **E**. BrdU in the granule cell layer following a 21 day incubation period. **F.** Some Copine-6 +ve granule cells have incorporated BrdU. **G**. The majority of Copine-6 cells in the glomerular layers did not incorporate BrdU. **H**. However, a small number of Copine-6 +ve periglomerular cells could be identified after 21 days incubation with BrdU (and also following 28 days, not shown) The low power images are shown to represent how few in number the adult born Copine-6 cells are in the OB and are not to prove co-reactivity. Individual cells were examined by z-stack to check the co-reactivity was not a consequence of tissue depth or cell overlap.

4.3.5. BrdU-analysis of embryonic mouse brain: Copine-6 cells are born during embryogenesis

BrdU analysis of the Copine-6 spiny interneurons in the corpus callosum of the adult brain shows that this cell population is not born during adult neurogenesis (see section 4.3.4). Since Copine-6 cells are detected in the embryonic brain, and from as early as day e18 Copine-6 cells resembling the spiny Copine-6 interneurons can be identified (see section 4.3.3), an embryonic birth-dating analysis using BrdU was carried out. For licencing reasons, BrdU administration into pregnant dams could only be carried out in mice. This change in species was not problematic since the Copine-6 spiny interneurons, although less abundant, are immunohistochemically identifiable in the brain of adult mice.

A range of embryonic BrdU injection pulses were carried out to ensure a full embryonic analysis. Pregnant dams were injected at several embryonic stages (see Table 3) and pups were maintained for a range of postnatal stages, up from p4 to p67. The results showed that the majority of Copine-6 spiny interneurons in the corpus callosum are born during embryogenesis. Immunohistochemical analysis of the postnatal mouse brains following embryonic BrdU administration showed that Copine-6 cells in the corpus callosum of different postnatal ages are labelled by BrdU following BrdU injection at embryonic day e10.5 (see Figure 4-19), e13.5 (see Figure 4-20), e14.5 (see Figure 4-21) and day e15.5 (see Figure 4-22). The majority of Copine-6 cells appear to be generated during embryonic days e13.5 to e.15.5, with a peak in Copine 6+BrdU+ labelling at e.14.5 (see Figure 4-23). This suggests that the majority of Copine-6 spiny interneurons may be born during early embryogenesis, and following their genesis the Copine-6 reactive cells remain within the corpus callosum throughout all post natal ages up to adult.

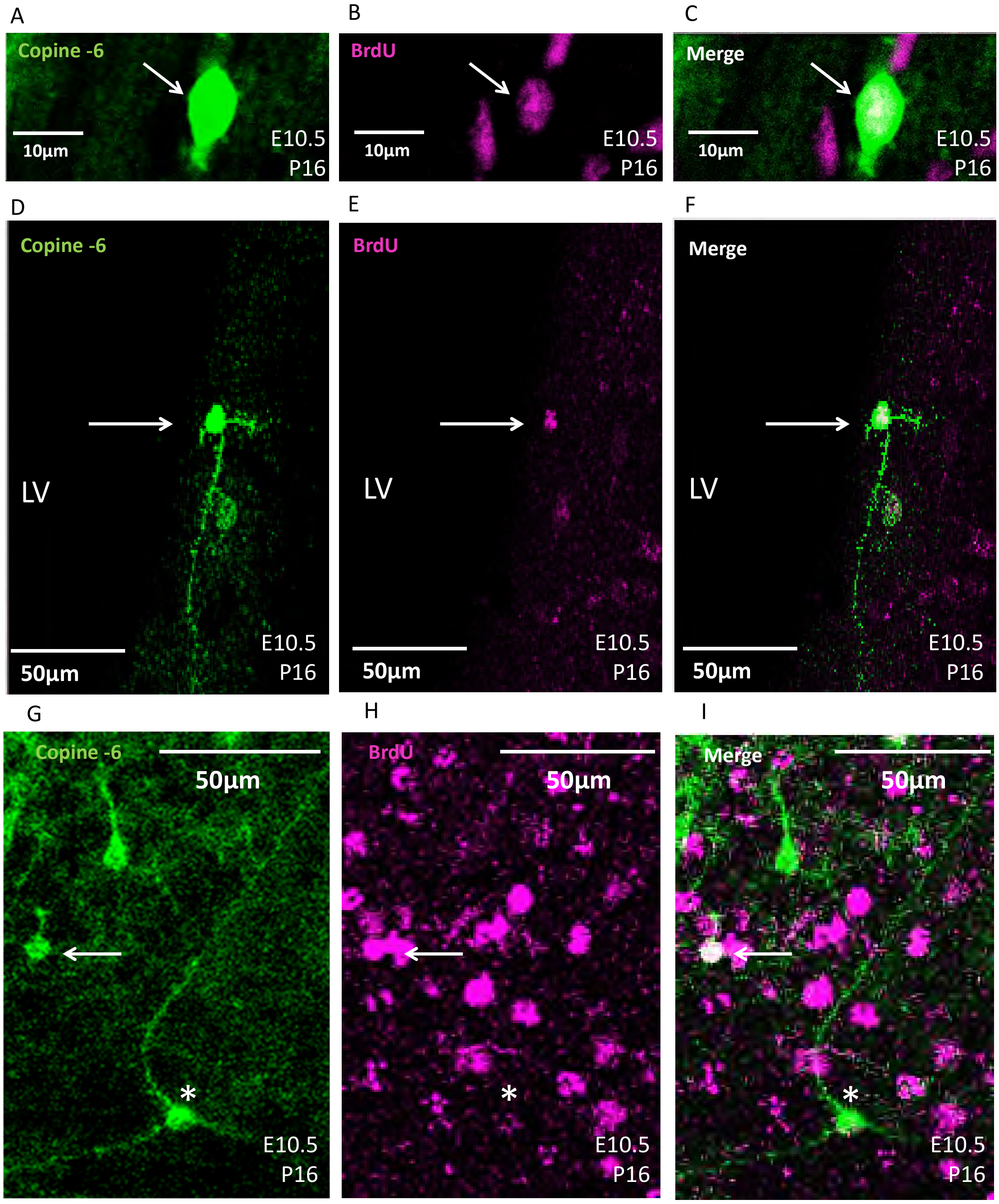

Figure 4-19 Some Copine-6 cells are born as early as embryonic day e10.5.

Copine-6 spiny interneurons in the corpus callosum and bordering the lateral ventricle (LV) have incorporated BrdU following BrdU administration at day e10.5 and brain processing at postnatal day 16 (p16). In all images the arrows point towards the BrdU+ Copine-6+ cells. **A**. The soma of a Copine-6 cell at the border of the LV and SVZ. **B**. BrdU labelling at the same region of the LV and SVZ. **C.** The Copine-6 cell clearly has BrdU incorporated into the nucleus. **D**. A Copine-6 cell at the border of the lateral ventricle with spiny arborisations. **E**. BrdU at the border of the lateral ventricle. **F**. The spiny Copine-6 cell is Brdu +ve. **G**. Copine-6 cells at the edge of the granule cell layer of the OB**. H**. BrdU labelling in the same regions. **I**. Some of the Copine-6 cells have incorporated BrdU following e10.5 administration (arrow). (*) indicates weak co-reactivity.

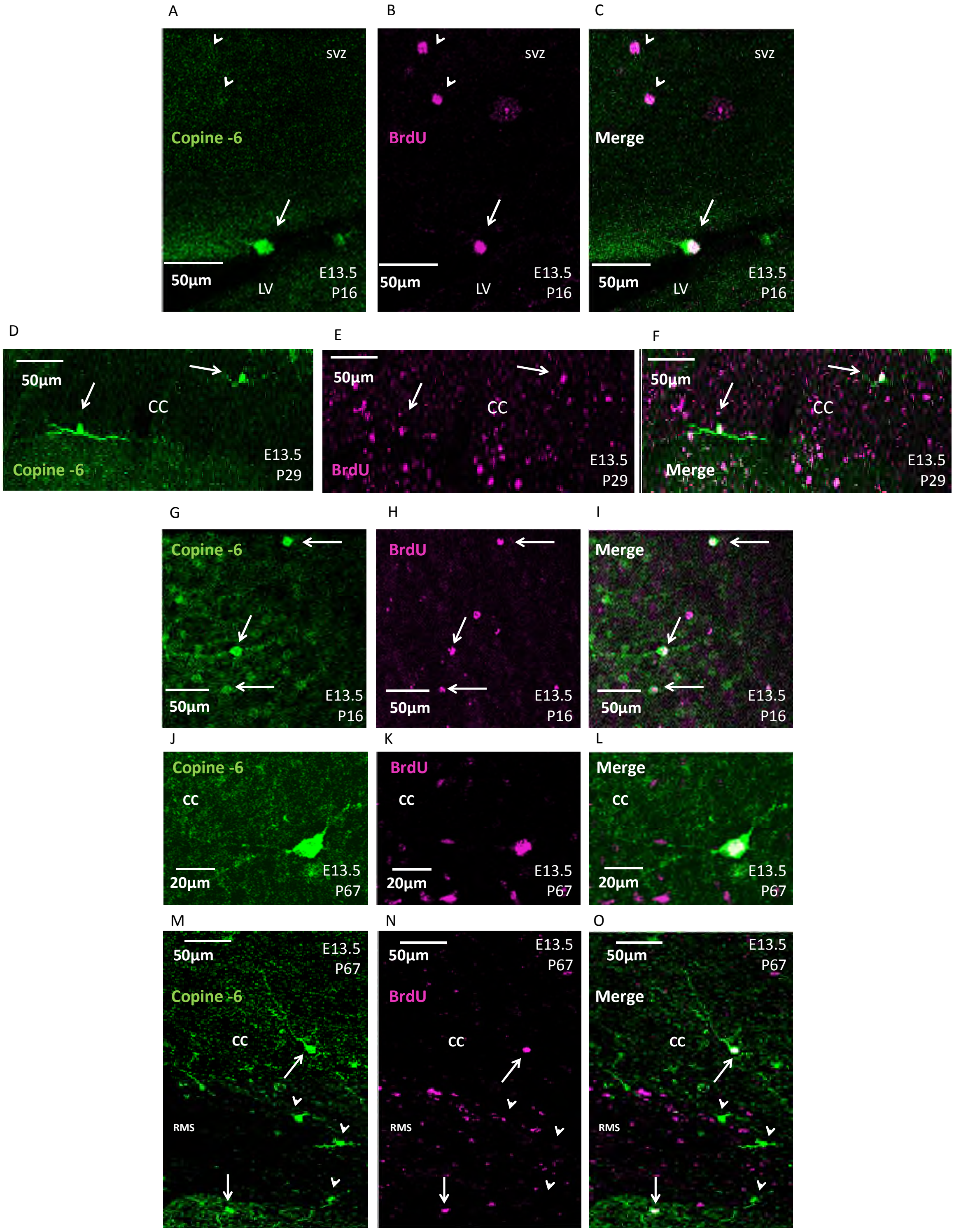

Figure 4-20 Copine-6 cells are also born during embryonic day e13.5.

A. A Copine-6 cell in the p16 brain bordering the LV. **B**. BrdU staining at the LV. **C**. The Copine-6 cell is BrdU +ve following administration of BrdU at e13.5 (arrow, arrowheads show BrdU +ve/Copine-6 –ve cells). **D**.Two Copine-6 cells in the corpus callosum (CC) and bordering the RMS. **E**. BrdU in the corpus callosum/RMS**. F**. The Copine-6 cells incorporated BrdU at e13.5 injection. **G**. Copine-6 in the olfactory bulb of the p16 mouse. **H**. BrdU in the olfactory bulb of the p16 mouse following e13.5 administration. **I**. Copine-6 cells are labelled by BrdU (arrows). **J**. A Copine-6 cell in the p67 (adult) mouse. **K.** BrdU in the corpus callosum of the p67 mouse after e13.5 adminstration. **L**. The Copine-6 is labelled by BrdU. **M**. Several Copine-6 cells in the corpus callosum of the p67 mouse. **N**. BrdU labelling at p67. **O**. Several cells are Copine-6 +ve/BrdU +ve (arrows). The arrowheads show Copine-6 cells that were not born at e13.5.

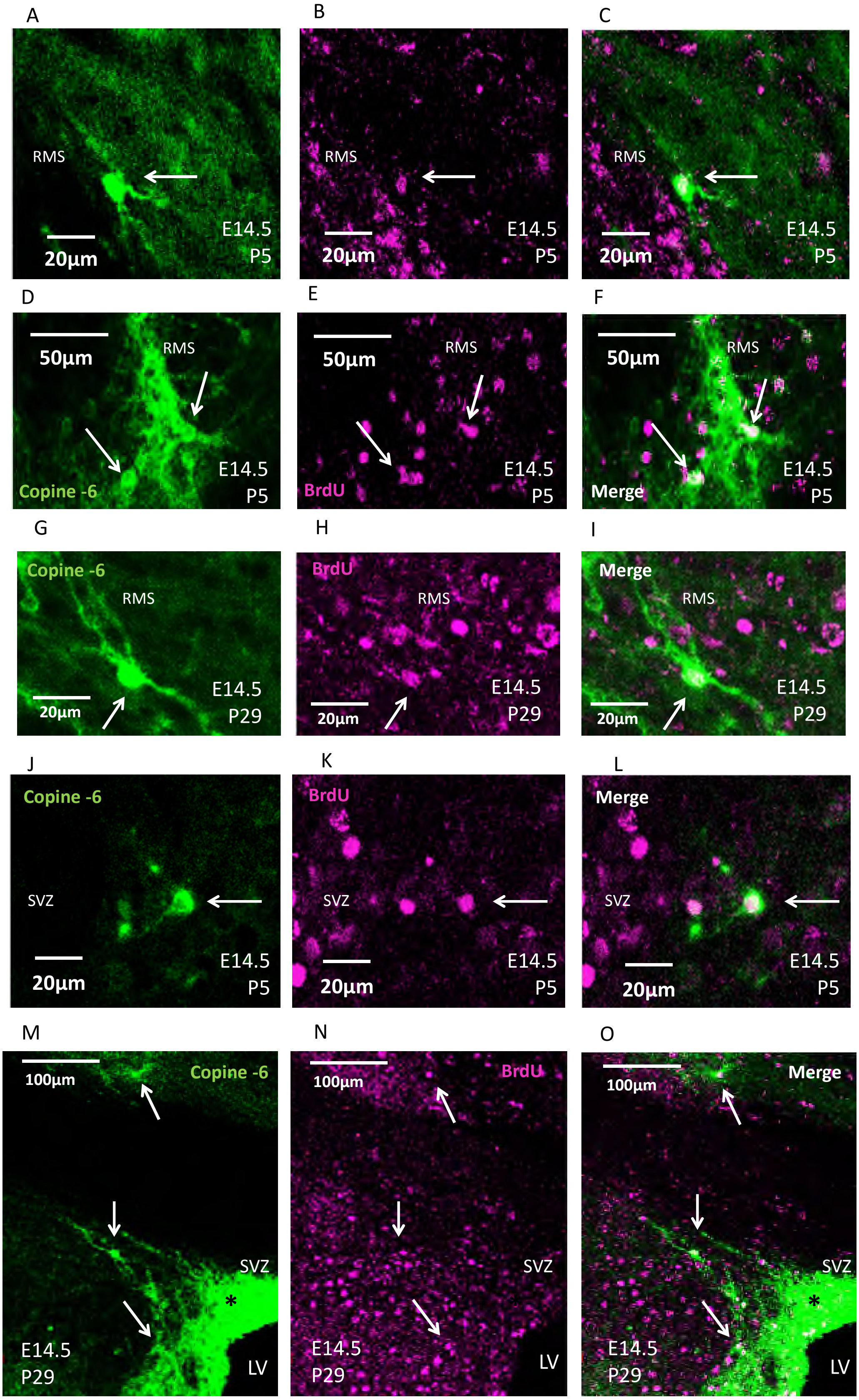

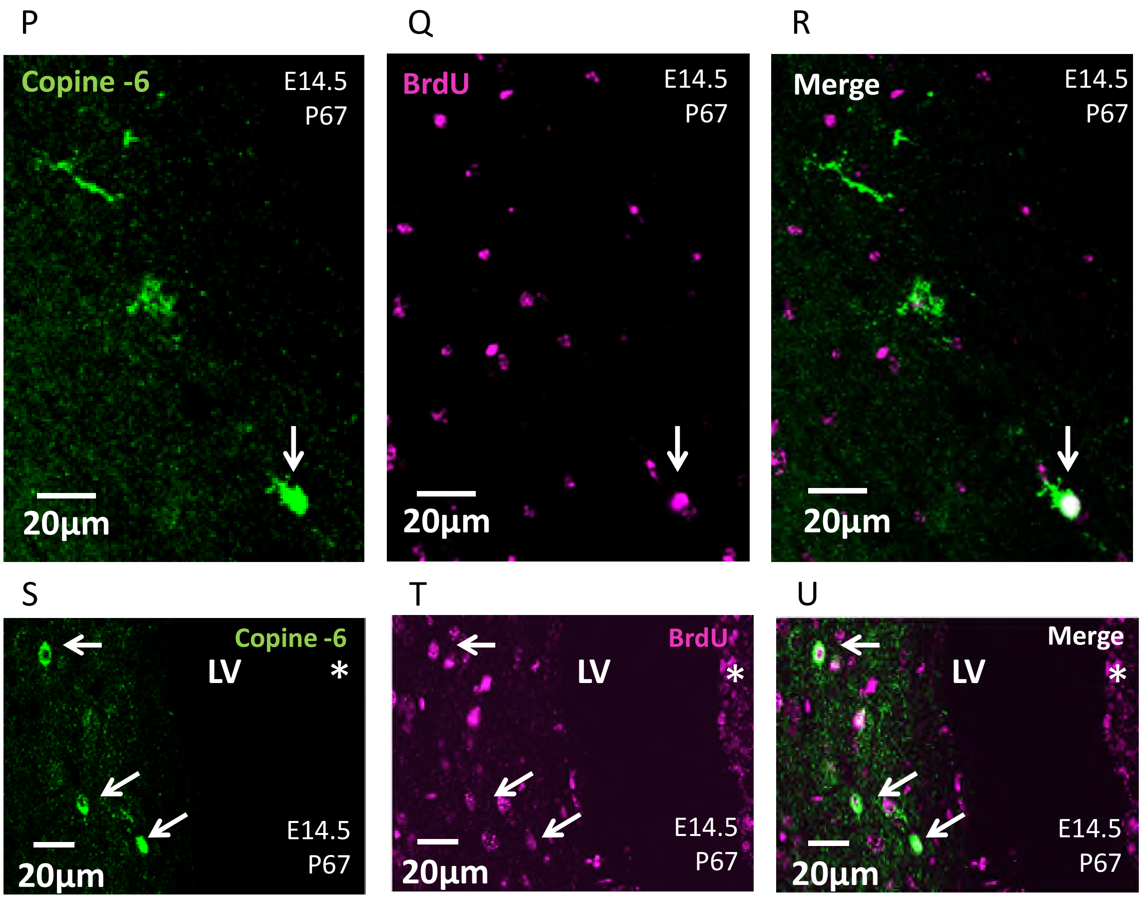

Figure 4-21 Copine-6 cells are also born during embryonic day e14.5.

A-C, D-F. Copine-6 cells are labelled by BrdU at the border of the rostral migratory stream (RMS) in postnatal brain at postnatal day 5 following administration at e14.5. **G-I**. Copine-6 cells are labelled by BrdU following injection at e14.5 in the postnatal day 29 mouse. **J-L**. BrdU also labels Copine-6 cells at the subventricular zone of the p5 brain, and **M-O.** in the p29 mouse (see arrows for co-reactivity). Copine-6 also labels many clustered cells at the subventricular zone in Images M and O, many of which are BrdU labelled (*). **P-R**. BrdU co-labelling of some Copine-6 spiny cells following e14.5 injection continues until adulthood (late postnatal day p67). **S-U**. Copine-6 cells lining the lateral ventricle (LV) are BrdU +ve, arrows. BrdU labelled progenitor cells lining the LV are indicated (*) All co-immunoreactive cells appear white and are indicated by the arrows.

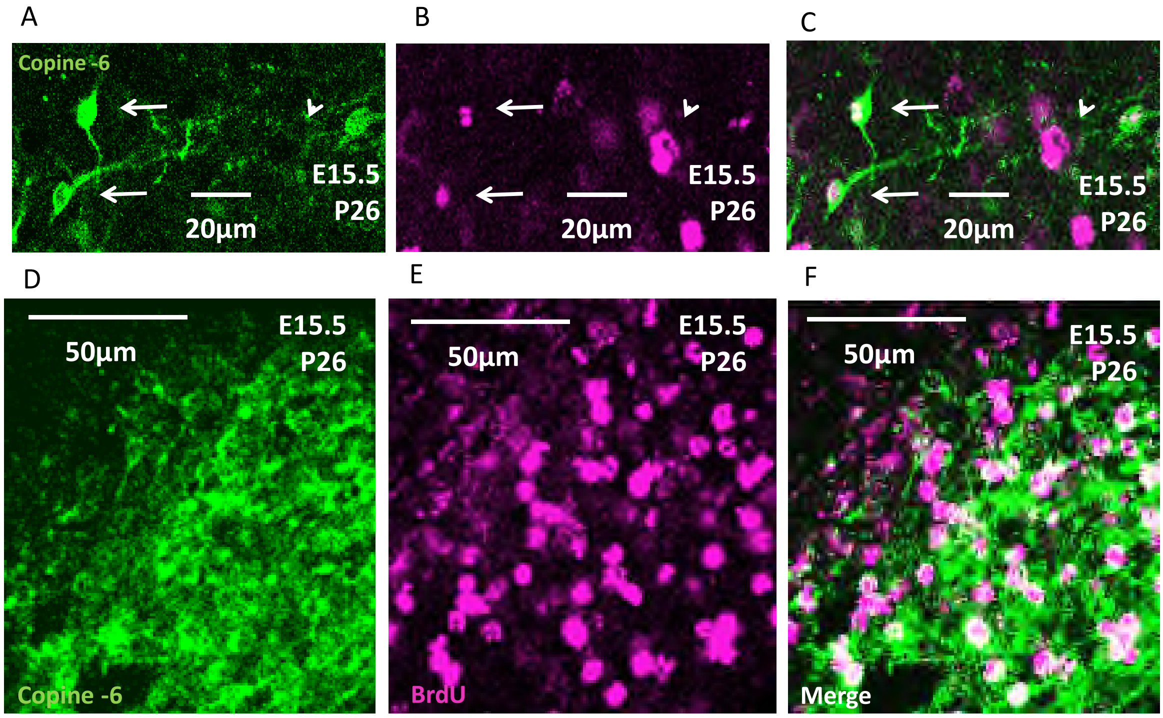

Figure 4-22 Copine-6 cells are also born during embryonic day e15.5.

A. Copine-6 cells in the rostral migratory stream of the postnatal day 26 brain **B**. BrdU labelling of cells in the RMS following administration at e15.5. **C**. Some Copine-6 cells have incorporated BrdU. (arrows) and other BrdU +ve cells can be identified that lack Copine-6 reactivity (arrowhead). **D.** Copine-6 in the granule cell layer of the OB. **E**. BrdU labelling in the olfactory bulb granule cell layer following e15.5 administration. **F.** Copine-6 +ve/BrdU +ve are in abundance. A low power image is shown to demonstrate the numerous Copine-6 cells with BrdU labelling. In all images the co-immunoreactivity appears white.

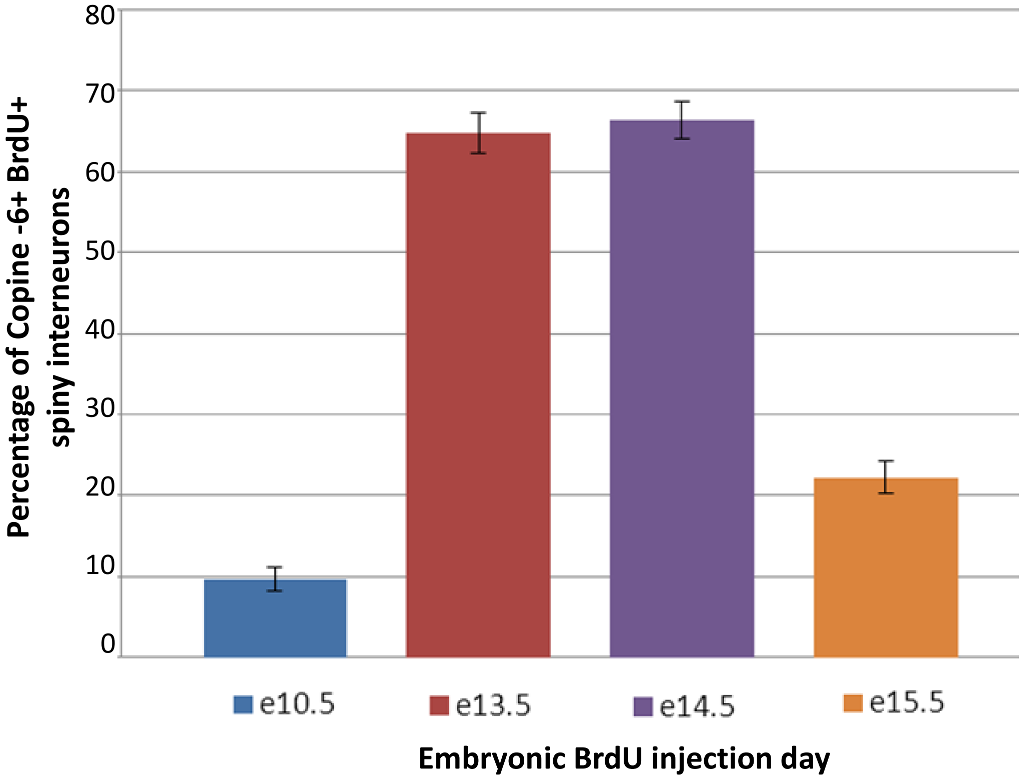

Figure 4-23 The majority of Copine-6 spiny interneurons are born during embryonic day e13.5 and e14.5.

Copine-6 spiny cells persist into postnatal stages of development following embryonic birthdating. Cell counts were conducted in postnatal mouse brains following embryonic administration of BrdU between days e10.5 and e15.5. BrdU was injected i.p into pregnant dams at the embryonic developmental timepoints stated above The pups were sacrificed at a variety of postnatal ages ranging from p4-p67(some animals were sacrificed earlier than others) with a minimum of 200 cells counted per animal. The data from a selection of the sacrificed mice is shown here. Following e10.5 administration, data from postnatal day 24 was analysed from two pups. For e13.5 injection, three pups were analysed at postnatal day 67. For embryonic injection day e14.5, four pups were sacrificed at postnatal day 67. Following embryonic day e15.5 injection, three postnatal pup brains were analysed at postnatal day 67. The percentage of Copine-6 spiny interneurons immunoreactive for BrdU were calculated from the total number of Copine-6 spiny cells. Error bars show standard error of the mean (±SE).

4.4. Discussion

In this chapter, a developmental profile of Copine-6 in rodent brain has been conducted.

Total protein content analysis initially identified a gradual increase in Copine-6 expression between embryonic day 18 to postnatal day 8 which plateaued from thereon but did not decrease. Copine-6 expression in the brain does not cease at any point, and since the expression is continuous from very early development this may point towards an continued function, perhaps related to neuronal maintenance. The immunohistochemical analysis of dissociated hippocampal neurons over different maturation stages indicates that although there is a gradual increase in expression intensity of the protein in those cells that are already immunopositive for Copine-6, the total number of cells expressing Copine-6 is relatively stable. In culture, the Copine-6 reactive neurons have a more intense labelling by the Copine-6 antibody as they mature, which correlates with the mature morphological changes in the cells such as the size of dendritic arbor and the number of spines. This finding was supported by the immunohistochemical analysis of Copine-6 in embryonic and postnatal rat brain which showed that not only is Copine-6 protein identified in all developmental stages examined, but Copine-6 cells were in the same anatomical locations from later embryonic stages (e18+) right through to adulthood. The majority of the Copine-6 cells were embryonically immature, especially those in the rostral migratory stream and ventricular regions, however they became more characteristic of the Copine-6 spiny interneurons (identified in Chapter 3) by mid-post natal (p4-p8) ages. Furthermore, although the protein immunoblot suggests otherwise, the Copine-6 antibody reaction in the embryo was not particularly weak and instead showed a relatively non-uniform labelling throughout much of the developing neocortex and hippocampus. This discrepancy in data between the immunoblot and the immunohistochemistry may be, as previously mentioned, due to Copine-6 being a very small fraction of total protein in the embryonic brain. This is consistent with the gradual increase in Copine-6 expression in cells during later embryonic development. Most of the cells in the e12 and e18 brain exhibited a migratory morphology, which was true for the neocortex, olfactory bulbs and hippocampus which would be as expected for these developmental times. From the mid (p4-p8) postnatal stages through to adulthood, the overall non-uniform Copine-6 expression intensity started to reduce and instead the immunoreactive cells were positioned in their destined anatomical locations and themselves became more strongly immunoreactive for the Copine-6 antibody. Cells became confined, as observed in the adult brain, to the olfactory granule and glomerular cell layers, the pyramidal cell layer of the hippocampus CA1-CA3, and to the neocortex.

These findings initially indicated that Copine-6 cells are present from very early embryogenesis, here documented by immunohistochemistry at day e12 (and, in the case of the spiny interneurons in the corpus callosum, also by BrdU analysis at day e10.5). Furthermore, since Copine-6 is found both at the ventricular and marginal zone of the e12 developing neocortex and has co-reactivity for Tuj-1, this also indicates that the cells are neurons, and have been programmed to be so from early (<e12) embryogenesis. Interestingly, it is thought that certain Tuj-1 cell populations close to the marginal zone of the early embryonic brain are retained to adulthood, and that they expand in number and are representative of the rostral migratory stream that continues through to adult neurogenesis (Pencea & Luskin, 2003). Since Copine-6 is subsequently found on the border of the rostral migratory stream and subventricular zone which can be seen in the embryonic day e18 brain onward, it would be plausible to consider that the Copine-6 cells in the e12 brain could belong to these cell populations that persist in the RMS.

In the embryonic rat brain, the majority of Copine-6 immunoreactive cells in the developing neocortex, subventricular zone and corpus callosum had an immature (nestin +) neuronal (Tuj-1) phenotype. Since nestin immmunoreactivity, which indicates immature and/or migrating new born cells, was lost through postnatal to adult stages of brain development, yet the Tuj-1 reactivity was maintained, this could be indicative of an embryonic birth date of some Copine-6 spiny interneurons in the corpus callosum if they indeed remain in this location in the adult rat brain. Indeed, the BrdU birth-dating analysis during embryonic neurogenesis confirmed that the majority of Copine-6 spiny interneuron in the corpus callosum of the postnatal and adult rodent brain are born between embryonic days e10-5 to e15.5, with a peak in Copine-6 cell genesis between e13.5 and e14.5. Since the BrdU labelling was identified in the spiny interneurons throughout the entire rostral portion of the corpus callosum, including those cells at the subventricular zone and lining the lateral ventricles, this indicates that although the cells have an early embryogenic birth-date, they remain within a site of adult neurogenesis right through to adulthood. BrdU analysis in the adult rat brain confirmed that the Copine-6 spiny interneurons are not born during adult neurogenesis and therefore their genesis appears to be restricted to a particular window of time, despite their location at this neurogenic site.

In the olfactory bulb, a similar pattern of embryonic birth-dating was observed for the Copine-6 immunoreactive cells in the granule and glomerular cell layers. Many cells were labelled by both BrdU and Copine-6 in the granule and glomerular cell layers of the olfactory bulb throughout embryogenesis, with the most cells co-labelled at e13.5-e14.5. Interestingly, a very small number of cells (some 10-20 per adult rat examined) in the olfactory granule and glomerular cell layer were also co-labelled for BrdU and Copine-6 following the administration of BrdU in the adult rat. This indicates that some of the olfactory interneurons that are Copine-6 immunoreactive are indeed born in the adult rat brain. However, these cell populations – although molecularly similar– are unlikely to represent the Copine-6 spiny interneurons in the corpus callosum (see Chapter 3). No Copine-6 spiny interneurons, or any population of Copine-6 cell for that matter, were labelled by BrdU following adult administration at any of the neurogenic regions including the SVZ, RMS and corpus callosum. Therefore, it will be suggested here that the expression of Copine-6 in the adult generated BrdU +ve olfactory interneurons begins only once the cells reach the olfactory bulb.

Owing to the molecular similarity between the Copine-6 spiny interneurons in the corpus callosum and the olfactory interneurons (see Chapter 3), it is plausible to consider that the Copine-6 spiny cells within the corpus callosum may be a subpopulation of interneurons initially destined for the olfactory bulb, which may have failed to migrate but have instead matured *en route* to the olfactory bulb. However, the sheer number and consistency of the Copine-6 spiny interneurons in the brain of multiple rodents could argue against a putative failure in migration, which would be more likely to result in cell death rather than neuronal maturation and integration. Perhaps it is more likely that these cells were destined to remain in the corpus callosum from birth, but originate from similar neuronal precursors to the olfactory bulb interneurons for which they share molecular similarities.

Due to Home Office licencing restrictions, a postnatal birth-dating analysis could not be conducted therefore it remains to be answered if the Copine-6 spiny interneurons continue to be generated during postnatal development. However, since the majority of Copine-6 spiny interneurons were born embryonically, yet remain in a location that is home to very few mature neurons (rather, bordering many immature migrating neurons), this leads us to question what the anatomical significance of these Copine-6 cells might be. In order to partially investigate this, an electron microscopic analysis of the Copine-6 spiny interneurons is subsequently carried out (See Chapter 5) to investigate if the cells are integrated into, or established as a cell network.

Chapter 5. **Electron Microscopic analysis of Copine-6 immuno-positive neurons**

5.1. Introduction

Immunohistochemical analysis of Copine-6 (Chapter 3) identified several populations of neurons in the adult rat brain, including a novel spiny interneuron population in layer VI of the neocortex, the rostral and caudal corpus callosum and the neostriatum. These interneurons have an unusual molecular phenotype compared to other cells in these locations. They are very close to the rostral migratory stream and the subventricular zone, the latter a region of adult neurogenesis, yet they originate during embryogenesis (Chapter 4) suggesting that they have remained in this location throughout development and are possibly integrated into neuronal networks. The cells have a mature GABAergic phenotype, with heterogenous calretinin and enkephalin immunoreactivity, and several of the Copine-6 immunoreactive spine-like protrusions are VGAT immunopositive with closely apposed gephyrin puncta, suggesting pre- and postsynaptic specialisations, respectively (Chapter 3). These putative synaptic connections are here analysed by electron microscopy.

5.1.1. Synaptic neurochemistry and the Copine-6 spiny cells in the corpus callosum

There are two main classes of neurotransmitter; small molecules such as amino acids (of which GABA and glutamate are the main inhibitory and excitatory amino acid neurotransmitters, respectively) and amines (such as serotonin and the catecholamines adrenaline and noradrenaline), and neuroactive peptides (such as enkephalin, somatostatin and neuropeptide Y). All neurotransmitters from each class are stored in intracellular vesicles. Small molecule transmitters are held within small vesicles of some 20-40nm diameter which accumulate within the presynaptic terminal and are released, usually following an action potential, by specialised exocytosis at the active zone, which is juxtaposed to a postsynaptic specialisation containing numerous clustered receptors and cytoskeletal proteins. This process results in fast chemical transmission. The postsynaptic density appears as a large electron dense band in electron micrographs of asymmetrical (typically excitatory, Type 1) synapses, and is less pronounced in symmetrical (typically inhibitory Type 2) synapses (Gray, 1959). Neuroactive peptides on the other hand are stored in larger ‘dense-core’ vesicles, measuring between 60-100nm, which are more electron dense than the smaller vesicles when observed by electron microscopy. These vesicles can be released alongside classical neurotransmitters during the action potential, but can also be released in a non-synaptic manner from other locations within the soma or dendrite of a neuron. The nonsynaptic release of these neurotransmitters and peptides is typically associated with slow, modulatory long distance signalling.

GABA is the major inhibitory neurotransmitter in the central nervous system, and is stored in small vesicles and released in a synaptic manner. Chapter 3 shows that the Copine-6 spiny cells in the white matter are GABAergic (GAD67+) and are immunoreactive for the vesicular GABA transporter (VGAT), a protein responsible for the uptake of GABA and/or glycine into synaptic vesicles. The VGAT immunoreactivity was present in several of the appendages emanating from the Copine-6 reactive dendritic branches, which may point towards a putative inhibitory presynaptic function for the Copine-6 interneurons (See Chapter 3). Furthermore, gephyrin, a scaffolding protein present at inhibitory post synaptic terminals, labels puncta in close apposition to the majority of the Copine-6+ and VGAT+ appendages, and also as puncta along the processes of the Copine –6 cells themselves. Although synaptic relationships can only be of predictive value at the level of light microscopic analysis, the VGAT and gephyrin labelling indicates that the Copine-6 spiny cells exhibit both pre- and post-synaptic connections, respectively, and some of the presynaptic connections may be onto other neuronal populations. In addition, some of the Copine-6 spiny cells in the white matter also contain enkephalin in some of the spiny protrusions, indicating that these cells may have peptidergic vesicles in the labelled immunoreactive spines. Visualisation of fine details such as pre- and postsynaptic architecture can be achieved with the high magnification and high resolution achieved with the electron microscope. Therefore this chapter concentrates on an electron microscopic analysis of the Copine-6 spiny cells in the white matter using traditional diaminobenzidine (DAB)-based immunoperoxidase methods.

Because the Copines are calcium dependent phospholipid binding proteins that are shown to translocate to the plasma membrane following an increase in intracellular calcium in HEK cells (Perestenko *et al*, 2010), it would be interesting to investigate the intracellular location of Copine-6 in neurons. Therefore, this chapter also analyses the intracellular localisation of the Copine-6 protein within two neuronal populations: the Copine-6 spiny interneurons in the corpus callosum, and pyramidal cells of the hippocampus, using silver intensified gold immunoparticle labelling and electron microscopy.

5.2. Methods

Tissue preparation for electron microscopy involves immunohistochemical methods similar to those employed for light microscopy, therefore the labelling of Copine-6 could easily be accomplished by application of the polyclonal rabbit Copine-6 antiserum. For visualisation, horseradish peroxidase (HRP) is conjugated to the secondary antibody and enzyme activity is demonstrated by diaminobenzidine (DAB) as chromogen and H2O2 as substrate. The enzyme mediated immuno-detection becomes visible owing to the brown polymeric oxidation product, which can be detected by both light and electron microscopy, with the help of heavy metal intensification, in my case OsO4 was used. The DAB product fills the immuno-reactive cell however fine detail is often lost or becomes distorted due to diffusion. To increase resolution silver intensified nanogold particles conjugated to the secondary antibody can be used to detect the bound primary antibody. The nanogold particles remain attached to the primary and secondary antibody complex, and when subjected to silver enhancement grow in size, revealing the specific immuno-reactive sites where the primary antibody is located. The particles are therefore distributed only where the antigen is present within the cell, allowing the morphological features of the labelled neurons to remain fully visible, rather than being compromised by the diffuse heavy labelling as often occurs with the DAB.

All procedures performed were carried out in accordance with the Animals Scientific Procedures Act of 1986 (UK). Every effort was made to minimise the number of animals used. For all immunohistochemical and electron microscopy studies, Sprague–Dawley rats (200-350g; Charles River, Margate, Kent, UK) were deeply anaesthetised using isofluorane (4% in O_2) plus pentobarbitone (200mg/kg; i.p.; Sagatal; Rhône Mérieux, Tallaght, Dublin, Ireland), and transcardially perfused via the ascending aorta using 100mL 0.1M phosphate buffered saline (PBS), followed by 300mL 4 % paraformaldehyde, 0.05 % glutaraldehyde and 0.2% picric acid in 0.1M PB (pH 7.4). Brains were immediately removed and postfixed in 4% paraformaldehyde in 0.1M PB for 24 hours before being sectioned at 70µM intervals in the sagittal plane on a Leica VT1000s vibrating microtome. Sections were collected and washed in 0.1M PB and incubated for 2 hours in 20% sucrose in 0.1M PB. Sections were permeabilised using x2 freeze-thaw cycles, using liquid nitrogen and 20% sucrose, then liquid nitrogen and 0.1M PB. Thawing was carried out once the sections were uniformly white. Sections were then washed x4 10 minutes in 0.1M PB, x1 10 minutes in Tris-buffered saline (TBS), and blocked in 20% normal goat serum in TBS for at least 1 hour. Primary antibody, rabbit Copine-6 antiserum was applied at 1:000 for 48 hours at 4˚c with gentle shaking.

5.2.1. Horseradish Peroxidase (HRP) + 3,3'-Diaminobenzidine (DAB), and Avidin-Biotin Complex (ABC) + 3,3'-Diaminobenzidine (DAB).

Following incubation with primary antibody sections were washed x3 10 minutes in TBS. For the simple HRP-DAB reaction, sections were incubated in secondary antibody, swine anti-rabbit-HRP (Dako, P0217) at 1:100 in TBS for 24 hours at 4˚C with gentle shaking. Sections were washed in Tris-buffer (TB) before continuing with Osmium tetroxide and Uranyl Acetate steps to increase contrast of the specimens for electron microscopy.

For the ‘ABC-DAB’ reaction, sections were incubated in secondary antibody, biotinylated -goat anti-rabbit (Vector Laboratories, BA-1000) at 1:100 in TBS for 24 hours at 4˚C with gentle shaking. Sections were washed x3 10minutes in TBS. 'ABC elite kit' (Vectorstain, Vector Labs) was used. 'AB' was applied at 1:100 in TBS for 24 hours at 4˚c with gentle shaking. Sections were then washed x3 10 minutes in 0.1M TB, before incubation with 0.5mg/mL DAB (Sigma Aldrich, DB001) in TB for 10 minutes in the dark. Peroxidase enzyme activity was visualised with DAB and 0.002% H_2O_2 (in dH_2O from stock) as substrate under the stereoscope to determine reaction time, individually for each experiment. The reaction was stopped using TB and sections were then washed x4 10 minutes in 0.1M PB before continuing with Osmium and Uranyl Acetate contrasting steps.

5.2.2. Silver intensified Gold

Following incubation with the primary antibody, sections were washed x3 10 minutes in TBS. Goat anti-rabbit nanogold (1.4nM) was applied at 1:100 in TBS for 24 hours at 4˚c. Sections were then washed x3 10 minutes in 0.1M PB, followed by x3 10 minute washes in 1x Aurion Enhancement Conditioning Solution diluted in ddH_2O (ECS, Aurion, Netherlands). Sections were then incubated in Silver enhancement reagents (R-Gent SE-EM, Aurion, 500-033) for time determined by each reaction (between 5-20 minutes). Sections were then washed x3 10 minutes in 1x ECS, followed by x3 10 minutes washes in 0.1M PB.

5.2.3. Controls

The antibody specificity of the Copine-6 antibody has been characterised in Chapter 2. For all immunohistochemical reactions, including Copine-6, control test sections were carried out to establish the specificity of the methods. For these controls, the entire set of secondary antibody combinations were applied to sections without any primary antibody to test for background reaction of the secondary antibodies. Application of the entire set of secondary antibodies in the presence of only one of the primary antibodies was used to test for cross reactivity between the different secondary antibodies and the primary antibody. This was carried out when new antibody combinations were being used. Some sections were reacted for calretinin as a positive control but were not processed further.

5.2.4. Postfixation, Uranyl Acetate staining, Dehydration and epoxy resin embedding.

All reactions described continue from this step onward (except for the controls, if they were negative). The sections were all washed x3 10 minutes in 0.1M PB, and incubated in osmium tetroxide solution for postfixation (either 0.5% or 1% in 0.1M PB, depending on amount of HRP endproduct) for 45 minutes at room temperature. Sections were washed x4 10 minutes in 0.1M PB, dehydrated for 10 minutes in 50% ethanol, followed by 10 minutes in 70% ethanol, then incubated in 1% Uranyl Acetate (in 70% ethanol) for 40 minutes at room temperature in the dark. Sections were dehydrated in graded, ascending concentrations of ethanol: they were washed twice in 70% ethanol, then further dehydrated for 10 minutes each in 90%, then 95% ethanol, and twice for 10 minutes in 100% ethanol. Sections were then incubated twice for 10 minutes in propylene oxide and subsequently transferred into epoxy resin. Sections were infiltrated with resin at room temperature for 24 hours, then they were warmed on a hot plate, and carefully placed on microscope slides without bubbles. Greased coverslips were placed over the sections and the resin was polymerised in the oven at 56˚c for 48 hours to ensure polymerisation.

5.2.5. Coating of Copper Grids

Single slot copper grids were coated with a polymer membrane for supporting serial electron microscopic sections. All procedures were carried out in the fume hood. 0.15g of Pioloform (Agar Scientific, R1275) was dissolved in 50mL chloroform (VWR Pro Lab, 22711.324) to make a 0.3% solution and was mixed well until completely dissolved. Copper grids were washed in acetone for 5 minutes. A glass dip-miser was washed in chloroform, and was then filled with the 0.3% Pioloform solution to approximately ¾ the height of a glass slide. A clean (unused) glass slide was then placed into the dip-miser, and the solution drained out of the bottom of the dip-miser. The speed at which the solution is drained affects how thick the membrane will be – slower draining creates thinner film. The slides were stood to dry for 30 seconds before cutting around the film edge with a scalpel blade. The slides were then placed vertically onto a petri dish filled with water, allowing the film to float onto the water by lowering vertically. The thickness of the film was checked at this stage; uniform grey film is an appropriate thickness, any tinge of gold is too thick. Grids were placed shiny side up onto the Pioloform membrane. Parafilm was placed over the grids on membranes, and was promptly picked up ensuring the membrane adhered to the parafilm. Excess moisture was removed and the grids were left to dry for 48 hours prior to use.

5.2.6. Cutting electron microscopic sections and electron microscopy

Following polymerisation, sections were viewed under the light microscope to identify the cells of interest. All cells were documented in the first instance by tracing with a pencil and tracing paper, using a drawing tube connected to a Leitz Dialux 22 microscope. Tissue regions of interest were then cut out of the 70µm thick sections using a scalpel blade, the diameter not exceeding 4mm x 4mm. Selected tissue sections were then re-embedded in resin using flat based tubes to create a block, and were incubated for 2 nights at 56˚c for polymerisation. Resin blocks were hand trimmed using a blade, the block face diameter not exceeding 1mm x 1mm. The block was then sequentially sectioned at 70nM thickness using Leica UltraCut UCT ultramicrotome and a Diatome 45˚ diamond knife. The block face was photographed at regular intervals using a Leitz Dialux 22 microscope connected to a digital camera (Canon D5126171). Ultrathin section ribbons were collected on pioloform-coated copper grids, excess water removed and carefully dried using a hairdryer. The ultrathin sectioning was paused at approximately 3.5µM intervals so that images could be taken of the block face, to ensure full sectioning of the cell in question. Where possible, sections were taken to span the entire cell, so as to include all dendritic arborisations on both sides of the soma in that section

Copper grids holding the sections were then viewed using Philips CM-100 transmission electron microscope.

5.3. Results.

The immunoperoxidase labelling produced a strong Copine-6 signal. Light microscopy showed that the regions, numbers and shape of the immunopositive cells labelled by DAB were identical to those identified previously using fluorescent immunohistochemistry (Chapter 3). There was some (albeit minimal) background nuclear staining in some cells particularly in the cortex and hippocampus. All controls were blank indicating that the background was a result of the primary antibody. The background staining may be real immmunoreactivity but was much weaker compared to the strongly immunopositive cells which contained DAB reaction product throughout the nucleus and cytoplasm. Only these strongly labelled Copine-6 spiny cells in the white matter and some pyramidal cells in the hippocampus were analysed by electron microscopy and the nuclear immmunoreactivity was noted in all cells but was not analysed further.

The immunolabelling for Copine-6 using ABC + DAB was very dark with bright background staining. The interference of this background labelling made it difficult to visualise any individual immuno-positive cells. Therefore the ABC + DAB processed tissue was abandoned, and electron microscopy was conducted only on the tissue labelled by the indirect HRP-conjugated secondary antibody reacted tissue.

5.3.1. Fine structure of the Copine-6 spiny interneurons in the corpus callosum

Regional and structural components of the Copine-6 cells in the white matter of the corpus callosum were strongly stained throughout the soma and processes.

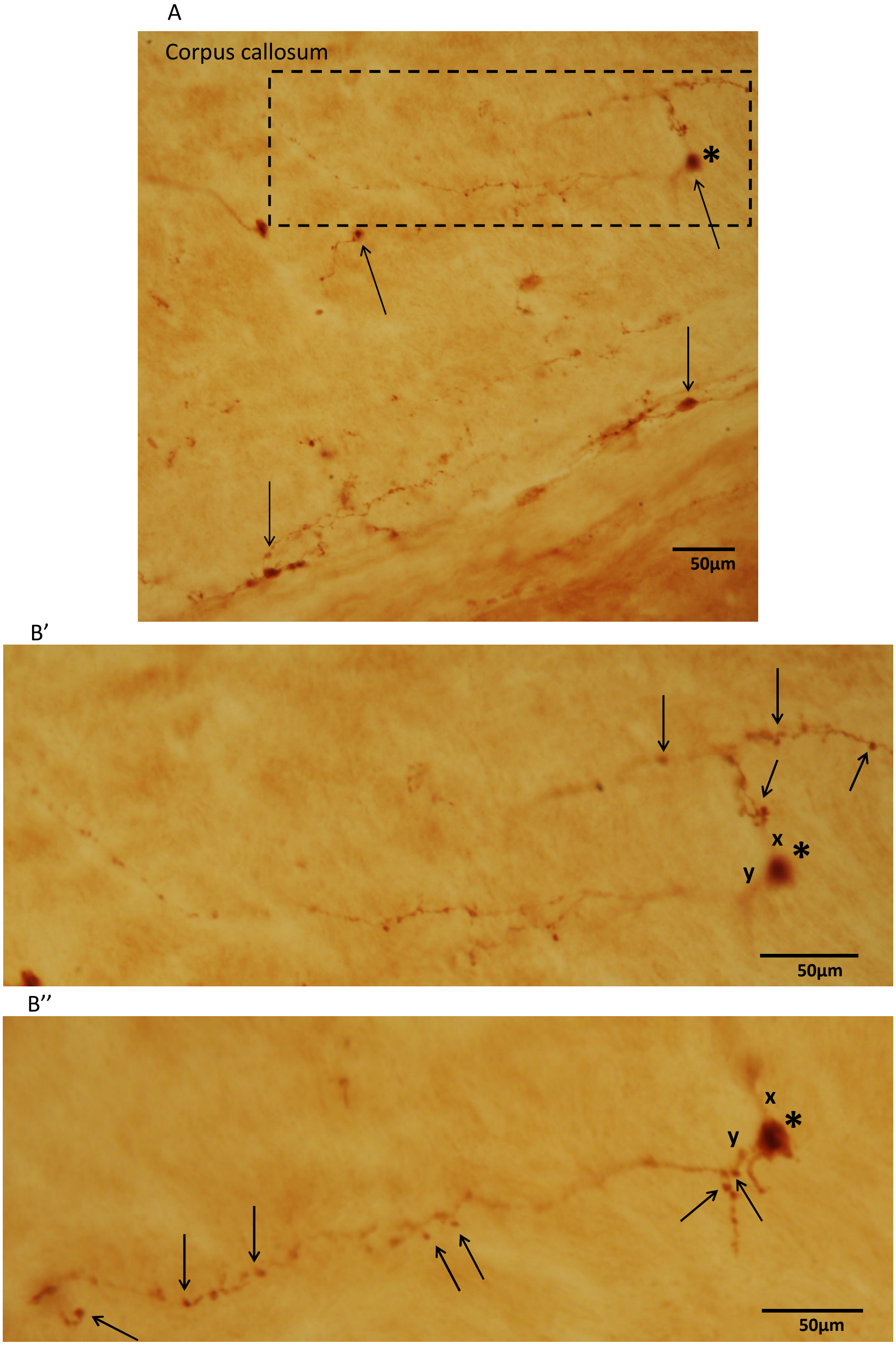

Figure 5-1 Copine-6 labelled cells in the corpus callosum of the adult rat, immunoperoxidase labelling.

A. Multiple Copine-6 immuno-positive soma (arrows) can be seen in the white matter. The cells have extensive dendritic arborisations with spiny protrusions. **B'** and **B''** show the cell outlined in image A at two different focal planes. The soma is labelled *****. The cell has a bipolar morphology, dendrite x visible in Image B', and dendrite y mostly visible in B'' depending on the point of focus. Along the entire length of all the dendrites, spine like protrusions can be seen (arrows).

The small soma, long bipolar dendritic arborisations and small 'spine-like' protrusions with long necks along the membrane of the dendrites are clearly labelled by the HRP reaction product (see Figure 5-1). The cells isolated for examination were all within the white matter in a rostral-caudal direction as described in Chapter 3, following the corpus callosum from the genu (above the striatum), past the lateral ventricle and subventricular zone, to the anterior hippocampal continuation (over and above the hippocampus). Often, multiple Copine-6 reactive cells or their processes could be isolated in the same ~1mm sized block for sectioning, since the cells are so tightly distributed in the white matter.

Ultrathin sections were taken to span the entire cell(s) under investigation wherever possible, therefore ensuring consistent analysis of all dendritic arborisations from each soma. This helped to ensure that no detail was missed. Wherever possible, the dendrites were traced back to a Copine-6 soma. However, often this was not possible, particularly because many of the dendrites were branched over several isolated sections with multiple dendrites from other Copine-6 cells within the selected area of tissue (see Figure 5-2). Therefore to avoid losing any important detail, any visible Copine-6 processes, dendrites or 'spines' within the region of corpus callosum were analysed, so the Copine-6 networks as a whole were investigated even though the soma couldn't always be identified. Furthermore, since no other Copine-6 reactive cell types have been identified in this region, all dendrites could be presumed as belonging to a spiny Copine-6 cell.

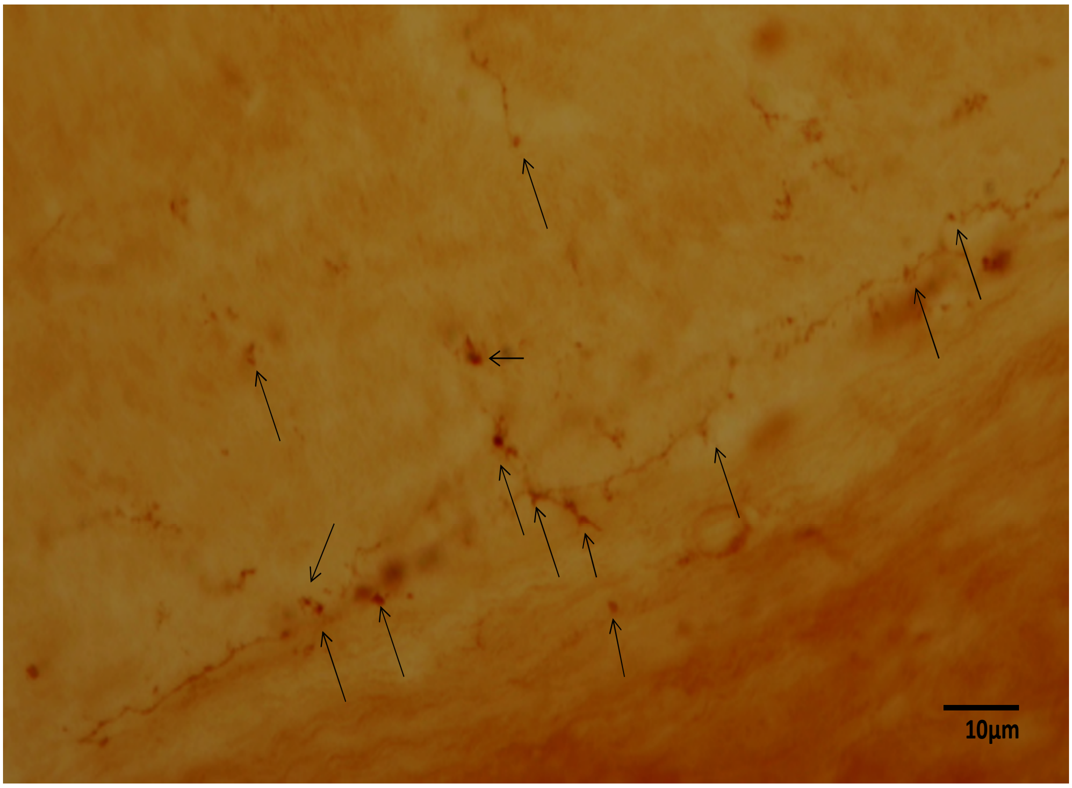

Figure 5-2 A x20 light microscope image demonstrating the abundance of Copine-6 spiny processes in the corpus callosum of the adult rat brain.

The most obvious spines are labelled by the arrows. The spine-like protrusions and processes cannot always be traced back to a particular soma in the same section or block. Since only Copine-6 spiny interneurons were labelled in this region of the white matter, all identified processes were examined.

The immunoperoxidase labelling of the Copine-6 cells in the corpus callosum illustrated a diffuse and widespread labelling throughout the soma, dendrites, and dendritic appendages of the Copine-6 cells. The nucleus of every Copine-6 cell in the white matter was large, and the perikaryon had a small rim of cytoplasm (see Figure 5-3 Image A). The cytoplasm was strongly labelled with DAB and there was also a‘grainy’ DAB labelling in the nucleus. It is not clear if this is artefact due to diffusion of the endproduct from the cytoplasm. The outer plasma membrane of the soma and associated processes were all labelled with the DAB product, and some organelles were visible by their lack of DAB labelling. In most of the cells identified, both the soma and primary dendrite(s) were visible in the same certain ultrathin sections (Figure 5-3 Images B and C).

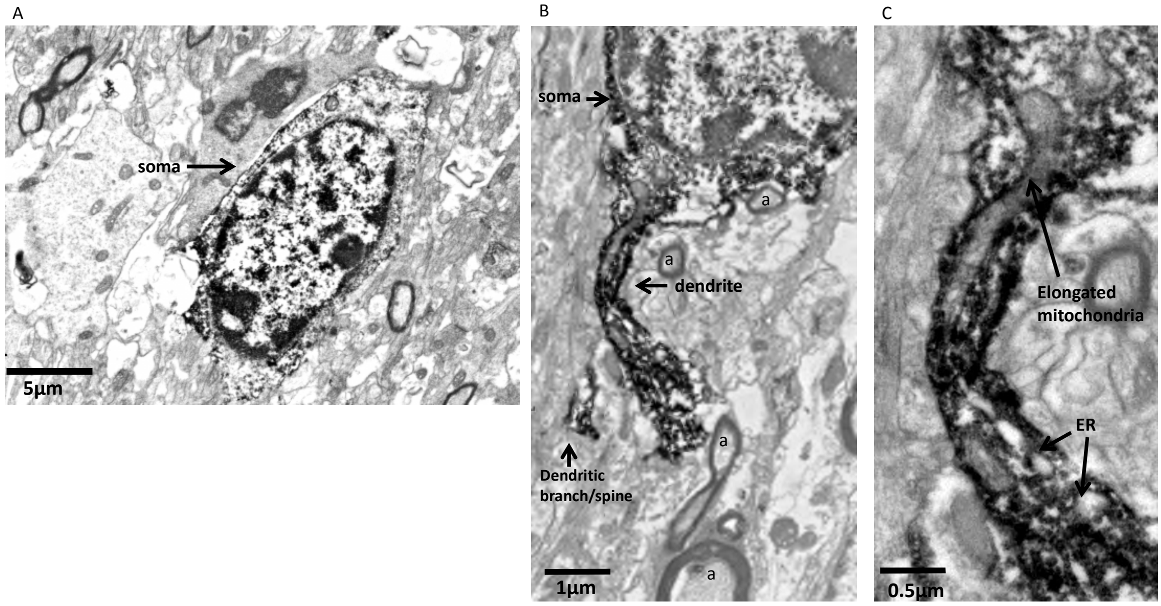

Figure 5-3 Copine-6 spiny interneurons labelled with HRP endproduct.

A. The soma is elongated with a large nucleus. **A+B.** The DAB reaction product labels the plasma membrane, nucleus and cytoplasm **B**. In some sections the dendrite can be seen in continuation with the perikaryon. **C**. Enlarged from image B to illustrate the elongated mitochondria and endoplasmic reticulum visible in the dendritic processes. The cells are located in the corpus callosum and are surrounded by axons (a).

5.3.2. Copine-6 spiny interneurons within the corpus callosum receive dendrodendritic synapses

The processes of the Copine-6 spiny interneurons are architecturally dendritic, as they receive afferent synapses. The cytoplasm is a continuation of the perikarya, typical of dendritic processes, in this case the dendrites are abundant in endoplasmic reticulum and elongated mitochondria (see Figure 5-3), and the presence of postsynaptic junctions on the Copine-6 labelled processes supports this dendritic classification (see Figure 5-5 and Figure 5-7).

Furthermore, there was no evidence of myelination in any of the processes. Indeed, this is in line with the axonless phenotype of these Copine-6 GABAergic spiny interneurons as molecularly defined in Chapter 3, although unmyelinated axon cannot be ruled out. Although the diffusion of the DAB reaction product made it difficult to clearly identify small structures within the Copine-6 dendrites, some endoplasmic reticulum and mitochondria were visible particularly since they were not permeable to the endproduct labelling.

The spine-like appendages of the Copine-6 spiny cells were distributed in a non-uniform manner along the surface of each dendrite (Figure 5-2) , and some dendrites exhibited more appendages than others. Some of the spine-like appendages were individually isolated from the dendrite in the electron microscopic section which made it difficult to trace them back to any particular process or soma when analysing consecutive sections. This is due to sectioning plane of particular spines and their parent dendrites. For this reason, to try to minimise loss of detail, the majority of cells were initially documented using a drawing tube connected to a light microscope so that the full arborisation of each cell and its processes could be observed by scanning through all possible focal planes in each section prior to resin embedding (for an example of such a trace, see Figure 5-4). Electron microscopic scanning through several of the ultrathin sections was subsequently carried out to follow the multiple spines, and these were then traced back to the processes or soma of interest based on the original hand traced drawing, wherever possible.

There was no evidence of myelination in the ‘spine like’ appendages, and their apparent continuation of the dendritic membrane suggests that they are dendritic spines. Several of the spine-like appendages were laden with vesicles (Figure 5-6, Figure 5-7 A1-2), and some showed evidence of receiving a synapse thus being postsynaptic (Figure 5-5, Figure 5-7). This included those that were and were not themselves vesicle laden. A dense post synaptic density in the Copine-6 process was visible in all cases, opposite a presynaptic bouton with vesicular accumulation. The dense postsynaptic density is typical of an asymmetric or type I synapse.

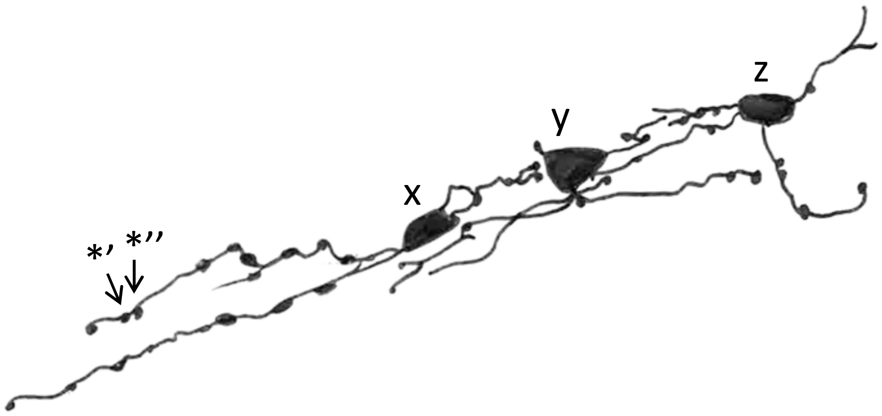

Figure 5-4 Three Copine-6 spiny interneurons in the corpus callosum.

The cells were hand traced using a light microscope at x40 magnification, scanning through all focal planes of the 70µm thick section. By this method the majority of processes could be seen to be associated with a particular soma. Any spines isolated by subsequent electron microscopic sectioning (such as *’ and *’’, which belong to soma X) could therefore be traced in the resin block after sectioning. Cells x and y were isolated for analysis Figure 5-5 A)

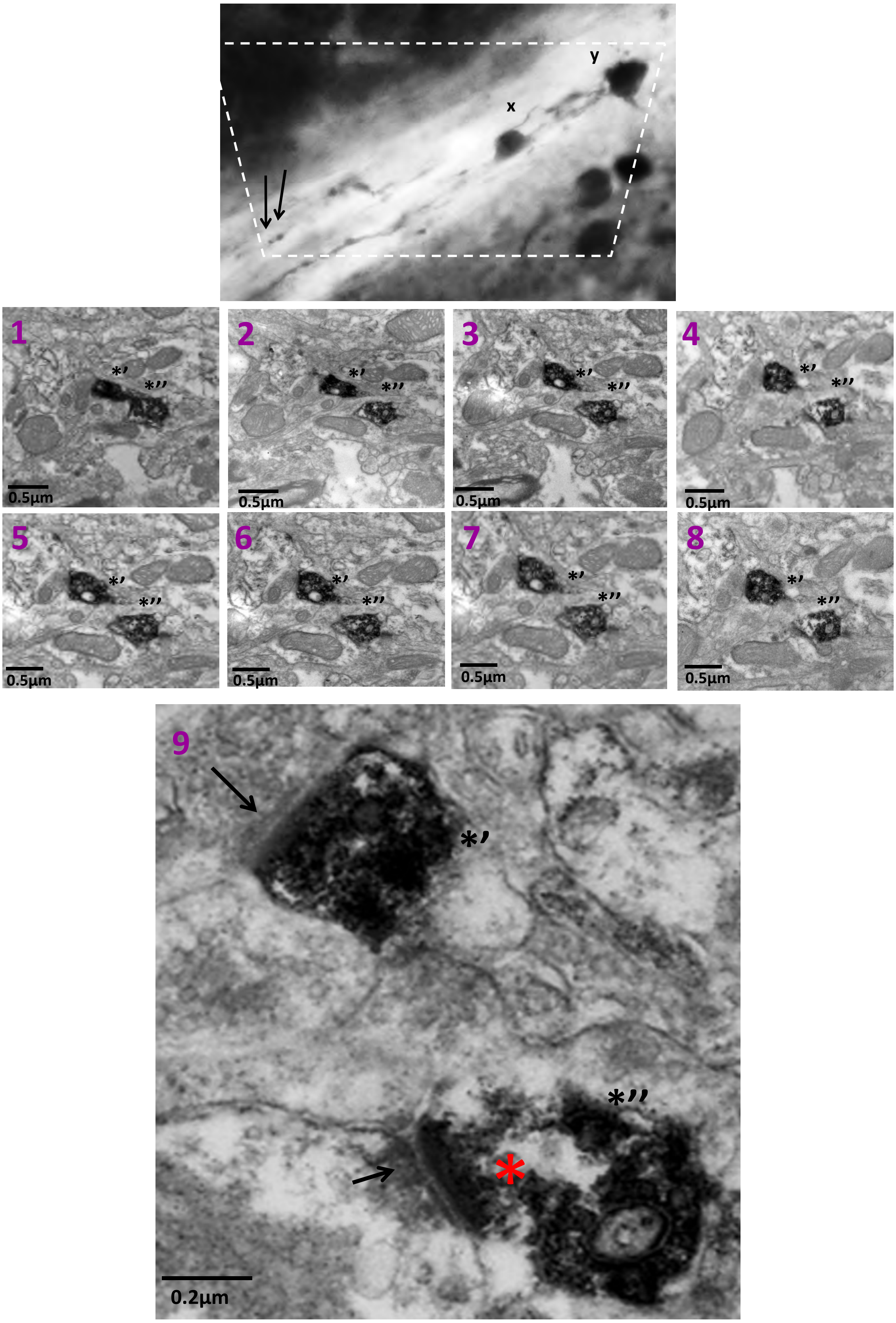

Figure 5-5 Ultrastructural analysis of two Copine-6 spiny appendages.

(Fig 5-5) A. Two Copine-6 soma and their associated processes and spines were identified using the light microscope (soma X and Y, and spines *’ and *’’). The block was cut as shown by the dotted white line. Ultrathin sections were taken spanning the entire thickness of each soma. **B.** The spines (*’ and *’’) were traced through consecutive sections and were structurally analysed. Ten ultrathin consecutive sections are shown (+/- 2-3 sections in between). **B1** shows the dendritic connection between the two spines. **B9** shows both spines as postsynaptic targets. Spine *' is postsynaptic to a Copine-negative presynaptic terminal (arrow, B.9). Spine *'' has an invaginated protrusion from another cell (asterisk*****), which was followed in serial sections. This spine is postsynaptic to a presynaptic terminal (arrow) but synaptic relationship with the invaginated process could not be established.

Within some (but not all) of these dendritic appendages, a large number of vesicles was present (see Figure 5-6 and Figure 5-7 Image A2). The interior of the vesicles lacked DAB reaction product and were between 0.03-0.06µm (30-60nm). The vesicles are translucent within the DAB reaction product. Not all Copine-6 spines could be shown to contain vesicles which may be due to overlying reaction product. No obvious vesicular clustering or docking – which would be typical of a presynaptic terminal – could be seen, although a presynaptic function of these cells cannot be ruled out.

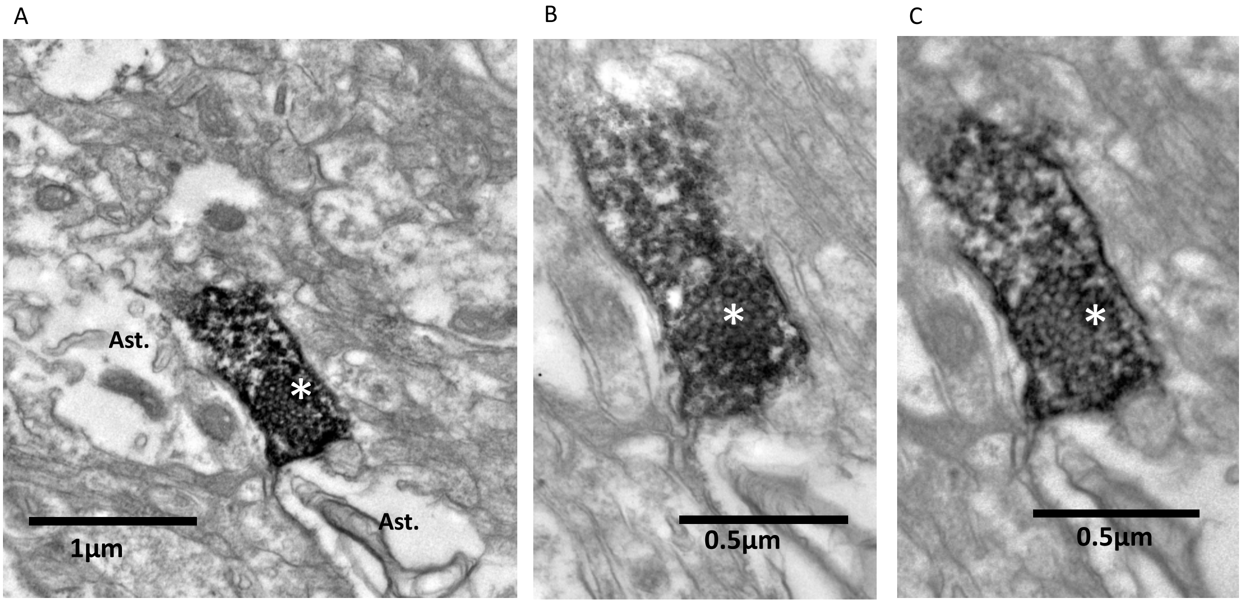

<u>Figure 5-6 A typical Copine-6 labelled vesicle-filled spine-like appendage.</u>

A. This process is isolated from any immediate dendrites in the ultrathin sections, typical of many of the spiny Copine-6 processes identified. The process is vesicle laden (*). **B** and **C** are enlarged micrographs of the same process in sections before and after Image A, respectively. The accumulation of vesicles within the appendage (*) is consistent throughout consecutive ultrathin sections. No obvious post synaptic cell could be identified in this example.

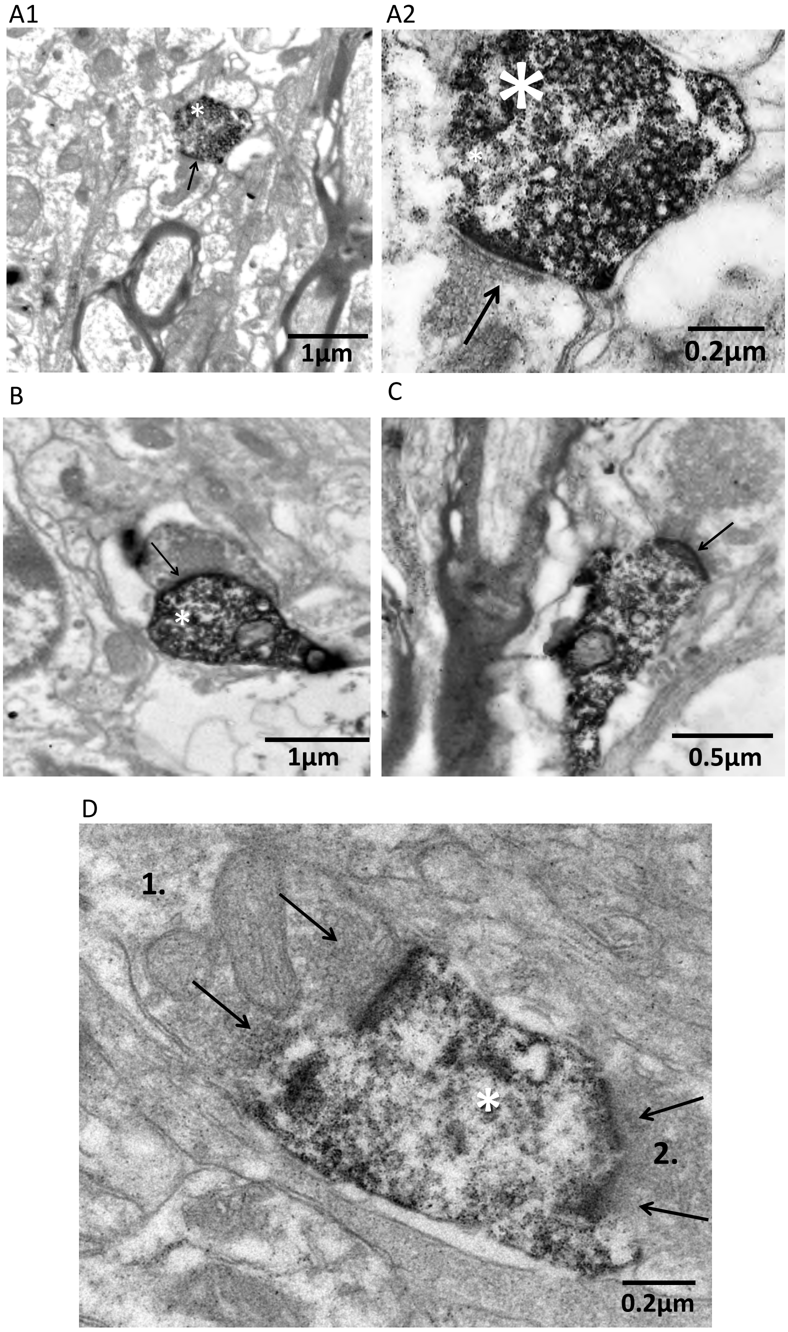

Figure 5-7 Postsynaptic Copine-6 processes.

A1. A vesicle laden Copine-6 spine (*) *receives* a synapse from a presynaptic terminal in the rostral corpus callosum. **A2**. Enlarged consecutive section of the vesicle laden spine. The arrow shows the direction of the synapse and (*) shows the vesicle accumulation in the Copine-6 immunopositive process. No postsynaptic cell could be identified that may be receiving a synapse from this Copine-6 spine despite the presence of vesicles. **B**. + **C**. Two additional examples of Copine-6 dendritic processes (*) receiving a synapse (arrow) from Copine-6 immunonegative presynaptic terminals in the white matter. **D**. A postsynaptic Copine-6 labelled process receiving four synapses from two separate processes (1. and 2.). In all cases, vesicular accumulation can be seen in the presynaptic process (arrows) and postsynaptic densities can be seen on the membrane of the Copine process (*).

Interestingly, only two putative cases of presynaptic Copine-6 reactive terminals in the corpus callosum were identified out of some 15+ vesicle laden appendages examined. One of these examples are documented here (Figure 5-8). Although the presynaptic processes could be traced to a soma and appeared to stem from a primary dendrite, it is not clear at this stage if they are indeed dendritic (and thus would form dendro-dendritic synapse), or if they are unmyelinated axon. I cannot exclude that reaction product had diffused into the bouton from nearby Copine-6 positive processes. Furthermore, both of the putative presynaptic Copine-6 boutons appear to be forming a synapse with a postsynaptic Copine – 6 positive terminal. There may be reciprocal synaptic connections between Copine-6 spiny interneurons through dendro-dendritic synapses, but testing this hypothesis requires better material for electron microscopy.

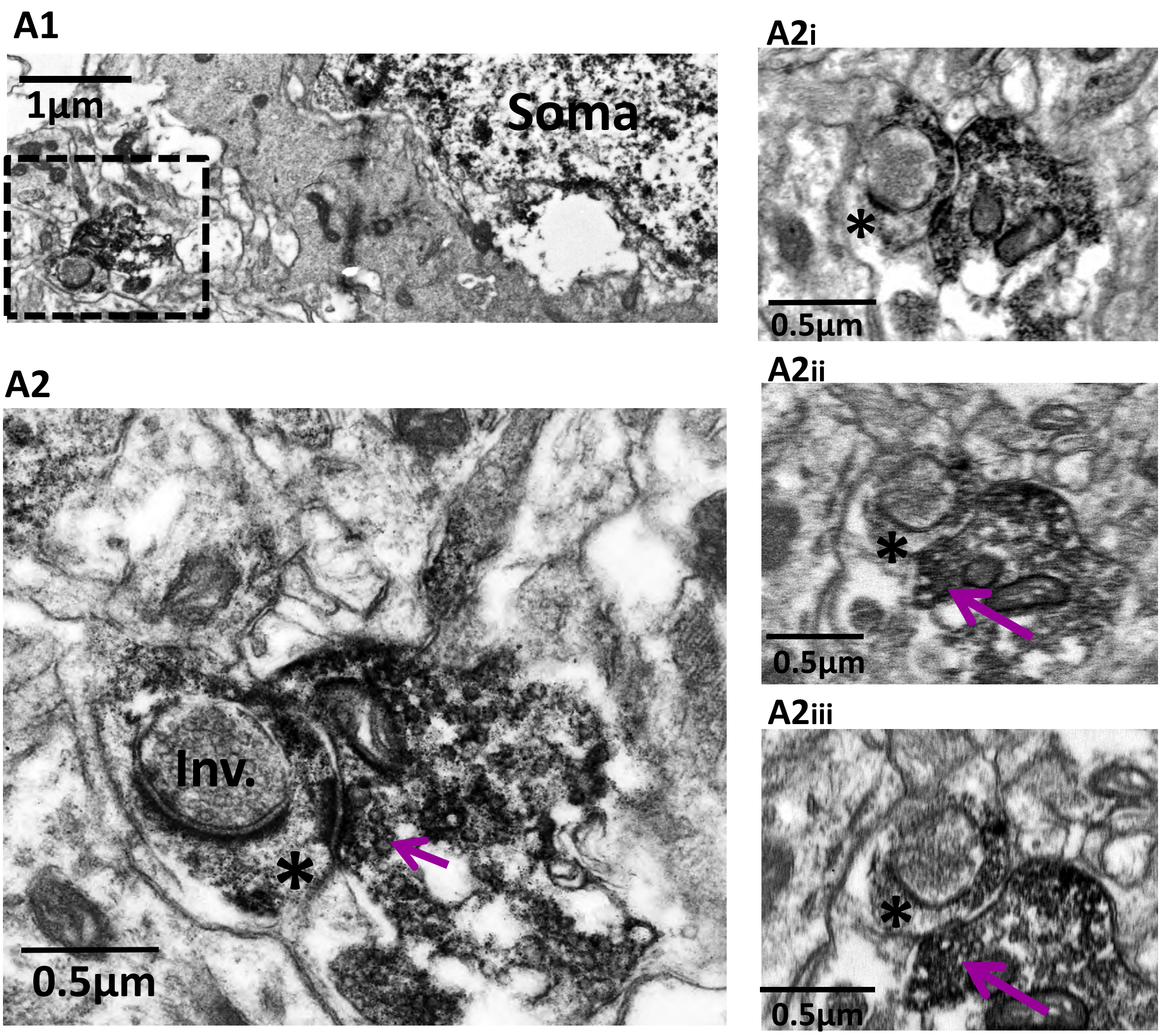

Figure 5-8 An example of putative Copine-6 presynaptic terminals.

A1. A putative pre- and post-synaptic Copine-6 process (boxed) which was traced back to the Copine-6 soma. The dotted box outlines the bouton analysed in subsequent images. **A2.** Enlarged image of the boxed Copine-6 process in A1. The arrow indicates the Copine-6 labelled process with a vesicular accumulation which appears to be presynaptic to a postsynaptic Copine-6 reactive terminal (*). It is not clear if the Copine-6 staining of the postsynaptic process is true labelling or whether it is due to diffusion of the labelling product. An invagination of the membrane (Inv.) also shows that this process might receive another synapse but this could not be traced back because of the plane of sectioning. **A2i-iii**. The consecutive sections demonstrate that the synapse can be seen to be consistent over several sections. The invagination (inv.) of the postsynaptic terminal membrane can be seen in all sections. A vesicular accumulation can also be seen in the invagination.

Although ultrathin continuous sections were examined in both cases where Copine-6 presynaptic terminals were suspected, I have not reached a conclusion and more examples need to be examined. The uncertainty of whether or not Copine-6 spiny cells are presynaptic may be, in part, due to the plane of sectioning (for example if the post synaptic cell or synaptic junction is above the plane at which the cell was sectioned). Furthermore, in the two examples presented, it is not clear if the reaction product in the 'presynaptic' element is due to diffusion from the 'postsynaptic' element. No presynaptic Copine-6 boutons were identified to be targeting a Copine-6 *negative* process, which supports the diffusion hypothesis. In order to investigate whether Copine-6 has a pre- or post-synaptic localisation, immunoreactivity was analysed by electron microscopy in the pyramidal cell of the hippocampus CA3 region. Preliminary results using silver intensified particle labelling is suggestive that Copine-6 can be both pre- and post-synaptic (Figure 5-12). Better material needs to be analysed before these observations can be concluded.

5.3.3. Intracellular localisation of Copine-6 protein using silver intensified nanogold particle labelling

The diffuse labelling by the DAB reaction product does not allow for the exact intracellular location of the Copine-6 protein to be established. Therefore, the silver intensified gold nanoparticle method was employed so that the intracellular structure of the neuron is preserved (i.e. not covered by precipitate), and the intracellular structures can be visualised alongside a particle antibody labelling. In these experiments, the 1.4nM nanogold particle gave good labelling, and the generated silver particle size was sufficient enough to allow identification of cellular structures without obscuring their appearance, at the same time as labelling the immunopositive regions sufficiently enough for them to be recognised.

By light microscopy, the silver intensified gold staining of the Copine-6 immunopositive cells in all locations was much weaker than the DAB labelling, as would be expected since the entire cell is not filled by the metals. Pyramidal cells of the CA3 region of the hippocampus were labelled more strongly than the spiny Copine-6 interneurons in the white matter. Cells taken for examination were isolated from the corpus callosum and from CA3 region of the hippocampus (see Figure 5-9 A and B respectively).

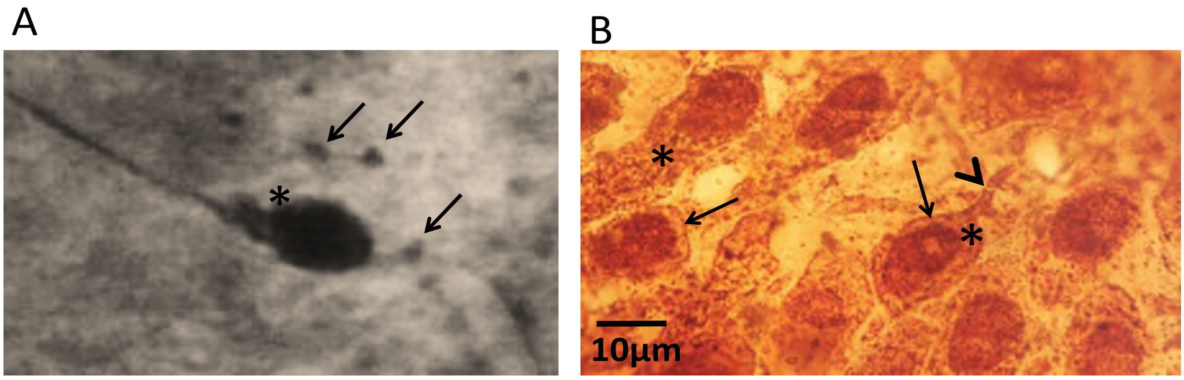

Figure 5-9 Silver intensified gold nanoparticle labelling of Copine-6.

A. A Copine-6 labelled spiny interneuron in the white matter of the corpus callosum. The nanoparticle labelling is quite weak but the soma (*), processes and spines (arrows) are visible. **B**. Copine-6 immunoreactive cells in the pyramidal cell layer of the CA3 region of the hippocampus. There is strong nuclear staining in these cells. Some of the cells have cytoplasmic labelling (*), and localised plasma membrane labelling (arrows). The arrowhead points towards the labelling of a pyramidal cell process. Image B is a stack of 4 planes of focus which were combined using extended focus autoblend (Photoshop) to eliminate inaccuracies.

When viewed by the electron microscope, the silver intensified nanoparticles were present in the soma and processes. They were considered to be immunopositive if they contained 4 or more nanoparticles which were seen consistently over four or more serial sections. Immunonegative cells contained none, or fewer than 2 nanoparticles that were not continuous over serial sections. All controls were blank.

The intracellular location of Copine-6 was the same in all neurons examined. In neurons of both the corpus callosum and the hippocampus, nanogold particles accumulated along the plasma membrane of the soma and dendrites. In most cases, the particles could be seen surrounding the majority of the inner plasma membrane (Figure 5-10).

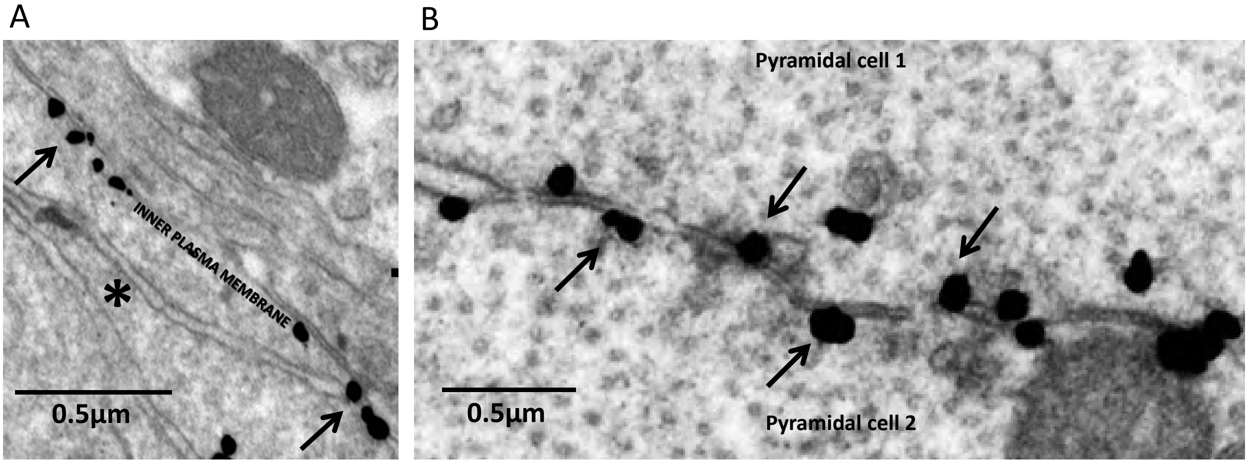

Figure 5-10 Copine-6 protein is localised to the inner face of the plasma membrane in neurons.

In all neurons examined, nanoparticle labelling of Copine-6 was lined along the inner face of the plasma membrane. **A**. The membrane labelling of a spiny Copine-6 immunopositive interneuron (*) in the corpus callosum. The nanogold particles accumulate along the membrane edge (arrows). **B**. Two aligned pyramidal cells of the CA3 region of the hippocampus, both with nanoparticle labelling on the inner face of the membrane of each soma.

In addition to somatic and dendritic plasma membrane labelling by the nanogold particles, Copine-6 was also identified on certain intracellular organelles. Consistently, nanoparticles labelled Copine-6 on the outer membrane of the endoplasmic reticulum, and also surrounding multivesicular bodies (MVBs) (see Figure 5-11). Again, this was true of all Copine-6 reactive neurons examined in the white matter and the hippocampal CA3 pyramidal cells which suggests that Copine-6 is located in the same regions of all types of neuron analysed.

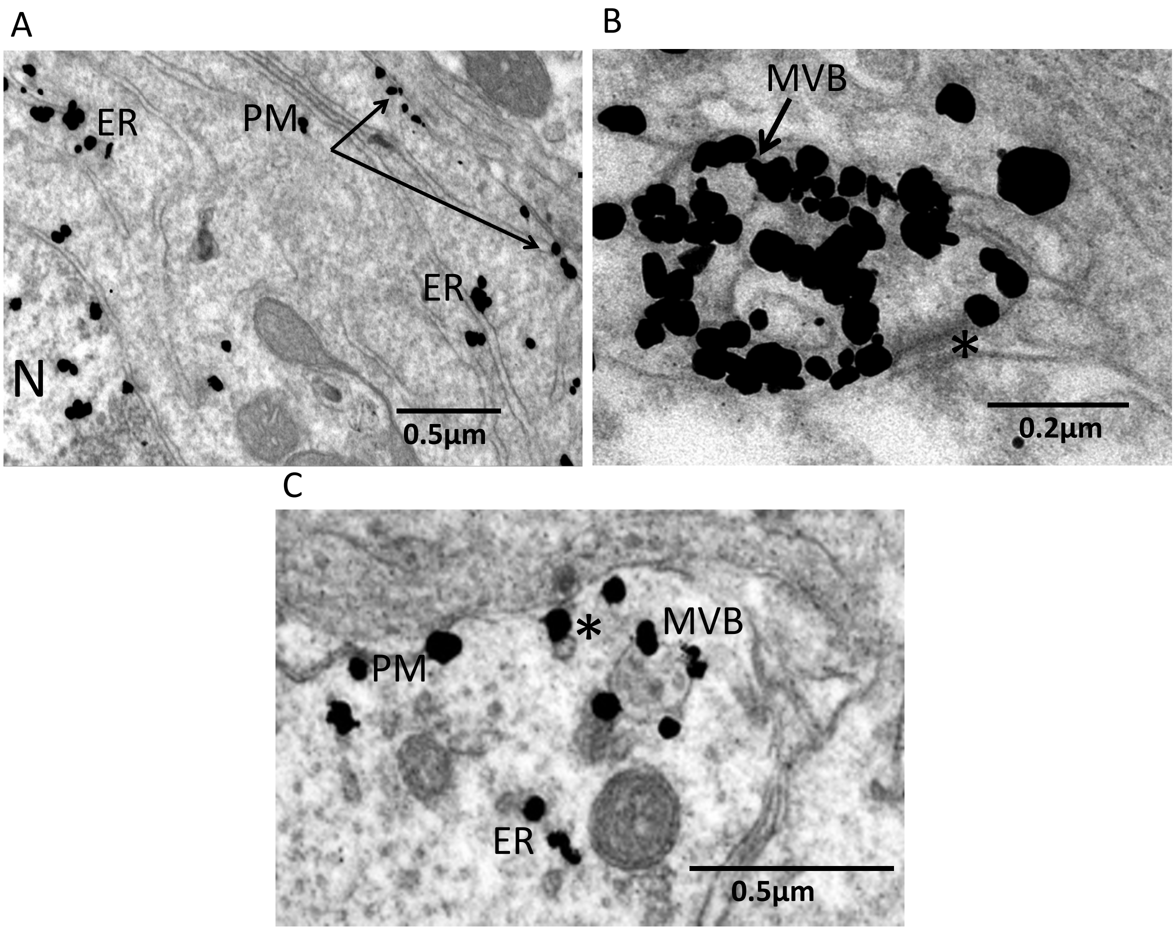

Figure 5-11 Copine-6 protein is localised to the ER and multivesicular bodies in neurons.

A. The soma of a spiny Copine-6 interneuron in the corpus callosum. Nanoparticle labelling can be seen along inner plasma membrane (PM) and the outer membrane of the endoplasmic reticulum (ER). The nucleus (N) shows nanoparticle labelling which may be an artefact. **B**. A spine of a Copine-6 interneuron in the corpus callosum which has strong nanoparticle labelling throughout. The arrow points to a multivesicular body which is surrounded by nanoparticles. Other structures in the spine are obscured by the particle staining. The spine appears to form a junction with a Copine-6 negative process (*), and the lack of vesicles in either of the processes points towards this being an adherens junction. **C**. A multivesicular body labelled by Copine-6 in a pyramidal cell of the CA3 region of the hippocampus. In this example, there is also an extension of the Copine-6 particle labelling to a vesicular structure which may be a fusing or budding membrane vesicle (*). Further analysis of such structures and more examples would be required before conclusions can be drawn.

B.

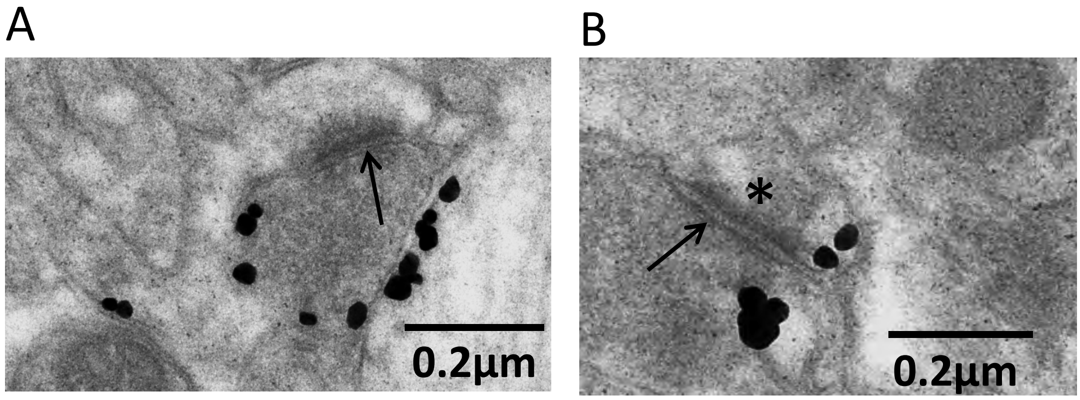

Figure 5-12 Preliminary evidence for pre- and post- synaptic Copine-6 labelling in CA3 pyramidal neurons in the hippocampus.

A. A presynaptic terminal with Copine-6 particle labelling in the pyramidal cell layer of the CA3 region of the hippocampus, forming a synapse (arrow) with a Copine-6 immunonegative process. **B**. An example of a postsynaptic Copine-6 process(*). The particle labelling in the presynaptic structure cannot be concluded as being Copine-6 immuno-positive since the labelling may be of the neighbouring process. The pre and post synaptic processes contained at least 2 gold particles per ultrathin section over 2-3 sections. Better material needs to be examined and this is a preliminary observation.

5.4. Discussion

5.4.1. Synaptic relationship of the Copine-6 spiny interneurons in the corpus callosum

Electron microscopic analysis of the architecture of the Copine-6 interneurons in the corpus callosum supports the immunohistochemical finding, as previously described in Chapter 3, that these are a population of axonless neurons. The bipolar processes emanating from the Copine-6 soma have here been considered to be architecturally dendritic and this would suggest that a novel subpopulation of interneuron has been identified which have not yet been described in the literature. Although these axonless cells in the white matter are likely to differ to the *uni*polar axonless neurons described by Monyer and collegues based on the number of processes alone, the possibility of some overlap cannot be ruled out at this stage (Le Magueresse *et al.*, 2011).

The fine structural analysis of the Copine-6 spiny interneurons shows that some of the Copine-6 spines contain numerous vesicles, which is consistent with the VGAT and enkephalin immunoreactivity identified in some of the appendages in Chapter 3. However, despite their ‘vesicle laden’ appearance, I have not found conclusive evidence that these spines are presynaptic to a postsynaptic cell. Only two putative presynaptic Copine-6 processes were found over the course of this study, both of which appeared to be in contact with a Copine-6 immunoreactive process. Although this could point towards the Copine-6 neurons communicating amongst themselves, they receive afferent synapses and therefore communicate with other neurons as recipients, therefore more analysis is required before a presynaptic function of these spiny interneurons is either confirmed or ruled out. It is acknowledged historically that the presence of vesicles within a spine is not sufficient evidence that they form a synapse (Pinching *et al*, 1971a, 1971b). However, the maintenance and accumulation of such a large number of vesicles in a specific location would entail a large energy demand, and suggests that this is a specialised region in these cells. It may also be possible that the Copine-6 spiny interneurons are forming a symmetrical (Gray's type II) synapse – particularly since they have a GABAergic phenotype – in which case it could be that the postsynaptic density of the receiving neuron is very small and difficult to distinguish in the sections of immunoreacted material (Colonnier, 1968). Or, in the knowledge that some of the Copine-6 spines are immunoreactive for enkephalin, it would be plausible to suggest at this stage that the vesicles and the contents are perhaps released in a nonsynaptic manner, in which case no true synaptic architecture would be visible. In order to investigate a role such as peptidergic signalling, more immunohistochemical analysis at the level of the electron microscope using double labelling for enkephalin and Copine-6, for example, would be required, and the vesicles themselves would require more detailed analysis.

Many Copine-6 spiny processes in the corpus callosum were identified as postsynaptic to unidentified presynaptic, most likely, axonal boutons. There is no doubt, therefore, that these cells are integrated into neuronal networks certainly by input. All of the identified postsynaptic Copine-6 processes had a large postsynaptic density, and there was always a well-defined accumulation of vesicles in the presynaptic terminal which indicates an asymmetrical, presumably glutamatergic, synapse onto the Copine-6 spiny interneuron population. The identification that the Copine-6 immunoreactive spine-like protrusions receive afferent synapses would indicate that these structures are architecturally dendritic. Yet the presence of vesicles in some of these varicosities, if synaptically functional, might also point towards them being an axonal profile (although the receiving of afferent synapses, despite the presence of vesicles, would strongly suggest otherwise). In the olfactory bulb, a very similar type of neuron exists, the olfactory granule cell, which exhibit reciprocal dendro-dendritic synapses between the spiny gemmules and mitral cells (Rall *et al.*, 1966) As in the case of the olfactory granule cell, the Copine-6 spiny cells might be able to form a dendro-dendritic synapse, however based on the current architectural analysis of the Copine-6 spiny cells, I cannot yet conclude their exact synaptic relationship. Dendro-dendritic synapses have been identified in the deep layers of the motor cortex, and the processes of these cells are documented to receive some ~15 synapses but make no more than 2 synapses onto neighbouring dendrites (Sloper & Powell, 1978). It could be the case, then, that a presynaptic Copine-6 spiny cell process has not been identified yet simply because they are low in number.

In the cells of the motor cortex and the granule cells of the olfactory bulb that form dendro-dendritic synapses, the vesicular accumulations are described to be few in number and the vesicles are restricted to the region of the synaptic membrane (Rall *et al.*, 1966; Sloper & Powell, 1978). This is very different to the vesicle laden appearance of the Copine-6 spiny neurons which do not appear to have a restricted vesicular accumulation at all, and rather exhibit a large number of vesicles *throughout* the cytoplasm. Again, investigation into the vesicles themselves – and their contents – is required which may assist in the analysis of the Copine-6 spiny interneurons synaptic behaviour.

In pyramidal cells of the CA3 region of the hippocampus, I document some preliminary evidence that Copine-6 may not have a restricted localisation to only pre- or post-synaptic structures. Furthermore, a large number of pyramidal cells in the CA3 are immunoreactive for Copine-6, which is apparently localised to the plasma membrane. These glutamatergic neurons also exhibit axons which may suggest that Copine-6 expression is not restricted to dendritic synapses. Interestingly, Copine-6 labelling throughout the entire hippocampus shows a ‘layered’ expression pattern(see Chapter 3, Section 3.3.1.4), which may point towards a specific pre- or post-synaptic expression of the Copine-6 protein in these different hippocampal regions. Furthermore, this layered expression pattern may be a reflection of the input or output to each region of the hippocampus, therefore more electron microscopic analysis would be required to observe the Copine-6 localisation in each layer.

5.4.2. Intracellular location of Copine-6 in neurons

In order to observe the intracellular location of the Copine-6 protein in neurons of the rat brain, cells of the CA3 region of the hippocampus and the Copine-6 spiny interneurons in the corpus callosum were examined using silver intensified gold nanoparticle labelling. In every neuron examined, Copine-6 was found lining the inner face of the plasma membrane, the outer face of the membrane of the endoplasmic reticulum, and surrounding the outer membrane of multi-vesicular bodies.

The location of the Copine-6 protein at the plasma membrane in the neurons suggests that the protein is bound to the membrane in a normal physiological state (i.e. in the absence of experimental intervention). Therefore, the intracellular calcium levels within neurons – which are constantly active as part of synaptic networks – are high enough to keep the Copine-6 at the plasma membrane. This is true for both the hippocampal pyramidal cells, and for the spiny interneurons in the corpus callosum. Since the neurons analysed were not subjected to experimental manipulation it is difficult to ascertain whether or not the Copine-6 protein remains bound to the plasma membrane at all times, or whether the protein translocates to the membrane following fluctuations in intracellular calcium. To date, the lipid binding properties of the Copines have only been explored in *in vitro* studies using lipid vesicles (Creutz *et al.*, 1998; Nakayama, Yaoi, & Kuwajima, 1999; Tomsig & Creutz, 2000a; Damer *et al.*, 2005), and more recently the calcium dependent translocation of Copines to the plasma membrane was shown *in vitro* using human embryonic kidney cells (HEK-293) (Perestenko *et al.*, 2010). In experiments on neurons in culture, Copine-6 has also been found adjacent to the plasma membrane, but when the cells are treated with antagonists of the NMDA receptor the protein becomes predominantly cytosolic, suggesting that it is neuronal activity that maintains its association with the membrane (unpublished, McIlhinney and Perestenko, personal communication). This suggests that since neurons are chemically and electrically active, the intracellular calcium concentrations are high enough to keep Copine at the inner surface of the membrane at all times. It is clear from the electron microscopic intracellular analysis of Copine-6 that in all neurons examined, Copine-6 is associated with the inner surface of the plasma membrane.

A rather striking Copine-6 nanoparticle labelling was seen surrounding the membrane of multivesicular bodies (MVBs), in soma and dendrites of all neurons. Multivesicular bodies were first described by Palay and Palade in 1955 as spherical, single membrane bound organelles containing multiple spherical or ellipsoidal vesicles (Peters *et al.*, 1991. pg 33), and MVBs have since been associated with endosomal membrane recycling and lysosomal degradation behaviour in dendrites and spines (for reviews see Spacek *et al*, 1997; Kennedy *et al*, 2011). Copine-6 nanoparticle labelling occurs predominantly on the outer face of the MVB membrane, which is topologically equivalent to the inner plasma membrane and indicates that similar lipid interactions may be occurring. The location of Copine-6 on the membrane of the MVB may, however, point towards a role of Copine-6 protein in membrane recycling. However it may be that Copine-6 protein itself may be subjected to membrane recycling.

Nanogold particle labelling of Copine-6 was also seen on the endoplasmic reticulum in all neuronal soma and dendrites examined. It appears that Copine-6 is preferentially associated with the smooth endoplasmic reticulum, which may implicate Copine-6 in membrane biosynthesis or trafficking. The smooth endoplasmic reticulum is associated with and often seen partnered with other intracellular organelles such as the Golgi apparatus and multivesicular bodies (Spacek *et al*, 1997; Kennedy *et al*, 2011), with a role in lipid biosynthesis and trafficking. All of these organelles are involved in the transfer and export of membrane associated components, therefore the presence of Copine-6 on each could indicate that it functions in this process.

In conclusion, the intracellular location of Copine-6 within neurons is shown here to be specific to the ER, multivesicular bodies and on the inner face of the plasma membrane. It cannot be excluded that the cytoplasmic Copine-6 appears to be associated with these organelles as a result of the fixation process, although the replicable localisation of the nanoparticles with the inner most plasma membrane and the outer membrane of the same specific organelles, and not with others such as mitochondrion, would suggest that this is a suggestive location for the Copine-6 protein. This is true for all neurons examined in this study and these intracellular locations may implicate Copine-6 in processes such as membrane biosynthesis or trafficking. Static electron micrographs, although a reliable indicator of protein location, need to be complimented with further investigations such as live imaging of cell trafficking processes, for example, before the function of Copine-6 in neurons can be concluded.

Chapter 6. **General Discussion**

The experiments examined in this thesis were conducted to investigate the general expression of the neuron-specific calcium-dependent phospholipid-binding protein, Copine-6, in the brain of rodents with the intention of searching for functional properties of the protein. Using the antibody to Copine-6 characterised here, I showed that Copine-6 expression is restricted to specific subpopulations of neurons in the neocortex, olfactory bulb, hippocampus and corpus callosum and dorsal striatum. Each of these cell populations were successfully characterised, based on molecular phenotypes already in use in the literature for neuronal identification. Although all of the Copine-6 labelled cell populations were analysed to some degree, the thesis focusses on an embryonically generated interneuron subpopulation labelled by Copine-6 in the corpus callosum. Despite molecular similarities between it and certain olfactory interneurons, the unusual location of the 'spiny' Copine-6 labelled interneurons within the white matter running in both a rostral and caudal direction means it is unlikely that these cells belong to an already recognised neuronal population, one moreover that arises early in development and persists throughout adulthood. It has been identified that the spiny Copine-6 interneurons are likely to be axonless as defined both by their lack of Ankyrin –G and the inability to find an axon profile in electron micrographs, and this is suggestive of their ability to form dendro-dendritic synapses, which would be the first to be identified in the corpus callosum, should their vesicular accumulations be of synaptic significance. This thesis therefore documents the discovery of a novel molecular marker for unique neuron subpopulations in different regions of the brain, and reports the discovery of a novel axonless neuron population labelled by Copine-6 in the corpus callosum.

The close proximity of the identified axonless interneurons to the subventricular zone and the 'tunnel-like' distribution surrounding the rostral migratory stream might indicate that other cells such as migrating or immature neuroblasts are influenced by this neuronal population. Indeed, the discovery that the Copine-6 cell spine-like protrusions are often vesicle laden and can contain GABA and also enkephalin supports the hypothesis that these cells certainly contain – and are likely to release – transmitter substances. However, the inability to find a synapse (despite the abundance of the Copine-6 ‘spines’ found to *receive* a synapse as recipients) suggests that either these cells form very few – and yet to be identified –putative dendro-dendritic synapses onto other neurons, or they do not form synapses at all and instead release their vesicular contents in a non-synaptic manner. Interestingly, it is shown that neuroblasts in the SVZ and RMS release GABA in a non-synaptic, non-vesicular manner, in order to control neurogenesis and the proliferation of GFAP-expressing cells (Wang *et al.*, 2003; Kriegstein, 2005; Liu *et al.*, 2005), therefore it would be plausible to consider that other (more mature) cells are able to retain the ability to release GABA in these locations by similar non-synaptic mechanisms. Although the mechanism by which GABA is released by the neuroblasts is not known (reviewed in Kriegstein, 2005), whether or not the Copine-6 cells actually release their stored GABA (or enkephalin) certainly requires further investigation. Basic electrophysiological properties of the Copine-6 spiny cells might give some insight into such behaviour which would be achievable by whole cell patch clamp techniques. Another possible situation in which a structural synapse would be absent is if the cells release their transmitter by volume transmission. Considered to be a large distance signalling with minimal spatial constraint in dopaminergic neurons in the striatum (Zoli *et al.*, 1999), volume transmission can be categorised into ‘open synapses’ i.e. those with a functional synapse with functional spillover of transmitter for long distance signalling, and ‘non-junctional varicosities’ in which there is a spatial mismatch between the release site and the targeted receptors. Although more analysis is required into the signalling mechanisms of the Copine-6 spiny cells, there is a possibility that these cells might release transmitter substances in such an extra-synaptic manner.

During the course of this thesis, I conducted some electrophysiological studies in collaboration with Dr. Karri Lamsa (Department of Pharmacology, University of Oxford). The spiny Copine-6 interneurons in the corpus callosum were investigated by patch clamping techniques on brain slices, however owing to the heavy content of myelin within the white matter this proved experimentally difficult and no data was achieved. The cells were initially difficult to find (without any prior labelling), and the white matter itself caused technical problems with the electrodes. Instead, the spiny Copine-6 cells in the olfactory bulb/RMS cultures were investigated by whole cell patch clamp, and although this has been excluded from this thesis owing to the small number of recordings, this on-going project may give some insight into the physiological properties of the Copine-6 spiny interneurons. In order to overcome the difficulties in recording from brain slices, transgenic animals could be produced in which GFP is expressed using the Copine-6 promoter. This would allow for visualisation of the cells in different brain slices for subsequent electrophysiological characterisation.

The studies presented here on the localisation and ultrastructural analysis of the Copine-6 cells in the corpus callosum suggest that they could be integrated into established neuronal networks by synaptic and/or peptide signalling. Vesicular release at synapses can be experimentally and pharmacologically manipulated and analysed by the use of compounds such as αα-latrotoxin (to stimulate massive neurotransmitter release), botulinum toxin (to abolish neurotransmitter release), or tetrodotoxin (to block action potentials). These examples each target different proteins, receptors and ion channels that are required for finely tuned synaptic mechanisms, and if experimentally coupled with electrophysiological paired recordings in wild type and treated acute slices or tissue culture, some insight into the Copine-6 spiny cell behaviour – and perhaps even cell targets – could be achieved. On this note, it has to also be considered that the signalling mechanism of the Copine-6 spiny cells may not be a classical one (i.e. it may not require the synaptic machinery blocked by such toxins), in which case the signalling behaviour of these unusual spiny cells might be uncovered. It is becoming increasingly clear that neurotransmission in the central nervous system can occur through many different signalling molecules, and the identification of enkephalin in the dendrites and 'spine-like' protrusions of Copine-6 spiny cells this does point toward these cells having dendritic peptidergic signalling. This may be acting pre-synaptically to retrogradely modulate neurotransmitter release of other neurons, be an autoregulation, or be extrasynaptically targeting other cells within the RMS. Alongside the GABA content (indicated by the presence of VGAT in some Copine-6 dendritic protrusions), it may be that these neurons have been developmentally conserved to continue a mode of paracrine signalling that is usually typical of neuroblasts (Kriegstein, 2005; Liu *et al.*, 2005), thereby retaining the ability to modulate and finely tune migration, proliferation and differentiation of cells in the RMS and SVZ. Another possibility is that these Copine-6 spiny cells in the corpus callosum may be 'misdirected' olfactory granule and/or periglomerular cells, which are generated at the subventricular zones and would usually migrate to the olfactory bulb. The molecular phenotype of the Copine-6 interneurons certainly suggests that they could belong to these olfactory cell populations, yet their integration into circuitry at the corpus callosum and at the top of the dorsal striatum, together with their mature morphology and biochemical content could suggest that these cells have a functional purpose and are therefore unlikely to be misdirected. Perhaps their molecular similarity to olfactory cells could be accounted for if these cells were generated from the same progenitor cells as the olfactory interneurons. This could initially be examined using immunohistochemical techniques, to observe the expression of established transcription factors that present in certain progenitor cell populations. However, since the expression of many transcription factors is down-regulated during development or following maturation of the neuron, immunohistochemical techniques past embryogenesis may not be sufficient to co-label Copine-6 cells and therefore genetic fate mapping may be required. Various retroviral or Cre- mediated lineage tracing methods provide successful labelling of progenitor cells and their progeny, and since the Copine-6 cells are likely to originate from an already identified progenitor cell population in the embryonic brain, already existing models could be used in the first instance. Transcription factors such as Dlx1/2, Nkx2.1, ER81 and Vax-1 have been identified to be expressed by specific progenitor cells originating in restricted prolific regions of the embryonic brain, which give rise to different interneurons of the olfactory bulbs and the neocortex (for a review (Wichterle *et al.*, 2001; Wonders & Anderson, 2006; Gelman & Marín, 2010;

Marín, 2013). Many of these transcription factors have been genetically manipulated successfully for the labelling cells *in vivo* using GFP driven under the control of their promoter, and such models – which would allow persistent labelling of progenitor cells and their progeny – could be used for subsequent immunohistochemical analysis to examine their location and to identify any Copine-6 protein expression. Furthermore, various different studies into cell origin and cell migration have been conducted in the embryonic and adult brain, particularly following mutation of such transcription factors (for a review, see Ghashghaei, Lai, & Anton, 2007). These have shown olfactory interneuron precursor cells to originate at multiple sites in the embryonic brain (Batista-Brito *et al.*, 2008), therefore it would be plausible to consider that the Copine-6 spiny cells may be derived from various different progenitor pools.

Classically the function of proteins has been studied by producing knockout animals in which the gene is disrupted and so expression of the protein is prevented. The phenotype of the knockout animal is then studied from which a function of the protein might be inferred. However, no Copine-6 knock out animal model has been produced to date, and evidence of strong Copine-6 expression in various neuronal populations throughout development of the rodent brain might suggest that a full knock out of the Copine-6 gene would prove lethal. However, advanced genetic manipulation techniques such as Cre-Lox technology could be employed to overcome this problem. This would involve transgenic breeding of mice expressing the Cre transgene (which recombines short target sequences such as Lox, and can be targeted to specific tissues or cell types), and the LoxP insert at specific sites in the DNA sequence to ‘flank’ a target gene/promotor/stop sequence. Expression of the CRE transgene can be regulated by putting it under the control of specific gene promotors, and this can result in tissue, cell and indeed developmentally regulated expression of the transgene. Recently a library of 20+ Cre mice were produced to examine neural circuitry of the cerebral cortex, more specifically the diversity of GABAergic interneurons, which can be used to trace cell fate and connectivity (Taniguchi *et al.*, 2011). Such technology will advance the study of neural circuitry, particularly if the library becomes extensive to more proteins. The Copine-6 gene itself, for example, could be floxed by the LoxP sites which, following generation of a Cre-type LoxP mouse, would result in deletion of the Copine-6 gene in those cells containing the Cre insertion. Therefore, cell specific conditional knock outs of Copine-6 could be generated. Furthermore, it is possible to insert 'inducible' Cre recombinase, which is a modified form of the Cre transgene that becomes active only following an inducing agent is administered, such as tetracycline or tamoxifen. This allows for the knockout of the target gene at different and specific times in the life of an animal. Such a method would be useful for investigating the function of Copine-6, particularly since its expression may have different function implications at different stages of development. A time-controlled knock out of the Copine-6 gene would therefore allow a full developmental functional study to be conducted.

Ideally, as mentioned above, a Cre-LoxP transgenic mouse would be produced with specific knock out of Copine-6 only in the spiny interneurons of the corpus callosum. This would allow for the effect of knock out to be attributed specifically to this cell population alone, rather than being associated with the other numerous cell types that are labelled by Copine-6. Although such a cell specific knock out is not currently possible, an ever growing number of cells types that can be specifically targeted are available, most of which manipulate the Cre/LoxP recombination system (for some examples, see (Tsien *et al.*, 1996; Yamashita *et al.*, 2006; Gong *et al.*, 2007; Taniguchi *et al.*, 2011; Wu *et al.*, 2011). These methods rely on the expression of particular proteins, neurotransmitters or transcription factors at certain developmental time points in particular cell populations, and it is plausible that such technology could eventually be used to specifically target the Copine-6 spiny cells, especially if a transcriptional promoter unique to these spiny cells (i.e. one that is not expressed by other Copine-6 expressing cell populations) can be identified and manipulated using the Cre/LoxP technology. All of these are avenues with the potential to aid our understanding of the function of this novel cell type in the corpus callosum.

The methods described above provide a means to examine the physiological role of Copine 6, yet the molecular function of the protein remains elusive. Electron microscopic analysis using nanoparticle labelling (Chapter 5) shows that in neurons, Copine-6 is restricted to the intracellular plasma membrane, the smooth endoplasmic reticulum (SER) and to multi-vesicular bodies (MVBs). Although the function of Copine-6 (indeed, any of the Copines) has not yet been established, it is reported that they translocate to the intracellular plasma membrane in transfected HEK 293 cells following an increase in intracellular calcium (Perestenko *et al.*, 2010). Copine-6, when constitutively expressed in HEK cells, was also found to associate with clathrin-coated membranes of internalised early endosomes, suggesting an endosomal targeting sequence within the Copine-6 vWA-domain (Perestenko *et al.*, 2010). This is in line with findings in *Dictyostelium*, showing the localisation of GFP-tagged CpnA with organelles of the endo-lysosomal pathway also in a calcium dependent manner (Damer *et al.*, 2005). During processes of endomembrane sorting, early endosomes mature into late endosomes, which can be identified by their characteristic accumulation of intraluminal vesicles, or multi-vesicular bodies (for a review see Gruenberg & Stenmark, 2004). MVBs contribute to the complex processes involved in protein and lipid degradation and recycling, and do so either by direct fusion of the MVBs with lysosomes for degradation of vesicular content, or by vesicle trafficking and recycling to and from the Golgi and plasma membrane. It is suggested that the formation of endosomal membranes is organised itself by specialised membrane domains such as lipids, protein-lipid, and protein-protein complexes, assembled at the membrane surface (Gruenberg, 2001). Interestingly, the previously identified association of Copine-6 with early endosomes in HEK cells (Perestenko *et al.*, 2010) and the association of Copine 6 with multi-vesicular bodies in neurons reported in this thesis, may point towards a function of the protein in such endomembrane sorting systems. Although some co-localisation studies on the early stages of endocytosis have already been conducted in the laboratory (Perestenko *et al.*, 2010, and McIlhinney *et al*, unpublished), the co-localisation of Copine-6 with multi-vesicular bodies has not fully been explored. The effect of Copine-6 knock down on MVBs following either si- (small-interfering), or sh- (small hairpin) RNA, both of which silence the Copine-6 gene, could initially be employed in neuronal tissue culture, primarily to investigate if there are any morphological, intracellular or functional changes within the endomembrane sorting system in the absence of Copine-6.

As an alternative to knockdown studies with Copine-6, mutations in the C2 or vWA domains of the Copine-6 could be introduced, targeting the calcium or manganese binding sites in these domains. If the domains function as predicted, such mutants could act as a dominant negative mutation (Jambunathan *et al.*, 2001), and by expressing these in neurons and monitoring their functional consequences insights into both the function of the protein and of the domains could be dissected. The use of tissue culture or slice culture also allows for a variety of transgenic techniques to be used in combination; for example an initial knock down of the Copine-6 protein by siRNA could then be followed by the introduction of a mutant or wild type Copine-6 domain by transfection or by biolistic gene transfer, in order to observe whether or not particular domains are able to rescue altered phenotypes at particular stages of development.

In addition, electrophysiological techniques could be employed to investigate the role of the Copine-6 protein itself. Knock down of Copine-6 by shRNA or siRNA in hippocampal cultures, for instance, which have strong Copine-6 expression, should give insights into how this affects the electrophysiology of the cells. Preliminary studies have established that Copine-6 knockdown by shRNA in hippocampal tissue cultures results in an increase in filopodia and changes in dendrite morphology (McIlhinney and Perestenko, personal communication), and electrophysiological experiments could contribute to understanding the functional significance of these changes.

As the Copines have been suggested to be associated with protein trafficking, their potential protein partners could be sought to provide clues as to their function. Whilst extensive proteomic studies using the Copines have been carried out in the laboratory these have been equivocal, and to date have not yielded definitive results. A yeast two-hybrid analysis using the difference domains of Copine-6 might provide another route to finding Copine interacting proteins. Indeed this approach has identified interacting partners for some of the Copines (Tomsig *et al.*, 2003) although in most cases the physiological significance of these has not been fully established.

A combination of the experimental approaches discussed above will be needed to understand the physiological function(s) of Copine-6 and which signalling pathways it might use to produce these functions. It is evident from the data so far that Copine-6 – indeed, all of the Copine family members – require further extensive analysis in order to discover their intracellular role(s). However, the data presented in this thesis compliments the Copine-6 literature to date, and the discovery that Copine-6 labels a novel axonless interneuron population in the corpus callosum of the rodent brain, with an unusual developmental and signalling phenotype, indicates that this protein is likely to be functionally important. Investigations using a combination of *in vivo* and *in vitro* techniques are imperative for gaining insight into this unusual protein family.

Chapter 7. **References**

Abrous, D.N., Koehl, M., & Moal, M.L.E. (2005) Adult Neurogenesis□: From Precursors to Network and Physiology. *Physiology Review*, **85**, 523–569.

Altman, J. (1962) Are new neurons formed in the brains of adult animals? *Science*, **135**, 1127–1128.

Altman, J. (1963) Autoradiographic investigation of cell proliferation in the brains of rats and cats. *The Anatomical record*, **145**, 573–591.

Altman, J. (1969) Autoradiographic and Histological Studies of Postnatal Neurogenesis. *Journal of Comparative Neurology*, **137**, 433–457.

Alvarez-Buylla, a, García-Verdugo, J.M., & Tramontin, a D. (2001) A unified hypothesis on the lineage of neural stem cells. *Nature reviews. Neuroscience*, **2**, 287–293.

Alvarez-buylla, A. & Garcıa-Verdugo, J.M. (2002) Neurogenesis in Adult Subventricular Zone. *The journal of neuroscience*, **22**, 629–634.

Anastasiades, P.G. & Butt, S.J.B. (2011) Decoding the transcriptional basis for GABAergic interneuron diversity in the mouse neocortex. *The European journal of neuroscience*, **34**, 1542–1552.

Anderson, S. a, Marín, O., Horn, C., Jennings, K., & Rubenstein, J.L. (2001) Distinct cortical migrations from the medial and lateral ganglionic eminences. *Development (Cambridge, England)*, **128**, 353–363.

Angelides, K.J., Elmer, L.W., Loftus, D., & Elson, E. (1988) Distribution and lateral mobility of voltage-dependent sodium channels in neurons. *The Journal of cell biology*, **106**, 1911–1925.

Angevine, J. & Sidman, R. (1961) Autoradiographic Study of Cell Migration during Histogenesis of Cerebral Cortex in the Mouse. *Nature*, **192**, 766–768.

Arlotta, P., Molyneaux, B.J., Chen, J., Inoue, J., Kominami, R., & Macklis, J.D. (2005) Neuronal subtype-specific genes that control corticospinal motor neuron development in vivo. *Neuron*, **45**, 207–221.

Ascoli, G. a, Alonso-Nanclares, L., Anderson, S. a, Barrionuevo, G., Benavides-Piccione, R., Burkhalter, A., Buzsáki, G., Cauli, B., Defelipe, J., Fairén, A., Feldmeyer, D., Fishell, G., Fregnac, Y., Freund, T.F., Gardner, D., Gardner, E.P., Goldberg, J.H., Helmstaedter, M., Hestrin, S., Karube, F., Kisvárday, Z.F., Lambolez, B., Lewis, D. a, Marin, O., Markram, H., Muñoz, A., Packer, A., Petersen, C.C.H., Rockland, K.S., Rossier, J., Rudy, B., Somogyi, P., Staiger, J.F., Tamas, G., Thomson, A.M., Toledo-Rodriguez, M., Wang, Y., West, D.C., & Yuste, R. (2008) Petilla terminology: nomenclature of features of GABAergic interneurons of the cerebral cortex. *Nature reviews. Neuroscience*, **9**, 557–568.

Bagley, J., LaRocca, G., Jimenez, D. a, & Urban, N.N. (2007) Adult neurogenesis and specific replacement of interneuron subtypes in the mouse main olfactory bulb. *BMC neuroscience*, **8**, 92.

Baimbridge, K.G., Celio, M.R., & Rogers, J. (1992) Calcium-binding proteins in the nervous system. *Trends in neurosciences*, **15**, 303–308.

Baimbridge, K.G. & Miller, J.J. (1982) Immunohistochemical localization of calcium-binding protein in the cerebellum, hippocampal formation and olfactory bulb of the rat. *Brain research*, **245**, 223–229.

Barinka, F. & Druga, R. (2010) Calretinin Expression in the Mammalian Neocortex□: A Review. *Physiological Research*, **59**, 665–677.

Batista-Brito, R., Close, J., Machold, R., & Fishell, G. (2008) The distinct temporal origins of olfactory bulb interneuron subtypes. *The Journal of neuroscience□: the official journal of the Society for Neuroscience*, **28**, 3966–3975.

Bayer, S., Zhang, X., Russo, R.J., & Altman, J. (1993) Three-Dimensional Reconstructions of the Developing Forebrain in the Rat Embryos. *Neuroimage*, **1**, 296–307.

Bayer, S.A. (1983) 3H-Thymidine-radiographic Studies of Neurogenesis in the Rat Olfactory Bulb. *Experimental brain research.*, **50**, 329–340.

Berridge, M.J. (1998) Neuronal Calcium Signaling. *Neuron*, **21**, 13–26.

Betz, H. (1998) Gephyrin, a major player in GABAergic postsynaptic membrane assembly? *Nature neuroscience*, **1**, 541–543.

Bhattacharya, S., Bunick, C.G., & Chazin, W.J. (2004) Target selectivity in EF-hand calcium binding proteins. *Biochimica et biophysica acta*, **1742**, 69–79.

Bogan, N., Brecha, N., Gall, C., & Karten, H. (1982) DISTRIBUTION OF ENKEPHALIN-LIKE IMMUNOREACTIVITY IN THE RAT MAIN OLFACTORY BULB. *Neuroscience*, **7**, 895–906.

Bonfanti, L. (2006) PSA-NCAM in mammalian structural plasticity and neurogenesis. *Progress in neurobiology*, **80**, 129–164.

Brazel, C.Y., Romanko, M.J., Rothstein, R.P., & Levison, S.W. (2003) Roles of the mammalian subventricular zone in brain development. *Progress in Neurobiology*, **69**, 49–69.

Britanova, O., De Juan Romero, C., Cheung, A., Kwan, K.Y., Schwark, M., Gyorgy, A., Vogel, T., Akopov, S., Mitkovski, M., Agoston, D., Sestan, N., Molnár, Z., & Tarabykin, V. (2008) Satb2 is a postmitotic determinant for upper-layer neuron specification in the neocortex. *Neuron*, **57**, 378–392.

Brose, N., Hofmann, K., Hata, Y., & Südhof, T.C. (1995) Mammalian homologues of Caenorhabditis elegans unc-13 gene define novel family of C2-domain proteins. *The Journal of biological chemistry*, **270**, 25273–25280.

Cajal, R. y (1901a) Estudios sobre la corteza cerebral humana. *Trab Inst Cajal Invest Biol*, **1**, 1–227.

Cajal, R. y (1901b) Textura del lóbulo olfativo accesorio. *Trab. Lab. Invest. Biol*, **1**, 141–149.

Camp, A.J. & Wijesinghe, R. (2009) Calretinin: modulator of neuronal excitability. *The international journal of biochemistry & cell biology*, **41**, 2118–2121.

Caudell, E.G., Caudell, J.J., Tang, C.H., Yu, T.K., Frederick, M.J., & Grimm, E. a (2000) Characterization of human copine III as a phosphoprotein with associated kinase activity. *Biochemistry*, **39**, 13034–13043.

Cauli, B., Audinat, E., Lambolez, B., Angulo, M.C., Ropert, N., Tsuzuki, K., Hestrin, S., & Rossier, J. (1997) Molecular and physiological diversity of cortical nonpyramidal cells. *Journal of Neuroscience*, **17**, 3894–3906.

Cauli, B., Porter, J.T., Tsuzuki, K., Lambolez, B., Rossier, J., Quenet, B., & Audinat, E. (2000) Classification of fusiform neocortical interneurons based on unsupervised clustering. *Proceedings of the National Academy of Sciences of the United States of America*, **97**, 6144–6149.

Caviness, V. & Sidman, R.L. (1973) Time of Origin of Corresponding Cell Classes in the Cerebral Cortex of Normal and Reeler Mutant Mice□: An Autoradiographic Analysis ’. *Journal of Comparative Neurology*, **148**, 141–152.

Caviness, V.S. & Takahashi, T. (1995) Proliferative events in the cerebral ventricular zone. *Brain & development*, **17**, 159–163.

Celio, M.R. (1986) Parvalbumin in Most γ-Aminobutyric Acid-Containing Neurons of the Rat Cerebral Cortex. *Science*, **231**, 995–997.

Celio, M.R. & Heizmann, C.W. (1981) Calcium Binding proteins parvalbumin as a neuronal marker. *Nature*, **293**, 300–302.

Church, D.L. & Lambie, E.J. (2003) The promotion of gonadal cell divisions by the Caenorhabditis elegans TRPM cation channel GON-2 is antagonized by GEM-4 copine. *Genetics*, **165**, 563–574.

Clapham, D.E. (1995) Calcium Signaling Review. *Cell*, **80**, 259–268.

Cohen, O.S., Mccoy, S.Y., Middleton, F. a, Bialosuknia, S., Zhang-James, Y., Liu, L., Tsuang, M.T., Faraone, S. V, & Glatt, S.J. (2012) Transcriptomic analysis of postmortem brain identifies dysregulated splicing events in novel candidate genes for schizophrenia. *Schizophrenia research*, **142**, 188–199.

Colonnier, M. (1968) Synaptic patterns on different cell types in the different laminae of the cat visual cortex. An electron microscope study. *Brain research*, **9**, 268–287.

Condé, F., Lund, J.S., Jacobowitz, D.M., Baimbridge, K.G., & Lewis, D. a (1994) Local circuit neurons immunoreactive for calretinin, calbindin D-28k or parvalbumin in monkey prefrontal cortex: distribution and morphology. *The Journal of comparative neurology*, **341**, 95–116.

Corbin, J.G., Nery, S., & Fishell, G. (2001) Telencephalic cells take a tangent: non-radial migration in the mammalian forebrain. *Nature neuroscience*, **4**, 1177–1182.

Coussens, L., Parker, P.J., Rhee, L., Yang-feng, T.L., Chen, E., Waterfield, M.D., Francke, U., Ullrich, A., & Francke, U.T.A. (1986) Multiple, distinct forms of bovine and human protein kinase c suggest diveristy in cellular signaling pathways. *Science*, **233**, 859–866.

Cowland, J.B., Carter, D., Bjerregaard, M.D., Johnsen, A.H., Borregaard, N., & Lollike, K. (2003) Tissue expression of copines and isolation of copines I and III from the cytosol of human neutrophils Abstract□: Copines are a recently identified group of proteins characterized by two Ca 2 -binding C2- C terminus . Although pEST sequences indicate the. *Journal of Leukocyte Biology*, **74**, 379–388.

Craig, A.M., Banker, G., Chang, W., McGrath, M.E., & Serpinskaya, a S. (1996) Clustering of gephyrin at GABAergic but not glutamatergic synapses in cultured rat hippocampal neurons. *The Journal of neuroscience□: the official journal of the Society for Neuroscience*, **16**, 3166–3177.

Creutz, C.E., Tomsig, J.L., Snyder, S.L., Gautier, M., Skouri, F., Beisson, J., & Cohen, J. (1998) The Copines , a Novel Class of C2 Domain-containing , Calcium- dependent , Phospholipid-binding Proteins Conserved from Paramecium to Humans. *Journal of Biological Chemistry*, **273**, 1393–1402.

Damer, C.K., Bayeva, M., Hahn, E.S., Rivera, J., & Socec, C.I. (2005) Copine A, a calcium-dependent membrane-binding protein, transiently localizes to the plasma membrane and intracellular vacuoles in Dictyostelium. *BMC Cell Biology*, **6**, 1471.

Damer, C.K., Smith, T.S., Pineda, J.M., & Donaghy, A.C. (2010) Copine A plays a role in the differentiation of stalk cells and the initiation of culmination in Dictyostelium development. *BMC developmental biology*, **10**, 59.

Davletov, B.A. & Sudhof, T.C. (1993) A Single C2 Domain from synaptotagmin I is sufficient for high affinity ca2+/phospholipid binding. *Journal of biological chemistry*, **268**, 26386–26390.

De Marchis, S., Bovetti, S., Carletti, B., Hsieh, Y.-C., Garzotto, D., Peretto, P., Fasolo, A., Puche, A.C., & Rossi, F. (2007) Generation of distinct types of periglomerular olfactory bulb interneurons during development and in adult mice: implication for intrinsic properties of the subventricular zone progenitor population. *The Journal of neuroscience□: the official journal of the Society for Neuroscience*, **27**, 657–664.

DeFelipe, J., López-Cruz, P.L., Benavides-Piccione, R., Bielza, C., Larrañaga, P., Anderson, S., Burkhalter, A., Cauli, B., Fairén, A., Feldmeyer, D., Fishell, G., Fitzpatrick, D., Freund, T.F., González-Burgos, G., Hestrin, S., Hill, S., Hof, P.R., Huang, J., Jones, E.G., Kawaguchi, Y., Kisvárday, Z., Kubota, Y., Lewis, D. a, Marín, O., Markram, H., McBain, C.J., Meyer, H.S., Monyer, H., Nelson, S.B., Rockland, K., Rossier, J., Rubenstein, J.L.R., Rudy, B., Scanziani, M., Shepherd, G.M., Sherwood, C.C., Staiger, J.F., Tamás, G., Thomson, A., Wang, Y., Yuste, R., & Ascoli, G. a (2013) New insights into the classification and nomenclature of cortical GABAergic interneurons. *Nature reviews. Neuroscience*, **14**, 202–216.

Demeulemeester, H., Arckens, L., Vandesande, F., Orban, G., Heizmann, C., & Pochet, R. (1991) Calcium binding proteins and neuropeptides as molecular markers of GABAergic interneurons in the cat visual cortex. *Experimental brain research.*, **84**, 538–544.

Demeulemeester, H., Vandesande, F., Orban, G. a, Brandon, C., & Vanderhaeghen, J.J. (1988) Heterogeneity of GABAergic cells in cat visual cortex. *The Journal of neuroscience□: the official journal of the Society for Neuroscience*, **8**, 988–1000.

Doetsch, F. & Alvarez-Buylla, a (1996) Network of tangential pathways for neuronal migration in adult mammalian brain. *Proceedings of the National Academy of Sciences of the United States of America*, **93**, 14895–14900.

Doetsch, F., Caillé, I., Lim, D. a, García-Verdugo, J.M., & Alvarez-Buylla, a (1999) Subventricular zone astrocytes are neural stem cells in the adult mammalian brain. *Cell*, **97**, 703–716.

Duncan, R., Betz, A., Shipston, M.J., Brose, N., Chow, R.H., & Neurobiologie, A.G.M. (1999) Transient, Phorbol Ester-induced DOC2-Munc13 interactions in vivo. *Journal of biological chemistry*, **274**, 27347–27350.

Duncan, R., Shipston, M., & Chow, R. (2000) Double C2 protein. A review. *Biochimie*, **82**, 421–426.

D'Arcangelo, G., Miao, G., Chen, S.-C., Soares, H., Morgan, J., & Curran, T. (1995) A protein related to extracellular matrix proteins deleted in the mouse mutant reeler. *Nature*, **374**, 719–723.

Eng, L.F., Vanderhaeghen, J.J., Bignami, a, & Gerstl, B. (1971) An acidic protein isolated from fibrous astrocytes. *Brain research*, **28**, 351–354.

Erondu, N. & Kennedy, B. (1985) Regional Distribution of Type II Ca * + / Calmodulin-dependent Kinase in Rat Brain. *Journal of Neuroscience*, **5**, 3270–3277.

Essrich, C., Lorez, M., Benson, J.A., Fritschy, J., & Lüscher, B. (1998) Postsynaptic clustering of major GABA A receptor subtypes requires the γ2 subunit and gephyrin. *Nature Neuroscience*, **1**, 563–571.

Falconer, D. (1951) Two new mutants "trembler" and "reeler", with neurological actions in the house mouse (mus musculus l.). *Journal of Genetics*, **50**, 192–201.

Fasolo, A., Peretto, P., & Bonfanti, L. (2002) Cell migration in the rostral migratory stream. *Chemical senses*, **27**, 581–582.

Francis, F., Koulakoff, a, Boucher, D., Chafey, P., Schaar, B., Vinet, M.C., Friocourt, G., McDonnell, N., Reiner, O., Kahn, a, McConnell, S.K., Berwald-Netter, Y., Denoulet, P., & Chelly, J. (1999) Doublecortin is a developmentally regulated, microtubule-associated protein expressed in migrating and differentiating neurons. *Neuron*, **23**, 247–256.

Freund, T. & Buzsaki, G. (1996) Interneurons of the Hippocampus. *Hippocampus*, **6**, 347–470.

Freund, T., Martin, K., Smith, A., & Somogyi, P. (1983) Glutamate Decarboxylase-Immunoreactive Terminals of Golgi-Impregnated Axoaxonic Cells and of Presumed Basket Cells i n Synaptic Contact with Pyramidal Neurons of the Cat ' s Visual Cortex. *Journal of Comparative Neurology*, **221**, 263–278.

Freund, T.F., Maglóczky, Z., Soltész, I., & Somogyi, P. (1986) Synaptic connections, axonal and dendritic patterns of neurons immunoreactive for cholecystokinin in the visual cortex of the cat. *Neuroscience*, **19**, 1133–1159.

Friedrich, R., Groffen, A.J., Connell, E., Van Weering, J.R.T., Gutman, O., Henis, Y.I., Davletov, B., & Ashery, U. (2008) DOC2B acts as a calcium switch and enhances vesicle fusion. *The Journal of neuroscience□: the official journal of the Society for Neuroscience*, **28**, 6794–6806.

Friedrich, R., Yeheskel, A., & Ashery, U. (2010) DOC2B, C2 domains, and calcium: A tale of intricate interactions. *Molecular neurobiology*, **41**, 42–51.

Fritschy, J.-M., Harvey, R.J., & Schwarz, G. (2008) Gephyrin: where do we stand, where do we go? *Trends in neurosciences*, **31**, 257–264.

Fritschy, J.M. & Mohler, H. (1995) GABAA-receptor heterogeneity in the adult rat brain: differential regional and cellular distribution of seven major subunits. *The Journal of comparative neurology*, **359**, 154–194.

Gabbott, P.L. & Somogyi, P. (1986) Quantitative distribution of GABA-immunoreactive neurons in the visual cortex (area 17) of the cat. *Experimental brain research.*, **61**, 323–331.

Garaschuk, O., Yaari, Y., Konnerth, A., Institut, I.P., & Saarlandes, U. (1997) Release and sequestration of calcium by ryanodine-sensitive stores in rat hippocampal neurones. *Journal of Physiology*, **502**, 13–30.

García-Verdugo, J.M., Doetsch, F., Wichterle, H., Lim, D. a, & Alvarez-Buylla, a (1998) Architecture and cell types of the adult subventricular zone: in search of the stem cells. *Journal of neurobiology*, **36**, 234–248.

Gelman, D.M. & Marín, O. (2010) Generation of interneuron diversity in the mouse cerebral cortex. *The European journal of neuroscience*, **31**, 2136–2141.

Geppert, M. & Südhof, T.C. (1998) RAB3 and synaptotagmin: the yin and yang of synaptic membrane fusion. *Annual review of neuroscience*, **21**, 75–95.

Gerke, V., Creutz, C.E., & Moss, S.E. (2005) Annexins: linking Ca2+ signalling to membrane dynamics. *Nature reviews. Molecular cell biology*, **6**, 449–461.

Ghashghaei, H.T., Lai, C., & Anton, E.S. (2007) Neuronal migration in the adult brain: are we there yet? *Nature reviews. Neuroscience*, **8**, 141–151.

Gleeson, J.G., Lin, P.T., Flanagan, L.A., & Walsh, C.A. (1999) Doublecortin Is a Microtubule-Associated Protein and Is Expressed Widely by Migrating Neurons. *Neuron*, **23**, 257–271.

Gonchar, Y. & Burkhalter, a (1997) Three distinct families of GABAergic neurons in rat visual cortex. *Cerebral cortex (New York, N.Y.□: 1991)*, **7**, 347–358.

Gonchar, Y., Pang, L., Malitschek, B., Bettler, B., & Burkhalter, a (2001) Subcellular localization of GABA(B) receptor subunits in rat visual cortex. *The Journal of comparative neurology*, **431**, 182–197.

Gonchar, Y., Wang, Q., & Burkhalter, A. (2007) Multiple distinct subtypes of GABAergic neurons in mouse visual cortex identified by triple immunostaining. *Frontiers in neuroanatomy*, **1**, 1–11.

Gong, S., Doughty, M., Harbaugh, C.R., Cummins, A., Hatten, M.E., Heintz, N., & Gerfen, C.R. (2007) Targeting Cre recombinase to specific neuron populations with bacterial artificial chromosome constructs. *The Journal of neuroscience□: the official journal of the Society for Neuroscience*, **27**, 9817–9823.

Gottschalk, A., Almedom, R.B., Schedletzky, T., Anderson, S.D., Yates, J.R., & Schafer, W.R. (2005) Identification and characterization of novel nicotinic receptor-associated proteins in Caenorhabditis elegans. *The EMBO journal*, **24**, 2566–2578.

Goulburn, A.L., Stanley, E.G., Elefanty, A.G., & Anderson, S. a (2012) Generating GABAergic cerebral cortical interneurons from mouse and human embryonic stem cells. *Stem cell research*, **8**, 416–426.

Gray, E.G. (1959) Axo-somatic and axo-dendritic synapses of the cerebral cortex: an electron microscope study. *Journal of anatomy*, **93**, 420–433.

Greengard, P., Valtorta, F., Czernik, A.J., & Benfenati, F. (1993) Synaptic Vesicle Phosphoproteins and Regulation of Synaptic Function. *Science*, **259**, 780–785.

Groffen, A.J. a, Friedrich, R., Brian, E.C., Ashery, U., & Verhage, M. (2006) DOC2A and DOC2B are sensors for neuronal activity with unique calcium-dependent and kinetic properties. *Journal of neurochemistry*, **97**, 818–833.

Gruenberg, J. (2001) The Endocytic Pathway: A Mosaic of Domains. *Nature reviews. Molecular cell biology*, **2**, 721–730.

Gruenberg, J. & Stenmark, H. (2004) The biogenesis of multivesicular endosomes. *Nature reviews. Molecular cell biology*, **5**, 317–323.

Hack, I., Bancila, M., Loulier, K., Carroll, P., & Cremer, H. (2002) Reelin is a detachment signal in tangential chain-migration during postnatal neurogenesis. *Nature neuroscience*, **5**, 939–945.

Harman, a W. & Maxwell, M.J. (1995) An evaluation of the role of calcium in cell injury. *Annual review of pharmacology and toxicology*, **35**, 129–144.

Heinrich, C., Keller, C., Boulay, A., Vecchi, M., Bianchi, M., Sack, R., Lienhard, S., Duss, S., Hofsteenge, J., & Hynes, N.E. (2010) Copine-III interacts with ErbB2 and promotes tumor cell migration. *Oncogene*, **29**, 1598–1610.

Heizmann, C.W. (1984) Parvalbumin, an intracellular calcium-binding protein; distribution, properties and possible roles in mammalian cells. *Experientia*, **40**, 910–921.

Heizmann, C.W. (1993) Calcium signaling in the brain. *Acta neurobiologiae experimentalis*, **53**, 15–23.

Heizmann, C.W. & Hunziker, W. (1991) Intracellular calcium-binding proteins:more sites than insights. *Trends in Biochemical science*, **16**, 98–103.

Hong, J., Yang, H., & Costa, E. (1977) On the location of methionine enkephalin neurons in rat striatum. *Neuropharmacology*, **16**, 451–453.

Hu, H., Tomasiewicz, H., Magnuson, T., & Rutishauser, U. (1996) The role of polysialic acid in migration of olfactory bulb interneuron precursors in the subventricular zone. *Neuron*, **16**, 735–743.

Hua, J., Grisafi, P., Cheng, S.H., & Fink, G.R. (2001) Plant growth homeostasis is controlled by the Arabidopsis BON1 and BAP1 genes. *Genes & development*, **15**, 2263–2272.

Inoue, Masanori; Kishimoto, Arira; Tarai, Yoshimi; Nishizuka, Y., Inoue, M., Kishimoto, A., Takai, Y., & Nishizuka, Y. (1977) Studies on a Cyclic Nucleotide-independent and Its Proenzyme in Mammalian Tissues. *The Journal of biological chemistry*, **252**, 7610–7616.

Jacobowitz, D.M. & Winsky, L. (1991) Immunocytochemical localization of calretinin in the forebrain of the rat. *The Journal of comparative neurology*, **304**, 198–218.

Jambunathan, N., Siani, J.M., & Mcnellis, T.W. (2001) A Humidity-Sensitive Arabidopsis Copine Mutant Exhibits Precocious Cell Death and Increased Disease Resistance. *The Plant cell*, **13**, 2225–2240.

Jewell, S. a, Bellomo, G., Thor, H., Orrenius, S., & Smith, M. (1982) Bleb formation in hepatocytes during drug metabolism is caused by disturbances in thiol and calcium ion homeostasis. *Science (New York, N.Y.)*, **217**, 1257–1259.

Jones, E.G. (2004) Cerebral Cortex. *Cerebral Cortex*, 769–773.

Jovanov-Milošević, N., Petanjek, Z., Petrović, D., Judaš, M., & Kostović, I. (2010) Morphology, molecular phenotypes and distribution of neurons in developing human corpus callosum. *The European journal of neuroscience*, **32**, 1423–1432.

Kaiserman-Abramof, I. & Peters, A. (1972) Some aspects of the morphology of Betz cells in the cerebral cortex of the cat. *Brain research*, **43**, 527–546.

Kato, T., Yokouchi, K., Li, Z., Fukushima, N., Kawagishi, K., & Moriizumi, T. (1999) Calretinin-immunoreactive neurons in rostral migratory stream: neuronal differentiation. *Neuroreport*, **10**, 2769–2772.

Kawaguchi, Y. (1995) Physiological Subgroups of Nonpyramidal Cells with Specific Characteristics in Layer II / III of Rat Frontal Cortex. *Journal of Neuroscience*, **15**, 2638–2655.

Kawaguchi, Y. & Kubota, Y. (1997) GABAergic cell subtypes and their synaptic connections in rat frontal cortex. *Cerebral cortex (New York, N.Y.□: 1991)*, **7**, 476–486.

Kawaguchi, Y. & Kubota, Y. (1998) Neurochemical features and synaptic connections of large physiologically-identified GABAergic cells in the rat frontal cortex. *Neuroscience*, **85**, 677–701.

Kennedy, M.J. & Ehlers, M.D. (2011) Mechanisms and function of dendritic exocytosis. *Neuron*, **69**, 856–875.

Khodosevich, K. & Monyer, H. (2011) Signaling in migrating neurons: from molecules to networks. *Frontiers in neuroscience*, **5**, 28.

Kirsch, J. & Betz, H. (1993) Widespread expression of gephyrin, a putative glycine receptor-tubulin linker protein, in rat brain. *Brain research*, **621**, 301–310.

Kohwi, M., Petryniak, M. a, Long, J.E., Ekker, M., Obata, K., Yanagawa, Y., Rubenstein, J.L.R., & Alvarez-Buylla, A. (2007) A subpopulation of olfactory bulb GABAergic interneurons is derived from Emx1- and Dlx5/6-expressing progenitors. *The Journal of neuroscience□: the official journal of the Society for Neuroscience*, **27**, 6878–6891.

Kojima, T., Fukuda, M., Aruga, J., & Mikoshiba, K. (1996) Calcium-dependent phospholipid binding to the C2A domain of a ubiquitous form of double C2 protein (Doc2 beta). *Journal of biochemistry*, **120**, 671–676.

Kordeli, E., Davis, J., Trapp, B., & Bennett, V. (1990) An isoform of ankyrin is localized at nodes of Ranvier in myelinated axons of central and peripheral nerves. *The Journal of cell biology*, **110**, 1341–1352.

Korteweg, N., Denekamp, F. a, Verhage, M., & Burbach, J.P. (2000) Different spatiotemporal expression of DOC2 genes in the developing rat brain argues for an additional, nonsynaptic role of DOC2B in early development. *The European journal of neuroscience*, **12**, 165–171.

Kosaka, K. & Kosaka, T. (2005) Synaptic organization of the glomerulus in the main olfactory bulb□: Compartments of the glomerulus and heterogeneity of the periglomerular cells. *Anatomical Science International*, 80–90.

Kosaka, K., Toida, K., Aika, Y., & Kosaka, T. (1998) How simple is the organization of the olfactory glomerulus□?: the heterogeneity of so-called periglomerular cells. *Neuroscience Research*, **30**, 101 – 110.

Kostovic, I. & Rakic, P. (1980) Cytology and time of origin of interstitial neurons in the white matter in infant and adult human and monkey telencephalon. *Journal of neurocytology*, **9**, 219–242.

Kostović, I., Judaš, M., & Sedmak, G. (2011) Developmental history of the subplate zone, subplate neurons and interstitial white matter neurons: relevance for schizophrenia. *International journal of developmental neuroscience□: the official journal of the International Society for Developmental Neuroscience*, **29**, 193–205.

Kretsinger, R.H. (1976) CALCIUM-BINDING PROTEINS. *Annual review of biochemistry*, **45**, 239–266.

Kretsinger, R.H. (1980) Structure and evolution of calcium-modulated proteins. *CRC critical reviews in biochemistry*, **8**, 119–174.

Kretsinger, R.H. & Nockolds, C.E. (1973) Carp Muscle Calcium Binding Protein. *Journal of biological chemistry*, **248**, 3313–3326.

Kriegstein, A., Noctor, S., & Martínez-cerdeño, V. (2006) Patterns of neural stem and progenitor cell division may underlie evolutionary cortical expansion. *Nature reviews. Neuroscience*, **7**, 883–890.

Kriegstein, A.R. (2005) GABA puts the brake on stem cells. *Nature neuroscience*, **8**, 1132–1133.

Kriegstein, A.R. & Noctor, S.C. (2004) Patterns of neuronal migration in the embryonic cortex. *Trends in neurosciences*, **27**, 392–399.

Kubota, Y., Hattori, R., & Yui, Y. (1994) Three distinct subpopulations of GABAergic neurons in rat frontal agranular cortex. *Brain research*, **649**, 159–173.

Langosch, D., Hoch, W., & Betz, H. (1992) The 93 kDa protein gephyrin and tubulin associated with the inhibitory glycine receptor are phosphorylated by an endogenous protein kinase. *FEBS letters*, **298**, 113–117.

Le Magueresse, C., Alfonso, J., Khodosevich, K., Arroyo Martín, A. a, Bark, C., & Monyer, H. (2011) “Small axonless neurons”: postnatally generated neocortical interneurons with delayed functional maturation. *The Journal of neuroscience : the official journal of the Society for Neuroscience*, **31**, 16731–16747.

Lee, J.O., Rieu, P., Arnaout, M. a, & Liddington, R. (1995) Crystal structure of the A domain from the alpha subunit of integrin CR3 (CD11b/CD18). *Cell*, **80**, 631–638.

Lee, T.-F. & Mcnellis, T.W. (2009) Evidence that the BONZAI1/COPINE1 protein is a calcium- and pathogen-responsive defense suppressor. *Plant Molecular Biology*, **69**, 155–166.

Leid, M., Ishmael, J.E., Avram, D., Shepherd, D., Fraulob, V., & Dollé, P. (2004) CTIP1 and CTIP2 are differentially expressed during mouse embryogenesis. *Gene expression patterns : GEP*, **4**, 733–739.

Lendahl, U., Zimmerman, L.B., & McKay, R.D. (1990) CNS stem cells express a new class of intermediate filament protein. *Cell*, **60**, 585–595.

Li, C., Ullrich, B., Zhang, J.J., Anderson, R.R., Brose, N., Südhof, T.C., & Sudhof, T.C. (1995) Ca++dependent and independent activities of neural and non-neural synaptotagmins. *Nature*, **375**, 594–599.

Li, Y., Gou, M., Sun, Q., & Hua, J. (2010) Requirement of calcium binding, myristoylation, and protein-protein interaction for the copine BON1 function in Arabidopsis. *The Journal of biological chemistry*, **285**, 29884–29891.

Lisman, J. (1989) A mechanism for the Hebb and the anti-Hebb processes underlying learning and memory. *Proceedings of the National Academy of Sciences of the United States of America*, **86**, 9574–9578.

Liu, X., Wang, Q., Haydar, T., & Bordey, A. (2005) Nonsynaptic GABA signaling in postnatal subventricular zone controls proliferation of GFAP-expressing progenitors. *Nature neuroscience*, **8**, 1179–1187.

Lledo, P.-M., Alonso, M., & Grubb, M.S. (2006) Adult neurogenesis and functional plasticity in neuronal circuits. *Nature reviews. Neuroscience*, **7**, 179–193.

Lledo, P.-M., Merkle, F.T., & Alvarez-Buylla, A. (2008) Origin and function of olfactory bulb interneuron diversity. *Trends in neurosciences*, **31**, 392–400.

Lledo, P.-M., Saghatelyan, A., & Lemasson, M. (2004) Inhibitory interneurons in the olfactory bulb: from development to function. *The Neuroscientist*, **10**, 292–303.

Lois, C. & Alvarez-Buylla, a (1994) Long-distance neuronal migration in the adult mammalian brain. *Science (New York, N.Y.)*, **264**, 1145–1148.

Luskin, M. & Menezes, J. (1994) Expression of Neuron-Specific Tubulin Defines a Novel Population in the Proliferative Layers of the Developing Telencephalon. *The journal of neuroscience*, **14**, 5399–5416.

Luskin, M.B. (1993) Restricted proliferation and migration of postnatally generated neurons derived from the forebrain subventricular zone. *Neuron*, **11**, 173–189.

Maitra, R., Grigoryev, D.N., Kumar Bera, T., Pastan, I.H., Lee, B., & Bera, T.K. (2003) Cloning, molecular characterization, and expression analysis of Copine 8. *Biochemical and Biophysical Research Communications*, **303**, 842–847.

Malinow, R., Schulman, H., & Tsien, R.W. (1989) Inhibition of postsynaptic PKC or CaMKII blocks induction but not expression of LTP. *Science (New York, N.Y.)*, **245**, 862–866.

Martens, S., Kozlov, M.M., & McMahon, H.T. (2007) How synaptotagmin promotes membrane fusion. *Science (New York, N.Y.)*, **316**, 1205–1208.

Martín-López, E., Corona, R., & López-Mascaraque, L. (2012) Postnatal characterization of cells in the accessory olfactory bulb of wild type and reeler mice. *Frontiers in neuroanatomy*, **6**, 15.

Marín, O. (2013) Cellular and molecular mechanisms controlling the migration of neocortical interneurons. *The European journal of neuroscience*, **38**, 2019–2029.

Marín, O. & Rubenstein, J.L.R. (2003) Cell migration in the forebrain. *Annual review of neuroscience*, **26**, 441–483.

McIntire, S.L., Reimer, R.J., Schuske, K., Edwards, R.H., & Jorgensen, E.M. (1997) Identification and characterization of the vesicular GABA transporter. *Nature*, **389**, 870–876.

Memberg, S.P. & Hall, A.K. (1995) Dividing Neuron Precursors Express Neuron-Specific Tubulin. *Journal of neurobiology*, **27**, 26–43.

Michishita, M., Videm, V., & Arnaout, M. a (1993) A novel divalent cation-binding site in the A domain of the beta 2 integrin CR3 (CD11b/CD18) is essential for ligand binding. *Cell*, **72**, 857–867.

Molyneaux, B.J., Arlotta, P., Menezes, J.R.L., & Macklis, J.D. (2007a) Neuronal subtype specification in the cerebral cortex. *Nature reviews. Neuroscience*, **8**, 427–437.

Molyneaux, B.J., Arlotta, P., Menezes, J.R.L., & Macklis, J.D. (2007b) Neuronal subtype specification in the cerebral cortex. *Nature reviews. Neuroscience*, **8**, 427–437.

Monyer, H. & Markram, H. (2004) Interneuron Diversity series: Molecular and genetic tools to study GABAergic interneuron diversity and function. *Trends in neurosciences*, **27**, 90–97.

Mullen, R.J., Buck, C.R., & Smith, a M. (1992) NeuN, a neuronal specific nuclear protein in vertebrates. *Development*, **116**, 201–211.

Nakayama, T., Yaoi, T., & Kuwajima, G. (1999) Localization and subcellular distribution of N-copine in mouse brain. *Journal of neurochemistry*, **72**, 373–379.

Nakayama, T., Yaoi, T., Kuwajima, G., Yoshie, O., & Sakata, T. (1999) Ca 2 + -dependent interaction of N-copine , a member of the two C2 domain protein family , with OS-9 , the product of a gene frequently amplied in osteosarcoma. *FEBS letters*, **453**, 77–80.

Nakayama, T., Yaoi, T., Yasui, M., & Kuwajima, G. (1998) N-copine: a novel two C2-domain-containing protein with neuronal activity-regulated expression. *FEBS letters*, **428**, 80–84.

Nalefski, E.A. & Falke, J.J. (1996) The C2 domain calcium-binding motif□: Structural and functional diversity. *Protein Science*, **5**, 2375–2390.

Nielsen, J. V, Blom, J.B., Noraberg, J., & Jensen, N. a (2010) Zbtb20-induced CA1 pyramidal neuron development and area enlargement in the cerebral midline cortex of mice. *Cerebral cortex (New York, N.Y.□: 1991)*, **20**, 1904–1914.

Olson, E.C. & Walsh, C.A. (2002) Smooth , rough and upside-down neocortical development. *Current opinion in genetics and development*, **12**, 320–327.

Orita, S., Sasaki, T., Naito, A., Komuro, R., Ohtsuka, T., Maeda, M., Suzuki, H., Igarashi, H., Takai, Y., & Susuki, H. (1995) Doc2: A Novel Brain Protein Having Two Repeated C2-like Domains. *Biochemical and Biophysical Research Communications*, **206**, 439–448.

O'Connor, S. & Jacob, T.J.C. (2008) Neuropharmacology of the olfactory bulb. *Current molecular pharmacology*, **1**, 181–190.

Parker, P.J., Coussens, L., Totty, N., Rhee, L., Young, S., Chen, E., Stabel, S., Waterfield, M.D., & Ullrich, A. (1986) The complete primary structure of protein kinase C - the major phorbol ester receptor. *Science*, **233**, 853–859.

Parnavelas, J.G. (2000) The origin and migration of cortical neurones: new vistas. *Trends in neurosciences*, **23**, 126–131.

Pencea, V. & Luskin, M.B. (2003) Prenatal development of the rodent rostral migratory stream. *The Journal of comparative neurology*, **463**, 402–418.

Perestenko, P. V, Pooler, A.M., Noorbakhshnia, M., Gray, A., Bauccio, C., & Jeffrey McIlhinney, R.A. (2010) Copines-1, -2, -3, -6 and -7 show different calcium-dependent intracellular membrane translocation and targeting. *The FEBS journal*, **277**, 5174–5189.

Peretto, P., Merighi, A., Fasolo, A., & Bonfanti, L. (1997) Glial tubes in the rostral migratory stream of the adult rat. *Brain research bulletin*, **42**, 9–21.

Perin, M., Fried, V., Mignery, G., Jahn, R., & Sudhof, T.C. (1990) Phospholipid binding by a synaptic vesicle protein homologous to the regulatory region of protein kinase C. *Nature*, **345**, 260–263.

Peters, A., Miller, M., & Kimerer, L.M. (1983) Cholecystokinin-like immunoreactive neurons in rat cerebral cortex. *Neuroscience*, **8**, 431–448.

Peters, A., Palay, S., & Webster, H. (1991) *The Fine Structure of the Nervous System*, Third. edn. Oxford University Press.

Philpot, B.D., Lim, J.H., & Brunjes, P.C. (1997) Activity-dependent regulation of calcium-binding proteins in the developing rat olfactory bulb. *The Journal of comparative neurology*, **387**, 12–26.

Pierce, K.L., Premont, R.T., & Lefkowitz, R.J. (2002) Seven-transmembrane receptors. *Nature reviews. Molecular cell biology*, **3**, 639–650.

Pinching, A.J. & Powell, T.P. (1971a) The neuron types of the glomerular layer of the olfactory bulb. *Journal of cell science*, **9**, 305–345.

Pinching, A.J. & Powell, T.P. (1971b) The neuropil of the glomeruli of the olfactory bulb. *Journal of cell science*, **9**, 347–377.

Pinching, A.J. & Powell, T.P. (1971c) The neuropil of the periglomerular region of the olfactory bulb. *Journal of cell science*, **9**, 379–409.

Powell, T. (1981) Certain aspects of the intrinsic organisation of the cerebral cortex. In Pompeiano, O. & Marsan, C. (eds), *Brain Mechanisms of Perceptual Awareness and Purposeful Behaviour*, Volume 8. edn. Raven Press, New York, pp. 1–19.

Price, J.L. & Powell, T.P. (1970a) An electron-microscopic study of the termination of the afferent fibres to the olfactory bulb from the cerebral hemisphere. *Journal of cell science*, **7**, 157–187.

Price, J.L. & Powell, T.P. (1970b) The synaptology of the granule cells of the olfactory bulb. *Journal of cell science*, **7**, 125–155.

Price, J.L. & Powell, T.P. (1970c) The morphology of the granule cells of the olfactory bulb. *Journal of cell science*, **7**, 91–123.

Rakic, P. (1995) Radial versus tangential migration of neuronal clones in the developing cerebral cortex: Commentary. *Proceedings of the National Academy of Sciences of the United States of America*, **92**, 11323–11327.

Rall, T. & Sutherland, E.W. (1958) Formation of a cyclic adenine ribonucleotide by tissue particles. *Journal of biological chemistry*, **232**, 1065–1076.

Rall, W., Shepherd, G., Reese, S., & Brightman, M. (1966) Dendrodendritic Synaptic Pathway for Inhibition in the Olfactory Bulb. *Experimental neurology*, **14**, 44–56.

Ramsey, C.S., Yeung, F., Stoddard, P.B., Li, D., Creutz, C.E., & Mayo, M.W. (2008) Copine-I represses NF-kappaB transcription by endoproteolysis of p65. *Oncogene*, **27**, 3516–3526.

Rasmussen, H. (1970) Cell Communication, Calcium Ion, and Cyclic Adenosine Monophosphate. *Science*, **170**, 404–412.

Raynal, P. & Pollard, H.B. (1994) Annexins: the problem of assessing the biological role for a gene family of multifunctional calcium and phospholipid binding proteins. *Biochemica et Biophysica Acta*, **1197**, 63–93.

Ribak, C., Vaughn, J., Saito, K., Barber, R., & Roberts, E. (1977) Glutamate Decarboxylase localization in neurons of the olfactory bulb. *Brain Research*, **126**, 1–18.

Ribak, C.E. (1978) Aspinous and sparsely-spinous stellate neurons in the visual cortex of rats contain glutamic acid decarboxylase. *Journal of neurocytology*, **7**, 461–478.

Riederer, B.M., Berbel, P., & Innocenti, G.M. (2004) Neurons in the corpus callosum of the cat during postnatal development. *Neuroscience*, **19**, 1–8.

Rizo, J. & Rosenmund, C. (2008) Synaptic vesicle fusion. *Nature Structural & Molecular Biology*, **15**, 665–674.

Rizo, J. & Sudhof, T.C. (1998) C2-domains, structure and function of a Universal Ca2+ -binding domain. *The Journal of biological chemistry*, **273**, 15679–15882.

Rodbell, M. (1980) The role of hormone receptors and GTP-regulatory proteins in membrane transduction. *Macmillan Journals*, **284**, 17–22.

Rogers, A.W. & Berry, M. (1965) The migration of neuroblasts in the developing cerebral cortex. *Journal of Anatomy*, **99**, 691–709.

Rogers, J.H. (1987) Calretinin: a gene for a novel calcium-binding protein expressed principally in neurons. *Journal of cell biology*, **105**, 1343–1353.

Rosengarth, A. & Luecke, H. (2004) Annexins□: calcium binding proteins with unusual binding sites. In *Handbook of Metalloproteins Volume 3*. pp. 649–663.

Résibois, a & Rogers, J.H. (1992) Calretinin in rat brain: an immunohistochemical study. *Neuroscience*, **46**, 101–134.

Savino, M., Apolito, M., Centra, M., Beerendonk, H.M. Van, Whitmore, S.A., Crawford, J., Callen, D.F., Zelante, L., & Savoia, A. (1999) Characterization of Copine VII , a New Member of the Copine Family , and Its Exclusion as a Candidate in Sporadic Breast Cancers with Loss of Heterozygosity at 16q24 . 3. *Genomics*, **61**, 219 –226.

Schanne, F.A.X., Kane, A.B., Young, E.E., Farber, J.L., & Url, S. (2013) Calcium Dependence of Toxic Cell Death□: A Final Common Pathway Reviewed work (s): Calcium Dependence of Toxic Cell Death□: A Final Common Pathway. *Science*, **206**, 700–702.

Schmidt, H. (2012) Three functional facets of calbindin D-28k. *Frontiers in molecular neuroscience*, **5**, 25.

Schwaller, B., Dick, J., Dhoot, G., Carroll, S., Vrbova, G., Nicotera, P., Pette, D., Bluethmann, H., Hunziker, W., Celio, M.R., Albéri, L., Lintas, A., Kretz, R., Schwaller, B., Villa, A.E.P., Olinger, E., Loffing, J., Gailly, P., Devuyst, O., Harris, R.L., Bennett, D.J., Levine, M.A., Putman, C.T., Schiaffino, S., & Reggiani, C. (1999) Prolonged contraction-relaxation cycle of fast-twitch muscles in parvalbumin knockout mice Prolonged contraction-relaxation cycle of fast-twitch muscles in parvalbumin knockout mice. *Am J Physiol Cell Physiology*, **276**, 395–403.

Schwaller, B., Meyer, M., & Schiffmann, S. (2002) “New” functions for “old” proteins: the role of the calcium-binding proteins calbindin D-28k, calretinin and parvalbumin, in cerebellar physiology. Studies with knockout mice. *The Cerebellum*, **1**, 241–258.

Scott, B.T., Simmerman, H.K., Collins, J.H., Nadal-Ginard, B., & Jones, L.R. (1988) Complete amino acid sequence of canine cardiac calsequestrin deduced by cDNA cloning. *The Journal of biological chemistry*, **263**, 8958–8964.

Seemann, J., Weber, K., & Gerke, V. (1996) Structural requirements for annexin I – S100C complex-formation. *Journal of biochemistry*, **319**, 123–129.

Seki, T. & Arai, Y. (1993) Distribution and possible roles of the highly polysialylated neural cell adhesion molecule (NCAM-H) in the developing and adult central nervous system. *Neuroscience Research*, **17**, 265–290.

Shao, X., Davletov, B.A., Sutton, R.B., Südhof, T.C., Sudhof, T.C., & Rizot, J. (1996) Bipartite Ca2+-Binding Motif in C2 Domains of Synaptotagmin and Protein Kinase C. *Science*, **273**, 248–251.

Shepherd, G.. (2004) *The Synaptic Organisation of the Brain*, 5th Editio. edn. Oxford University Press.

Shepherd, G.M., Chen, W.R., Willhite, D., Migliore, M., & Greer, C. a (2007) The olfactory granule cell: from classical enigma to central role in olfactory processing. *Brain research reviews*, **55**, 373–382.

Silva, A., Paylor, R., Wehner, J.M., & Tonegawa, S. (1992) Impaired spatial learning in alpha-calcium-calmodulin kinase II mutant mice. *Science (New York, N.Y.)*, **257**, 206–211.

Silva, A.J., Stevens, C.F., Tonegawa, S., & Wang, Y. (1992) Deficient Hippocampal Long-term Potentiation in a alpha-calcium calmodulin kinase II mutant Mice. *Science*, **257**, 201–206.

Sloper, J.J., Hiorns, R.W., & Powell, T.P.S. (1979) A Qualitative and Quantitative Electron Microscopic Study of the Neurons in the Primate Motor and Somatic Sensory Cortices. *Philosophical Transactions of the Royal Society B: Biological Sciences*, **285**, 141–171.

Sloper, J.J. & Powell, T.P. (1978) Dendro-dendritic and reciprocal synapses in the primate motor cortex. *Proceedings of the Royal Society of London. Series B, Containing papers of a Biological character. Royal Society (Great Britain)*, **203**, 23–38.

Somogyi, P. (1989) Synaptic Organization of GABAergic Neurons and GABA A Receptors in the Lateral Geniculate Nucleus and Visual Cortex. In Lam, D.. & Gilbert, C. (eds), *Neural Mechanisms of Visual Perception*. Portfolio Publishing Co. Texas, pp. 35–62.

Somogyi, P., Hodgson, a. J., Chubb, I.W., Penke, B., & Erdei, a. (1985) Antisera to gamma-aminobutyric acid. II. Immunocytochemical application to the central nervous system. *Journal of Histochemistry & Cytochemistry*, **33**, 240–248.

Somogyi, P., Hodgson, A., Smith, D., Nunzi, G., Gorio, A., & Wu, J. (1984) Different populations of GABAergic neurons in the visual cortex and hippocampus of cat contain somatostatin or cholecystokinin immunoreactive material. *Journal of Neuroscience*, **4**, 2590–2603.

Somogyi, P., Priestley, J. V, Cuello, a C., Smith, a D., & Takagi, H. (1982) Synaptic connections of enkephalin-immunoreactive nerve terminals in the neostriatum: a correlated light and electron microscopic study. *Journal of neurocytology*, **11**, 779–807.

Somogyi, P. & Soltész, I. (1986) Immunogold demonstration of GABA in synaptic terminals of intracellularly recorded, horseradish peroxidase-filled basket cells and clutch cells in the cat's visual cortex. *Neuroscience*, **19**, 1051–1065.

Somogyi, P., Tamás, G., Lujan, R., & Buhl, E.H. (1998) Salient features of synaptic organisation in the cerebral cortex. *Brain research. Brain research reviews*, **26**, 113–135.

Spacek, J. & Harris, K.M. (1997) Three-dimensional organization of smooth endoplasmic reticulum in hippocampal CA1 dendrites and dendritic spines of the immature and mature rat. *The Journal of neuroscience□: the official journal of the Society for Neuroscience*, **17**, 190–203.

Sugita, S., Ho, a, & Südhof, T.C. (2002) NECABs: a family of neuronal Ca(2+)-binding proteins with an unusual domain structure and a restricted expression pattern. *Neuroscience*, **112**, 51–63.

Südhof, T.C. & Rizo, J. (1996) Synaptotagmins: C2-domain proteins that regulate membrane traffic. *Neuron*, **17**, 379–388.

Taniguchi, H., He, M., Wu, P., Kim, S., Paik, R., Sugino, K., Kvitsiani, D., Kvitsani, D., Fu, Y., Lu, J., Lin, Y., Miyoshi, G., Shima, Y., Fishell, G., Nelson, S.B., & Huang, Z.J. (2011) A resource of Cre driver lines for genetic targeting of GABAergic neurons in cerebral cortex. *Neuron*, **71**, 995–1013.

Taylor, N. (1974) Chick Brain Calcium-Binding Protein Comparison with Intestinal Vitamin D-Induced Calcium Binding Protein. *Archives of Biochemistry and Biophysics*, **161**, 100–108.

Temple, S. (2001) The development of neural stem cells. *Nature neuroscience insight review*, **414**, 112–117.

Tobimatsu, T. & Fujisawa, H. (1989) Tissue-specific expression of four types of rat calmodulin-dependent protein kinase II mRNAs. *The Journal of biological chemistry*, **264**, 17907–17912.

Tomsig, J.L. & Creutz, C.E. (2000a) Biochemical characterization of copine: a ubiquitous Ca2+-dependent, phospholipid-binding protein. *Biochemistry*, **39**, 16163–16175.

Tomsig, J.L. & Creutz, C.E. (2000b) Biochemical Characterization of Copine□: A Ubiquitous Ca 2 + -Dependent ,. *Biochemistry*, **39**, 16163–16175.

Tomsig, J.L., Snyder, S.L., & Creutz, C.E. (2003) Identification of targets for calcium signaling through the copine family of proteins. Characterization of a coiled-coil copine-binding motif. *The Journal of biological chemistry*, **278**, 10048–10054.

Tomsig, J.L., Sohma, H., & Creutz, C.E. (2004) Calcium-dependent regulation of tumour necrosis factor-alpha receptor signalling by copine. *The Biochemical journal*, **378**, 1089–1094.

Tretter, V., Mukherjee, J., Maric, H.-M., Schindelin, H., Sieghart, W., & Moss, S.J. (2012) Gephyrin, the enigmatic organizer at GABAergic synapses. *Frontiers in cellular neuroscience*, **6**, 23.

Tsien, J.Z., Chen, D.F., Gerber, D., Tom, C., Mercer, E.H., Anderson, D.J., Mayford, M., Kandel, E.R., & Tonegawa, S. (1996) Subregion- and cell type-restricted gene knockout in mouse brain. *Cell*, **87**, 1317–1326.

Verhage, M., De Vries, K.J., Røshol, H., Burbach, J.P., Gispen, W.H., & Südhof, T.C. (1997) DOC2 proteins in rat brain: complementary distribution and proposed function as vesicular adapter proteins in early stages of secretion. *Neuron*, **18**, 453–461.

Wang, D.D., Krueger, D.D., & Bordey, a (2003) GABA depolarizes neuronal progenitors of the postnatal subventricular zone via GABAA receptor activation. *The Journal of physiology*, **550**, 785–800.

Wang, Z., Meng, P., Zhang, X., Ren, D., & Yang, S. (2011) BON1 interacts with the protein kinases BIR1 and BAK1 in modulation of temperature-dependent plant growth and cell death in Arabidopsis. *The Plant journal□: for cell and molecular biology*, **67**, 1081–1093.

Wichterle, H., Garcia-Verdugo, J.M., & Alvarez-Buylla, a (1997) Direct evidence for homotypic, glia-independent neuronal migration. *Neuron*, **18**, 779–791.

Wichterle, H., Turnbull, D.H., Nery, S., Fishell, G., & Alvarez-Buylla, a (2001) In utero fate mapping reveals distinct migratory pathways and fates of neurons born in the mammalian basal forebrain. *Development (Cambridge, England)*, **128**, 3759–3771.

Wonders, C.P. & Anderson, S. a (2006) The origin and specification of cortical interneurons. *Nature reviews. Neuroscience*, **7**, 687–696.

Wu, S., Esumi, S., Watanabe, K., Chen, J., Nakamura, K.C., Nakamura, K., Kometani, K., Minato, N., Yanagawa, Y., Akashi, K., Sakimura, K., Kaneko, T., & Tamamaki, N. (2011) Tangential migration and proliferation of intermediate progenitors of GABAergic neurons in the mouse telencephalon. *Development (Cambridge, England)*, **138**, 2499–2509.

Wyss, J.M., Stanfield, B., & Cowan, W. (1980) Structural abnormalities in the olfactory bulb of the Reeler mouse. *Brain research*, **188**, 566–571.

Yamashita, T., Ninomiya, M., Hernández Acosta, P., García-Verdugo, J.M., Sunabori, T., Sakaguchi, M., Adachi, K., Kojima, T., Hirota, Y., Kawase, T., Araki, N., Abe, K., Okano, H., & Sawamoto, K. (2006) Subventricular zone-derived neuroblasts migrate and differentiate into mature neurons in the post-stroke adult striatum. *The Journal of neuroscience□: the official journal of the Society for Neuroscience*, **26**, 6627–6636.

Yang, S. & Hua, J. (2004) A Haplotype-Specific Resistance Gene Regulated by BONZAI1 Mediates Temperature-Dependent Growth Control in Arabidopsis. *The Plant cell*, **16**, 1060–1071.

Yao, J., Gaffaney, J.D., Kwon, S.E., & Chapman, E.R. (2011) Doc2 is a Ca2+ sensor required for asynchronous neurotransmitter release. *Cell*, **147**, 666–677.

Yoshimura, R., Ito, K., & Endo, Y. (2009) Differentiation/maturation of neuropeptide Y neurons in the corpus callosum is promoted by brain-derived neurotrophic factor in mouse brain slice cultures. *Neuroscience letters*, **450**, 262–265.

Young, K.M., Fogarty, M., Kessaris, N., & Richardson, W.D. (2007) Subventricular zone stem cells are heterogeneous with respect to their embryonic origins and neurogenic fates in the adult olfactory bulb. *The Journal of neuroscience□: the official journal of the Society for Neuroscience*, **27**, 8286–8296.

Zhao, C., Deng, W., & Gage, F.H. (2008) Mechanisms and functional implications of adult neurogenesis. *Cell*, **132**, 645–660.

Zoli, M., Jansson, a, Syková, E., Agnati, L.F., & Fuxe, K. (1999) Volume transmission in the CNS and its relevance for neuropsychopharmacology. *Trends in pharmacological sciences*, **20**, 142–150.